2013

Understanding the Posttranslational Regulation of the Response Regulator Rcsb and Acetyl Phosphate as an Acetyl Group Donor in E. Coli

Linda Hu
Loyola University Chicago

LOYOLA UNIVERSITY CHICAGO

UNDERSTANDING THE POSTTRANSLATIONAL REGULATION OF THE RESPONSE REGULATOR RCSB AND ACETYL PHOSPHATE AS AN ACETYL GROUP DONOR IN *E. COLI*

A DISSERTATION SUBMITTED TO

THE FACULTY OF THE GRADUATE SCHOOL

IN CANDIDACY FOR THE DEGREE OF

DOCTOR OF PHILOSOPHY

PROGRAM IN MICROBIOLOGY AND IMMUNOLOGY

BY

LINDA I-LIN HU

CHICAGO, IL

DECEMBER 2013

ACKNOWLEDGEMENTS

I would like to first thank my husband Nestor. His love and encouragement has been critical throughout my graduate school career. Having him with me has made any challenge feel conquerable. He is my weapon of choice. I also thank my family for all of their patience, love, and support. I thank my father in particular. He inspired me to pursue my dreams and encouraged me to not be afraid because he believed in me. I would also like to thank my amazing friends, Caela, Greg, and Bruno, who have been my sources of fun, encouragement, and support. I am blessed to have these wonderful people in my life.

I thank my advisor Dr. Alan J. Wolfe for the opportunity to be part of his laboratory. From him, I have learned what it means to be a mentor and what it takes to become a great scientist. I also thank all past and present members of the laboratory for being a great support for my personal and professional growth.

Lastly, I thank the members of my committee, Drs. Karen Visick, Adam Driks, Thomas Gallagher, Christopher Wiethoff, and Sean Crosson, for their guidance in my development as a scientist. I would also like to thank the members of the Microbiology and Immunology department for all of their help. It has been a pleasure and an honor to have received my education from Loyola.

For Nestor and Daddy, my daily sources of love, encouragement, support, friendship, and inspiration

From a few peaks rising above the fog we try to imagine what the hidden landscape underneath might look like.

Pieter W. Postma

TABLE OF CONTENTS

LIST OF TABLES

LIST OF FIGURES

LIST OF ABBREVIATIONS

PTM	Posttranslational modification
KAT	Lysine acetyltransferase
GNAT	GCN5-related N-Acetyltransferase
HDAC	Histone deacetylase
KDAC	Lysine deacetylase
VC	Vector control
TB	Tryptone broth
TB7	Tryptone broth pH 7
TBK	Tryptone broth with potassium chloride
RNAP	RNA polymerase
CoASH	Coenzyme A
AcCoA	Acetyl coenzyme A
AcP	Acetyl phosphate
NAM	Nicotinamide
SC	Spectral counts

ABSTRACT

The observation that Nε-lysine acetylation occurs on a hundreds of proteins in bacteria is a recent discovery. To study the mechanisms that regulate acetylation and to determine if acetylation affects physiology, I studied the *Escherichia coli* response regulator and transcription factor RcsB, which was reported to be acetylated *in vitro*. To monitor RcsB activity, I measured transcription from the *rprA* promoter, which requires RcsB. I confirmed that RcsB is activated by phosphorylation through the Rcs phosphorelay and acetyl phosphate and showed that acetyl phosphate could phosphorylate RcsB. However, a mutant that accumulates acetyl phosphate (*ackA*) exhibited reduced *rprA* transcription instead of the predicted increase. To test if acetylation affected RcsB activity *in vivo*, I analyzed the effect of the only known *E. coli* protein deacetylase CobB on *rprA* transcription and RcsB acetylation and determined that the *cobB* mutant showed reduced *rprA* promoter activity and hyperacetylated RcsB. Perhaps more surprisingly, RcsB isolated from the *ackA* mutant was also hyperacetylated. Using a genetic approach, I identified an AckA- and CobB-sensitive RcsB lysine that controls its activity. Since RcsB acetylation increases when acetyl phosphate accumulates, we hypothesize that acetyl phosphate is a novel acetyl donor for protein acetylation.

CHAPTER ONE

LITERATURE REVIEW

Introduction

After protein synthesis, a wide repertoire of post-translational modifications (PTMs) can alter the protein and its function. The Uniprot database currently lists 435 PTMs (The UniProt Consortium, 2010). These PTMs are often mediated by enzymes and can change protein function through the addition of functional groups, chemical modifications, proteolytic cleavage, or protein isomerization. These modifications can impact protein function through changes in protein stability, interactions with other proteins, DNA, lipids, cofactors, or cellular localization. PTMs are critical regulators of physiology because PTMs can affect many cellular functions, including signaling pathways, gene expression, DNA repair, cell division, and metabolism. Dysfunctional regulation of PTMs can lead to various disease states in humans (1).

PTMs can allow an organism to quickly respond to a stimulus by directly altering protein function, bypassing the otherwise necessary energy and time investments for DNA replication, transcription, and translation of appropriate effectors to carry out the altered biological function. Since PTMs can be reversible, the cell can also quickly turn off a response.

More than one PTM of the same or different type can alter protein function by modifying one or more sites on a protein. Since a protein can adopt these various PTM combinations, a single protein has multiple distinct protein isoforms, and thus has the potential to have more than one biological output. PTMs have been considered "nature's escape from genetic imprisonment" (2) by expanding the functional potential of an organism's genome.

The following sections focus on acetylation, one of the most common PTMs. I will discuss the types of acetylation, the mechanisms of acetylation, and the effects of acetylation. The purpose will be to gain an understanding of acetylation in eukaryotes and apply this knowledge towards acetylation in bacteria.

Acetylation

The Chemical Reaction

Two types of acetylation exist. Acetylation occurs through the transfer of an acetyl functional group onto either the amino terminus of the first amino acid of a protein, called Nα-acetylation, or onto the epsilon amino group of a lysine side chain, called Nε-acetylation.

Both Nα- and Nε-acetylation require the proper microenvironment. Acetylation requires that the acetyl donor, e.g. acetyl-coenzyme A (AcCoA), be brought into close proximity to the amino group of the substrate. This step can be facilitated either by an acetyltransferase that can interact with both the acetyl donor and the target of acetylation or by a high local concentration of the acetyl donor. Acetylation also requires a neutral amino group, which can undergo nucleophilic

attack of the carbonyl group. Deprotonation of the amino group can occur by the presence of an acetyltransferase, an amino acid that can act as a general base, or by an increase in pH. Nucleophilic attack of the carbonyl carbon of AcCoA forms an unstable tetrahedral intermediate and the electron dense oxygen expels the thiolate group, resulting in an acetylated amino group and free CoASH (**Figure 1**; (3,4)).

Nα-Acetylation

While the focus of my dissertation is Nε-acetylation, understanding what is known concerning Nα-acetylation could help direct analyses of the regulation and effect of Nε-acetylation in bacteria.

Nα-acetylation was discovered by Phillips in 1963 (5). He found that acetyl groups were present on histones and that the amino terminus of the histone polypeptide chain was acetylated.

Nα-acetylation occurs either on the deformylated N-terminal methionine or, following cleavage of the N-terminal methionine, on the newly exposed amino acid. These reactions are irreversible modifications that are extremely common in eukaryotes, but rare in bacteria. While 60% of yeast and 80% of human proteins exhibit Nα-acetylation (6), in bacteria, only some ribosomal proteins are known to be Nα-acetylated (7).

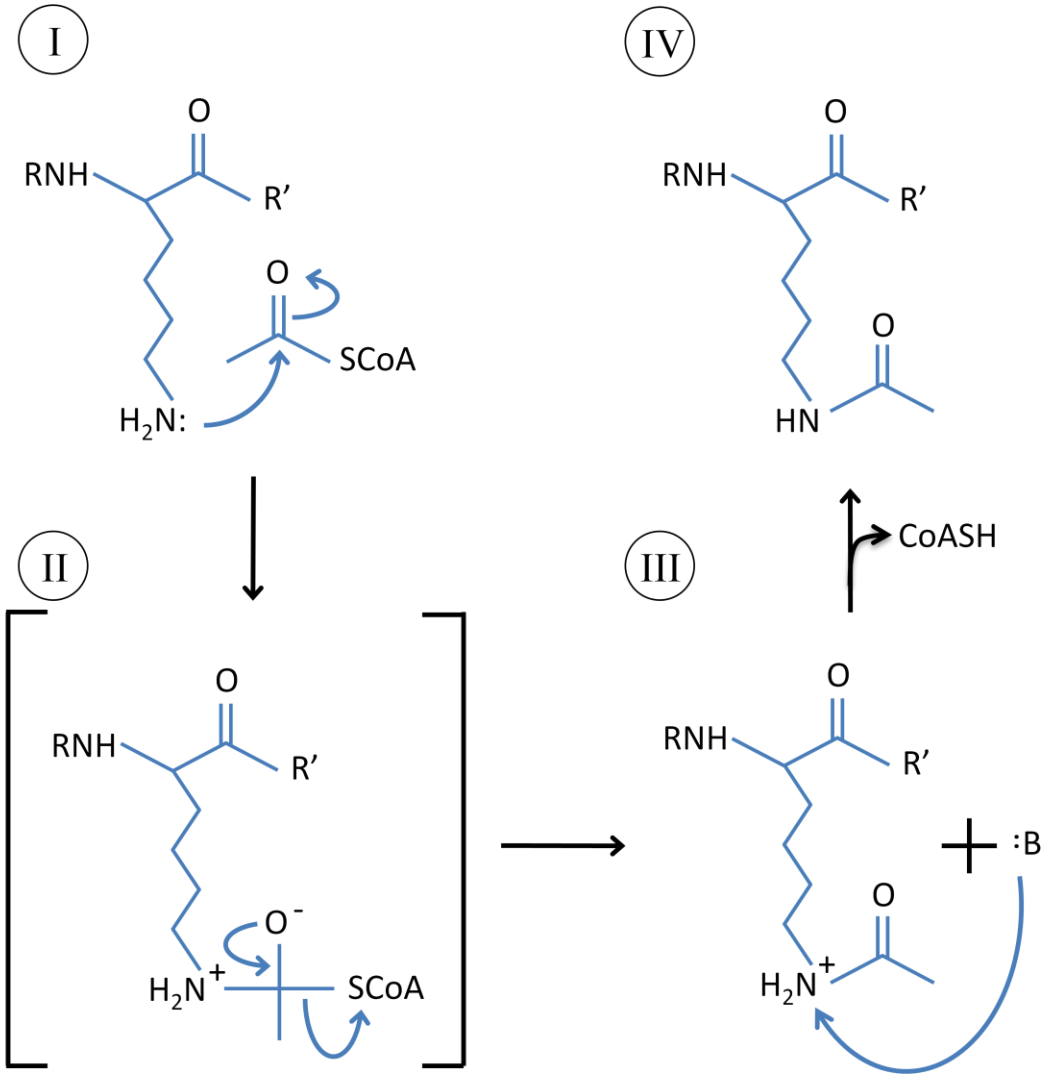

Figure 1. Electron transfer during direct Nε-acetylation from acetyl-CoA.
At neutral pH, the ε-amino group is positively charged. This residue is deprotonated by a base (not shown in figure). (I) The lysine ε-amino group can now act as a nucleophile to attack the electrophilic carbonyl carbon of acetyl-CoA (II) forming a tetrahedral intermediate. The electron dense oxygen expels the thiolate group (-SCoA). (III) A base (:B) deprotonates the amino group (IV), resulting in an acetylated lysine side chain and CoASH. The figure is from Hu *et. al.*, 2010, which was adapted from Walsh 2006.

While Nα-acetylation in bacteria occurs post-translationally, in eukaryotes, acetylation is primarily co-translational, occurring on nascent polypeptides. This co-translational modification is facilitated by the direct interaction of ribosomes with the required acetyltransferases (8-11).

There are several known Nα acetyltransferases (NATs or more recently called Naa (12)). NatA-F are found in all domains of life (13). NATs are known to differ in their substrate specificity, depending on the first few amino acids of the target: the most common NatA substrates include Ser- and Thr-N termini, while NatB and NatC prefer Met-N termini. Two analyses of the acetylated and non-acetylated N-termini in yeast, human, bovine, and rat (13) or in yeast alone (14) found a strong preference for the acidic aspartyl and glutamyl residues adjacent to the acetylated first amino acid residue. N-termini with the sequences X-Asp or X-Glu were acetylated more often than N-termini with the sequences X-Lys or X-Arg, while X-Pro was not acetylated (13,14). This information has been used to develop computer programs to predict acetylation (13,14); however, these acetylation prediction programs have not been reliable. One possible explanation is that that the sequence alone is not the sole determinant for acetylation. It is unclear whether a motif for either Nα-acetylation or Nε-acetylation exists in *E. coli*.

The best understood function of Nα-acetylation is to regulate protein stability. The earliest function attributed to Nα-acetylation was to inhibit protein degradation by the ubiquitin system (15). Recently, however, Nα-acetylation is

proposed to promote protein degradation by generating signals that a certain ubiquitin ligase can recognize (16). Since a large percentage of eukaryotic proteins are Nα-acetylated, global degradation of these proteins is non-intuitive. Instead, there are likely additional, unknown regulators that control protein stability in addition to the effect of Nα-acetylation.

Nε -Lysine Acetylation

While the first Nε-acetylated bacterial protein was reported in 1992 (17), the discovery of Nε-acetylation was made by Allfrey and colleagues 30 years earlier in 1964 on histones (18). They analyzed the effect of incubating calf thymus nuclei with radioactive acetate and found that "…the radioactive material was *N*-acetyl-lysine. Since lysine does not occur in the NH2-terminal or COOH-terminal positions of the *f2a1* [histone 4], the site of substitution was presumably on the ε-amino nitrogen of the dibasic amino acid." Allfrey verified this conclusion by demonstrating that the radioactivity in the samples co-eluted with an ε-acetyllysine standard on an amino acid analyzer column. Because of this influential paper and his subsequent contributions, Allfrey is considered a founding father of epigenetics.

In contrast to Nα-acetylation, Nε-acetylation is reversible, making this form of acetylation dynamic. Nε-acetylation only targets lysine residues, increasing the length and neutralizing the charge of the lysine side chain. These changes can alter the protein, including changing protein conformation, activity, stability, interactions

with other molecules, and localization (4). Since Nε-acetylation is the focus of this dissertation, I will refer to it as 'acetylation,' unless otherwise noted.

Histone acetylation was identified almost 50 years ago (5,19). Since then, we have learned that histones are subject to a myriad of PTMs, leading to the concept that PTMs can generate a molecular language on histones (20,21). The 'histone code hypothesis' has been generalized to a PTM code, describing the effect of combinations of PTMs on protein function.

p53 is a prototype for both the PTM code and non-histone acetylation. p53 is a transcription factor that also has cytosolic, transcription-independent functions (22) with at least 50 sites that are known to be posttranslationally modified (23). These PTMs include phosphorylation, ubiquitylation, and acetylation. Although intricate, complex, and incomplete, there are aspects of p53 regulation that are understood. p53 may be regulated by single 'off-on' modifications. For instance, acetylation of lysine-317 is proposed to turn off DNA damage-induced, p53-dependent apoptosis (24). p53 also may be regulated by sequential multiple modifications. Under stress, phosphorylation of serine-15 appears to start a sequential PTM pathway, leading to the phosphorylation of several residues, phosphorylation recruits the acetyltransferases CBP and p300, which acetylate and increase p53 affinity for DNA targets (23,25-27). Lastly, different combinations of simultaneous modifications have been demonstrated, correlating to changes in p53 activity (28). A similar PTM code appears to exist on the *E. coli* signal transduction

protein CheY (discussed in detail later), but it is unknown if other bacterial proteins are regulated by a PTM code.

Recent reports show that protein acetylation extends far beyond these few examples. The mammalian acetylome includes more than 2700 acetylated proteins that are involved in almost every aspect of cellular physiology, including central metabolism, mRNA splicing, protein synthesis and degradation, cell morphology and cell division (29-31). In these studies, it was evident that many mitochondrial proteins are acetylated. Since mitochondria are closely related to α-proteobacteria (32,33), could global protein acetylation exist in bacteria?

The Discovery and Impact of Nε-Lysine Acetylation in Bacteria

Before 2008, lysine acetylation was believed to be rare in bacteria. However, the first bacterial global proteomic analysis identified 85 *E. coli* proteins with 125 lysine-acetylated sites (34). Yu and colleagues grew *E. coli* W3110 in nutrient rich LB medium to mid-exponential and stationary phase. Upon harvesting samples, they added 50 mM nicotinamide, a lysine deacetylase inhibitor, lysed the cells, and digested the proteins with trypsin. Affinity immunoprecipitation with anti-acetyllysine antibody enriched for acetylated peptides and nano-HPLC/MS/MS analysis identified acetylated lysines. This study revealed different *E. coli* acetylation profiles in exponential phase and stationary phase, suggesting that acetylation for some proteins is dependent on growth phase. The majority of the proteins (68%) were acetylated specifically in stationary phase, 23% were acetylated only in

exponential phase, and the remaining 11% were detected as acetylated in both conditions. A functional classification of the acetylated proteins suggested the cellular processes that may be regulated by acetylation. Most of the acetylated proteins are involved in protein synthesis (28%), carbohydrate metabolism (19%), nucleotide (11%) or amino acid (8%) biosynthesis, the TCA cycle (8%), and transcription (7%). The remaining acetylated proteins are involved in protein folding, detoxification, and energy or fatty acid metabolism. Since this seminal article, several global proteomic analyses have followed, adding to this growing field of bacterial protein acetylation.

Zhang and coworkers published the second *E. coli* global protein acetylation study. *E. coli* DH5α was aerated in LB medium at 37°C and grown to exponential phase (35). An analysis of the functional annotations of the 91 proteins and 138 acetylated sites confirmed the previously reported functional classifications of acetylated *E. coli* proteins (35). Acetylation is sensitive to hypoxic growth conditions, suggesting that lysine acetylation is a stress response. Since 24% of the acetylated *E. coli* proteins have at least 25% sequence identity to a mammalian protein and acetylation is a prominent modification in mitochondria, the authors proposed that lysine acetylation is an evolutionarily conserved mechanism of regulation. Additionally, the acetylated peptides showed a preference for histidines and tyrosines in the C-terminal direction adjacent to the acetylated lysine, which is similar to what was reported for mitochondrial lysine acetylation (30).

Wang and colleagues reported that lysine acetylation is abundant (191 proteins and 235 acetylated sites) in *Salmonella enterica* (36). Of these acetylated proteins, 90% of the central metabolic enzymes were targeted. They tested the effect of metabolic flux on the acetylation profiles of these enzymes. On the basis of a comparison of cells grown in defined medium supplemented with the glycolytic carbon source glucose to the same cells grown on the gluconeogenic carbon source citrate, the authors proposed that the acetylation of metabolic enzymes changes in response to the carbon source and that the lysine acetyltransferase (KAT) Pat and the lysine deacetylase (KDAC) CobB are involved in regulating these changes.

Acetylation is not limited to Gram-negative bacteria. An extensive acetylproteome was identified in the Gram-positive organism *Bacillus subtilis* with 185 proteins and 332 acetylated sites (37). There is some conservation of acetylated proteins. The *B. subtilis* acetylproteome was 30% and 12% conserved compared to the *E. coli* and *S. enterica* acetylproteomes, respectively. Since 10% of *B. subtilis* proteins are modified by both acetylation and serine/threonine/tyrosine phosphorylation, a bacterial PTM code involving phosphorylation and acetylation may exist. An analysis of the acetylated sites revealed that glutamic acid, proline, aspartic acid, and lysine were frequently in the +1 position relative to the acetylated lysine residue, suggesting that a consensus acetylation motif may exist in *B. subtilis*. Consensus acetylation motifs of five bacterial and eukaryotic acetylproteomes were

compared and there was no one common signature sequence, which may indicate that the mechanisms that regulate the acetylproteomes are different.

Bacterial PTMs may also form a protein modification code through phosphorylation and acetylation. In *Mycoplasma pneumoniae*, combinations of lysine acetylation and serine/threonine/tyrosine phosphorylation form a complex regulatory network (38,39). In total, 72 proteins with 93 phosphorylated sites and 221 proteins with 719 acetylated sites were identified. Consistent with the hypothesis that lysine acetylation is an evolutionarily conserved mechanism of protein regulation, many lysines that were acetylated in *M. pneumoniae* proteins were conserved within three amino acids in eukaryotic orthologs. The phosphoproteome and the acetylproteome affect one another. Deleting the kinases (or the phosphatase) or the acetyltransferase changed the profiles of the opposing proteome, i.e. the acetylproteome or the phosphoproteome, respectively. It is possible that phosphorylation and acetylation affect one another in *E. coli*.

A global proteomic study coupled to a structural analysis provided insight into the effect of acetylation in *Thermus thermophilus* and possibly other organisms (40). 127 proteins with 197 acetylated lysines and 4 Nα-acetylation sites were identified. Of these proteins, 20% of the proteins had more than one site modified. Almost all (94%) of the acetylated *T. thermophilus* proteins have orthologs in archaea (*Sulfolobus solfataricus*), bacteria (*E. coli*, *B. subtilis*, *Halobacterium salinarum*, and *Deinococcus radiodurans*), or eukaryotes (*Saccharomyces cerevisiae*,

Arabidopsis thaliana, *Mus musculus*, and *Homo sapiens*), suggesting that acetylation may regulate conserved proteins. In fact, 22% of acetylated *T. thermophilus* proteins are conserved in all 9 organisms. Since 56% of the acetylated *T. thermophilus* lysines were conserved in the orthologous proteins, acetylation may occur on these proteins and possibly have an effect on protein function. An analysis of the primary amino acid sequences flanking acetylated lysines demonstrated a high frequency of negatively charged amino acids. Most of the acetylated lysines were on the surface of tertiary or quaternary structures while some acetylation occurred in positions that are important for binding to ligands or enzyme activity. 56% of the surface-exposed acetylated lysines were near acidic amino acids or oxygen atoms. Neutralization of the positively charged lysine may disrupt these stabilizing electrostatic interactions or hydrogen bonds, leading to possible changes in protein conformation and protein function.

Before the global proteomic analyses that identified hundreds of acetylated proteins in bacteria, acetylation was known to regulate bacterial chemotaxis and acetate metabolism by affecting two proteins, the chemotaxis response regulator (RR) CheY and acetyl-coenzyme A synthetase (Acs; Acs will be discussed in detail later). In contrast to Acs in which acetylation 'turns off' Acs activity, acetylation of CheY is more complex, with multiple lysines acetylated and more than one mechanism of acetylation and deacetylation. CheY acetylation was detected *in vivo* on six lysinyl residues (41,42). These acetylated lysines reside on the CheY surface

and reduce CheY binding to three proteins: the CheY kinase CheA, the CheY phosphatase CheZ, and the switch of the flagellar motor FliM (43,44). CheY acetylation can occur through autoacetylation using AcCoA as the acetyl donor or through an Acs-mediated reaction using either AcCoA or acetate (and ATP) as the acetyl donors (17,45,46). Acetylation of CheY is reversible; acetylated CheY is deacetylated by Acs or by the KDAC CobB (45).

Acetylation of neighboring lysines on the exposed surface of the α subunit of RNA polymerase (RNAP) elicits opposite effects on RNAP activity. RNAP is a multi-subunit enzyme, consisting of two α subunits, β, β', and ω. WT *E. coli* cells exposed to moderate amount of glucose (0.4% or 22 mM) activate the stress responsive *cpxP* promoter (47). This glucose-induced activation requires the KAT YfiQ and is inhibited by the KDAC CobB. Consistent with the hypothesis that acetylation of Lys-298 of the α subunit of RNAP activates *cpxP* transcription, glucose-induced *cpxP* transcription required Lys-298, and acetylation of Lys-298 was dependent on both glucose and YfiQ. In contrast, acetylation of Lys-291 appears to reduce *cpxP* transcription. This occurs when the intracellular concentration of the metabolic intermediate and signaling molecule acetyl phosphate (AcP) accumulates, either in *ackA* mutant cells exposed to moderate concentrations of glucose (0.4%) or in WT cells grown in the presence of a large amount of glucose (4%) (48). Compared to WT cells exposed to 0.4% glucose, the *ackA* mutant exposed to the same concentration of glucose exhibited a reduced *cpxP* promoter response, suggesting that an

accumulation of AcP inhibits glucose-induced transcription. Acetylation of Lys-291 of the α subunit of RNAP appears to inhibit RNAP activity at the *cpxP* promoter because Lys-291 required for the inhibitory behavior, Lys-291 was acetylated in the *ackA* mutant exposed to glucose, and WT cells overexpressing a genetic mimic of constitutively acetylated Lys-291 (K291Q) inhibited *cpxP* transcription even in the absence of glucose.

Acetylation may regulate transcription factor activity. To identify substrates of the *S. enterica* KAT Pat, a chip mounted with *E. coli* proteins was incubated with purified Pat and radiolabeled AcCoA. Pat acetylated RcsB, McbR, RpsD, MltD, YcjR, and YbaB (49). Thao *et al*. showed that RcsB was acetylated by both *S. enterica* Pat and *E. coli* YfiQ and acetylation was detectable on only one residue, Lys-180. Lys-180 is in the DNA-binding domain of RcsB. Acetylation of Lys-180 reduced binding to the *flhDC* promoter *in vitro* and Lys-180 was required for RcsB-mediated inhibition of *flhDC* promoter activity. These results demonstrated that this residue was critical for RcsB function. Site-directed acetylation of Lys-180 on RcsB was performed and it was determined that CobB can deacetylate acetyl-Lys-180, indicating that RcsB is reversibly modified. While RcsB was found to be reversibly acetylated by Pat/YfiQ and CobB *in vitro*, it was not demonstrated whether RcsB was acetylated *in vivo* and if acetylation affected RcsB activity.

Acetylation may regulate protein stability in bacteria. RNase R is an *E. coli* exoribonuclease that is acetylated on Lys-544 by the *E. coli* KAT YfiQ (50,51).

Acetylated RNase R can bind to *trans*-translation machinery RNA tmRNA and the tmRNA binding protein SmpB (52). This complex promotes an interaction with proteases HslUV and Lon and leads to RNase R degradation (53).

These examples of acetylated proteins provide us with valuable information concerning the regulation and the effect of bacterial acetylation. However, the scope of knowledge is still very limited if one considers the hundreds of known acetylated bacterial proteins. Therefore, there is a necessity for studies on either other acetylated bacterial proteins or a more complete, global analysis into the function of acetylation.

Acetyltransferases

Acetylation can occur enzymatically, through the action of acetyltransferases. Acetyltransferases were originally identified in the 1970-1980s as required for modification of aminoglycoside antibiotics and were the basis for the first sequence comparison that led to the identification of the general control non-derepressible 5 (Gcn5)-related acetyltransferase (GNAT) family (54,55).

The GNAT and MYST families are the largest groups of acetyltransferases. GNATs include NATs and PCAF (p300/CBP-associated factor). Other acetyltransferases are p300/CBP (adenoviral E1A-associated protein of 300 kDa and CREB-binding protein), SRC, and the TAFII group of transcription factors (56-59).

Acetyltransferases have a conserved catalytic core of three-beta sheets and a helix. While the core is structurally conserved, there is little to no sequence similarity between the acetyltransferase sub-families. The GNAT core has three conserved sequence motifs (A, B, and D) and some GNAT members also have a fourth conserved sequence motif C (60). Motif A is the most conserved and binds AcCoA (61,62). Members of the MYST sub-family have homology to motif A only. The acidic, negatively charged residues of Motif B accommodate a positively charged substrate, such as a lysine side chain. The core is flanked by variable helices and loops on the N- and C-termini. Together, the core and the variable regions form a groove that accommodates their respective protein targets and possible coactivators.

The mechanism through which acetyl transfer occurs has been described for GNATs (63) and MYSTs (64,65). These families of acetyltransferases are proposed to catalyze acetylation by directly transferring an acetyl group onto the substrate, in which a ternary complex between AcCoA, the substrate, and the acetyltransferase is formed (64-66). At neutral pH, the epsilon amino group of the lysine side chain is protonated due to its high pKa of 10 and does not undergo nucleophilic attack of AcCoA. The acetyltransferase can deprotonate and thus activate the lysine for acetylation using a catalytic general base such as aspartic or glutamic acid. Structural and mutational analyses of Gcn5 suggest that deprotonation occurs through a conserved glutamate residue (Glu-173) in the core (67,68). Mutational

analysis of Gcn5 Glu-173 determined that the residue was not involved in binding to AcCoA or the histone substrate. Instead, Glu-173 was involved in catalysis because Glu-173 was not required at high pH, a condition that non-enzymatically deprotonates lysine. These results indicate that the function of Glu-173 is to act as a general base to deprotonate lysine for nucleophilic attack of AcCoA at neutral pH.

Several other divergent acetyltransferases have residues that are required for catalytic activity and could act as general bases and deprotonate the lysine target (64,67,69,70). For example, human NAT Naa50p catalysis depends on tyrosine and histidine (Tyr-73 and His-112) to act as general bases (69) and cAMP-regulated *Mycobacterium* Rv0998 catalytic acitivity depends on Glu-235 positioned where the conserved Glu-173 is in Gcn5 (70). Instead of a catalytic general base, some acetyltransferases have a series of residues that may form a water channel or a 'proton wire,' shuttling protons from the active site to internal proton acceptors or to the solvent (63,71,72).

Thus, there are multiple approaches to accomplish lysine deprotonation, which suggests that this step is critically important for acetylation to occur.

Acetylation can also occur non-enzymatically. For example, non-enzymatic acetylation of CheY occurs in the presence of AcCoA or acetic anhydride (44,46). Although the GCN5-like 1 protein is an indirect regulator of mitochondrial protein acetylation (73), a mitochondrial KAT has not yet been identified and such an enzyme has proven to be elusive. Therefore, non-enzymatic acetylation is also

suspected to occur in the mitochondria. The mechanism of non-enzymatic acetylation is unknown but could involve this critical step of deprotonation of lysine residues prior to acetyl transfer.

Lysine Deacetylases

Lysine acetylation is reversible through the action of deacetylases. The first histone deacetylase (HDAC), called HDA1, was identified in 1996. It was reported that cytostatic agent and deacetylase inhibitor trapoxin enhanced histone acetylation and blocked cell cycle progression in mammalian cells (74). Schreiber and co-workers used trapoxin to purify HDA1 (75). Since then, four deacetylase classes I-IV have been identified based on sequence homology and phylogenetic analyses (76-80). Homologs of these four classes have been found in bacteria (80).

Classes I, II, and IV are commonly referred to as either zinc-dependent deacetylases or the classical HDACs. However, it is important to mention that class III deacetylases are also zinc-dependent. Furthermore, while these enzymes are historically referred to HDACs, they have functions that do not involve histones; several members of classes I, II, and IV can shuttle between the nuclear and cytoplasmic compartments (80) and some HDACs can deacetylate nonhistone proteins, such as tubulin (81) and p53 (82). Classes I and II are the largest groups of deacetylases with 10 members. Class IV consists of one member (HDAC 11) that shares some similarity to classes I and II, but a phylogenetic analysis of the catalytic core region of HDAC-like genes in all fully sequenced organisms showed that HDAC

IV-related genes form a distinct group (77). Class III is comprised of the NAD^+-dependent deacetylases, typically called sirtuins, after the yeast silent mating type information regulator 2 (Sir2)(83). The following will describe some of what is known about the classical HDACs and sirtuins.

Classical HDACs

While its function remains unknown, the structure of the histone deacetylase-like protein (HDLP) isolated from the hyperthermophilic bacterium *Aquifex aeolicus* provided the first model for the classical HDAC structure and function (84-86). HDLP structure consists of an eight-stranded parallel beta sheet flanked by four alpha helices. On one side of the beta sheet is a cluster of alpha helices and loops on the C-terminal ends of the beta sheet. These helices and loops form a hydrophobic channel with the bound zinc ion at the base, near the end of the channel. The carbon chains of two HDAC inhibitors, which are structurally similar to an acetylated lysine, can bind within this channel, suggesting that this channel is the acetyl-lysine binding pocket on HDACs, (84). Further highlighting the importance of this region, highly conserved residues of the class I and II HDACs map to the channel of the HDLP structure (86).

Structural variations to this channel may regulate substrate binding. A comparison of a class I HDAC (HDAC8) with HDLP identified some structural variations that appear to provide a more accessible substrate binding pocket that is both wider and longer (87,88). Substrate specificity may be regulated by the loops

that line the channel since a comparison of HDLP, HDAC8, and an amidohydrolase from a *Bordetella*/*Alcaligenes* strain revealed the most structural variability in the loops (85).

These enzymes utilize Zn-dependent hydrolysis of the acetyl-amide bond. Zn is coordinated by conserved aspartyl and histidinyl residues in the channel and HDAC inhibitors vorinostat and trichostatin A (87,88). Zn coordinates with the hydroxymate moiety of these inhibitors, suggesting that Zn is important because Zn coordinates with the acetyl group of an acetylated substrate. Once the acetylated substrate is positioned properly, a water molecule can hydrolyze the acetyl-lysine bond by attacking the carbonyl carbon of the acetyl group.

Sirtuins

Organisms from all three domains of life and in some viruses possess sirtuins (89). Sirtuins are structurally, functionally, and evolutionarily unrelated to the 'classical' HDACs. Unlike the HDACs that catalyze the hydrolysis of an acetyllysine, these enzymes require nicotinamide adenine dinucleotide (NAD^+) as a co-substrate in deacetylation. Certain sirtuins exhibit more general functions than just deacetylating lysines. Some of the human sirtuins deacetylate proteins *in vitro* poorly. One of these sirtuins is human SIRT5, which can de-succinylate and de-malonylate (90). Therefore, it has been proposed that sirtuin deacetylases would be better referred to as sirtuin de-acylases (83).

Sir2 is the founding member of the sirtuin family of deacetylases. A spontaneous *sir2* mutant (originally called *mar1* for mating type regulator) led to sterility of yeast and transcriptional inhibition of mating information loci (91). This finding contributed to the current popular concept of transcriptional silencing by acetylation.

A comparison of over 40 sirtuin structures revealed a conserved two domain catalytic core (92). One is a structural motif called a Rossmann fold that is responsible for recognizing the NAD^+ cofactor. The second domain binds zinc and is a less conserved structure amongst the sirtuins. A channel is formed between these two domains and connecting loops. This cleft binds the acylated substrate and the NAD^+. The channel is composed of conserved and variable residues that are responsible for substrate binding and reaction catalysis (93).

Sirtuins are proposed to catalyze a direct reaction that transfers an acetyl group from acetyllysine to NAD^+ (**Figure 2**, (92,94)). Unlike many NAD^+-dependent metabolic reactions that reduce NAD^+ to produce NADH, sirtuins actually couple deacetylation to NAD^+ hydrolysis. Except for SIRT6, sirtuin enzymes require binding to acetyllysine prior to NAD^+ binding (95,96). In the absence of acetyllysine substrate, NAD^+ binds in a non-productive conformation. Once an acetyllysine substrate is present, NAD^+ binds in a productive conformation within the conserved catalytic pocket. The carbonyl oxygen undergoes nucleophilic attack on NAD^+, cleaving NAD^+ and releasing nicotinamide as a byproduct. A peptidylimidate

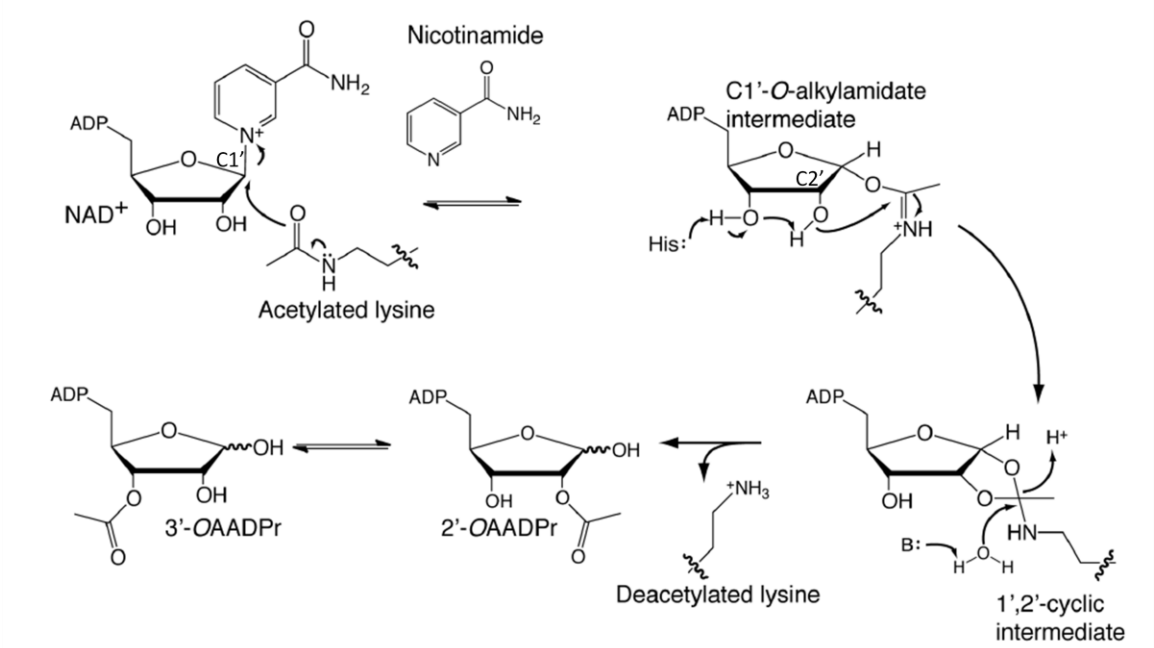

Figure 2. The proposed mechanism of NAD⁺-dependent sirtuin catalyzed deacetylation. The carbonyl oxygen of the acetylated lysine attacks C1' of the nicotinamide ribose ring. Nicotinamide (NAM) is expelled and an alkylamidate intermediate is formed. In the presence of NAM, the intermediate can reverse back to reactants. Otherwise, a conserved histidine in the active site can directly or indirectly deprotonate the C2' hydroxyl group. The activated oxygen reacts with the alkylamidate carbon to form a cyclic intermediate. A base activates a water molecule, which disrupts the tetrahedral intermediate. A deacetylated lysine is released along with O-acetyl-ADP-ribose (OAADPr), which isomerizes between 3'-OAADPr and 2'-OAADPr. This figure was adapted from Feldman, *et al.* 2012.

intermediate (also called an alkylamidate intermediate) is formed. This reactive intermediate is essentially an acetylated lysine covalently bound to the NAD⁺ ribose ring. The intermediate is subject to intramolecular reactions that can reverse the reaction or, driven by conserved catalytic base residues that activate nucleophilic reactions, proceed forward to the products, producing a deaceylated lysine and a mix of 2'- and 3'-*O*-acetyl-ADP ribose (97). The physiological function of these

acetyl-ADP ribose metabolites is yet unclear, but some evidence exists that they might be signaling molecules (98).

Sirtuins are widely distributed in nature. Phylogenetic analyses of the conserved core domain have classified sirtuins into five classes (78,79). Classes I, II, and -IV are eukaryotic and class U, for 'undifferentiated,' represent bacterial and archaeal sirtuins.

Class III is a mix, composed of eukaryotic, bacterial, and archaeal sirtuins (78). Human SIRT 5 is a member of class III, suggesting that SIRT5 may be evolutionarily the most ancient of the seven human sirtuins. This is consistent with the localization of SIRT5 predominately to the mitochondria. Class IIIa, which includes SIRT5, is mostly eukaryotic, Class IIIb is mostly archaeal, while class IIIc, which includes the one known *E. coli* deacetylase CobB, is mostly bacterial.

The phylogenetic analyses suggested that CobB is the only sirtuin in *E. coli* and thus the only regulator of protein deacetylation. The identification of the bacterial SIR2 homolog CobB arose from analyzing the regulation of cobalamin (vitamin B12) biosynthesis in *Salmonella typhimurium* LT2 (99,100). Phosphoribosyltransferase CobT transfers the phosphoribosyl group from nicotinate mononucleotide to 5,6-dimethylbenzimidazole (Me_2Bza), making α-ribazole-5'-phosphate, a required precursor for the nucleotide loop assembly step in cobalamin biosynthesis. Unexpectedly, the *cobT* mutant requires Me_2Bza for growth. Another pathway in cobalamin biosynthesis that can compensate for the loss of

CobT was proposed to be activated by the presence of high concentrations of Me_2Bza. The *cobT cobB* double mutant was deficient in cobalamin biosynthesis, suggesting that CobB provides this alternative to CobT. *E. coli* CobB has inefficient NAD^+-dependent ADP-ribosyltransferase activity using Me_2Bza (101) but can efficiently deacetylate acetylated histones in an NAD^+-dependent manner (102). These results suggest that protein acetylation is present in bacteria and that some of the regulation of acetylation is similar to eukaryotic organisms.

Due to the implicated functions of sirtuins in the regulation of metabolism and aging (103), there is great interest in the development of small molecule modulators of sirtuin activity (104). Nicotinamide, a product of deacetylation, is a well-known inhibitor of sirtuin activity (105). Nicotinamide is a non-competitve inhibitor of sirtuins with an IC50 of 150 μM. It functions by interacting with a deacetylation intermediate. Through a process called nicotinamide base-exchange, the reaction is reversed, regenerating NAD^+ and acetyllysine.

Therefore, nicotinamide has provided insight into the mechanism of sirtuin catalysed deacetylation. Nicotinamide and other deacetylase inhibitors could prove to be useful in organisms in which the understanding of the function of acetylation is incomplete.

E. coli metabolism

Glucose Metabolism and the Effects on Coenzyme A Pools

It was recently discovered that the level of protein acetylation is sensitive to the metabolic status of the cell. For instance, acetylation increases in the presence of glucose (36). The addition of glucose in growth media has therefore been a method to enrich for acetylated proteins and may be a useful approach to understand the regulation and effect of acetylation in bacteria. The following section on *E. coli* metabolism will address bacterial glucose metabolism and its effect on the acyl carrier molecule coenzyme A (CoASH).

When bacteria are exposed to multiple carbon sources, the preferred and quickly metabolizable carbon source (like glucose) will be assimilated first. This occurs by repressing the genes that encode enzymes that are required for uptake and metabolism. This phenomenon is called carbon catabolite repression (CCR) and the phosphoenolpyruvate (PEP):carbohydrate phosphotransferase system (PTS) plays a significant role in regulating CCR in both the Gram-negative *Enterobacteriaceae* and the Gram-positive *Firmicutes* (106-108).

The PTS transports and phosphorylates carbon sources using PEP as the phosphoryl group donor. *E. coli* has more than 15 different carbohydrate specific PTSs (107). Each PTS uses a common signal transduction pathway, consisting of two cytoplasmic proteins (enzyme I and histidine phosphocarrier protein HPr) and a carbohydrate specific, membrane-bound protein (enzyme II (EII)), which can be

either one or two proteins. In *E. coli*, the glucose-specific EII consists of a cytoplasmic EIIA(Glc) protein and a two-domain, membrane-bound protein EIIBC(Glc). Transport of glucose occurs via a phosphorylation cascade that proceeds from PEP → enzyme I → HPr → EIIA(Glc) → EIIB(Glc). Phosphorylated EIIB(Glc) phosphorylates glucose as EIIC(Glc) transports it across the membrane. The result is cytoplasmic glucose-6-phosphate.

Glucose-exposed *E. coli* cells inhibit alternative sugar transport systems. The inhibitory mechanism takes advantage of the fact that glucose transport increases the levels of both non-phosphorylated EIIA(Glc) and non-phosphorylated EIICB(Glc). The non-phosphorylated EIIA(Glc) affects the activity of global transcription regulators and inhibits transporters of alternative sugars. Bacterial catabolic enzymes are commonly not synthesized unless the substrate is present; therefore, phosphorylated EIIA(Glc) indirectly decreases transcription of catabolic operons by inhibiting the transportation of their inducers. Non-phophorylated EIICB(Glc) binds and limits a global repressor of sugar metabolism Mlc. The Mlc regulon includes *ptsG*, which encodes EIICB(Glc). Consequently, glucose uptake relieves transcriptional repression of *ptsG.* Additionally, phosphorylated EIIA(Glc) activates adenylate cyclase activity. The result is accumulation of cAMP, which binds to the cAMP receptor protein (CRP, also known as CAP or the catabolite activator protein). The cAMP-CRP complex binds to hundreds of DNA sites within the *E. coli*

chromosome and regulates transcription from hundreds of promoters (109). Therefore, CCR impacts global transcription (107,108).

Under these catabolite repressing or under oxygen limiting conditions, the tricarboxylic acid cycle (TCA) is limited and acetogenesis occurs (108). The mechanism through which CCR limits respiration not completely understood. However, it is known that oxygen limiting conditions can activate the oxygen-sensitive transcription factors ArcA and FNR, repressing the *sdh-suc* operon that encodes three enzymes in the TCA cycle succinate dehydrogenase, succinyl-CoA synthetase complex, and 2-ketoglutarate dehydrogenase. Instead of fully oxidizing AcCoA to carbon dioxide and generating energy, an altered TCA cycle synthesizes succinyl-CoA and 2-ketoglutarate and, thus, functions as a biosynthetic system. Under these conditions, glycolysis and acetogenesis via the phosphotransacetylase (Pta) and acetate kinase (AckA) pathway is critical to supply energy to the cell.

Non-esterified CoASH acts as a monitor, sensing the extracellular and intracellular changes. For example, CoASH is sensitive to environmental stresses, including pH, temperature and osmotic stress. CoASH and AcCoA pools were reduced at pH 9. AcCoA synthesis is high at 40°C, but is not detectable at 50°C (110).

However, CoASH is best known for its capacity to act as an efficient monitor of nutrient status in *E. coli.* Because CoASH functions as an acyl carrier, CoASH is important for many biosynthetic and metabolic pathways; therefore, CoASH and its thioesters are intermediates in many essential metabolic pathways.

According to a sensitive method that can detect various CoA species (111), the concentration of CoASH is tightly regulated and thus maintained within a range of 0.30-0.52 mM (110). This regulation of the intracellular level of CoASH is due to a combination of CoASH degradation (112) and a negative feedback loop on CoASH biosynthesis (113,114). The negative feedback loop involves pantothenate kinase (CoaA), encoded by an essential gene (114). CoaA catalyzes the first step in CoA biosynthesis, a rate-controlling reaction of phosphorylating the vitamin pantothenic acid. This reaction is inhibited by CoASH and its thioester derivatives with CoASH being a stronger inhibitor of pantothenate kinase activity than its esterified derivatives.

The limited pool of CoASH responds quickly to metabolizable carbon sources like glucose; almost 70% of CoASH is acylated to AcCoA within 10 minutes (115). These results are consistent with a previous study in which a mutant strain of *E. coli* was griwb in the presence of the radiolabelled CoASH precursor β-alanine, and determined that glucose-exposed *E. coli* converts the majority of CoASH into AcCoA (80%) and succinyl-CoA (5%), restricting the free CoASH pool (116). CoASH is sensitive to the presence of glucose because the conversion of CoASH to AcCoA saturates at 0.5 mM glucose. When these carbon sources are depleted, AcCoA is quickly deacylated to free CoASH (115).

Therefore, changes in the composition of the CoA pools reflect the metabolic state of the cell. Since the CoASH response to assimilable carbon sources is

predominately conversion to AcCoA, the changes to the AcCoA and CoASH concentrations are inversely related. Chohnan and coworkers thus proposed that the AcCoA-to-CoASH ratio is "an important index of facultative anaerobes that reflects the state of carbon and energy metabolism *in vivo*" (110). Since AcCoA is a conventional acetyl group donor for acetylation, it is possible that manipulating the AcCoA-to-CoASH ratio could alter the acetyl donor pool and, thus, protein acetylation.

The Pta-AckA Pathway and Acetyl Phosphate

Short chain fatty acids (SCFA) are available in high concentrations (70-130 mM) in the human gastrointestinal tract, a region of the body that is colonized by a rich and complex community of bacteria (117,118). Acetate, propionate, and butyrate constitute the dominant SCFA species. Bacteria have evolved mechanisms to scavenge and activate these abundant carbon sources (108,119). Two pathways perform this function: the Pta-AckA pathway and the Acs pathway. This section will discuss the Pta-AckA pathway and focus on its regulation of the metabolic intermediate AcP. The following section will introduce the function and regulation of the Acs pathway.

Pta and AckA, encoded by the *ackA pta* operon, comprise a reversible, low affinity pathway, identified in many bacteria, some archaea and in lower eukaryotes, including fungi, green algae *Chlamydomonas* and water mold *Phytophthora* (120).

Pta interconverts AcCoA and orthophosphate with AcP and CoASH, while AckA interconverts AcP and ADP with excreted acetate and ATP (**Figure 3**).

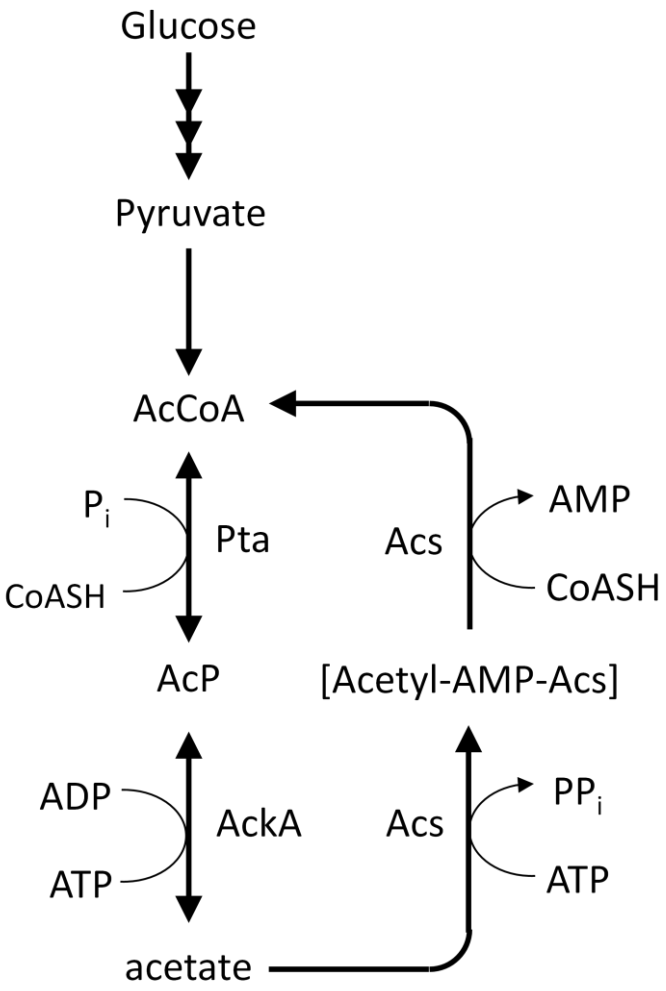

Figure 3. The Pta-AckA and Acs pathways.
Glucose is metabolized to AcCoA. Pta reversibly converts inorganic phosphate and AcCoA to generate AcP and CoASH. AckA reversibly converts AcP and ADP to ATP and excreted acetate. Acs activates acetate to AcCoA by converting acetate and ATP to an Acs-bound acetyl-AMP intermediate that produces AcCoA and AMP in the presence of CoASH.

Pta and AckA have Km values for substrates between 7 and 10 mM (121). Therefore, unless the concentration of environmental acetate is high, such as during high cell density fermentation, the Pta-AckA pathway is predominantly an acetate dissimilation pathway. The Pta-AckA pathway produces or consumes acetate, recycles the limited CoASH, generates ATP, and modulates the metabolites and signaling molecules AcCoA and AcP levels.

AcP is the high-energy intermediate of the pathway. Compared to the $\Delta G°$ of hydrolysis for ATP (-30.5 kJ/mol in complex with Mg^{2+}), AcP stores more energy with a $\Delta G°$ of hydrolysis of -43.3 kJ/mol) (122). AcP can be present at high concentrations in bacteria and is considered a critical signaling molecule. The level of intracellular AcP was estimated to reach between 3 and 4.5 mM in WT cells and 15 mM in the *ackA* mutant during exponential growth (123). AcP is involved in regulating the expression of 100 genes (124) and multiple bacterial phenotypes, including chemotaxis, flagella biosynthesis and capsule production (125), respiratory or fermentative metabolism (126), protein folding and degradation (127), and biofilm formation (124).

Like AcCoA, AcP is regulated by to metabolism. In particular, the intracellular concentration of AcP is influenced by the carbon source. For example, the levels of AcP correlate with the acetogenicity of the carbon source. When *E. coli* grown in minimal growth medium supplemented with the non-acetogenic carbon source glycerol, the level of intracellular AcP was <40 μM. When the carbon source

was the acetogenic glucose or pyruvate, the AcP concentration was 300 μM and 1500 μM, respectively (128). Thus, it is possible that glucose induces protein acetylation due to either an accumulation of the conventional acetyl donor AcCoA and/or AcP.

Function and Regulation of Acetyl Coenzyme A Synthetase

Activation of acetate by Acs is a conserved mechanism found in all three domains. Acs is a high affinity acetate assimilation pathway. Acs has a Km of 200 μM for acetate (129) and is important when cells are grown on low concentrations of acetate (≤2.5 mM) (121). ADP-forming Acs reversibly converts acetate and ATP to ADP, orthophosphate, and AcCoA in one step (**Figure 3**). AMP-forming Acs converts acetate to AcCoA in a two step process. In the first step, acetate is activated to acetyl-AMP. Acs converts acetate and ATP to pyrophosphate and an acetyl-AMP-bound Acs intermediate. The second step converts acetyl-AMP to AcCoA. CoASH and acetyladenylate react to produce AcCoA and AMP (**Figure 3**). Although Acs activity is reversible *in vitro*, pyrophosphatases remove pyrophosphate *in vivo*, a necessary substrate for the acetyladenylate-bound Acs to generate acetate and ATP, and thus their action limits Acs reversibility.

The KDAC CobB directly activates Acs by deacetylating acetylated Acs. On low acetate concentrations, both the *acs* and *cobB* mutants grow poorly. When Acs was purified from the *cobB* mutant, there was reduced AcCoA synthetase activity *in vitro* (130,131). Activity was restored when inactive Acs was incubated with both

purified CobB and NAD^+ (131). These results are consistent with an inactive form of Acs in the absence of CobB deacetylation. Starai and coworkers determined if this inactive form of Acs is acetylated Acs, and found that Acs was acetylated in the *cobB* mutant on one site Lys-609 (131). This acetylation event blocks the first step of acetate assimilation that activates acetate to acetyl-AMP while not affecting the second step, the conversion of acetyl-AMP to AcCoA (131).

A member of the GNAT family of acetyltransferases Pat (protein acetyltransferase) acetylates and inhibits Acs. Starai and Escalante-Semerena discovered Pat through a random transposon mutagenesis of the *cobB pta* double mutant and identified a *pat cobB pta* triple mutant that could grow on low concentrations of acetate (132). Reversible acetylation of Lys-609 of Acs by Pat and CobB was demonstrated: Pat can acetylate Lys-609 of Acs using AcCoA and CobB can deacetylate Pat-acetylated Acs *in vitro*.

Pat consists of two domains, a smaller domain with sequence homology to acetyltransferases and a second domain that is found in NDP-forming acetyl-CoA synthetases. Starai and Escalante-Semerena proposed that Pat homologs evolved from NDP-forming Acs's (132). NDP-forming Acs homologs have a conserved catalytic histidine. The authors suggest that Pat was not able to activate acetate to AcCoA *in vitro* because of the substitution of the conserved catalytic histidine with an asparagine residue in Pat. A thorough analysis of this hypothesis has not yet been performed.

Two-component Signal Tranduction in Bacteria

The focus of my dissertation was to analyze the regulation and effect of acetylation in bacteria. I studied the transcription factor RcsB, a two-component response regulator that has been reported to be reversibly acetylated *in vitro*. This section will introduce the function and regulation of two-component systems (TCSs).

Bacteria coordinate gene transcription in response to a wide spectrum of environmental stimuli. The transcriptional response allows the bacterium to adapt effectively and thus survive external pressures. Stimuli that can affect transcription include pH, temperature, osmotic stress, and nutrition availability. Bacteria organize responses to each of these stimuli, in part, through phosphorylation-dependent signal transduction pathways. These pathways, called two-component systems (TCS), are critical in coupling environmental stimuli to the transcriptional response (133-137).

Most bacterial genomes encode multiple TCSs, which consist of two core signaling transduction proteins (**Figure 4A**): a sensor protein (aka histidine kinase (HK) or sensor kinase (SK)) and a RR (133,134). The *E. coli* genome encodes 62 putative TCS proteins (138), consisting of 30 SKs and 32 RRs. The numbers of hypothetical TCS genes vary amongst bacteria with 366 in *Ktedonobacter racemifer* DSM 44963, 70 in *Bacillus subtilis*, and 0 in *Mycoplasma* (139,140). TCSs appear to be less common in eukaryotes with only a few known examples, including in the

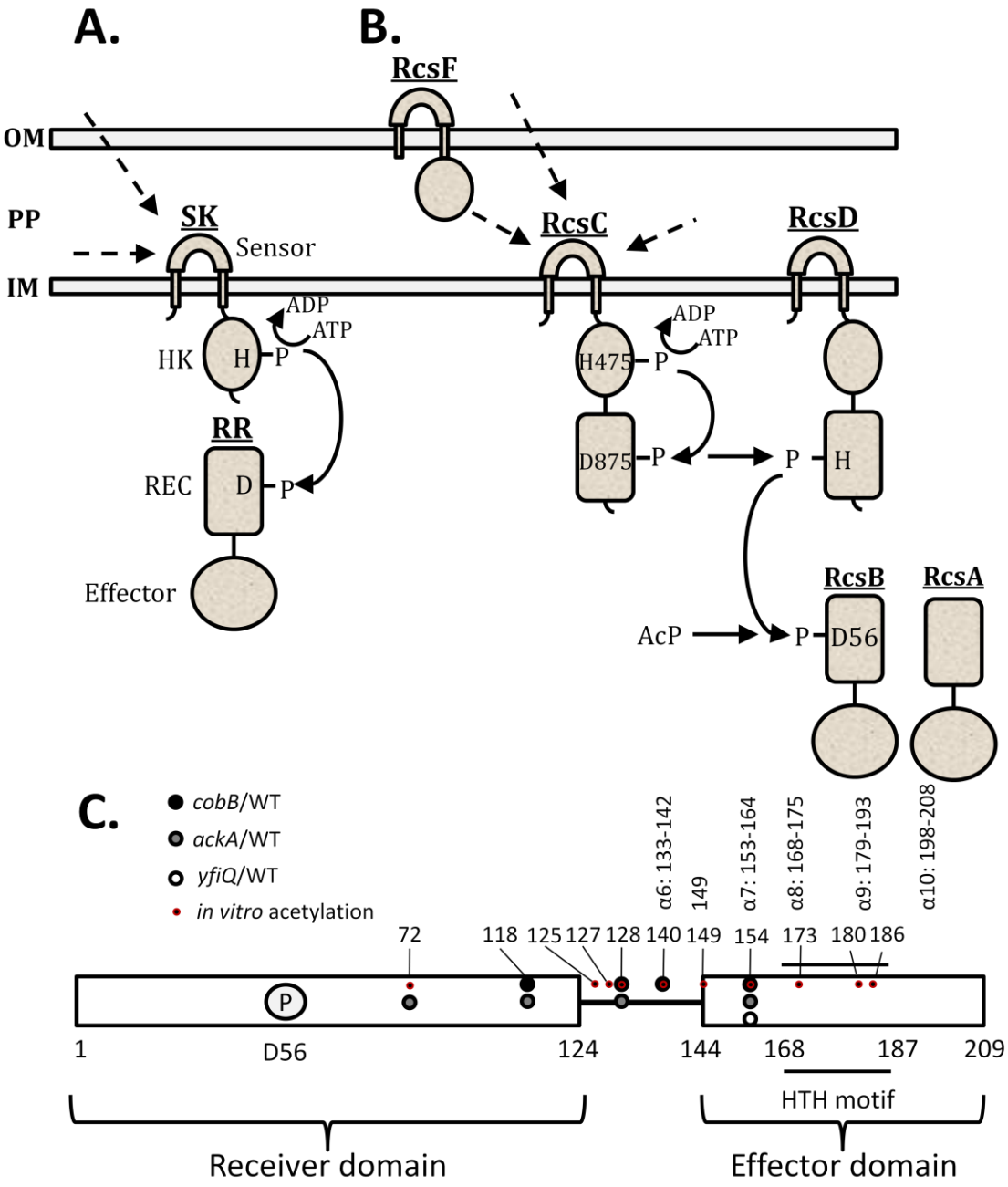

Figure 4. Two component signaling, the Rcs phosphorelay, and the domains of RcsB.

A. Two-component signal transduction. A sensor kinase (SK) can detect cytoplasmic, periplasmic, extracellular signals. The SK autophosphorylates on a conserved

histidine using ATP as a phosphoryl group donor. The response regulator (RR) catalyzes the phosphoryl transfer from the SK onto a conserved aspartate on the receiver domain (REC) of the RR.
B. The Rcs phosphorelay. The hybrid SK RcsC can detect signals and autophosphorylate on a conserved histidine residue using ATP as the phosphoryl group donor. The phosphoryl group is transferred onto an aspartate residue on an attached REC domain. The histidine-containing phosphotransmitter RcsD transfers the phosphoryl group to a conserved aspartate residue on the REC domain of RcsB. Alternatively, acetyl phosphate (AcP) can donate phosphoryl groups to RcsB. RcsB can then homodimerize or heterodimerize with proteins, including the co-activator RcsA.
C. Depiction of RcsB REC and effector domains separated by a linker and the sites that were most acetylated under *in vivo* and *in vitro* conditions. The phosphoryl acceptor site D56 is marked in the REC domain. The numbers below the drawing are based on the domain cut-offs reported in Gottesman, 2005. The rotated numbers above the drawing represent the five alpha helices that were identified by crystallization of the RcsB carboxy terminus by Pristovek *et al.*, 2003. Pristovek reported that α6 is a linker helix, α7 is a supporting helix, α8 is the scaffold helix, α9 is the DNA recognition helix, and α10 may be involved in protein dimerization. The black, grey, and white circles indicate the strain conditions (*cobB*, *ackA*, and *yfiQ*, respectively) under which certain RcsB lysines were more acetylated relative to the level of acetylation in WT cells (Tables 2-4). The sites that were more acetylated from *in vitro* acetylation (with AcCoA alone or with AcCoA + YfiQ) are indicated with red dots (Table 5).

budding yeast *Saccharomyces serevisiae*, the fungus *Candida albicans*, and the plant *Arabidopsis thaliana* (134).

Most, but not all, TCS sensor proteins possess N-terminal transmembrane regions and are, thus, positioned to sense and gather information about the environment while others are cytoplasmic sensor proteins (141). Sensor proteins consist of a conserved kinase core and a variable sensing domain. The sensing domain recognizes specific stimuli and, in response, autophosphorylates at a conserved histidine residue using ATP as the phosphoryl donor.

Autophosphorylation occurs through a bimolecular reaction within sensor kinase homodimers in which each monomer catalyzes the phosphorylation of the conserved histidine on its partner (134). The RR then catalyzes the phosphotransfer reaction from the phosphorylated sensor protein to a conserved aspartate residue on the RR receiver (REC) domain, which can mediate a wide variety of functions.

The interaction between the sensor and the RR is specific. *In vitro* studies of various combinations of sensor proteins and RRs revealed a 1000-fold increase in phosphotransfer between cognate SKs and RRs relative to non-cognate pairs, indicating that SKs possess a strong preference for their partner RR (142). However, 'cross-talk' or signaling between non-cognate sensor proteins and RRs is known to occur in the absence of the cognate histidine kinase.

TCS RRs usually consist of a conserved N-terminal regulatory or REC domain that catalyzes autophosphorylation and a C-terminal effector domain. These domains can interact in diverse ways to regulate the function of the effector (143). The REC domain is composed of a five-stranded parallel β sheet located between two helical components made of two and three helices. This structurally conserved domain contains the conserved aspartic acid that is the site of phosphorylation. The REC domain also contains critical catalytic residues that are important in positioning a divalent metal ion that is necessary for phosphorylation. Finally, this domain contains residues required for auto-dephosphorylation (144).

RRs regulate diverse functions. Through their variable C-terminal effector domains, RRs can regulate diverse functions. The majority of RRs are known or putative transcription factors: 65% of the 9000 RRs from 400 sequenced bacterial and archaeal genomes contain DNA-binding domains (139,143). However, some RRs contain enzymatic (11%), protein binding (2%), or RNA binding domains (1%).

RRs also can autophosphorylate, in the absence of its cognate sensor kinase (123,125,128,145-150). AcP can function as a global signal in bacteria due to its ability to donate phosphoryl groups to certain RRs (128,149,151). The efficiency and kinetics of phosphorylation are different between RRs and the phosphoryl group donors and the stability of phosphorylation can vary between RRs, suggesting that there are differences in catalysis or substrate binding amongst the RRs. For instance, CheY rapidly autophosphorylated with AcP while PhoB did so much more slowly (128).

Phosphotransfer from a sensor protein is more rapid than RR autophosphorylation by AcP and other small molecule phosphodonors. For example, characterizations of the chemotaxis RR CheY with AcP demonstrated that the affinity for AcP is very low ($K_s >> 0.1$ M) and the rate of autophosphorylation does not saturate; therefore, it was proposed that RRs catalyze autophosphorylation and sensor proteins somehow contribute to the rate of catalysis, possibly by increasing the effective concentration of phosphate (152,153). The stability of the

phosphorylated-aspartate residue may be limited by RR auto-dephosphorylation, phosphatase activity of the sensor protein, or a dedicated phosphatase (134).

The phosphorylation of a RR is proposed to induce conformational changes that increase the pool of active RRs (143). Phosphorylation of the REC domain forms a high energy acyl-phosphate bond. The energy stored within this bond is proposed to induce changes in protein conformation. Phosphorylation brings a conserved phenylalanine/tyrosine residue from an outward facing position near the hydrophobic environment of the active site. This change leads to a subtle alteration in the α4-β5-α5 surface of the REC domain. In many TCS, this surface of the REC domain is important in signal transduction by forming homodimers or by interactions with other proteins. Despite the high structural conservation of the REC domain, dimerization via the α4-β5-α5 surface can occur in many ways, depending on the direction and the nature of the secondary structures involved in the interaction.

The role of phosphorylation in activation depends on the RR. Generally, phosphorylation is thought to act as a simple switch to turn on RR activity. However, activation is not necessarily dependent on phosphorylation. Volkman and co-workers in 2001 compared the NMR analyses of an unphosphorylated, inactive NtrC and a carbamoylphosphate-activated NtrC and identified activated NtrC in the unphosphorylated NtrC (154). This finding suggested that RRs are dynamic and may exist in equilibrium between active and inactive states, and phosphorylation that

stabilizes the active conformation, shifting the equilibrium in favor of the activated state.

The Rcs Phosphorelay: A complex TCS

A more complex form of the TCS is the phosphorelay. The flow of phosphoryl groups in the conventional TCS is His→Asp. Phosphorelays transfer phosphoryl groups through the pattern His→Asp→His→Asp, providing more steps to be regulated. In the presence of an activating signal, the SK of a phosphorelay autophosphorylates a conserved histidine residue and then transfers the phosphoryl group to an aspartate residue that is located in a REC domain that may or may not be attached to the SK. The phosphoryl group is then passed to a conserved histidine residue in a domain called a histidine phosphotransferase (HPt). The HPt acts as a phosphorylated intermediate, passing its phosphoryl group to the conserved aspartyl residue in the REC domain of the cognate RR.

One example of a well-studied phosphorelay is the regulator of capsule synthesis (Rcs) phosphorelay (**Figure 4B**). The Rcs phosphorelay is an envelope stress response pathway that can sense extracytoplasmic signals, such as changes in temperature, changes in osmolarity, or peptidoglycan disruption (155,156). The pathway consists of the hybrid SK RcsC, the HPt RcsD, the RR RcsB, the outer membrane lipoprotein RcsF, and the accessory regulator RcsA (156). RcsC is a hybrid protein composed of the SK and the first REC domain. RcsC is proposed to be functionally conserved throughout the Enterobacteriaceae and possesses both

kinase and phosphatase activities to regulate RcsB phosphorylation and dephosphorylation (125,157,158). RcsF-dependent or –independent mechanisms can activate RcsC (157,159,160). RcsC undergoes autophosphorylation on conserved His-475 and transfers the phosphoryl group to conserved Asp-875 on RcsC. Via its conserved histidinyl residue, RcsD shuttles the phosphoryl group from RcsC to conserved Asp-56 on the phosphoreceiver domain of RcsB. Alternatively, RcsB can receive a phosphoryl group from AcP (125) (**Figure 4B**).

RcsB regulates the transcription of 5% of the *E. coli* genome and 20% of the *S. enterica* genome. RcsB can either homodimerize or heterodimerize with other proteins, including RcsA, a RR-like transcription factor that lacks the conserved aspartate. Instead of phosphorylation regulating RcsA activity, the steady state level of RcsA is regulated by the protease Lon under certain growth conditions (156,161-163)

The RcsB homodimer regulation of transcription is best understood at three *E. coli* promoters: *osmCp1*, *rprA*, and *flhDC. osmCp1* is one of two overlapping promoters that encodes the peroxiredoxin OsmC (164-166). The activity of this promoter is regulated by two transcription factors, NhaR and RcsB. Osmotic or membrane stresses activate *osmC* transcription through either NhaR or RcsB, respectively. The *rprA* promoter requires RcsB and encodes a small RNA RprA. RprA activates translation of the stationary phase sigma factor RpoS by disrupting a translation initiation inhibitory stem-loop in the untranslated region of the *rpoS*

mRNA (158,167,168). The *flhDC* promoter encodes the flagellar master regulator, a hexameric transcription factor that controls flagellar gene expression. *flhDC* transcription is controlled by a complex network of several transcription factors that together sense a large variety of environmental signals. One of these transcription factors is RcsB. Upon activation, RcsB represses *flhDC* transcription (163). At the *osmC* and *rprA* promoters, the RcsB homodimer binds a 14-nucleotide sequence adjacent to the -35 region of the promoter. From this position, RcsB likely activates transcription by contacting RNAP. In contrast, RcsB binds about 10 nucleotides downstream of the transcription start site of the *flhDC* promoter (163). From this location, RcsB would be expected to interfere with the binding of RNAP to DNA.

RcsB is a 216 amino acid protein. The REC domain (amino acids 1-124) is separated from the helix-turn-helix (HTH)-containing effector domain (amino acids 144-209) by a linker region (amino acids 125-143) (**Figure 4C**; (156)). The linker provides conformational flexibility and was demonstrated to be involved in RR interdomain signaling (169). A functional analysis of the RcsB linker has not been performed but such an analysis has been done on OmpR and PhoB, representative RRs with a winged HTH-containing effector domain and a structurally conserved RR REC domain. OmpR has a linker length of 15 amino acids and the PhoB linker is 6 amino acids long. An analysis of chimeras that fused OmpR and PhoB REC domains, linkers, and effector domains found that the unstructured linkers are important for

DNA binding, activation of the effector domain in transcription, and conformational changes that mediate interdomain interactions. Such intrinsically unstructured regions are commonly involved in targets for post-translational regulation (170). For example, a recent proteomic analysis in mice revealed of the 500+ phosphorylation sites identified, 86% of the sites were mapped to unstructured regions of proteins (171). Therefore, linkers and unstructured regions of proteins may be critical regulators of protein activity. If the unstructured regions of RcsB and other *E. coli* proteins are enriched for acetylation was unknown.

The effector domain of RcsB binds to DNA through a HTH structure that is typical of the NarL/FixJ and LuxR/UhpA subfamilies of RRs. The crystal structure of the carboxy terminus of RcsB is characteristic for members of these groups (172,173). RcsB has a four helix (α7-α10) effector domain, a helical linker (α6), and a 7-amino acid polypeptide chain. The linker and the chain would connect the REC domain to the effector domain. α8-α9 form the HTH. The scaffolding helix α8 is connected by a sharp turn to α9, the DNA recognition helix. Titration analysis determined that several RcsB residues are involved in RcsA-independent DNA binding to an RcsA-RcsB heterdimer target called an RcsAB box (Lys-154, Val-158, Leu-167, Thr-169, Arg-177, Ser-178, Ile-179, Thr-181, Ile-182). Based on structural homology to a *B. subtilus* sporulation transcriptional regulator GerE (174) and the *Agrobacterium tumefaciens* quorum-sensitive transcriptional regulator TraR (175), the authors proposed that α10 may be involved in dimerization. Suggesting that a

conformational change is necessary for RcsB activation, the α6 linker helix interfered with this putative dimerization helix. α7 is a supporting structure that appears to stabilize several hydrophobic interactions between α7, α8, and α9 and between RcsB and DNA via Lys-154. The involvement of the amino terminus of α7 in secondary interactions with DNA through a basic patch is a common feature of several HTH containing proteins (176). Therefore, there are several critical regulatory regions of RcsB and modifications to these structures may affect its activity.

CHAPTER TWO

MATERIALS AND METHODS

Bacterial strains, bacteriophage, plasmids, and primers.

All bacterial strains, bacteriophage, plasmids, and primers used in this dissertation are listed in **Table 1**. Mutant strains were constructed by generalized transduction with P1kc (for details, see *Generalized P1 transduction*). Construction of monolysogens using λ bacteriophage carrying various transcriptional fusions was performed and verified as described previously (177,178). Plasmid derivatives were constructed either via cloning or by site-directed mutagenesis (for details, see *Plasmid Construction* and *Site-Directed Mutagenesis*).

Culture conditions.

For strain construction, cells were grown in Luria Broth (LB) containing 1% (w/v) tryptone, 0.5% (w/v) yeast extract, and 0.5% (w/v) sodium chloride; LB plates also contained 1.5% agar. For promoter activity assays, cells were grown in either tryptone broth with potassium chloride (TBK, containing 1% (w/v) tryptone and 0.5% (w/v) potassium chloride) or tryptone broth buffered at pH 7 (TB7, containing 1% (w/v) tryptone, no salt, buffered with 100 mM potassium phosphate). For TBK, potassium chloride was used instead of sodium chloride because sodium has a negative effect on the survivability of WT cells at alkaline pH (179). Cell growth was

monitored spectrophotometrically (DU640; Beckman Instruments, Fullerton, CA) by determining the optical density at 600 nm (OD600).

The working concentrations of antibiotics were as follows: ampicillin, 100 μg/mL; kanamycin, 40 μg/mL; spectinomycin 100 μg/mL; tetracycline, 15 μg/mL and chloramphenicol, 25 μg/mL or 17.5 μg/mL. Stock solutions were typically prepared at 1000 times the working concentration. Stock solutions of ampicillin, kanamycin and spectinomycin were dissolved in water and filter sterilized. Optimally, the filter has been pre-rinsed with water before sterilizing the antibiotic solution because *E. coli* can grow on the filtrate, suggesting the presence of some carbon source that primes the filter (Marvin Whitely from The University of Texas at Austin, personal communication, October 11, 2012). Stock solutions of tetracycline and chloramphenicol were dissolved in 50% and 100% ethanol, respectively, and filter sterilized. All antibiotic stocks were stored at -20°C. When necessary, isopropyl β-D-1-thiogalatopyranoside (IPTG) was added to the media at the indicated concentration to induce gene expression from a plasmid vector.

Generalized P1 transduction.

A single colony was inoculated in LB and grown overnight at 37°C aerobically with agitation at 250 RPM. In the morning, 50 μL of overnight culture were added to 5 mL of TB for transduction (TBT) (TB containing 0.2% [w/v] glucose from a 20% [w/v] stock solution, 10 mM $CaCl_2$, 10 mM $MgSO_4$, and 0.4 mM $FeCl_3$). The culture was grown until it reached an OD600 of approximately 0.5. One mL of cells was infected

with 10-100 µL of phage lysate and incubated statically at 37°C for 30 minutes. After incubation, 200 µL of 1M sodium citrate (pH 5.5) was added to prevent a second round of phage absorption. The cells were pelleted using a table-top centrifuge at 16000 RCF for 1 minute at room temperature. The supernatant was decanted and the pellet resuspended with 500 µL LB and 200 µL 1M sodium citrate. The cells were then incubated aerobically at 37°C with agitation at 250 RMP for 70 minutes to give them time to develop antibiotic resistance. After the second round of incubation, the cells were pelleted as described before. The supernatant was decanted and the pellet was resuspended with 50 µL 1 M sodium citrate. The entire cell suspension was plated onto LB agar plates with appropriate antibiotics required for the desired selection.

Plasmid construction.

Plasmid pPHB1 was constructed by Shaun R. Brismaide (UW-Madison) as follows. Alleles *phbCAB*$^{+}$ were amplified from *Ralstonia solanacearum* strain GMI1000 (a gift from Caitilyn Alen, UW-Madison) using forward primer 5'—ATC GAA CCC GGG ATG GCA TCG CGT CAC AA—3' and reverse primer 5'—AGC ATG AGT GCC CCG GGT CAG CCC ATG T—3'. Bases underlined indicate the *Sma*I restriction site engineered into each primer. The resulting ~4-kb fragment was A-tailed and gel-purified using the QIAquick® gel extraction kit (Qiagen). This product was ligated into the multiple cloning site of plasmid pGEM-T-Easy (Promega). The resulting plasmid was ~7-kb and was named pPHB1.

Plasmid pPHB3 was constructed by Shaun R. Brismaide (UW-Madison) as follows. The *Rs phbCAB*$^{+}$ genes were cut out of pPHB1 using *Sma*I. The resulting ~4-kb fragment was gel-extracted and ligated into plasmid pTAC-85 (180) that had been cut with *Nco*I and the resulting single-stranded DNA overhangs blunted with mung bean nuclease and dephosphorylated using shrimp alkaline phosphatase. The resulting plasmid was ~9.1-kb and was named pPHB3.

Plasmid pLIH002. To construct a single copy plasmid that permits expression of moderate amounts of WT RcsB, we constructed a derivative of CopyControl™ pCC1™ (EpiCentre) that carries the WT *rcsB* allele. We began with pVEC, a derivative of pCC1™, in which the plasmid-encoded *lacZα* is disrupted by an approximately 1360-bp kanamycin resistance cassette (**Table 1**, (181)). To replace the kanamycin resistance cassette with the WT *rcsB* allele, we first constructed a derivative of pVEC that lacked the kanamycin cassette. pVEC was BamHI-digested, ligated, transformed into TransforMax™ EPI300™-T1^{R} Chemically Competent E. coli (EpiCentre^{R}), and plated onto an LB plate containing chloramphenicol (17 μg/ml) and 5-bromo-4-chloro-indolyl-β-D-galactopyranoside (X-gal). A blue transformant was verified and designated pLIH001 (**Table 1**). We then amplified the WT *rcsB* allele from the chromosome of strain AJW3759 (**Table 1**), using primers rcsBFBamHI (5'-GGATCCAGGAAGGTAGCCTATTACATGAAC-3') and rcsBRBamHI (5'- GGATCCTTAGTCTTTATCTGCCGGACTTAAGG-3'). The resulting amplicon was purified using the CloneJET™ PCR Purification Kit (Thermo Scientific)

and cloned into pJET1.2 using the CloneJET™ PCR Cloning Kit (Thermo Scientific). The ligated product was transformed into competent DH5α and plated onto LB ampicillin plates. WT *rcsB* allele was excised from pJET1.2 with BamHI, gel extracted, subcloned into BamHI-digested pLIH001, transformed into EPI300 cells, and plated onto LB plates containing chloramphenicol and X-gal. White colonies were used to inoculate LB supplemented with chloramphenicol (17 μg/ml) to maintain the plasmid and CopyControl™ BAC Autoinduction Solution (EpiCentre®) to amplify the plasmid and shaken overnight at 37°C. Plasmid DNA was purified and sequenced using primer pCC1RBZ (5'- GTAAAACGACGGCCAGTGAATTG-3'). The resulting plasmid was named pLIH002. For experiments that involved pLIH002 or derivatives, pVEC functioned as the negative control.

Site Directed Mutagenesis.

Site-directed mutagenesis of *rcsB* in pLIH002 was conducted using QuikChange® Lightning Multi Site-Directed Mutagenesis Kit (Agilent Technologies) in accordance with the manufacturer's instructions using the mutagenic primers listed in **Table 1**. The mutations were confirmed by sequence analysis of the purified mutagenized plasmids.

Transformation.

Three distinct transformation methods were used: transformation buffers (TBF), transformation storage solution (TSS), and electroporation.

TBF – 50 µL of an overnight culture of the recipient cells was diluted into 5 mL of LB. The culture was incubated with aeration rotating at 250 RPM at 37°C until OD600 reached 0.4-0.6. 1 mL of the culture was chilled on ice and then pelleted at 4°C for 1 minute at 16000 RCF using a tabletop centrifuge. The pellet was resuspended with 400 µL of ice cold TBF1 and pelleted. The pellet was resuspended with 40 µL of ice cold TBF2. 0.5 - 3 µL of plasmid DNA was mixed with the chemically competent cells and incubated on ice for 30 minutes. The DNA-cell mixture was heat shocked for 1 minute at 42°C and immediately placed on ice for 2 minutes. 300 µL of room temperature LB was added to the DNA-cell mixture. The cells were incubated at room temperature or 37°C, rotating at 250 rpm for 30 minutes to 1 hour. After incubation, typically 50 – 100 µL of cells were plated onto LB agar plates containing the appropriate concentration of antibiotic required for selection of transformants. For poor efficiency transformations, the entire 300 µL of cells was pelleted, resuspended with 50 µL of LB, and plated onto LB plates containing the appropriate antibiotic. Outgrowth was often, but not always, carried out overnight at 37°C.

TSS – 1 ml of overnight cell culture was pelleted at room temperature for 1 minute at 16000 RCF using a tabletop centrifuge. The pellet was resuspended with 100 µl TSS [10% (w/v) poly(ethylene glycol), 5% (v/v) DMSO and 50 mM $MgSO_4$ or $MgCl_2$ in LB]. After resuspension, 50 ng of plasmid DNA was added to the resuspended cells, the mixture was incubated on ice for 30 minutes. After ice

incubation, 0.9 mL of LB was added, and the cells were incubated for 1 hour at 37°C with aeration. After 37°C incubation, the cells were pelleted one more time as described above, the supernatant was decanted, and the cells were resuspended in 250 µL LB. 25-100 µl of the resuspended cells were used for plating on an LB agar plate containing the appropriate antibiotic for selection.

Electroporation - For electroporation, the recipient cells were made competent by inoculating 30 mL of LB in a 250 mL baffled flask with 500 µL of overnight culture. The culture was incubated with aeration rotating at 250 RPM at 37°C until OD600 reached 0.4-0.6. The culture was transferred into Oakridge tubes and spun down at 14000 RCF for 15 minutes at 4°C. After pelleting the cells, the supernatant was aspirated, and the cell pellet was gently resuspended with 1 mL of ice-cold sterile water. After resuspension, an additional 9 mL of ice cold water was added to the tube, bringing the total volume to 10 mL and the cells were spun one more time at 14000 RCF for 15 minutes at 4°C. At the end of the second spin, the supernatant was gently decanted immediately, as the pellet is not very compact and stable at this point. The pellet then was resuspended one more time with 1 mL of ice cold water, transferred to a 1.5 mL eppendorf tube, and spun down at 16000 RCF for 1 minute, using a table top centrifuge at 4°C. The supernatant was aspirated, the pellet was resuspended with 200 µl of ice cold water, divided into 50 µl aliquots and stored at -80°C for future use.

Transformation began by mixing 50 ng of purified plasmid DNA with 50 µL of electro-competent cells. The DNA-cell mixture was then transferred to a chilled 1 mm electroporation cuvette and electroporated at 1.8 KV. After electroporation, the cells were immediately rescued by the addition of 1 mL of room temperature LB, transferred to a small test tube or 1.5 mL eppendorf tube, and incubated at 37°C, rotating at 250 RPM for 30 minutes to 1 hour. After incubation, 20-100 µL of cells were plated onto LB agar plates containing the appropriate concentration of antibiotic required for selection of transformants. Outgrowth was often, but not always, carried out overnight at 37°C.

Promoter activity assays.

To monitor promoter activity from λ(*PrprA-lacZ*), λ(*PosmC-lacZ*), λ(*PflhDC-lacZ*), or λ(*PosmB-lacZ*)cells that were frozen at -80°C were grown on LB plates containing the appropriate concentration of antibiotic and incubated at 37°C overnight. Three independent colonies representing three biological replicates were used to inoculate 5 mL of TB unbuffered (TB) or TB that was buffered at pH 7.0 (TB7) and grown aerobically with agitation at 250 rpm at 37°C. The overnight cultures were diluted into 20 – 25 mL of TB or TB7 in 250 mL flasks to final OD600 of 0.03 – 0.05. At regular intervals, 50 µL aliquots were harvested and added to 50 µL of All-in-One β-galactosidase reagent (Pierce Biochemical). β -galactosidase activity was determined quantitatively Y-PER β-galactosidase assay kit (Pierce Biochemical), using a microtiter format. Three microtiter wells containing 50 µL of

TB or TB7 and 50 µL of All-in-One β-galactosidase reagent (Pierce Biochemical) was included on each microtiter plate as a negative control. The microtiter plates were incubated at 37°C until a light yellow color was visible. Promoter activity was plotted versus time or OD600. For some experiments, only the peak activity is shown. Each experiment included three independent measurements and was repeated at least once.

Hydroxylamine assay to measure AcP.

A standard curve was constructed by diluting known concentrations of AcP in *in vitro* acetylation buffer (150 mM Tris-HCl pH 7.3, 10mM $MgCl_2$, 150 mM NaCl, and 10% glycerol) to a final volume of 300 µl per reaction. 50 µl of neutralized hydroxylamine HCl solution (2M Hydroxylamine HCl neutralized with KOH pellets can be stored at room temperature for ~30 days or 4°C for ~90 days) was added and incubated at 60°C for 5 minutes. 100 µl of development solution (50:50 FeCl3/HCl:TCA = 0.5 M FeCl3 in 5 M HCl + 30% TCA) was added and immediately, color change is visible. The reactions were transfered into plastic cuvettes, bubbles were removed because they seemed to affect the readings, and the reactions were analyzed at 540 nm using a spectrophotometer. Absorbance was compared to the known AcP concentration. Readings from experimental samples were compared to the standard curve to extrapolate the concentration of AcP in the experimental samples. This protocol was based on a published method to measure AcP (182).

Nile Red.

Nile Red was used to detect the production and accumulation of polyhydroxybutyrate (PHB) on LB agar plates by *E. coli* cells carrying plasmid p*PHB3*. p*PHB3* carries three genes (*phbCAB*) under the control of an IPTG-inducible promoter and confers ampicillin resistance. A single colony was streaked onto LB agar plate containing 25 μg/ml Nile Red, 50 μM IPTG, and 25 μg/ml ampicillin. The plates were incubated overnight at 37°C. After incubation, PHB accumulation was detected by exposing the plates to ultraviolet light (λ=312 nm).

LTQ-Orbitrap Velos-LC-MS/MS Spectrometry and Protein Identification.

For identification of *in vivo* acetylation sites, cells transformed with pHis6*rcsB* (which expresses His-tagged RcsB) were grown aerobically at 37°C at 250 rpm in TB7 until stationary phase and cell lysates were prepared. For identification of *in vitro* acetylation sites, His-tagged RcsB and YfiQ proteins were purified from *E. coli* cells (see below). The proteins in the *in vivo* and *in vitro* samples were separated by SDS-polyacrylamide gel electrophoresis. To normalize the number of cells to lyse per milliliter, the inverse of the culture A_{600} was used (183). To avoid cross-contamination, we electrophoresed the samples from each strain and/or condition on separate SDS-polyacrylamide gels with bioreplicates separated by an empty lane(s). Electrophoresis was terminated before proteins could run off the bottom of the gel. The gel was cut down the middle of the empty lane to separate the bioreplicates. Each half of the gel was stained with SimplyBlue™ SafeStain

(Invitrogen) and destained with water. The bands were then excised and subjected to tryptic digestion, as described previously (184). Peptides eluted from tryptic digests of gel pieces were subjected to reversed phase column chromatography (self-packed C18 column, 100 μm diameter x 200 mm length) operated on an Easy-nLC II (Thermo Fisher Scientific, Waltham, MA). Elution was performed using a binary gradient of buffer A (0.1% (v/v) acetic acid) and buffer B (99.9 % (v/v) acetonitrile; 0.1% (v/v) acetic acid) over a period of 100 min with a flow rate of 300 nl/min. MS and MS/MS data were acquired with the LTQ-Orbitrap-Velos mass spectrometer (Thermo Fisher Scientific) equipped with a nanoelectrospray ion source. The Orbitrap Velos was operated in data-dependent MS/MS mode using the lock-mass option for real time recalibration. After a survey scan in the Orbitrap (r = 30,000), MS/MS data were recorded for the 20 most intensive precursor ions in the linear ion trap. For MS/MS analysis, singly charged ions were not taken into account.

Post-translational lysine acetylation sites on proteins were identified by searching all MS/MS spectra in .dta format against an *E. coli* database (extracted from the Uniprot-KB database: http://www.uniprot.org/uniprot/?query=Escherichia+coli+K12&sort=score), using **Sorcerer™-SEQUEST®** (Sequest v. 2.7 rev. 11, Thermo Electron including Scaffold_3_00_05, Proteome Software Inc., Portland, OR). The Sequest search was carried out considering the following parameters: a parent ion mass tolerance - 10 ppm, fragment ion mass tolerance of 1.00 Da. Up to two tryptic mis-cleavages were

allowed. Methionine oxidation (+15.99492 Da), cysteine carbamidomethylation (+57,021465 Da) and lysine acetylation (+42.010571 Da) were set as variable modifications. Proteins were identified by at least two peptides applying a stringent SEQUEST filter. Sequest identifications required deltaCn scores of greater than 0.10 and XCorr scores of greater than 2.2, 3.3 and 3.8 for doubly, triply and quadruply charged peptides. Acetylated peptides that passed these filter criteria were examined manually and accepted only when b- or y- ions confirmed the acetylation site.

Cloning, Recombinant Expression, and Purification.

For *in vitro* studies, we transformed the chloramphenicol resistant ASKA plasmids that encode YfiQ or RcsB with a noncleavable N-terminal polyhistidine tag (185) into kanamycin resistant BL21 Magic cells (186). The ASKA-encoded, polyhistidine tagged protein was expressed in the presence of 34 μg/ml chloramphenicol and 35 μg/ml kanamycin and purified with IMAC followed by size exclusion chromatography as described (Kuhn *et al*., submitted, (187)).

Dynamic light scattering.

For characterization of molecular size in solution, dynamic light scattering (DLS) provides a measure of the translational diffusion coefficient of protein in solution. All DLS measurements were performed on a Zetasizer Nano-S Zen 1600 DLS instrument with a 633 nm wavelength laser. The fluctuations in light intensity, due to the Brownian motion of the molecules, were measured by a photodiode at a 90°

angle. Photons were counted and the time dependence of the light intensity fluctuations was analyzed by autocorrelation. Assumptions include a solution viscosity equal to 1.019 and that the proteins are spherical in nature. The proteins were centrifuged for 5 min with 14,000 x g prior to collecting scattering data. Experiments were run at 25°C and at least 6 measurements were taken at each condition. Regularization histogram analyses of samples were carried out using the Zetasizer Nano software.

In vitro acetylation.

In vitro acetylation of proteins was conducted with two distinct acetyl donors: acetyl-CoA (AcCoA) and acetylphosphate (AcP).

AcCoA. Two different methods were used to detect *in vitro* acetylated proteins using AcCoA as the acetyl group donor: detection by anti-acetylated lysine western immunoblot and detection of AcCoA hydrolysis.

In vitro *acetylation followed by anti-acetyllysine Western immunoblot*.

20 μM RcsB, 2 μM YfiQ, and 0.4 mM AcCoA were incubated at 37°C for 1 hour in 50 mM Tris HCl (pH 8), 10% glycerol, 1 mM DTT, 10 mM sodium butyrate, and 0.1 mM EDTA (36). The reaction was stopped by the addition of equal volume of 2X SDS loading buffer (120 mM Tris-Cl [pH 6.8], 4% SDS, 0.2% bromophenol blue, 20% glycerol and 10% 2-Mercaptoethanol, which was added immediately prior to use). The EDTA was left out when *in vitro* acetylation preceded phosphorylation, because

EDTA chelates the zinc needed to perform Phos-Tag™ SDS-PAGE. The samples were heated at 95°C for 2 minutes, resolved using a 12% acrylamide SDS-PAGE gel, and subject to an anti-acetylated lysine western immunoblot.

In vitro *acetylation followed by measurement of AcCoA hydrolysis.*

Compared to the *in vitro* acetylation assay described previously (36), this biochemical *in vitro* assay detects acetylation by measuring the hydrolysis of AcCoA. Biochemical assays were performed as described previously (188) with some modifications. First, reactions were performed in the presence of 150 mM NaCl at 25°C for 1 hr to prevent protein precipitation during the reaction. Additionally, after stopping the reactions with guanidine HCl, samples were transferred to Nanosep 10K MWCO centrifugation devices (Pall Life Sciences, VWR) and centrifuged at 13,000 rpm for 10 minutes to separate CoA and the protein. The Ellman's reagent was then added to the flow-through and monitored as described (188). This biochemical *in vitro* acetylation assay was performed in the absence of DTT because it generates false positive signals. Reactions reached completion within one hour, and a saturating concentration of RcsB was determined to be 0.15 mM. High concentrations of YfiQ (100 μg) were necessary to detect activity. Several possibilities exist, including competition for binding between AcCoA and the polyhistidine tag (188).

AcP. *In vitro* acetylation of purified LpdA with AcP was carried out by mixing 1.25 μM LpdA peak 1 with AcP at concentrations ranging from 0-80 mM in buffer

containing 150 mM Tris-HCl pH ranging from 7.1 – 8.0, 10mM $MgCl_2$, 150 mM NaCl, and 10% glycerol. The reaction was incubated at 37°C for 0 to 7 hours. The reaction was stopped by the addition of 2X SDS loading buffer. Protein acetylation by AcP was detected by Western immunoblot analysis using an antibody against acetylated lysine (Cell Signaling) at a ratio of 1:1000.

In vitro phosphorylation.

In vitro phosphorylation was carried out by incubating lithium potassium AcP (Sigma) with purified His-tagged RcsB at 30°C for 30 min in buffer containing 40 mM Tris-HCl pH 8.0, 10 mM $MgCl_2$, 40 mM KCl and 1 mM DTT (48). The reaction was quenched by the addition of SDS loading buffer.

Detection of phosphorylated RcsB.

Similar to a previously reported procedure (48), phosphorylated RcsB from *in vitro* phosphorylation was separated from non-phosphorylated RcsB using zinc(II) Phos-Tag™ SDS-PAGE (10% acrylamide (37.5:1), 350 mM Tris, pH 6.8, 0.1% SDS, 75 μM Phos-Tag (NARD Institute LTD), and 150 μM $Zn(NO_3)_2$). Purified protein was detected either by staining the gel with SimplyBlue™ (Invitrogen) or by Western immunoblot analysis. If the protein was detected by Western immunoblot analysis, the gel is incubated at room temperature with gentle shaking for 15 minutes in Towbin buffer (50 mM tris and 40 mM glycine) containing 1 mM EDTA to chelate the zinc and then for another 15 minutes in only Towbin buffer prior to transfer of the proteins onto a membrane.

Western immunoblot analysis.

The protein samples were resolved by electrophoresis on a SDS-PAGE 10%, 12%, or 15% polyacrylamide gel. The gel and PVDF or nitrocellulose membrane were equilibrated in transfer buffer for 15 minutes at room temperature with shaking. The proteins were transferred to the membrane either at 25 V for 16 hours at 4°C or using TurboTransfer at 25V for 30 minutes at room temperature. The membrane was blocked for 1 hour with 5% milk in Phosphate-buffered saline with Tween-20 (PBS/T: 0.136 M NaCl, 2.7 mM KCl, 10 mM Na_2HPO_4, 1.7 mM KH_2PO_4, 0.05% Tween) or Tris-buffered saline with Tween-20 (TBS/T: 20 mM Tris base, 0.136 M NaCl, 0.1% Tween) at room temperature with gentle shaking. The membrane was briefly washed with PBS/T or TBS/T prior to incubation with the primary antibody.

The conditions used for primary antibody incubation varied depending on whether acetylation, RcsB protein, or His-tagged fusion proteins were detected. Acetylation was detected by incubating the membrane with anti-acetyllysine primary antibody (Cell Signaling Technology® #9441L) diluted 1:1000 in 5% BSA (w/v) TBS/T solution.. Detection of RcsB protein occurred by incubating the membrane with rabbit anti-RcsB antibody (Jorge Escalante-Semerena, UW-Madison) diluted 1:10,000 in 5% milk (w/v) PBS/T solution for 3 hours at room temperature with gentle shaking. The histidine tag was detected by incubating the membrane with 5 µg HRP-conjugated anti-His6 antibody (GenScript A00612) per 1 ml of PBS/T for 1 hour at room temperature with gentle shaking. The membrane

was washed three times, 5 minutes each, with PBS/T or TBS/T at room temperature with gentle shaking. Secondary goat anti-rabbit (Cell Signaling Technology®) immunoglobulin G antibody conjugated to horseradish peroxidase diluted 1:1000 dilution in 5% milk (w/v) PBS/T was used for 1 hour at room temperature with gentle shaking. The membrane was again washed three times. Enhanced chemiluminescence Western immunoblotting reagents (Cell Signaling Technology®) were used for visualization, according to the manufacturer's instructions.

When necessary, the membrane was stripped with OneMinute® Western Blot Stripping Buffer (GM Biosciences), according to the manufacturer's instructions.

Motility assays.

Three independent colonies representing three biological replicates were used to inoculate 5 mL of TB and grown aerobically at 250 rpm at room temperature. The overnight cultures were diluted into 5-8 mL of TB in test tubes to final OD600 of 0.1. 5 µl was inoculated on the surface of tryptone motility plates [TB supplemented with 0.25% (w/v) agar] and incubated at 28°C and the diameter was measured over time. Each experiment included at least three replicates and was repeated at least once.

Table 1. Bacterial strains, bacteriophage, plasmids, and primers used in this study.

Strain, phage, plasmid, or primer	Relevant Characteristic	Source/Reference
Strains		
BW25113	F- λ- Δ(*araD-araB*)567 Δ(*rhaD-rhaB*)*568* Δ*lacZ4787 rrnB3 rph-1 hsdR514*	(189)
AJW678	*thi-1 thr-1*(Am) *leuB6 metF159*(Am) *rpsL136* Δ*lacX74*	(190)
AJW3759	BW25113 λΦ(P*rprA142-lacZ*)	λ: λ*rprA142* → BW25113
AJW2628	BW25113 λΦ(P*osmC-lacZ*)	λ: λ*osmC* → BW25113
AJW2634	BW25113 λΦ(P*osmB-lacZ*)	λ: λ*osmB* → BW25113
AJW2640	BW25113 λΦ(P*flhD4-lacZ*)	λ: λ*flhD4* → BW25113
AJW3331	AJW678 λΦ(P*rprA142-lacZ*)	λ: λ*rprA142* → AJW678
AJW4884	AJW3759 Δ*rcsB*::*FRT*	P1: JW2205 (191) → AJW3759, then removed antibiotic marker
AJW3976	AJW3759 Δ*rcsC*::*tet*	P1: MZ63 (192) → AJW3759
AJW3981	AJW3759 Δ*ackA*::*FRT-kan-FRT*	P1: JW2293 (191) → AJW3759
AJW4533	AJW3759 Δ*speE*::*FRT*	P1: JW0117 (191) → AJW3759
AJW4589	AJW3759 Δ*speG*::*FRT*	P1: JW1576 (191) → AJW3759
AJW4592	AJW3759 Δ*speG*::*FRT* Δ*speE*::*FRT-kan-FRT*	P1: JW0117 (191) → AJW4589
JE8659	Δ*cobB*::*cat*	Escalante-Semerena (U. of Georgia)
AJW5011	AJW3759 Δ*cobB*::*cat*	P1: JE8659 → AJW3759
AJW3797	AJW3759 Δ*yfiQ*:: *FRT-kan-FRT*	P1: JW2568 (191) → AJW3759
EPI300TM-T1R	*F– mcrA Δ(mrr-hsdRMS-mcrBC) φ80dlacZΔM15lacX74 recA1 endA1 araD139 (ara-leu)7697 galU galK rpsL nupG trfA tonA dhfr*	Epicentre® Biotechnologies
BL21 (DE3) Magic	a derivative of BL21 cells carrying a plasmid encoding rare tRNAs	(186)

Phages		
λ*rprA142*	142 bp *rprA* promoter region transcriptionally fused to *lacZ*	(158)
λ*flhD4*	*flhD* promoter region (-1057 to +34) transcriptionally fused to *lacZ*	(163)
λ*osmC*	*osmC* promoter region (-95 to +420) transcriptionally fused to *lacZ*	(193)
λ*osmB*	465 bp *osmB* promoter region, includes *osmBp1* and *osmBp2*, transcriptionally fused to *lacZ*	(194)
Plasmids		
pVEC	Single-copy, *lacZ* null derivative of pCC1 (Epicentre^R), control for pLIH002 and pLIH003 Cm^R	(181)
pLIH001	pVEC derivative with kanamycin cassette removed	This study
pLIH002	pLIH001 carrying *rcsB*(WT) Cm^R	This study
pLIH003	pLIH001 carrying *rcsBD56A* allele Cm^R	This study
pLIH004	pLIH001 carrying *rcsBK154Q* allele Cm^R	This study
pLIH005	pLIH001 carrying *rcsBK154R* allele Cm^R	This study
pLIH006	pLIH001 carrying *rcsBK154A* allele Cm^R	This study
pTrc99a	Vector control for pPSG980 Ap^R	(195)
pPSG980	pTrc99a carrying Φ(P*lac*UV5–*rcsC*) Ap^R	(196,197)
pMH300	pTrc99a carrying Φ(P*lac*UV5–*rcsF*) Ap^R	(157)
pREII-*rpoA*	Expresses WT *rpoA* or Lys-to-Ala substitutions of RpoA Ap^R	(198)
pREII-ΔαCTD	Expresses the amino terminus of RpoA Ap^R	R. Gourse (U. of Wisconsin-Madison)
pTAC-85	Vector control for pPHB3 Ap^R	J. Escalante-Semerena (U. of Georgia)
pPHB3	pTAC-85 expressing 3 genes (*phbCAB*) from an IPTG-inducible	J. Escalante-Semerena (U. of

	promoter Ap^R	Georgia)
pCA24n	Control plasmid Cm^R	(185)
pCA24n-*rcsB*	pCA24n expressing 6xHis-RcsB from an IPTG-inducible promoter Cm^R	(185)
pCA24n-*coaA*	pCA24n expressing 6xHis-CoaA from an IPTG-inducible promoter Cm^R	(185)
pCA24n-*speG*	pCA24n expressing 6xHis-SpeG from an IPTG-inducible promoter Cm^R	(185)
pHis6*rcsB*	pIM10 vector expressing 6xHis-RcsB from an IPTG-inducible promoter, Kn^R Sp^R	(199)
Primers (5'-3')		
rcsBFBamHI	GGATCCAGGAAGGTAGCCTATTACATGAAC	This study
rcsBRBamHI	GGATCCTTAGTCTTTATCTGCCGGACTTAAGG	This study
pCC1RBZ	GTAAAACGACGGCCAGTGAATTG	This study
rcsBK154Q	ACAAGCGTCTCTCGCCACAGGAGAGTGAAGTTCTGCG, AAA→CAG	This study
rcsBK154A	TGACAAGCGTCTCTCGCCAGCAGAGAGTGAAGTTCTGC, AAA→GCA	This study
rcsBK154R	ACAAGCGTCTCTCGCCAAGAGAGAGTGAAGTTCTG, AAA→AGA	This study
rcsBD56A	CATGTGTTGATTACCGCTCTCTCCATGCCTGGC, GAT→GCT	This study

CHAPTER THREE

RESULTS

Analysis of the RcsB-regulated *osmC* promoter

Introduction

Previous studies established that activity of the *E. coli* RR RcsB could be regulated by phosphorylation (156,200) and, more recently, by acetylation (49). Biochemical evidence suggests that the KAT YfiQ can acetylate RcsB in the presence of the acetyl group donor AcCoA (49). Despite this finding, however, there is no evidence that acetylation of RcsB occurs *in vivo*. Equipped with RcsB-regulated promoters transcriptionally fused to *lacZ* and the means to genetically manipulate *in vivo* protein acetylation levels and the AcCoA-to-CoA ratio, I tested my hypothesis that acetylation can regulate RcsB activity *in vivo.* I first identified RcsB-regulated phenotypes that appear to be regulated by acetylation and then analyzed the mechanism.

Promoter screen for putative regulation by acetylation

There is evidence to support the hypothesis that glucose metabolism regulates protein acetylation in bacteria. This includes the observations that *E. coli* cells exposed to glucose rapidly increase intracellular concentrations of AcP (123) and AcCoA (110), and that both AcP (201,202) and AcCoA (132,203-205) could be

acetyl group donors for protein acetylation. Furthermore, exposure to glucose is reported to increase acetylation of RNA polymerase in *E. coli* (47,48) and global protein acetylation in *Salmonella enterica* (36).

We therefore reasoned that growth of *E. coli* in the presence of glucose might induce an acetylated RcsB-regulated phenotype. Given that RcsB is a transcription factor that regulates approximately 5% of the *E. coli* genome (156,206) and 20% of the *Salmonella enterica* genome (207), we screened several RcsB-regulated promoters for their response to glucose. To do so, I introduced λ hybrids carrying these promoters transcriptionally fused to *lacZ* into the λ attachment site of strain BW25113, a commonly used *E. coli* reference strain that is deleted for the endogenous *lacZ* gene (178). By colony PCR, I verified that the resultant lysogens were present in single copy (177). I grew these lysogens at 37°C in 1% tryptone buffered at pH 7 with 0.1 M potassium phosphate buffer (TB7) with or without 0.4% (w/v) glucose (22 mM). At regular intervals, samples were harvested for analysis of growth (monitored as optical density at 630 nM; OD_{630}) and promoter activity (monitored in terms of β-galactosidase activity in Miller units). When grown in TB7 supplemented with glucose (closed symbols), cells of the BW25113 reference strain (herein called wild-type, WT) appeared to grow better than cells grown in the absence of glucose (open symbols) (**Figure 5A**). In the absence of glucose, all reporter strains showed a similar low level of promoter activity as they transitioned into stationary phase (i.e., between 300 and 400 minutes (**Figure 5B and 5C**).

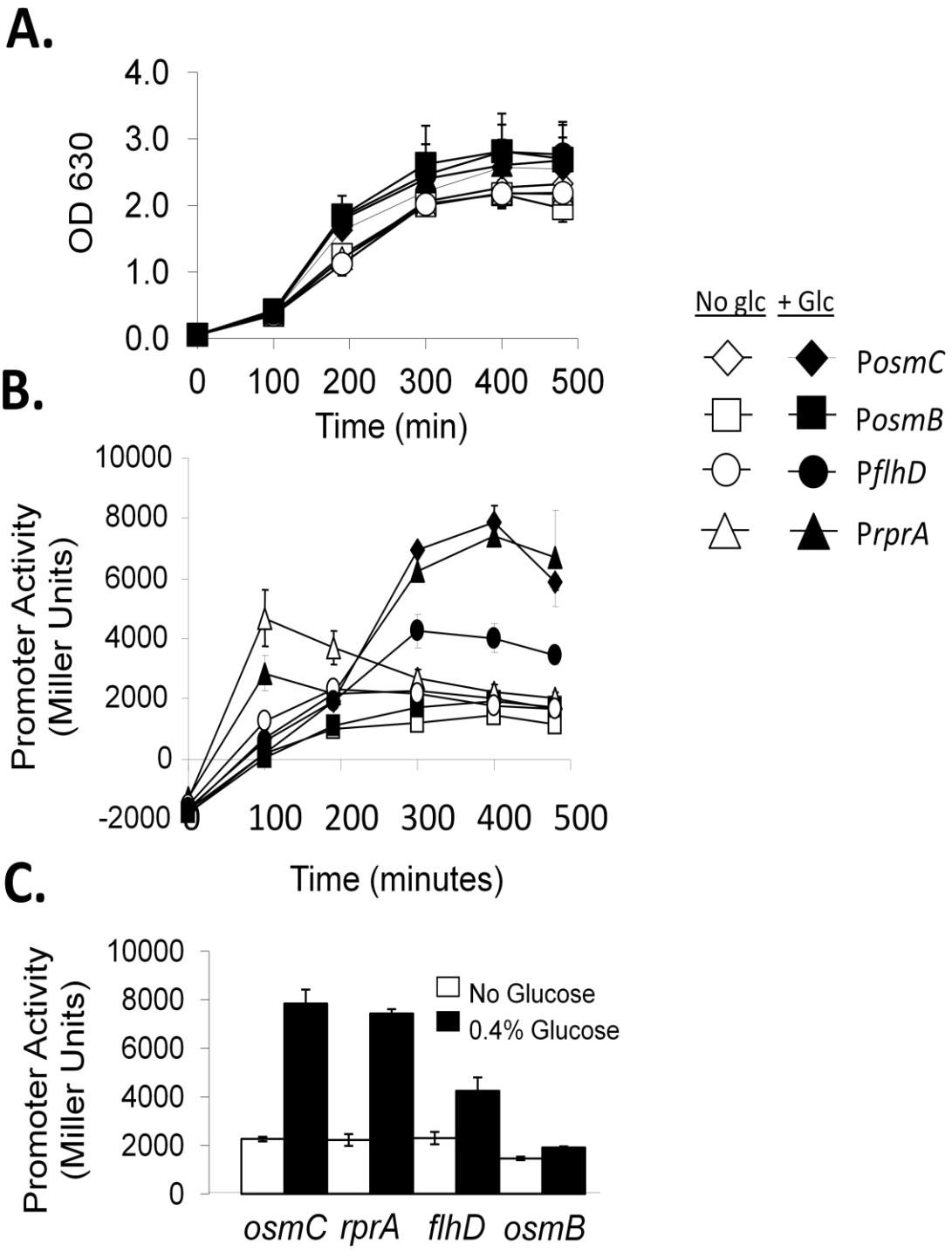
A.
OD 630
4.0
3.0
2.0
1.0
0.0
0
100
200
300
400
500
Time (min)
B.
Promoter Activity (Miller Units)
10000
8000
6000
4000
2000
0
-2000
Time (minutes)
No glc
+ Glc
PosmC
PosmB
PflhD
PrprA
C.
Promoter Activity (Miller Units)
No Glucose
0.4% Glucose
osmC
rprA
flhD
osmB

Figure 5. The effect of glucose on RcsB-regulated promoters.
Δ*lacZ* cells carrying chromosomal transcriptional promoter-*lacZ* fusions (AJW2628: *osmC*; AJW2634: *osmB*; AJW2640: *flhD*; AJW3759: *rprA* promoters) were aerated overnight at 37°C in TB7 growth medium supplemented with or without 0.4% (w/v) glucose. Samples were harvested at regular intervals assayed for OD630 (A) and β-galactosidase activity (B).
C. A histogram was constructed showing average maximum promoter activity in the presence (black bars) and absence of glucose (white bars). The values represent the means +/- standard deviations of triplicate independent cultures.

In the presence of glucose, however, the *osmC* promoter (hereafter denoted P*osmC*) and the *rprA* promoter (P*rprA*) were activated strongly, and the *flhD* promoter (P*flhD*) activated moderately, while the *osmB* promoter (P*osmB*) did not activate detectably.

To test if induction of promoter activity was specific to glucose or not, I grew the WT cells lysogenized with the *osmC* promoter fusion (strain AJW2628) in TB7 in the presence or absence of either 0.8% (w/v) pyruvate or 0.4% (w/v) glucose. The difference in the percentages normalizes for the amount of carbon (3 carbons in pyruvate and 6 carbons in glucose) in the medium. Both pyruvate and glucose induced P*osmC* activity, but pyruvate induced a weaker response than did glucose (**Figure 6**). Since induction, at least from the *osmC* promoter, is not specific to glucose, then induction of promoter activity may be dependent on some factor that is common to both glucose and pyruvate. Why exposure to glucose yields a stronger response than pyruvate remains unknown.

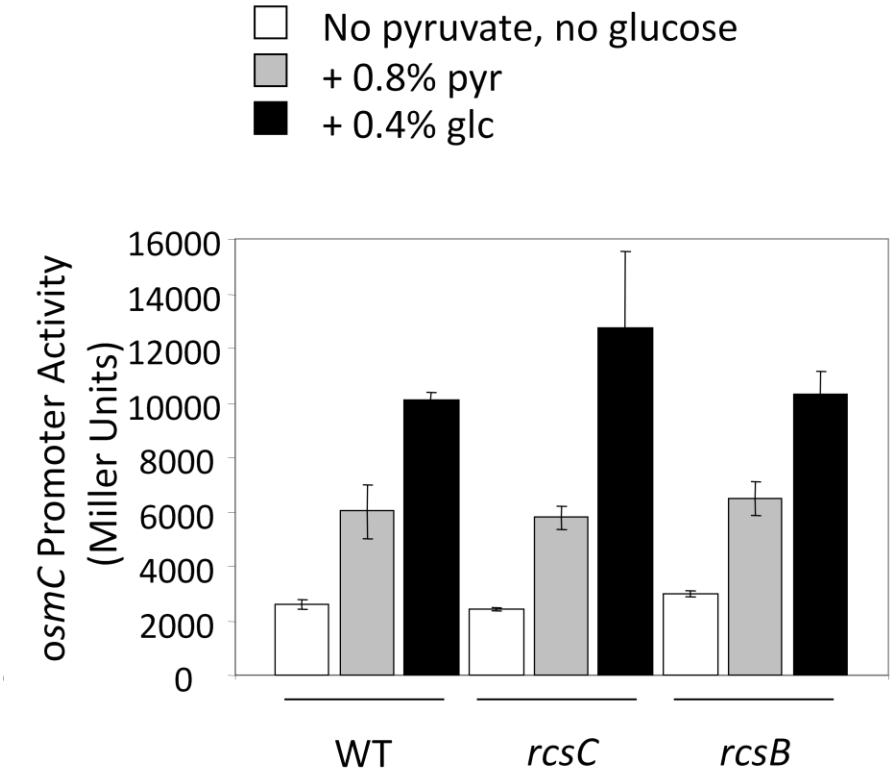

Figure 6. Comparing the effects of glucose and pyruvate at the *osmC* promoter. WT (AJW2628) and the isogenic *rcsC* (AJW3389) and *rcsB* (AJW3391) mutants were grown in TB7 in the presence and absence of 0.8% (w/v) pyruvate or 0.4% (w/v) glucose. Samples were harvested throughout growth and maximum promoter activity is plotted. These values represent the means of triplicate independent cultures and standard deviation.

Determining whether phase of growth affects the response to glucose

Since each glucose-responsive promoter exhibited peak responses as the cultures transitioned to stationary phase (**Figure 5**) and since each strain had been exposed to glucose throughout growth, I tested if the timing of glucose exposure regulates glucose-induced transcription. I grew WT cells lysogenized with the *rprA* promoter fusion (strain AJW3759) in TB7 alone and, at every hour starting at time

zero, added 0.4% glucose. As negative and positive controls, I grew cells grown in TB7 alone or TB7 plus 0.4% glucose. Samples were harvested throughout growth to analyze growth and P*rprA* activity. There were subtle differences in growth patterns (**Figure 7A**). Cells exposed to glucose earlier in growth, between 0 and 2 hours of inoculation (darker symbols), grew slightly faster during exponential phase and reached a maximum OD600 that was moderately greater than cells grown in the absence of glucose (white symbols). Cells exposed to glucose later, between 3 and 6 hours after inoculation (lighter symbols), reached a maximum OD600 that was greater than the other cultures. Consistent with our previous observations (**Figure 5B**), in the absence of glucose, WT cells (**Figure 7B**, shown as open symbols and 'no glc') exhibited exponential phase P*rprA* activity; when glucose was added at 0 hours, the cells exhibited P*rprA* activity in both exponential and stationary phase (**Figure 7B**, shown as black symbols with '0'). Consistent with stationary phase P*rprA* activity being dependent on exposure to glucose early in growth, cultures that were supplemented with glucose after 5 or 6 hours (i.e., when cultures were in mid-exponential phase or transitioning into stationary phase) exhibited little to no P*rprA* response to glucose (**Figure 7B**, shown as lighter gray symbols and '5' or '6'). Cultures that were supplemented with glucose early in growth (i.e., within 3 hours or when cultures were in lag to mid-exponential phase (**Figure 7B**, shown as darker gray symbols and '1-3')) exhibited P*rprA* responses similar to those observed when glucose was added at 0 hours. Adding glucose to the medium at 4 hours, when

cultures were in mid-exponential phase, had an intermediate effect on P*rprA* activity (**Figure 7B**, '4'). Thus, exposure to glucose early in the growth curve appears to be required for a response in stationary phase. This observation suggests that a trait associated with lag to mid-exponential phase is important. The identity of this trait remains unknown.

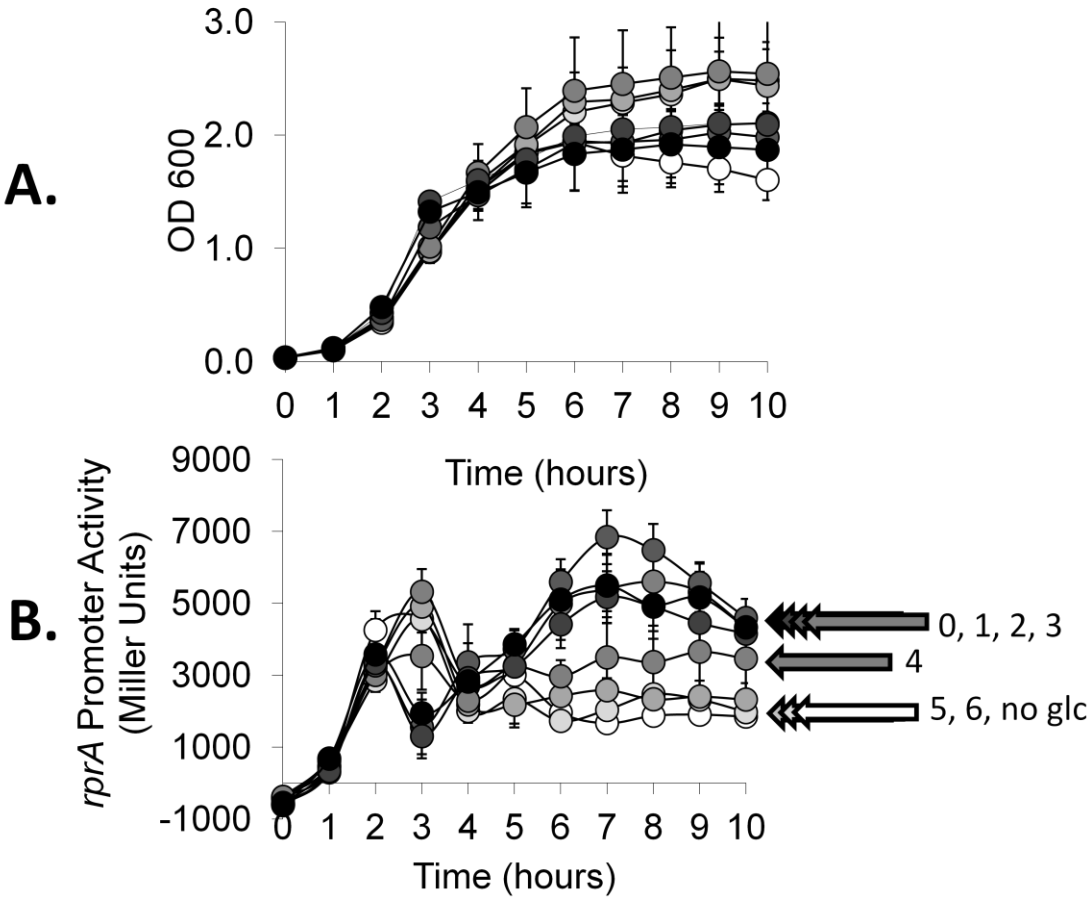

Figure 7. The effect of exposing cells to glucose at various points in the growth phase. In triplicate, I grew 8 sets of λ*rprA* lysogens (AJW3759) at 37˚C in TB7 overnight. In the morning, I diluted the overnight cultures to an OD600 of 0.03 in fresh TB7. The cells were exposed 0.4% glucose at each subsequent hour, symbolized by gradually lighter shading. One set of triplicates was grown in the absence of glucose (white symbols, 'no glc') and

another triplicate set was grown in the presence of 0.4% (w/v) glucose (black symbols). For each of the remaining 6 triplicate sets, I added an appropriate volume of 20% (w/v) glucose to achieve a final concentration of 0.4% (w/v) glucose in one hour intervals. The numbers indicate at which hour glucose was added. I harvested samples at regular intervals for growth (A) and β-galactosidase assays (B). These values represent the averages and standard deviations of triplicate independent cultures.

Analysis of the AcCoA:CoA ratio in glucose-induced P*osmC* and P*rprA* activities

Two effects of glucose is to elevate levels of both AcCoA and AcP (110,128), both of which can be acetyl donors for protein acetylation. An increase in AcCoA occurs at the expense of the limited CoA (112,113), resulting in an increase in the AcCoA-to-CoA (AcCoA:CoA) ratio (110). If the glucose-induced transcription involved acetylation, we predicted that reducing the AcCoA:CoA ratio (by genetic means) would decrease the intensity of glucose-induced promoter activity. To determine if the response to glucose depended on a large AcCoA:CoA ratio, we obtained the plasmid pPHB3 from the laboratory of Jorge Escalante-Semerena. When exposed to IPTG, pPHB3 expresses a three enzyme pathway (PhbC, PhbA, and PhbB) that uses AcCoA to produce the bioplastic polyhydroxybutyrate (PHB) with the release of free CoA (208). Thus, expression of the PHB pathway should cause the AcCoA:CoA ratio to decrease by draining acetyl groups from AcCoA, while also increasing the free CoA pool.

I used transformation to introduce this PHB synthetic pathway into *E. coli* cells that carried the promoter fusions. When exposed to IPTG, the resultant pPHB3 transformants expressed the PHB synthetic pathway, producing large, cytoplasmic

PHB aggregates visible by microscopy (**Figure 8A-C**, performed by my colleagues Dr. Bruno P. Lima and Noriko Shibata) and formed fluorescent colonies when grown on agar plates containing the stain Nile Red (**Figure 8D and 8E,** (209,210)).

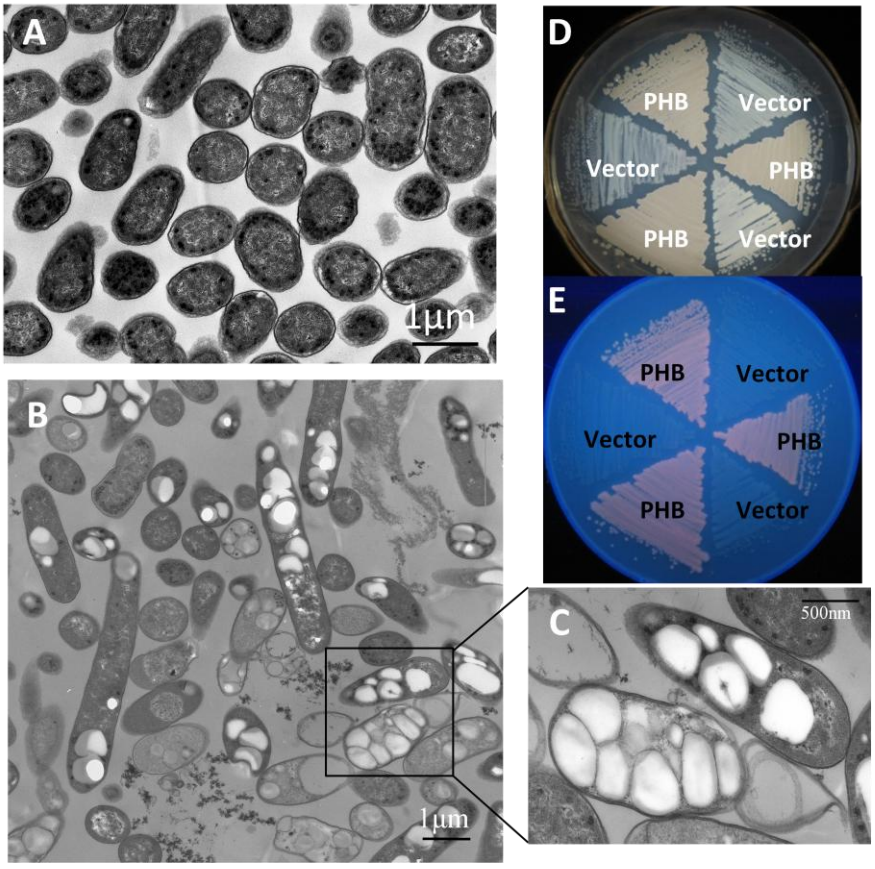

Figure 8. Visualizing PHB biosynthesis.
TEM images of PHB granules in cells. Cells were transformed with the IPTG-inducible PHB expression plasmid and grown at 37°C in TB7 supplemented with 50 µM IPTG, which either lacked (A) or contained 0.4% (w/v) glucose (B).
C) Higher magnification of cells in Panel B. TEM images were taken by Noriko Shibata and Dr. Bruno Lima.
D and E) Visualizing PHB production by UV fluorescence. Strains transformed with either the IPTG-inducible PHB expression plasmid or the vector control were grown

at 37°C on LB plates buffered at pH 7 with 0.1 M Tris containing 2% (w/v) glucose and Nile Red. Images were taken on a visible light box (D) and on a UV light box (E).

Once I knew that the PHB plasmid worked, I grew the transformants in the presence or absence of 0.4% glucose, with and without IPTG. I harvested samples at regular intervals to monitor growth and β-galactosidase activity and plotted the maximum promoter activities. While IPTG-induced PHB expression alone had limited effects on promoter activities (**Figure 9A**, light gray hatched bars), PHB expression substantially reduced glucose-induced P*osmC*, P*rprA*, and P*flhD* activities (**Figure 9A,** black hatched bars). Therefore, the AcCoA:CoA ratio may regulate *osmC, rprA*, and *flhD* transcription.

Since glucose induced the strongest responses from the *osmC* and *rprA* promoters, it is possible that they are more sensitive to a signal that is upregulated in the presence of glucose. Furthermore, these two promoters are relatively simple compared to the *flhD* promoter, which is complex and responsive to a large number of environmental variables. To reduce complications in our investigation into the nature of the glucose response, I chose to use P*osmC* and P*rprA* as the means to measure RcsB activity *in vivo*. I will first describe the glucose-induced regulation of P*osmC.*

While the PHB pathway would directly decrease AcCoA and increase CoA pools, the accumulation of PHB could interfere with promoter activity. Another genetic approach to test if transcription is regulated by the AcCoA:CoA ratio would

be to increase the CoA level. By overexpressing *coaA*, which encodes enzyme pantothenate kinase, the first enzyme in the CoA biosynthetic pathway, we increase the CoA pool in the cell (211). I began by transforming the IPTG-inducible *coaA* expression plasmid (p*coaA* from the ASKA collection, (185)) or the vector control (pCA24n) into the WT strain that carries P*osmC* (strain AJW2628). My colleague Dr. Bruno Lima grew the resultant transformants in TB7 in the presence or absence of 0.4% glucose and 50 μM IPTG. He harvested samples at regular intervals to monitor growth and β-galactosidase activity and plotted the maximum P*osmC* activity (**Figure 9B**). Compared to VC-transformed cells grown in the presence of glucose (**Figure 9B,** bar 5), p*coaA* transformed cells exhibited a moderate reduction in P*osmC* activity (**Figure 9B,** bar 6). A similar reduction in glucose-induced P*osmC* activity was observed with IPTG alone (**Figure 9B,** bar 7). Glucose-induced P*osmC* activity was reduced to the basal level when the *coaA* expression plasmid was induced with IPTG (**Figure 9B,** bar 8). These data support the hypothesis that excess carbon, in the form of glucose, activates *osmC* transcription through a high AcCoA:CoA ratio.

Determining the roles of RcsC and RcsB in glucose-induced *osmC* transcription

To determine if RcsB or the sensor protein RcsC were required, I grew WT, *rcsB*, and *rcsC* strains in TB7 in the presence or absence of glucose. Glucose-induced P*osmC* activity occurred whether or not RcsB or RcsC was present (**Figure 10A**). Pyruvate-induced P*osmC* activity also occurred in an RcsB- and RcsC-independent

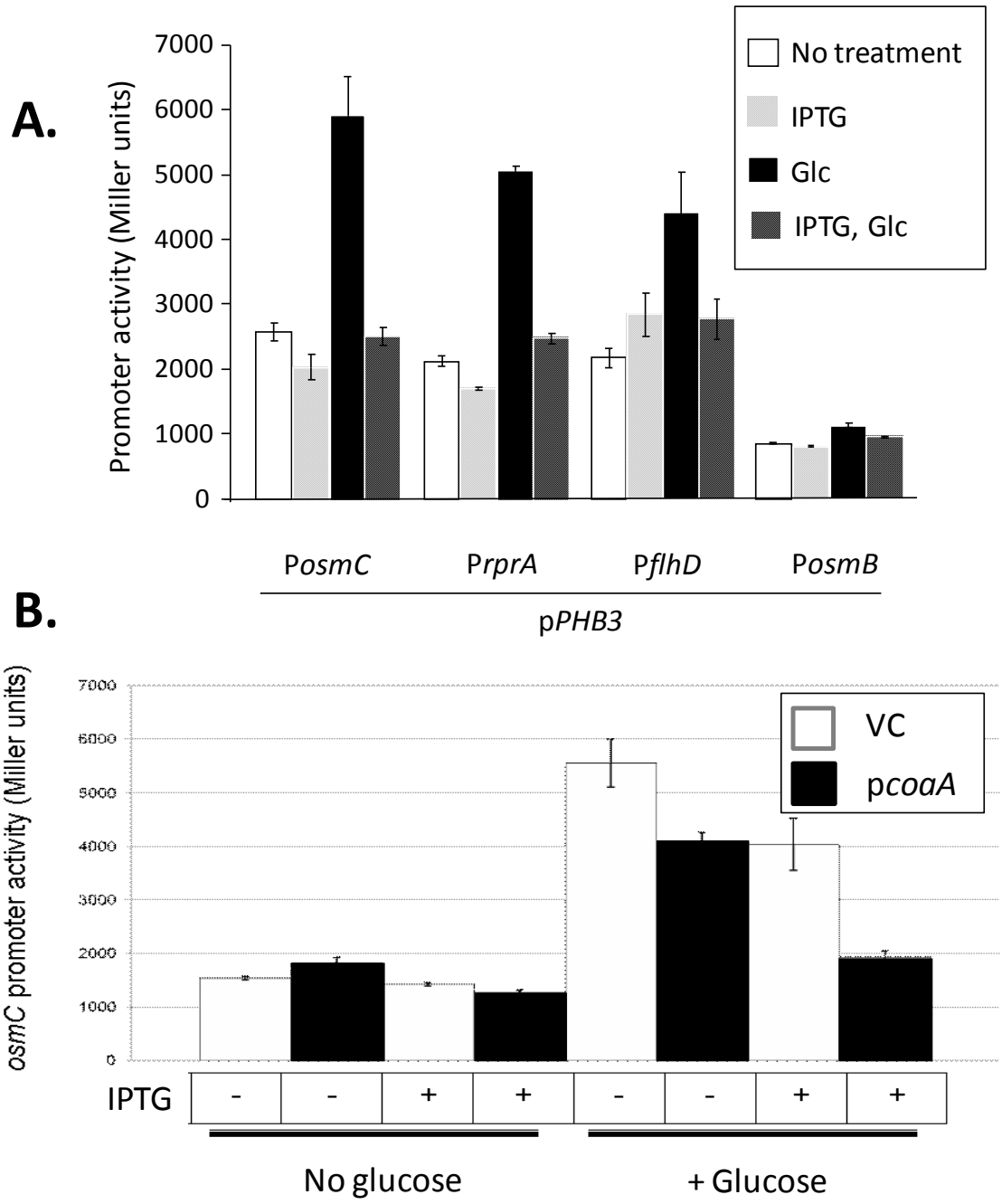

Figure 9. The effect of the AcCoA:CoA pool on promoter activity.
A) Testing if glucose-induced transcription is sensitive to PHB induction. λ*osmC*, λ*rprA*, λ*flhD*, and λ*osmB* cells (AJW2628, AJW3759, AJW2640, AJW2634,

respectively) were transformed with the IPTG-inducible PHB expression plasmid and aerated at 37°C in TB7 supplemented with 0.4% glucose (w/v) and 50 μM IPTG where indicated. The values represent the average maximum β-galactosidase activities +/- standard deviations of triplicate independent cultures.
B) Testing if glucose-induced transcription is sensitive to an increase in the CoA pool. λ*osmC* cells (AJW2628) transformed with either an IPTG-inducible vector carrying *coaA* (black bars) or the vector control (white bars) were aerated at 37°C in TB with 0.5% KCl, pH 7 buffered with 0.1 M Tris with 0.4% (w/v) glucose and 50 μM IPTG where indicated. β-galactosidase activity was assayed from samples harvested at regular intervals. The values represent the average maximum β-galactosidase activities +/- standard deviations of triplicate independent cultures. The *coaA* overexpression experiment was performed by Dr. Bruno Lima and the data are reproducible.

manner (**Figure 6**). To determine whether PHB induction affected RcsB-independent, glucose-induced P*osmC* activity, I compared the effect of glucose in WT cells and in an *rcsB* null mutant and found that the response to glucose was reduced when pPHB3 expression was induced regardless of RcsB status (**Figure 10B**). These results suggest that a high AcCoA:CoA ratio activates *osmC* transcription independently of RcsB. Given that the *rcsB* null exhibited P*osmC* activity that is either equal to or greater than WT cells, RcsB may even be an inhibitor of glucose-induced *osmC* transcription.

Analysis of αCTD lysines in the regulation of glucose-induced *osmC* transcription

The high AcCoA:CoA ratio-mediated P*osmC* activity suggests that another regulator of *osmC* transcription is sensitive to the glucose-induced, high AcCoA:CoA ratio. Dr. Lima reported that, in the presence of 0.4% glucose, several subunits of

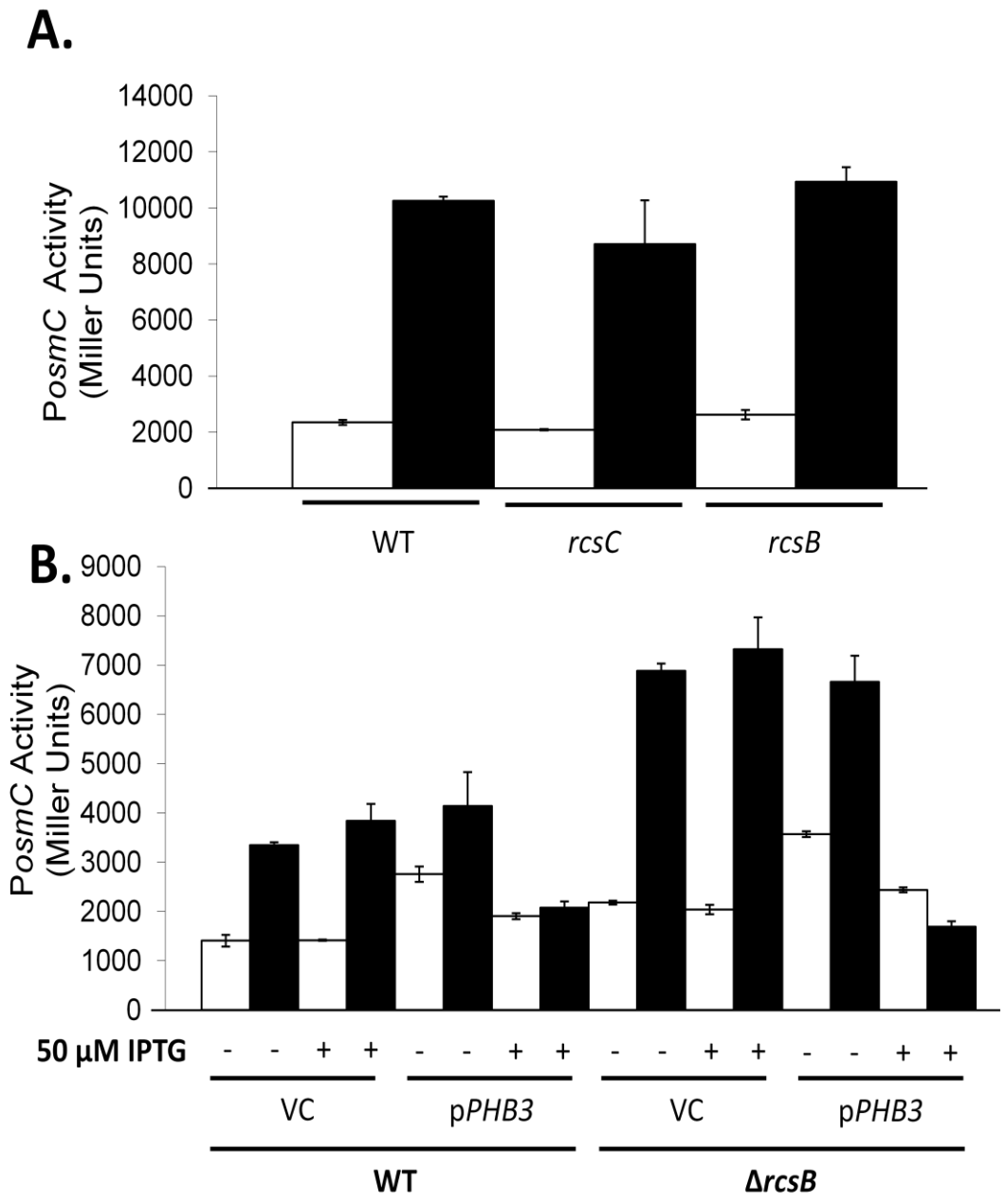

Figure 10. The effect of RcsC, RcsB, and the AcCoA:CoA ratio in glucose-induced *osmC* transcription.

A) Testing if RcsC or RcsB are required for the *osmC* response to glucose. WT (AJW2628) and isogenic *rcsC* (AJW3389) or *rcsB* (AJW3391) λ*osmC* lysogens were aerated at 37˚C in TB7 supplemented with (open bars) or without 0.4% glucose

(black bars). The values represent the average maximum β-galactosidase activity +/- standard deviations of triplicate independent cultures.
B) Determining if RcsB is required for PHB-mediated reduction in glucose-induced *osmC* transcription. WT (AJW2628) and isogenic *rcsB* (AJW3391) λ*osmC* lysogens were transformed with either the VC (pTAC-85) or a PHB expression plasmic (p*PHB3*). Transformants were aerated at 37˚C in TB7 supplemented with (open bars) or without 0.4% glucose (black bars) and in the presence (+) or absence (-) of 50 μM IPTG. The values represent the average maximum β-galactosidase activity +/- standard deviations of triplicate independent cultures.

RNA polymerase (RNAP) were acetylated and that acetylation of the α subunit, in particular, appeared to regulate the *cpxP* response to glucose (47,48). Additionally, the carboxyl terminal domain of α (αCTD) of RNAP has been shown by proteomic analysis to be acetylated ((34) and Kuhn *et al.*, in preparation), and the αCTD is frequently a target for transcriptional regulation (212). We therefore hypothesized that glucose-induced P*osmC* activity involved the acetylation of the α subunit of RNAP.

RNAP is a large multi-component complex consisting of two α subunits, one β subunit, one β' subunit, and one σ factor. Since α subunits are required for initializing the assembly of the RNAP, *rpoA*, the gene that encodes α, is essential for viability (213,214). To circumvent this problem, we used a partial diploid system consisting of an λ*osmC* lysogen carrying transformed with either a WT or mutagenized *rpoA* gene cloned onto a multicopy plasmid (described in (198) and generously provided by Dr. Richard Gourse). These cells would overexpress either a WT or mutant *rpoA*. If glucose-induced transcription required a lysine on the αCTD, then overexpressing a lysine-to-alanine mutant of the *rpoA* gene would repress

glucose-induced promoter activity. Cells transformed with either the plasmid-encoded WT (p*rpoA*(WT)) or the lysine-to-alanine αCTD derivatives (p*rpoA*(K271A, K291A, K297A, K298A, or K304A) were grown in TB7 supplemented with or without 0.4% glucose. Of the five lysine residues on the αCTD, WT cells carrying p*rpoA*(K271A) exhibited the weakest response to glucose (**Figure 11A**). This RpoA(K271)-regulated, glucose-induced P*osmC* activity was RcsB-independent (**Figure 11B**), consistent with our previous observations that the P*osmC* response to glucose is independent of RcsB. These results suggest that Lys-271 of the αCTD is important for glucose-induced *osmC* transcription.

Although these results suggest that Lys-271 of the αCTD is important for glucose-induced *osmC* transcription, the αCTD is not required for the P*osmC* response to glucose as overexpression of a truncated derivative of α that lacks both the flexible linker and the CTD does not interfere with glucose-induced P*osmC* activity (**Figure 12B**). This K271A-dependent inhibition may be a general phenomenon at RcsB-regulated promoters given that P*rprA* lysogens also exhibited *rpoA*(K271A)-inhibited, αCTD-independent glucose-induced activity (**Figure 12 A and B**). The function of K271 is unknown but we infer that Lys-271 of the αCTD may overcome an inherent inhibition of the αCTD and/or RcsB.

The effect of the CobB and YfiQ on glucose-induced P*osmC* activity

The high AcCoA:CoA ratio-mediated P*osmC* activity is consistent with the hypothesis that the activation of *osmC* transcription involves acetylation.

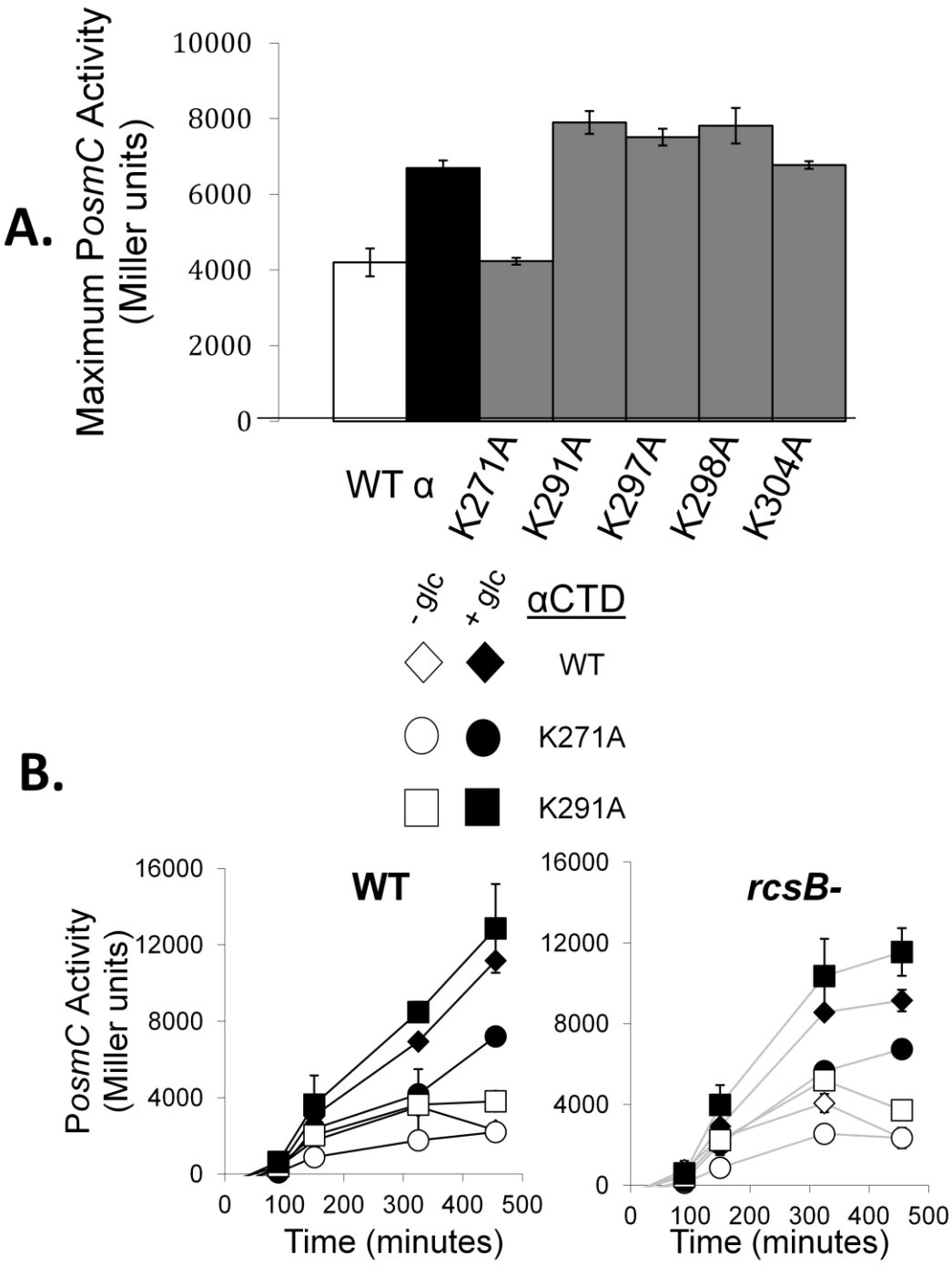
A.
Maximum PosmC Activity
(Miller units)
10000
8000
6000
4000
2000
0
WT α
K271A
K291A
K297A
K298A
K304A
B.
- g/c
+ g/c
αCTD
WT
K271A
K291A
WT
rcsB-
PosmC Activity
(Miller units)
16000
12000
8000
4000
0
0 100 200 300 400 500
Time (minutes)

Figure 11. The function of the αCTD of RNA polymerase and RcsB in glucose-induced *osmC* transcription.
A) Analysing the requirement for αCTD lysine residues. WT cells carrying λ*osmC* (AJW2628) were transformed with either a multi-copy plasmid that expressed WT *rpoA* or *rpoA*(K-to-A) mutants. Transformants were grown in TB7 in the presence (black and gray bars) or absence of glucose (white bars). Values represent the average maximum *osmC* promoter activity of triplicate independent cultures +/- standard deviations.
B) *osmC* promoter activity of WT (AJW2628) and the isogenic *rcsB* null mutant (AJW3391) transformed with a multi-copy plasmid that expressed WT *rpoA*, *rpoA*(K271A), or *rpoA*(K291A) mutants, grown in TB7, with (black symbols) and without glucose (white symbols). Values represent the average *osmC* promoter activity of triplicate independent cultures +/- standard deviations.

Therefore, to determine if glucose-induced P*osmC* activity was regulated by acetylation, I mutated the known effectors of acetylation and deacetylation, the KAT YfiQ and the KDAC CobB, by growing WT, *yfiQ*, and *cobB* strains in the presence or absence of glucose. P*osmC* in the *yfiQ* mutant responded to glucose (~6-fold) at a level similar to the WT response; therefore, YfiQ is not required for glucose-induced *osmC* transcription (**Figure 13A**). However, the basal level of P*osmC* activity was diminished in the *yfiQ* mutant; thus, YfiQ appears to regulate glucose-independent *osmC* transcription. The effect of CobB on P*osmC* activity is unclear. In the experiment that compared the *yfiQ* mutant to WT, the *cobB* mutant did not respond to glucose (**Figure 13A**), consistent with the hypothesis that CobB-mediated deacetylation of some protein is required for glucose-induced *osmC* transcription. However, when the experiment was repeated approximately 7 months later, the

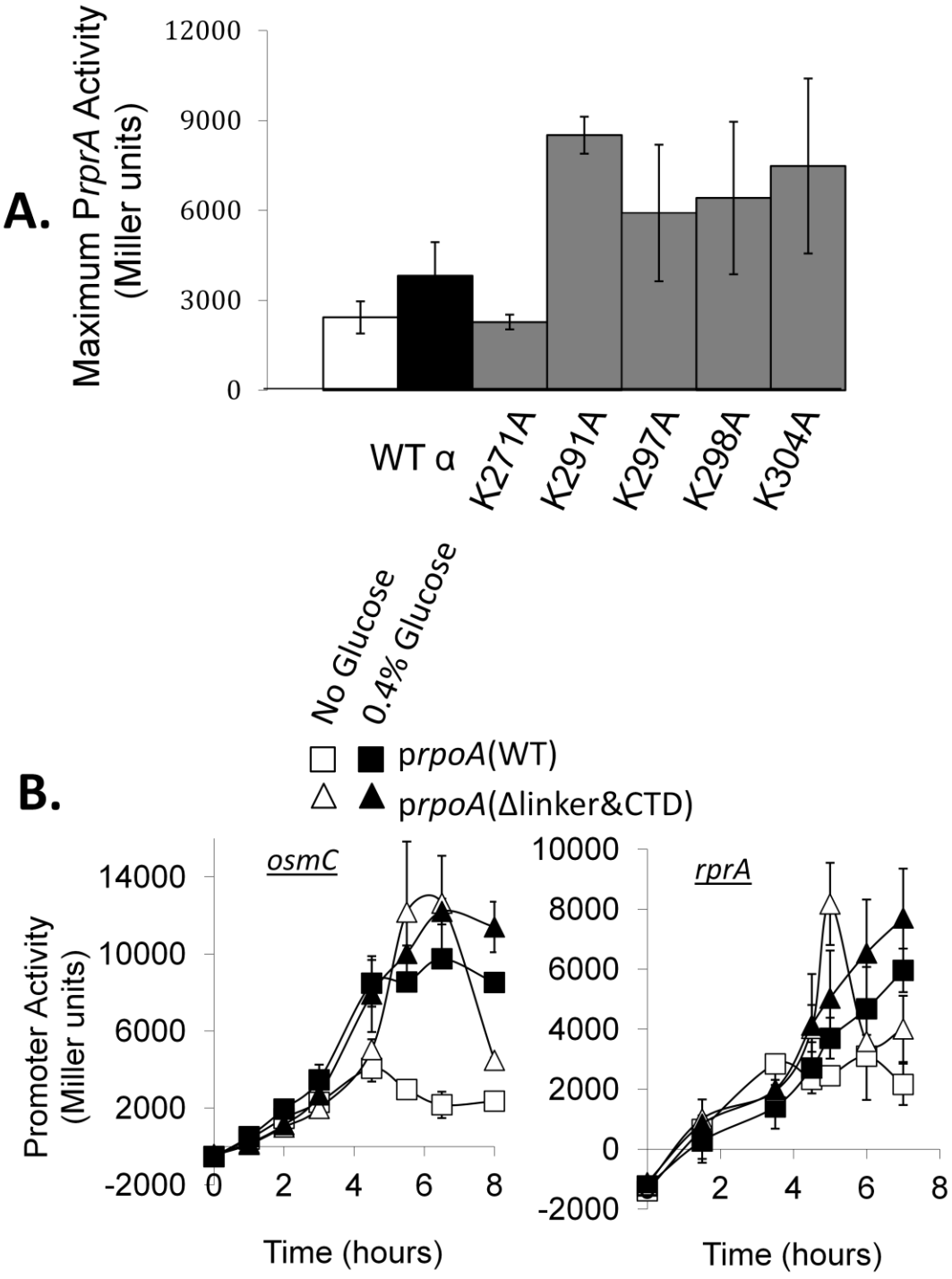
A.
Maximum PrprA Activity
(Miller units)
12000
9000
6000
3000
0
WT α
K271A
K291A
K297A
K298A
K304A
B.
No Glucose
0.4% Glucose
prpoA(WT)
prpoA(Δlinker&CTD)
osmC
rprA
Promoter Activity
(Miller units)
14000
10000
6000
2000
-2000
10000
8000
6000
4000
2000
0
-2000
0
2
4
6
8
Time (hours)
Time (hours)

Figure 12. The function of the αCTD of RNA polymerase and RcsB in glucose-induced *rprA* transcription.
A) Analysing the requirement for αCTD lysine residues. WT cells carrying λ*rprA* (AJW3759) were transformed with either a multi-copy plasmid that expressed WT *rpoA* or *rpoA*(K-to-A) mutants. Transformants were grown in TB7 in the presence (black and gray bars) or absence of glucose (white bars). Values represent the average maximum *rprA* promoter activity of triplicate independent cultures +/- standard deviations.
B) Analysing the requirement for the αCTD in glucose-induced *osmC* and *rprA* transcription. WT cells carrying λ*osmC* (AJW2628) or λ*rprA* (AJW3759) were transformed with plasmids encoding either WT (p*rpoA*(WT), squares) or αCTD derivatives that lack the linker and the αCTD (p*rpoA*(Δlinker&CTD), triangles). Cells were aerated at 37˚C in TB7 either in the presence (black symbols) or absence (white symbols) of 0.4% glucose. Values represent the average *osmC* promoter activity of triplicate independent cultures +/- standard deviations.

cobB mutant exhibited a WT-like response to glucose (**Figure 13B**). Therefore, the manner in which CobB regulates *osmC* transcription remains unclear.

Analyzing the role of Acs in glucose-induced *osmC* transcription

While Acs function is typically associated with scavenging acetate from the environment and activating the acetate to AcCoA (108,119), Acs also was reported to acetylate the RR CheY when incubated with AcCoA or with acetate and ATP (45), suggesting that it possesses protein acetyltransferase activity. I tested if Acs was involved in the P*osmC* response to glucose. I grew WT cells in the AJW678 strain background (AJW3487) and the *acs* mutant in TBK buffered with 0.1 M Tris pH 7, in the presence and absence of glucose. The *acs* mutant response to glucose was weak, in contrast to its WT parent, which exhibited a strong increase in P*osmC* activity when glucose was present (**Figure 14A**). This effect of Acs appears to have some

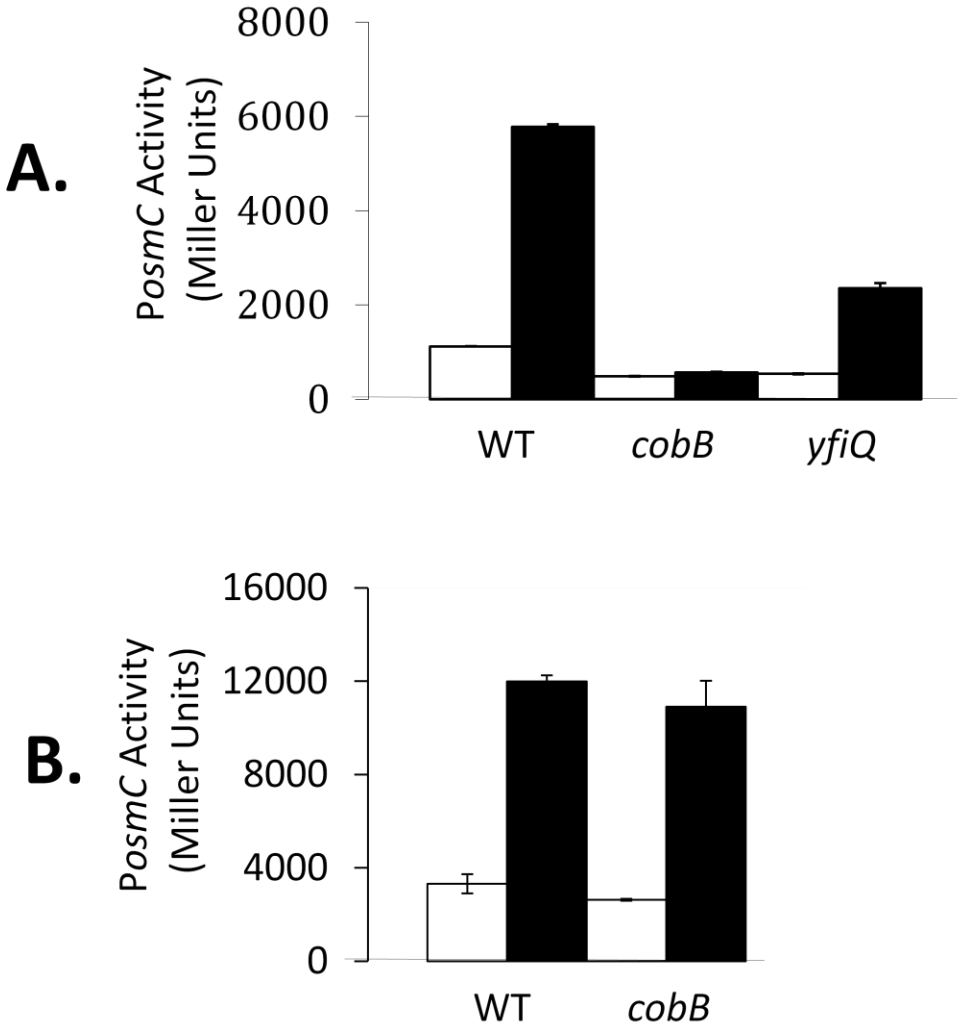

Figure 13. The function of the αCTD of RNA polymerase and RcsB in glucose-induced *rprA* transcription.

A) Testing if the *osmC* response to glucose required the KDAC CobB or the KAT YfiQ. β-galactosidase activity of WT (AJW2628) and isogenic *cobB* (AJW3529) and *yfiQ* (AJW3530) λ*osmC* lysogens aerated at 37˚C in TBK buffered at pH 7 with 0.1 M Tris in the presence (black bars) or absence (white bars) of 0.4% glucose. Values represent maximum average β-galactosidase activity +/- standard deviation of triplicate independent cultures.

B) Results from a repeat, testing if the *osmC* response to glucose required the KDAC CobB. The experiment was performed as described in A.

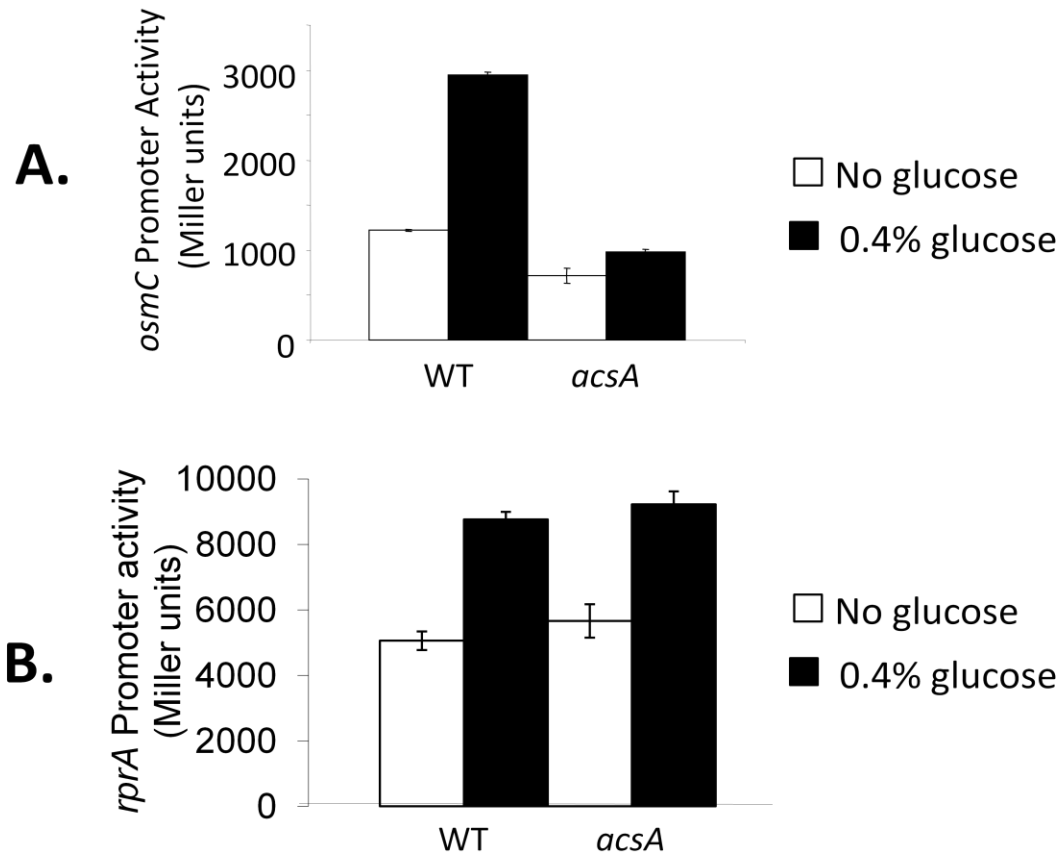

Figure 14. Testing if glucose-induced *osmC* and *rprA* responses require Acs.
A) β-galactosidase activity of WT (AJW3487) and *acsA* λ*osmC* in the 678 strain background aerated at 37˚C in TBK buffered with 0.1 M Tris pH 7 in the presence or absence of 0.4% glucose. Values represent maximum average β-galactosidase activity +/- standard deviation of triplicate independent cultures.
B) WT (AJW3759) and isogenic *acsA* mutant (AJW3800) λ*rprA* lysogens in the BW25113 strain background aerated at 37˚C in TBK buffered with 0.1 M Tris pH 7 in the presence or absence of 0.4% glucose. Values represent maximum average β-galactosidase activity +/- standard deviation of triplicate independent cultures.

specificity since the *rprA* promoter response to glucose is unaffected by the absence of Acs (**Figure 14B**). However, it should be noted that these experiments were performed in two different *E. coli* strain backgrounds (AJW678 and BW25113). If strain differences are not responsible for the effect of Acs on glucose-induced transcription, then it is possible that Acs is a protein acetyltransferase that can target proteins besides CheY. Alternatively, Acs could be an indirect regulator, affecting metabolic flux, and impacting *osmC* transcription.

Summary

It was reported that RcsB can be acetylated *in vitro,* but it was not known if RcsB was acetylated *in vivo* nor was it known if acetylation had any physiological affect on RcsB activity. I hypothesized that RcsB was acetylated *in vivo* and that acetylation affected RcsB activity as a transcription factor. I screened various RcsB-regulated transcriptional reporter constructs for a possible effect of acetylation. I predicted that manipulating global acetylation by growing *E. coli* in the presence of glucose may impact RcsB acetylation and that this change in acetylation may alter the RcsB-regulated transcriptional reporter construct. I demonstrated that P*osmC* and P*rprA* are most activated by glucose and activation occurs through a mechanism that requires a high AcCoA:CoA ratio, consistent with an acetylation-regulated phenotype that involves the acetyl donors AcCoA or AcP. The glucose-induced, AcCoA:CoA ratio-sensitive activation of P*osmC* does not require RcsB, RcsC, or the αCTD of RNAP, but does require Acs, suggesting that, if acetylation regulates *osmC* transcription, then acetylation of an unknown protein is critical and Acs is involved through an unknown mechanism.

The Effect of Acetylation on RcsB-dependent *rprA* Transcription in *E. coli*

Introduction

RcsB is proposed to be regulated by acetylation. Biochemical evidence suggests that the KAT YfiQ, AcCoA, and the KDAC CobB can regulate RcsB acetylation (49). It was not, however, demonstrated if RcsB acetylation occurs *in vivo* nor was the effect of acetylation on RcsB activity determined. I hypothesize that acetylation of RcsB occurs and that this acetylation affects RcsB activity as a transcription factor.

Because glucose-induced P*osmC* activity did not require RcsB, I chose to monitor the effect of acetylation on RcsB activity using the canonical RcsB-dependent promoter *rprA*, whose activity I had established as sensitive to the AcCoA:CoA ratio, consistent with an effect of acetylation on RcsB function. If RcsB does become acetylated, then it is possible that AcP, an emerging global regulator of acetylation (202), may also affect RcsB. To identify acetylated RcsB, we used mass spectrometry. To analyze the function of the observed acetylation, we analyzed the activity of RcsB lysine mutants at the *rprA* promoter.

The *rprA* promoter, however, is known to be regulated by the phosphorylation status of RcsB. Therefore, in order to use P*rprA* activity as a tool to study the effect of RcsB acetylation, I had to clarify the role of RcsB phosphorylation in transcription from P*rprA*. Like other RRs, RcsB is phosphorylated on a conserved

aspartyl residue (D56). Biochemical evidence shows that phosphorylation of D56 occurs via the Rcs phosphorelay, while genetic evidence suggests that RcsB phosphorylation status can be regulated by either AcP or the Rcs phosphorelay (125,156). Furthermore, the Rcs phosphorelay can either phosphorylate or dephosphorylate RcsB due to the bifunctionality of the SK RcsC (125,157,158). Under conditions in which RcsC has net phosphatase activity, it is proposed that AcP may act as a phosphoryl group donor to RcsB (125). At the *rprA* promoter, it is unknown whether D56 is required and the roles of RcsC and AcP are not fully understood. Finally, there is no biochemical evidence to support the genetic evicence that RcsB can autophosphorylate in the presence of AcP. By disrupting the Rcs phosphorelay and the Pta-AckA pathway, I was able to test the roles of these proposed sources of RcsB activation at the *rprA* promoter. Using a phosphate-binding molecule (Phos-Tag) that can detect the labile phosphoryl aspartate of phospho-RRs, I tested if AcP can donate phosphoryl groups to RcsB *in vitro* and if phosphorylation affects RcsB acetylation.

The role of D56 and RcsC in RcsB-dependent *rprA* transcription

I first tested if activity from P*rprA* required RcsB. WT λP*rprA-lacZ* lysogen (AJW3759) and the isogenic *rcsB* null mutant (AJW4884) were grown at 37°C in TB7 in the presence or absence of glucose. P*rprA* activity depended on RcsB under both conditions (**Figure 15A**). Importantly, we noticed that the peak of P*rprA* activity that occurred during exponential growth even in the absence of glucose and this

activity depended on RcsB (**Figure 15**). Although glucose-induced P*rprA* activity was sensitive to a high AcCoA:CoA ratio, and thus was a reasonable means to study the possible effect of acetylation on RcsB, glucose is not necessary for RcsB-dependent regulation of *rprA* transcription in exponential phase. I therefore decided to simplify my experimental approach and analyze the possible effect of acetylation on RcsB activity during exponential phase in the absence of glucose.

First, I tested whether exponential phase P*rprA* activity required D56. Overexpression of WT RcsB in an *rcsB* null mutant did not recapitulate WT behavior (**Figure 16A**). Therefore, I cloned *rcsB* into a single copy plasmid (pLIH001, which is a derivative of pVEC) and used site-directed mutagenesis to generate various *rcsB* alleles. From this single copy plasmid, I expressed WT *rcsB* (pLIH002, **Table 1**) or the mutant *rcsB-D56A* (pLIH003, **Table 1**) in an *rcsB* null mutant of the λP*rprA-lacZ* lysogen (strain AJW4884) and found that WT *rcsB* complemented exponential phase P*rprA* activity, while the *rcsB-D56A* allele did not (**Figure 16B**). I tried to verify that pLIH003 expresses RcsB-D56A using polyclonal anti-RcsB antibodies obtained from Dr. Sandy Thao in Dr. Jorge Escalante-Semerena laboratory. I was not successful, however, probably because the single copy of the gene does not express a detectable amount of RcsB. Instead, therefore, I used genetics to demonstrate that this plasmid expresses RcsB, showing that the activity of endogenous WT RcsB is inhibited when WT cells are transformed with pLIH003 (**Figure 16C**). Therefore, I conclude that

RcsB-D56A is expressed and I propose that exponential phase *rprA* transcription requires D56 of RcsB, and thus active phosphorylated RcsB.

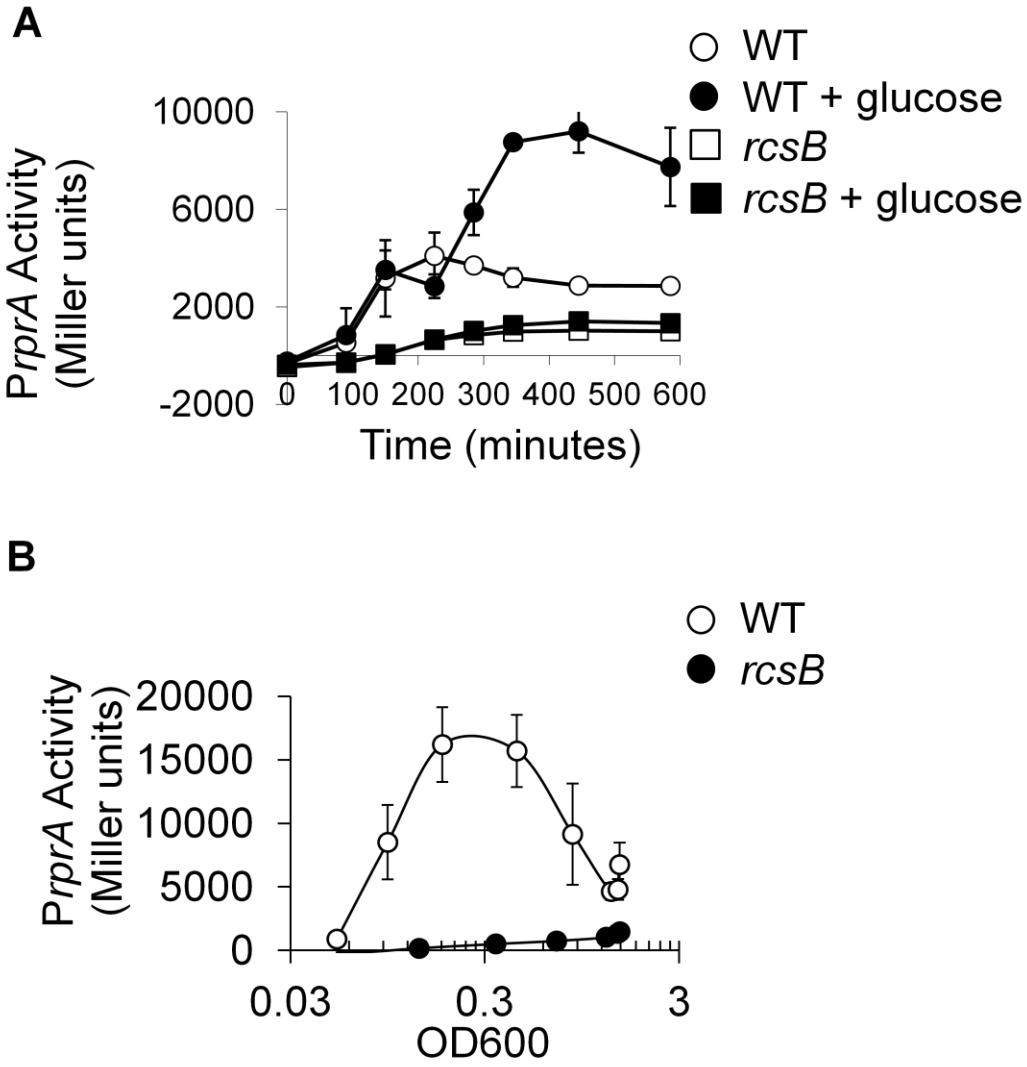
A
WT
WT + glucose
rcsB
rcsB + glucose
PrprA Activity
(Miller units)
10000
6000
2000
-2000
0
100
200
300
400
500
600
Time (minutes)
B
WT
rcsB
PrprA Activity
(Miller units)
20000
15000
10000
5000
0
0.03
0.3
3
OD600

Figure 15. The effect of glucose and RcsB at the *rprA* promoter.
A) P*rprA* activity of WT (AJW3759) and the isogenic *rcsB* mutant (AJW4884) when grown in TB7 in the presence and absence of glucose. Cells were harvested at multiple points throughout growth to measure β-galactosidase activity. The values represent the means of triplicate independent cultures with standard deviations.
B) P*rprA* activity of WT cells (AJW3759) and the isogenic *rcsB* (AJW4884) mutant when grown in TB7. The values represent the means of triplicate independent cultures with standard deviations.

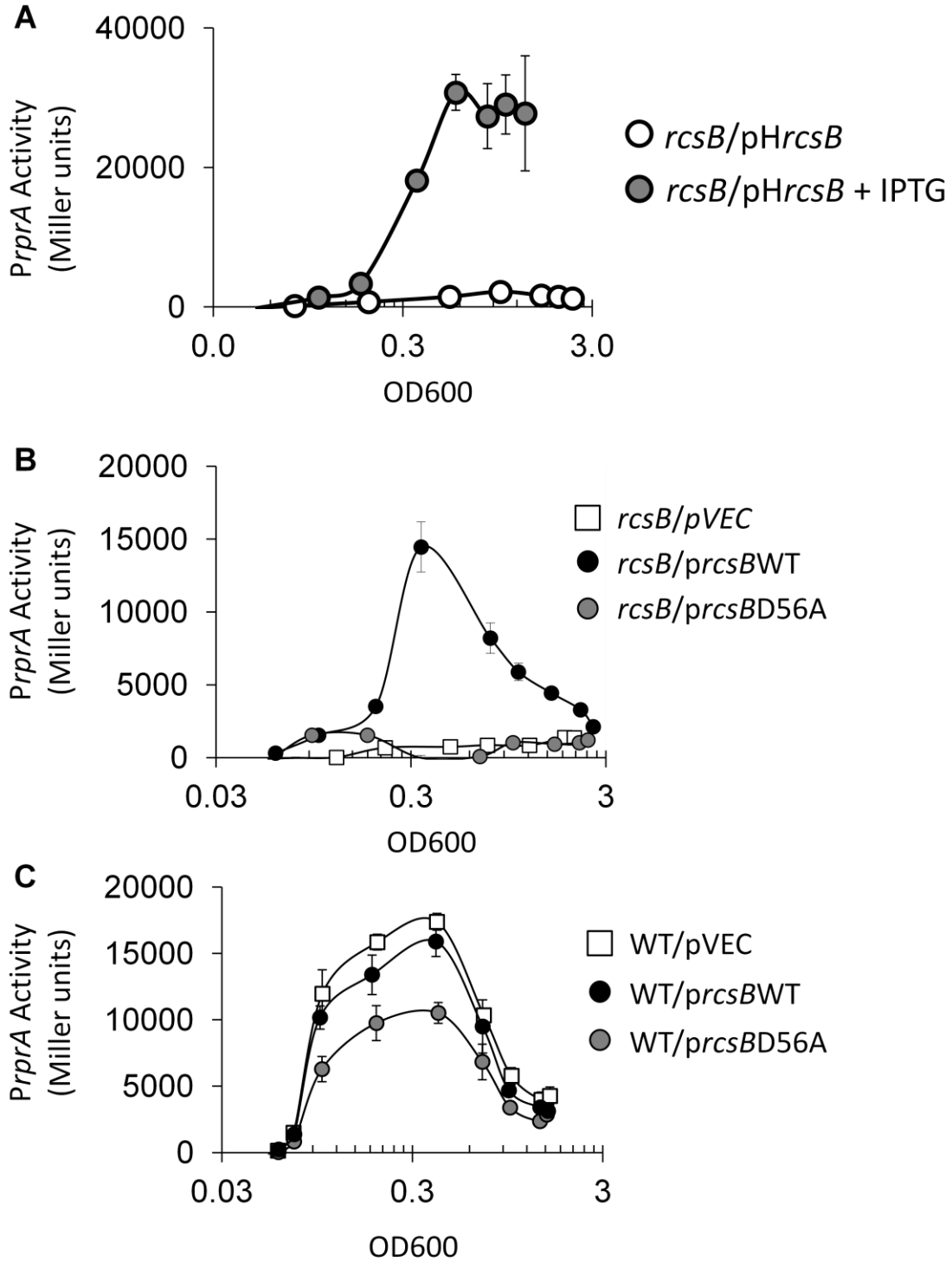
A
40000
20000
0
PprrA Activity
(Miller units)
0.0
0.3
3.0
OD600
rcsB/pHrcsB
rcsB/pHrcsB + IPTG
B
20000
15000
10000
5000
0
PprrA Activity
(Miller units)
0.03
0.3
3
OD600
rcsB/pVEC
rcsB/prcsBWT
rcsB/prcsBD56A
C
20000
15000
10000
5000
0
PprrA Activity
(Miller units)
0.03
0.3
3
OD600
WT/pVEC
WT/prcsBWT
WT/prcsBD56A

Figure 16. Testing if the activation of the *rprA* promoter requires the conserved aspartate residue 56 of RcsB

A) P*rprA* activity of an *rcsB* null mutant (AJW4884) transformed with an IPTG-inducible, His6-tagged RcsB overexpression plasmid (pHis6*rcsB*) and grown at 37°C in TB7 supplemented with 10 μM IPTG. The values represent the means of triplicate independent cultures with standard deviations.

B) P*rprA* activity of an *rcsB* null mutant (AJW4884) transformed with a *lacZ* null derivative of the single-copy expression plasmid pVEC or with a variant of that vector that encodes WT RcsB (pLIH002) or RcsBD56A (pLIH003) aerated at 37°C in TB7 supplemented with 50 μM IPTG. The values represent the means of triplicate independent cultures with standard deviations.

C) P*rprA* activity of WT cells (AJW3759) transformed with pVEC or pVEC encoding WT RcsB (pLIH002) or RcsBD56A (pLIH003) aerated at 37°C in TB7 supplemented with 50 μM IPTG. The values represent the means of triplicate independent cultures with standard deviations.

Because RcsC has been reported to function as either a kinase or a phosphatase (125,157,215), we assessed the influence of RcsC on P*rprA* activity. Consistent with RcsC activating *rprA* transcription, the *rcsC* null mutant exhibited reduced P*rprA* activity (**Figure 17A**). We conclude that endogenous RcsC functions as a kinase in this genetic background grown under these conditions. In contrast, overexpression of RcsC inhibited P*rprA* activity (**Figure 17B**) and reduced mucoidy on TB plates (**Figure 17C**), which is consistent with the report that RcsC overexpression decreases phospho-RcsB-dependent mucoidy (125). We propose that the equilibrium between RcsC kinase and phosphatase activities is sensitive to RcsC concentration.

In vitro phosphorylation of RcsB by acetyl phosphate

Using genetic approaches, AcP has been shown to activate the Asp-56-dependent RcsB activity required for mucoidy and for inhibition of flagellar biogenesis (125). AcP also has been shown both biochemically and genetically to donate phosphoryl groups to RRs (215). However, there is no biochemical evidence that AcP donates phosphoryl group to RcsB. To test whether AcP can act as a phosphoryl group donor for RcsB, we used Phos-Tag™, a dinuclear metal complex (*i.e.* 1,3-bis[bis(pyridin-2-ylmethyl)amino]propan-2-olato dizinc(II)) that has affinity for phosphomonoester dianions, such as the one found in a phosphorylated RR. When included in an SDS-PAGE, Phos-Tag™ slows the migration of the phosphorylated protein, allowing it to be distinguished from the non-

phosphorylated protein by mobility shift. When purified RcsB was incubated with AcP, we observed a shifted band that was sensitive to heat (**Figure 18**), indicative of a heat-labile aspartyl phosphate. I have also confirmed that the shifted and unshifted bands contained His6-tagged RcsB by anti-His6 immunoblot analysis and mass spectrometry (data not shown). We conclude that this shifted band is composed of phosphorylated RcsB and that RcsB can catalyze its own phosphorylation using AcP as the phosphodonor.

The effect of acetyl phosphate on P*rprA* activity

Since AcP can donate its phosphoryl group to RcsB *in vitro* and AcP can activate various RcsB-regulated phenotypes (125), I asked whether AcP activates *rprA* transcription *in vivo.* The enzyme phosphotransacetylase (Pta) converts AcCoA to AcP, while acetate kinase (AckA) converts AcP to acetate (**Figure 3**). Deletion of both *ackA* and *pta* results in the lack of AcP (123). In contrast, deletion of *ackA* alone causes accumulation of AcP (123). If AcP activated the observed Asp-56-dependent *rprA* transcription, then P*rprA* activity would be expected to decrease in the *ackA pta* double mutant and increase in the *ackA* null mutant. As predicted, the *ackA pta* double mutant displayed a small but reproducible reduction in *rprA* transcription whether or not *rcsC* was intact (**Figure 17A**). These results support the hypothesis that both AcP and RcsC contribute to RcsB phosphorylation. Contrary to expectations, however, P*rprA* activity was reduced in the *ackA* mutant rather than increased (**Figure 17A** and **19A**). This result suggests that the accumulation of some

metabolic intermediate in the *ackA* mutant inhibits RcsB activity. We reasoned that this inhibitory mechanism might involve protein acetylation because we have observed that a deletion of *ackA* changes the acetylation profile of RNA polymerase (48) and enhances global *E. coli* protein acetylation (Kuhn *et al.*, in preparation). We thus considered the possibility that protein acetylation was involved in the reduced *rprA* transcription exhibited by the *ackA* mutant.

The effect of the deacetylase CobB on P*rprA* activity

Consistent with the hypothesis that acetylation may regulate *rprA* transcription, it was reported that RcsB could be acetylated *in vitro* on one lysine residue, that this acetylation reduces RcsB DNA binding affinity, and that this acetylation can be reversed by the KDAC CobB (49). I therefore tested if protein acetylation inhibited *rprA* transcription. In the absence of CobB, the only known *E. coli* KDAC, there was a strong reduction in *rprA* transcription compared to that of its WT parent (**Figure 19A**). To determine if CobB activity was important for P*rprA* activity, WT cells were grown in the presence of nicotinamide, an inhibitor of sirtuin KDACs like CobB (216). Similar results were obtained with nicotinamide (**Figure 19B**), suggesting that CobB activity is a critical enhancer of *rprA* transcription. We propose that CobB enhances *rprA* transcription by deacetylating some protein, possibly RcsB, which inhibits *rprA* transcription in its acetylated form.

Determining if acetylated RcsB exists *in vivo*

Since CobB affects an RcsB-dependent phenotype, I tested if RcsB was acetylated *in vivo.* At first, I was unable to detect endogenous RcsB because the concentration of RcsB was low. I therefore used pHis6*rcsB* (199) to overexpress RcsB in WT cells and grew the resultant transformants in TB7. I grew four biological replicates in parallel and prepared cell lysates. I excised RcsB protein from SDS polyacrylamide gels and our collaborators Dr. Haike Antelmann, Bui Khan Chi, Katrin Basell, and Dorte Becher from the Institute for Microbiology at Ernst-Moritz-Arndt-University of Greifswald evaluated the acetylation status using Orbitrap Velos LC-MS/MS analysis. To ensure comparable protein abundances for tryptic digestion and MS analysis, RcsB protein obtained from all strains were processed in parallel and similar protein concentrations were loaded onto each SDS polyacrylamide gel. This allowed us to use the Scaffold software to perform a practical, label-free, semi-quantitative comparison of abundances (given as spectral counts, SC; (217)) for each detected peptide that contained an acetylated lysine (**Tables 2 and 3, Tables S1-S3** in (218)).

We detected acetylated RcsB *in vivo.* In four parallel bioreplicates of the WT strain overexpressing RcsB, Orbitrap Velos mass spectrometry reproducibly detected acetylation of four lysine residues: Lys-72, Lys-125, Lys-128, and Lys-154. Each acetylated lysine was identified by at least 1 SC in at least 2 replicates, with an

average of 4.0 total SC over all four replicates (**Tables 2 and 3, Table S1A-D** in (218)).

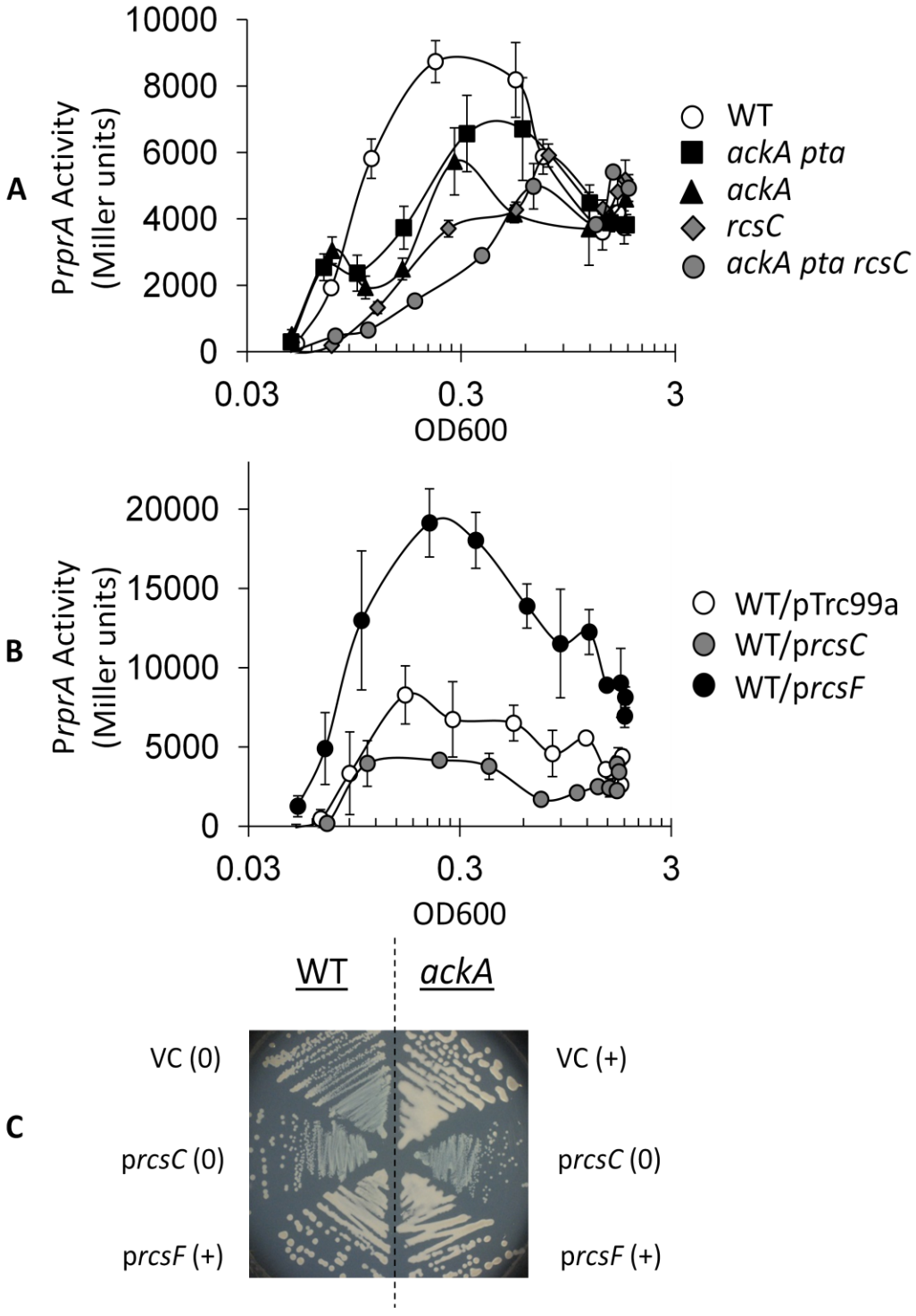
A
PprrA Activity (Miller units)
10000
8000
6000
4000
2000
0
0.03
0.3
3
OD600
WT
ackA pta
ackA
rcsC
ackA pta rcsC
B
PprrA Activity (Miller units)
20000
15000
10000
5000
0
0.03
0.3
3
OD600
WT/pTrc99a
WT/prcsC
WT/prcsF
C
WT
ackA
VC (0)
VC (+)
prcsC (0)
prcsC (0)
prcsF (+)
prcsF (+)

Figure 17. The effect of the Pta-AckA pathway, RcsC, and RcsF on *rprA* promoter activity and *ackA*-induced mucoidy.
A) P*rprA* activity of WT cells (AJW3759), *ackA* (AJW3981), *ackA pta* (AJW4030), *rcsC* (AJW3976), and *ackA pta rcsC* (AJW5187) aerated at 37°C in TB7. The values represent the means of triplicate independent cultures with standard deviations.
B) P*rprA* activity of WT cells (AJW3759) transformed with the RcsC expression plasmid p*rcsC* (pPSG980), the RcsF expression plasmid (pMH300), or the vector control (pTrc99a) and aerated at 37°C in TB7 supplemented with 50 μM IPTG to induce *rcsC* or *rcsF* expression. The values represent the means of triplicate independent cultures with standard deviations.
C) AJW678 WT or the isogenic *ackA* mutant (AJW1939) transformed with the vector control (pTrc99a), an RcsC overexpression plasmid (pPSG980), or an RcsF overexpression plasmid (pMH300) were grown on TB plates supplemented with ampicillin and 50 μM IPTG at 22°C for 2 days. The image was taken on a light box. "+" indicates mucoidy and "0" indicates no observable mucoidy.

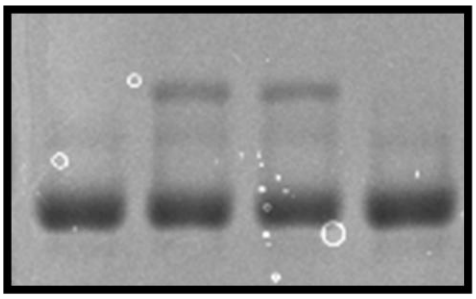

AcP	-	+	+	+
Heat	-	-	-	+

RcsB

Figure 18. AcP can induce a temperature-sensitive shift in RcsB migration through a Phos-Tag containing SDS-PA gel.
Purified His_6-RcsB peak 2 was incubated in the absence (lane 1) or presence of 5 mM AcP (lanes 2, 3, 4) for 30 minutes at 30°C. A fraction of the reaction was heated at 95°C for 15 minutes to hydrolyze the phosphoryl group (lane 4). The reactions were separated in a Phos-Tag™ SDS-PA gel and the gel was stained with coomassie brilliant blue.

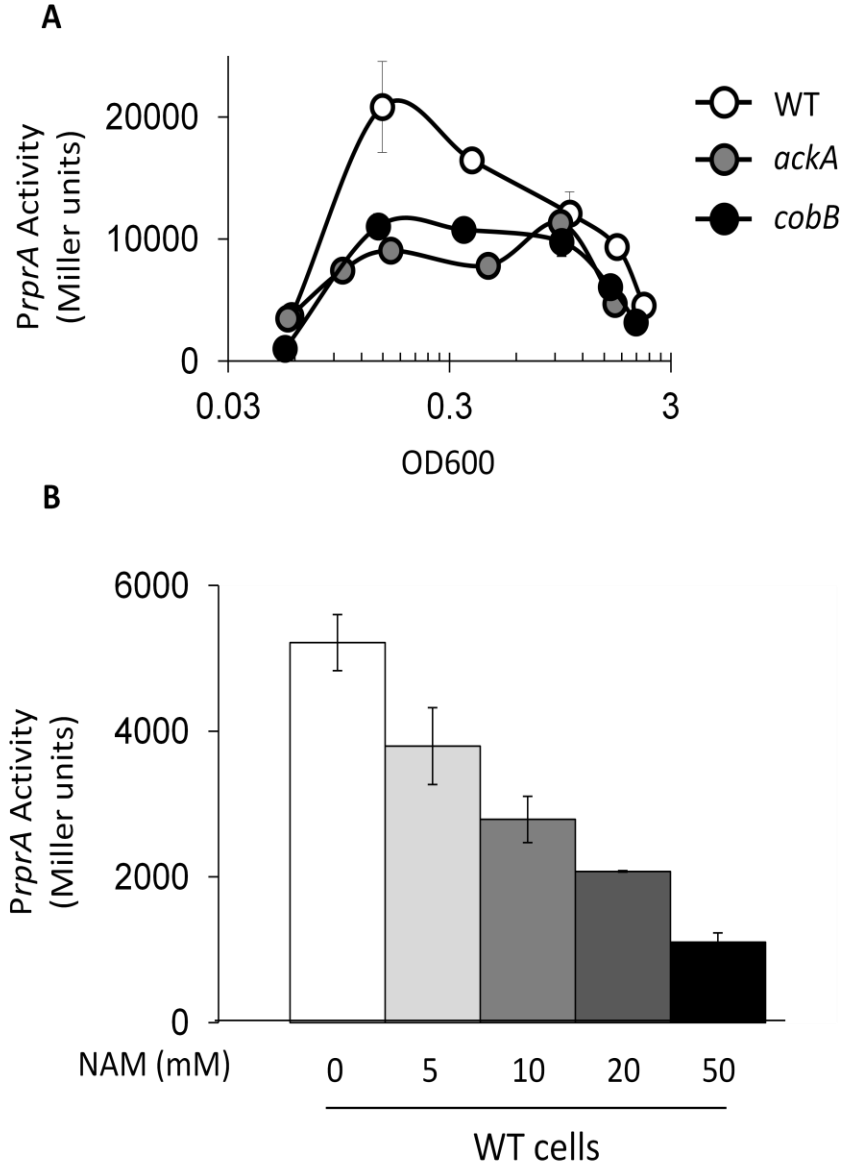
A
PprrA Activity
(Miller units)
20000
10000
0
0.03
0.3
3
OD600
WT
ackA
cobB
B
PprrA Activity
(Miller units)
6000
4000
2000
0
NAM (mM)
0
5
10
20
50
WT cells

Figure 19. The effect of CobB activity on *rprA* promoter activity.
A) WT λ*rprA* cells (AJW3759) and the isogenic *ackA* (AJW3981) and *cobB* (AJW5011) mutants were aerated at 37°C in TB7. Cells were harvested at multiple points throughout growth to measure OD600 and β-galactosidase activity. The values represent the means of triplicate independent cultures with standard deviations.
B) Peak β-galactosidase activity between OD600 0.6 – 0.8 of WT (AJW3759) cells aerated at 37°C in TB7 with and without increasing concentrations of nicotinamide (NAM). The values indicate the average of triplicate independent cultures with standard deviations.

Table 2. Spectral counts of lysine acetylated RcsB peptides isolated from WT cells, *cobB* mutants, and WT cells exposed to nicotinamide (NAM) [1,4]

	Average SC[2]			SC Ratio[2]	
Acetylated lysine	WT	*cobB*	WT + NAM	*cobB*/WT	NAM/WT
72	1.0	0.8	1.0	0.8	1.0
118	0.0	3.0	2.3	>3.0[3]	>2.3
125	1.5	2.0	1.5	1.3	1.0
128	0.5	0.8	1.0	1.5	2.0
140	0.0	2.0	0.8	>2.0	>0.8
149	0.0	1.5	1.5	>1.5	>1.5
154	1.0	2.0	2.0	2.0	2.0
173	0.0	0.0	0.5	NA	>0.5
180	0.0	0.5	0.0	>0.5	NA
Total SC	4.0	12.5	10.5	3.1	2.6

[1]Average spectral counts (SC) of detected lysine acetylation sites in the wild type (WT), its isogenic *cobB* mutant (*cobB*) and in the WT treated with NAM (WT+NAM).
[2]Using data obtained from Scaffold 3 proteome software, the spectral counts of four biological replicates for each strain/condition were counted manually, were averaged over the four replicates, and were compared as ratios of the mutant or the treated WT relative to the untreated WT.
[3]When the SC of a peptide with an acetylated lysine in the *cobB* mutant or in the NAM-treated WT is greater than the SC of the same peptide in the untreated WT control, the ratio is underlined. A ratio of >n refers to any acetylated peptide that was not detected in WT (SC=0), but detected in the *cobB* mutant or the NAM-treated WT (SC=n).
[4]The spectral counts of the detected lysine acetylation sites in each replicate and the peptide scores and mass deviations as well as the complete MS/MS spectra and fragment ion series can be found in **Tables S1A-D**, **S2A-D**, and **S3A-D**, where A-D denote the four bioreplicates in (218). As an example of the information available in these supplemental tables, '**Table S1A**' is provided in this study as **Table 3**.

Table 3. Identity, MS-MS spectra and B & Y-fragment ion series for acetylated RcsB peptides detected in samples isolated from WT cells.

Acetylated RcsB peptide data	SEQUEST	SEQUEST					Neutral							
Sequence	Prob	XCorr	DCn	NTT	Modifications	m/z Precursor Ion	Molecular Mass	Charge	Delta AMU	Delta PPM	Start	Stop	Other Proteins	Spectrum ID
(K)YGDGITLIk$_{72}$(+42)YIK(R)	95%	3.3368	0.5606	2	Acetyl (+42)	713.4027	1424.7909	2	-0.0009687	-0.6794	64	75		110218_OV3_P3_KG_HA_LH1A.13352.13352.2.dta
(K)YGDGITLIk$_{72}$(+42)YIK(R)	95%	4.3257	0.6152	2	Acetyl (+42)	713.4034	1424.7922	2	0.0003743	0.2625	64	75		110218_OV3_P3_KG_HA_LH1A.13315.13315.2.dta
(K)ALAALQk$_{125}$(+42)GK(K)	95%	2.9464	0.6351	2	Acetyl (+42)	471.2923	940.5700	2	-0.0007547	-0.8015	119	127		110218_OV3_P3_KG_HA_LH1A.04990.04990.2.dta
(K)ALAALQk$_{125}$(+42)GK(K)	95%	2.7962	0.6330	2	Acetyl (+42)	471.2923	940.5700	2	-0.0006937	-0.7368	119	127		110218_OV3_P3_KG_HA_LH1A.04949.04949.2.dta
(K)k$_{128}$(+42)FTPESVSR(L)	95%	1.8227	0.2948	2	Acetyl (+42)	546.7877	1091.5608	2	-0.0003717	-0.3402	128	136		110218_OV3_P3_KG_HA_LH1A.05728.05728.2.dta
(K)k$_{128}$(+42)FTPESVSR(L)	95%	1.9638	0.4599	2	Acetyl (+42)	546.7900	1091.5655	2	0.004389	4.017	128	136		110218_OV3_P3_KG_HA_LH1A.05645.05645.2.dta
(R)LSPk$_{154}$(+42)ESEVLR(L)	95%	1.7692	0.4068	2	Acetyl (+42)	600.3368	1198.6590	2	0.003195	2.663	151	160		110218_OV3_P3_KG_HA_LH1A.06910.06910.2.dta

Acetylated RcsB peptide coverage

All detected acetylated peptides are highlighted in yellow and the modified amino acids (Lys-acetyl and Met-oxidation) are marked in green. All acetylated peptides are listed in the Table above.

sp|P69407|RCSB_ECOLI (100%), 23.672,3 Da
Capsular synthesis regulator component B GN=rcsB PE=1 SV=1
4 unique peptides, 4 unique spectra, 7 total spectra, 40/216 amino acids (19% coverage)

MNNMNVIIAD DHPIVLFGIR KSLEQIEWVN VVGEFEDSTA LINNLPKLDA HVLITDLSMP GDKYGDGITL
IKYIKRHFPS LSIIVLTMNN NPAILSAVLD LDIEGIVLKQ GAPTDLPKAL AALQKGKKFT PESVSRLLEK
ISAGGYGDKR LSPKESEVLR LFAEGFLVTE IAKKLNRSIK TISSQKKSAM MKLGVENDIA LLNYLSSVTL
SPADKD

Table 3 continued.

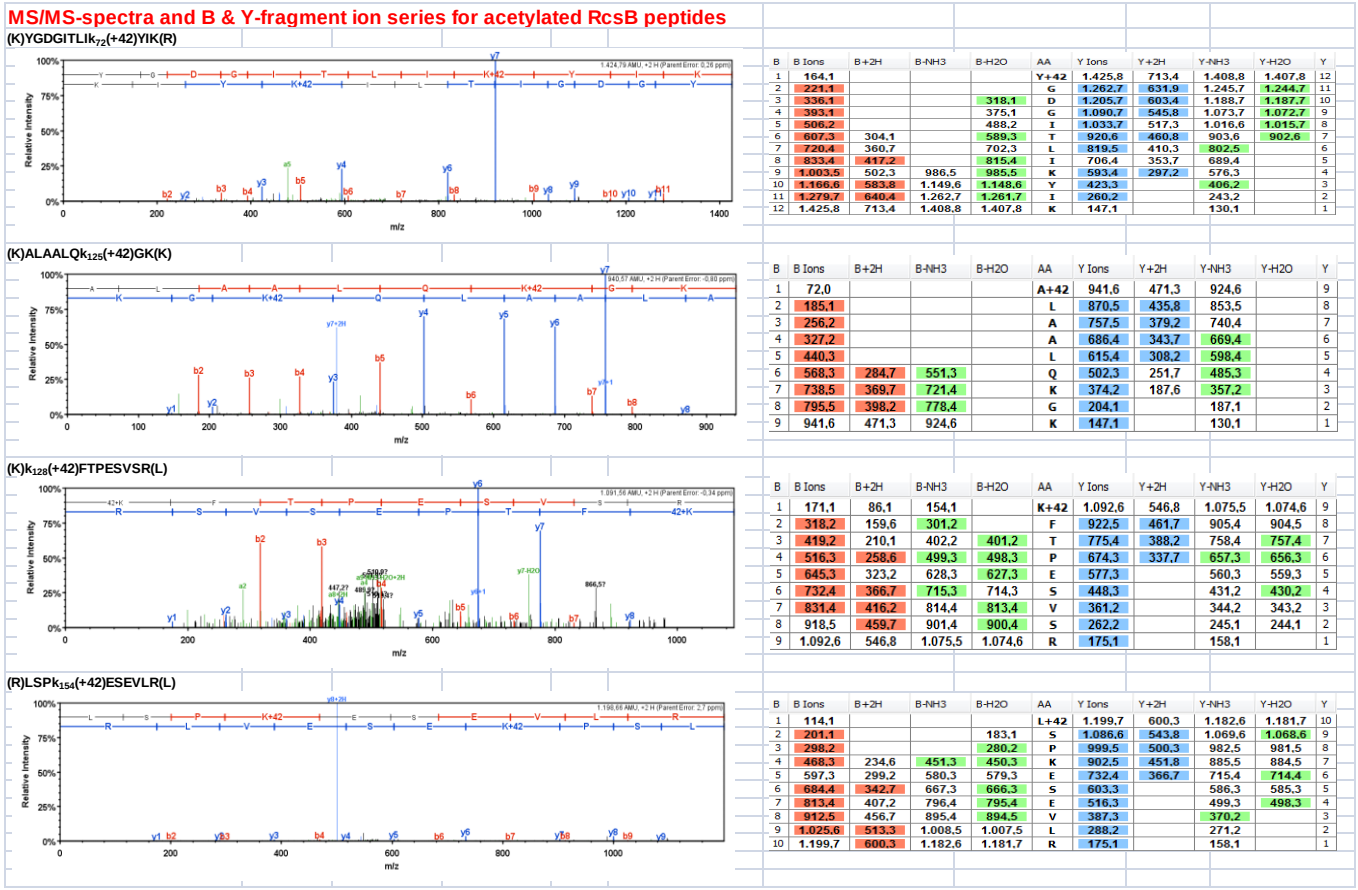

B	B Ions	B+2H	B-NH3	B-H2O	AA	Y Ions	Y+2H	Y-NH3	Y-H2O	Y
1	164.1				Y+42	1.425.8	713.4	1.408.8	1.407.8	12
2	221.1				G	1.262.7	631.9	1.245.7	1.244.7	11
3	336.1			318.1	D	1.205.7	603.4	1.188.7	1.187.7	10
4	393.1			375.1	G	1.090.7	545.8	1.073.7	1.072.7	9
5	506.2			488.2	I	1.033.7	517.3	1.016.6	1.015.7	8
6	607.3	304.1		589.3	T	920.6	460.8	903.6	902.6	7
7	720.4	360.7		702.3	L	819.5	410.3	802.5		6
8	833.4	417.2		815.4	I	706.4	353.7	689.4		5
9	1.003.5	502.3	986.5	985.5	K	593.4	297.2	576.3		4
10	1.166.6	583.8	1.149.6	1.148.6	Y	423.3		406.2		3
11	1.279.7	640.4	1.262.7	1.261.7	I	260.2		243.2		2
12	1.425.8	713.4	1.408.8	1.407.8	K	147.1		130.1		1

B	B Ions	B+2H	B-NH3	B-H2O	AA	Y Ions	Y+2H	Y-NH3	Y-H2O	Y
1	72,0				A+42	941,6	471,3	924,6		9
2	185,1				L	870,5	435,8	853,5		8
3	256,2				A	757,5	379,2	740,4		7
4	327,2				A	686,4	343,7	669,4		6
5	440,3				L	615,4	308,2	598,4		5
6	568,3	284,7	551,3		Q	502,3	251,7	485,3		4
7	738,5	369,7	721,4		K	374,2	187,6	357,2		3
8	795,5	398,2	778,4		G	204,1		187,1		2
9	941,6	471,3	924,6		K	147,1		130,1		1

B	B Ions	B+2H	B-NH3	B-H2O	AA	Y Ions	Y+2H	Y-NH3	Y-H2O	Y
1	171,1	86,1	154,1		K+42	1.092,6	546,8	1.075,5	1.074,6	9
2	318,2	159,6	301,2		F	922,5	461,7	905,4	904,5	8
3	419,2	210,1	402,2	401,2	T	775,4	388,2	758,4	757,4	7
4	516,3	258,6	499,3	498,3	P	674,3	337,7	657,3	656,3	6
5	645,3	323,2	628,3	627,3	E	577,3		560,3	559,3	5
6	732,4	366,7	715,3	714,3	S	448,3		431,2	430,2	4
7	831,4	416,2	814,4	813,4	V	361,2		344,2	343,2	3
8	918,5	459,7	901,4	900,4	S	262,2		245,1	244,1	2
9	1.092,6	546,8	1.075,5	1.074,6	R	175,1		158,1		1

B	B Ions	B+2H	B-NH3	B-H2O	AA	Y Ions	Y+2H	Y-NH3	Y-H2O	Y
1	114,1				L+42	1.199,7	600,3	1.182,6	1.181,7	10
2	201,1			183,1	S	1.086,6	543,8	1.069,6	1.068,6	9
3	298,2			280,2	P	999,5	500,3	982,5	981,5	8
4	468,3	234,6	451,3	450,3	K	902,5	451,8	885,5	884,5	7
5	597,3	299,2	580,3	579,3	E	732,4	366,7	715,4	714,4	6
6	684,4	342,7	667,3	666,3	S	603,3		586,3	585,3	5
7	813,4	407,2	796,4	795,4	E	516,3		499,3	498,3	4
8	912,5	456,7	895,4	894,5	V	387,3		370,2		3
9	1.025,6	513,3	1.008,5	1.007,5	L	288,2		271,2		2
10	1.199,7	600,3	1.182,6	1.181,7	R	175,1		158,1		1

RcsB was overexpressed from the p*His6-rcsB* plasmid in WT cells in TB7 supllemented with 50 µM IPTG. Proteins from whole cell lysates were separated by SDS-PAGE and RcsB bands were tryptically digested as described (219). The resulting peptides were analyzed using LC-MS/MS analysis as described in the Methods and analyzed using the Scaffold software. Table 3 shows the Xcorr, deltaCn scores, m/z of the precursor ions, neutral molecular masses of the CID MS/MS spectrum of the acetylated

peptides are shown, in which the complete b and y ion series are cognizable and labeled in red and blue, respectively. Table 3 is representative of the information provided in supplemental tables from (218).

Determining if CobB affects RcsB acetylation *in vivo.*

CobB activity appears to increase *rprA* transcription and CobB was reported to deacetylate Lys-180-acetylated RcsB *in vitro* (49). We thus tested whether CobB affected RcsB acetylation *in vivo.* RcsB was prepared for mass spectrometry as described above except that RcsB was overexpressed either in the *cobB* mutant or in WT cells exposed to 20 mM nicotinamide grown in TB7.

Consistent with CobB deacetylating RcsB *in vivo*, the *cobB* mutant exhibited an increase in the number of acetylated RcsB lysines*.* In the *cobB* mutant, mass spectrometry reproducibly detected acetylation of 8 lysine residues: the four listed above plus Lys-118, Lys-140, Lys-149, and Lys-180 **(Table 2, Tables S2A-D** in (218)**)**. In the WT strain treated with NAM, mass spectrometry also reproducibly detected acetylation of 8 lysine residues: seven identified in the *cobB* mutant and Lys-173 **(Table 2, Tables S3A-D** in (218)**)**. Furthermore, the acetylated peptides were more abundant in the *cobB* mutant (average total SC of 12.5) and in the NAM-treated parent strain (average total SC of 10.5) than in the parent control (average total 4.0 SC). However, these increases in SC were not distributed evenly over all acetylated lysines, suggesting that CobB does not regulate all acetylated RcsB lysines similarly. For example, the average SC for peptides containing acetylated Lys-72 or Lys-125 did not differ significantly between strains/conditions; in contrast, we reproducibly detected acetylation of 3 residues (Lys-118, Lys-140, and Lys-149) in the *cobB* mutant and the NAM-treated parent that were not detected in the untreated parent (**Table 2**). Thus, CobB may promote deacetylation of certain RcsB lysines *in vivo*.

Determining if AckA impacts RcsB acetylation *in vivo*

We hypothesized that an *ackA* mutation affects RcsB acetylation. We did so, in part, because Dr. Bruno Lima previously reported that the *cpxP* promoter response to glucose is reduced in the *ackA* mutant, that the acetylation profile of RNA polymerase is altered in the *ackA* mutant, and that this alteration is likely involved in the reduced transcription (48). I also observed that the *ackA* mutant phenocopies the *cobB* mutant (**Figure 19A**), a condition that affects RcsB acetylation (**Table 2**). We therefore tested if RcsB acetylation is enhanced in the absence of *ackA*. I overexpressed RcsB in the WT strain and its isogenic *ackA* and *cobB* mutants, separated the proteins by SDS-PAGE, and subjected the tryptic digests to mass spectrometry as described above. Once again, I performed replicate experiments in parallel, and processed the same amount of protein from all samples so that we could compare the spectral counts for each acetylated peptide in each mutant relative to WT.

As predicted, the acetylation profile of RcsB isolated from the *ackA* mutant (**Table 4, Tables S6A-B** in (218)) generally resembled that of the *cobB* mutant (**Table 4, Tables S5A-B** in (218)). Of the 7 acetylated RcsB lysines from the *cobB* mutant, 6 lysines were reproducibly acetylated in the *ackA* mutant. Several acetylated lysines (Lys-118, Lys-128, and Lys-154) were detected more often in both mutants than in their WT parent. Like RcsB from the *cobB* mutant (average total 14.5 SC), acetylated peptides from the *ackA* mutant were two-fold more abundant (average total 17 SC) than the same peptides from WT cells (average total 8.5 SC). We conclude that disruption of *ackA* promotes acetylation of some RcsB

lysines *in vivo.* We further propose that the reduction in *rprA* transcription in the *ackA* and *cobB* mutants results from the same mechanism, an increase in RcsB acetylation.

When comparing the results of this experiment (**Table 4**) to those of the previously described experiment (**Table 2**), we noticed a general increase in the numbers of detected acetylated lysine residues and their spectral counts. We attribute this difference primarily to the larger amounts of RcsB analyzed in the second experiment and to the use of a different liquid chromatography (LC) column prior to Orbitrap Velos MS. The general pattern however, was reproducible: acetylated peptides were more abundant in the *cobB* mutant (average total SC of 14.5) than in the parent control (average total 8.5 SC) (**Table 4**), supporting our conclusion that CobB may deacetylate RcsB *in vivo*. For the parent, we reproducibly detected acetylation of 5 lysine residues, each identified by 1-2 SC per replicate (**Table 4, Tables S4A-B** in (218)). For the *cobB* mutant, we observed reproducible acetylation of 7 lysines, each identified by 1-4 SC per replicate (**Table 4, Tables S5A-B** in (218)). Moreover, some acetylated peptides were reproducibly more abundant than the same peptides from the parent, consistent with our previous observations and supporting the prediction that CobB deacetylates certain RcsB lysines *in vivo*.

Genetic analysis into the function of acetylated RcsB lysines in *rprA* transcription

In the absence of *ackA* or *cobB*, P*rprA* activity was reduced and RcsB acetylation increased. One RcsB lysine (Lys-154) that was reproducibly more acetylated in the mutants relative to the WT parent (**Tables 2** and **4)** was found to be critical for RcsB activity. While there is a method that can generate site-specific acetylated proteins (220), we currently do not have this system functioning in our laboratory. Instead, to assess the effect of acetylation on RcsB function, we applied an approach commonly used in studies of acetylation in eukaryotes (221), converting this AckA- and/or CobB-sensitive lysine to a glutamine (which mimics a neutral, acetylated lysine) or to an arginine (which mimics a positive, non-acetylatable lysine). We introduced these *rcsB* variants (carried by pVEC) into the *rcsB* null strain (AJW4884) and monitored P*rprA* activity. The acetylated and non-acetylated mimics of Lys-154 exhibited opposite behaviors. The mimic of acetylated Lys-154 (RcsB-K154Q) exhibited a strong reduction in P*rprA* activity, a behavior that was indistinguishable from that of the vector control (**Figure 20A**), the non-phosphorylatable mutant RcsB-D56A, and the RcsB-K154A mutant (data not shown). This contrasted with the behavior of the non-acetylated mimic (RcsB-K154R), which more closely resembled that of the WT RcsB (**Figure 20A**). We next tested whether the inability of RcsB-K154Q to support P*rprA* activity was due to a lack of expression or a loss of function. I attempted to detect RcsB expressed from the pCC1 single copy plasmid system, but RcsB is not tagged, the anti-RcsB antibody (J. Escalante-Semerena laboratory) exhibited non-specific binding, and the amount

of RcsB expressed from the pCC1 plasmid is low. Instead, we took advantage of the report that RcsB inhibits migration through semi-solid agar by repressing transcription of *flhDC*, which encodes the master regulator of flagella biosynthesis (125,163). We asked if expression of the *rcsB* mutants could inhibit migration of the highly motile strain AJW3331 (AJW678 background). Indeed, each mutant *rcsB* allele (D56A, K154A, K154Q, and K154R) inhibited migration to a level similar to that of the WT allele (**Figure 20B**). We have not tested if growth was affected but the results are consistent with the expression of mutant RcsB and that they retain function. We therefore propose that the positive charge of Lys-154 is critical to RcsB-dependent activation of *rprA* transcription and that acetylation of Lys-154 may regulate RcsB activity. We were intrigued with the observation that RcsB-D56A was able to inhibit migration since this mutant lacks the conserved phospho-acceptor site. These results may suggest that binding to DNA does not require phosphorylation of RcsB and that phosphorylation impacts another step that is critical for RcsB activity.

The effect of acetylation on phosphorylated RcsB

Because an increase in the number of detectably acetylated RcsB lysine residues correlated with a reduction in phospho-RcsB dependent P*rprA* activity, I tested whether acetylation reduced the level of RcsB phosphorylation. I first acetylated purified RcsB using AcCoA alone or using both AcCoA and YfiQ, and then incubated the reaction mixtures with increasing amounts of AcP. We separated the mixtures by Phos-Tag™ SDS-PAGE and compared the ratio of phosphorylated-to-unphosphorylated RcsB with and without prior *in vitro* acetylation. When the AcP

concentration was physiologically relevant (≤5 mM; (123)), the percentage of phosphorylated RcsB following AcCoA- or AcCoA/YfiQ-mediated acetylation was reduced relative to the control that was not previously acetylated *in vitro* (**Figure 21**). While the effect of acetylation on phosphorylation is small, this observation that acetylation reduces the amount of phosphorylated RcsB is highly reproducible. These results suggest that RcsB is regulated by more than one modification and that this may be an example of a bacterial post-translational modification code (21). These results are consistent with acetylation inhibiting RcsB activity at the *rprA* promoter by reducing RcsB phosphorylation.

Summary

Using a combination of genetics and biochemistry, I tested the hypothesis that RcsB acetylation exists *in vivo* and that acetylation affects RcsB activity as a transcriptional regulator. I identified that RcsB is acetylated *in vivo* and I verified that RcsB function is sensitive to CobB activity (49) and showed that CobB regulates the acetylation status of RcsB *in vivo.* Consistent with the observation that Dr. Bruno Lima made at another stress-responsive promoter, I showed that the Pta-AckA pathway influences protein acetylation. This is the first published evidence that *in vivo* acetylation of a bacterial transcription factor could regulate its activity.

Table 4. Spectral counts of lysine acetylated RcsB peptides isolated from WT cells or *yfiQ, cobB,* or *ackA* mutant cells [1,4]

	Average SC[2]				SC Ratio[2]		
Acetylated lysine	**WT**	***cobB***	***ackA***	***yfiQ***	***cobB*/WT**	***ackA*/WT**	***yfiQ*/WT**
63	**1.0**	**1.0**	**1.5**	**0.0**	**1.0**	**1.5**	**0.0**
72	**2.0**	**0.5**	**4.5**	**2.0**	***0.3***[3]	**2.3**[3]	**1.0**
118	**1.5**	**3.5**	**4.5**	**2.5**	**2.4**	**3.0**	**1.7**
125	**1.5**	**1.5**	**2.0**	**1.5**	**1.0**	**1.4**	**1.0**
128	**0.5**	**2.0**	**1.0**	**0.0**	**4.0**	**2.0**	**0.0**
140	**0.0**	**1.5**	**0.5**	**0.0**	**>1.5**	**>0.5**	**0.0**
149	**0.0**	**0.5**	**0.0**	**0.0**	**>0.5**	**0.0**	**0.0**
154	**0.5**	**3.0**	**2.0**	**1.0**	**6.0**	**4.0**	**2.0**
173	**1.5**	**0.0**	**0.0**	**1.5**	**0.0**	**0.0**	**1.0**
180	**0.0**	**1.0**	**1.0**	**0.0**	**>1.0**	**>1.0**	**0.0**
Total SC	**8.5**	**14.5**	**17.0**	**8.5**	**1.7**	**2.0**	**1.0**

[1]Average spectral counts (SC) of detected lysine acetylation sites in the wild type (WT), and its isogenic *cobB, ackA* and *yfiQ* mutants.
[2]Using data obtained from Scaffold 3 proteome software, the spectral counts of two biological replicates for each strain were counted manually, were averaged over the two replicates, and were compared as ratios of the mutants relative to the untreated WT.
[3]When the SC of a peptide with an acetylated lysine in a mutant is less than the SC of the same peptide in the WT control, the ratio is italicized. When the SC of a peptide with an acetylated lysine in a mutant is greater than the SC of the same peptide in the WT control, the ratio is underlined. A ratio of >n refers to any acetylated peptide that was not detected in WT (SC=0), but detected in a mutant (SC=n).
[4]The spectral counts of the detected lysine acetylation sites in each replicate and the peptide scores and mass deviations as well as the complete MS/MS spectra and fragment ion series can be found in **Tables S4A-B**, **S5A-B**, **S6A-B** and **S7A-B** in (218), where A-B denote the two bioreplicates.

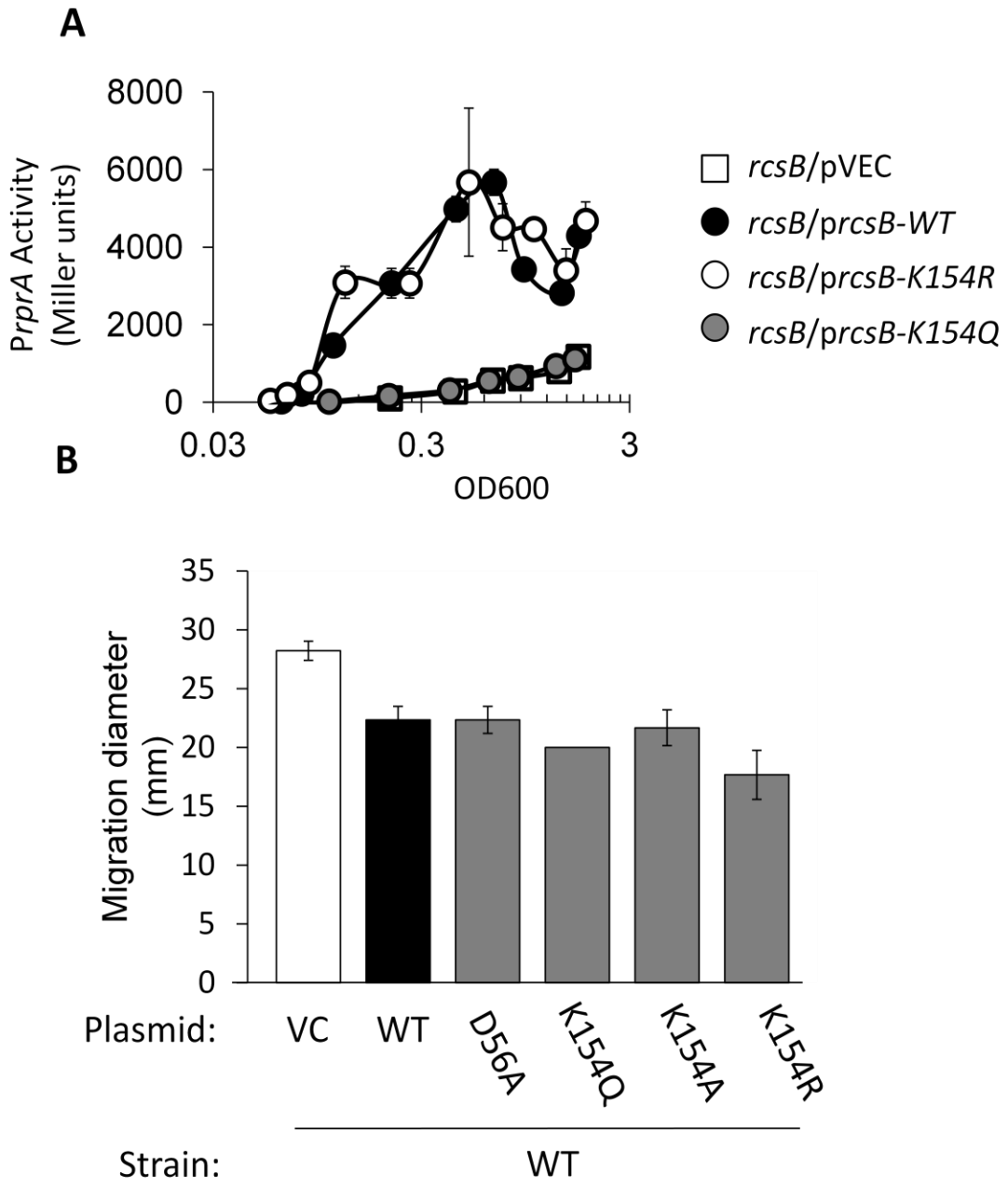
A
8000
6000
4000
2000
0
PprrA Activity
(Miller units)
0.03
0.3
3
OD600
rcsB/pVEC
rcsB/prcsB-WT
rcsB/prcsB-K154R
rcsB/prcsB-K154Q
B
35
30
25
20
15
10
5
0
Migration diameter
(mm)
Plasmid:
VC
WT
D56A
K154Q
K154A
K154R
Strain:
WT

Figure 20. Analyzing the role of Lys-154 on *rprA* transcription and migration.
A) P*rprA* activity of *rcsB* mutant (AJW4884) transformed with the single copy plasmid pVEC or pVEC carrying WT and mutant *rcsB*-K154 alleles. Cells were aerated at 37°C in TB7 supplemented with 50 μM IPTG.
B) Migration analysis of the highly motile WT strain (AJW3331) in the AJW678 strain background transformed with pVEC or pVEC carrying WT and mutant *rcsB* alleles. The histogram shows the last measurement of an 8.5 hour time course experiment. These results are representative of the whole experiment.

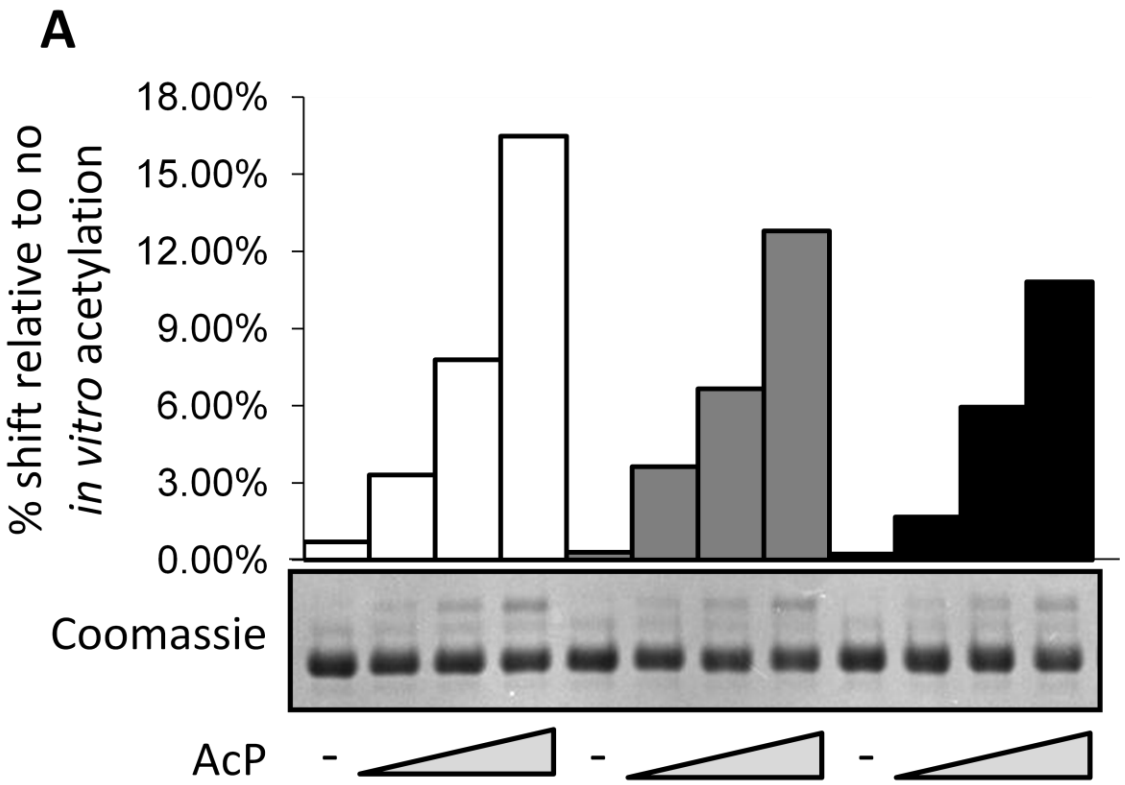
A
% shift relative to no
in vitro acetylation
18.00%
15.00%
12.00%
9.00%
6.00%
3.00%
0.00%
Coomassie
AcP
-
-
-

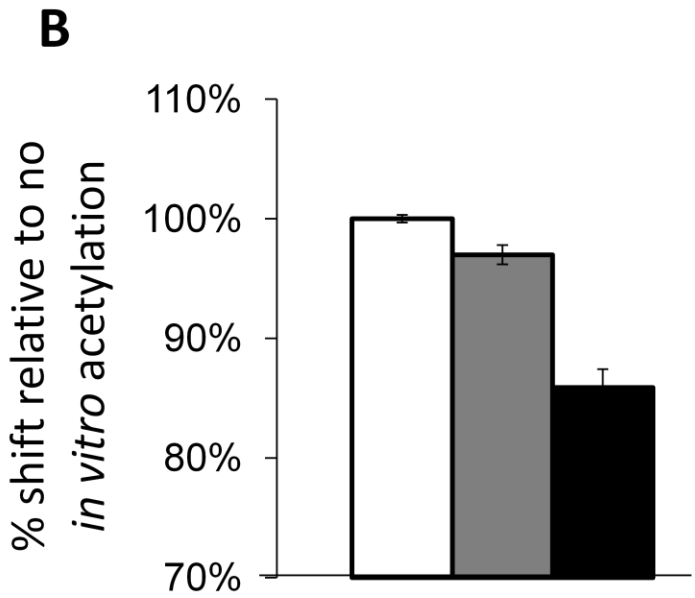
B
% shift relative to no
in vitro acetylation
110%
100%
90%
80%
70%

Figure 21. The effect of RcsB acetylation on RcsB phosphorylation *in vitro.*
A) *In vitro* acetylation followed by *in vitro* phosphorylation with increasing concentrations of AcP. 50 µl reactions of purified 20 µM RcsB were incubated in the absence of AcCoA (white bars), in the presence of 0.4 mM AcCoA (grey bars), or in the presence of AcCoA and 2 µM YfiQ (black bars) for 1 hour at 37°C. Fractions of these reactions were used for *in vitro* phosphorylation incubating each with AcP at 0, 1.25 mM, 2.5 mM, and 5 mM for 30 minutes at 30°C. The proteins were resolved by 13% SDS-PAGE at 4°C and stained with Coomassie brilliant blue. The values represent the percent phosphorylated shift relative to the total signal intensity (shifted and unshifted bands). Quantification was performed using AlphaView.
B) *In vitro* acetylation with AcCoA (grey bars) or AcCoA and YfiQ (black bars) followed by *in vitro* phosphorylation with 5 mM AcP. Reactions were performed in duplicate and set up as described for Figure 21A. The absence of *in vitro* acetylation (white bar) was set to 100%. The values represent the averages and the standard deviation.

Biochemical and Functional Analysis of YfiQ on RcsB and *rprA* transcription

Introduction

RcsB is acetylated *in vivo* and its acetylation is regulated by CobB and AckA (218). Since YfiQ was reported to acetylate RcsB on Lys-180 in the DNA binding domain, using AcCoA as the acetyl donor *in vitro* (49), YfiQ may regulate RcsB acetylation *in vivo.* However, Lys-180 was not the only acetylated site nor was Lys-180 the most common or highly acetylated site. Therefore, I repeated the reported *in vitro* experiment, investigating the effect of purified YfiQ on the acetylation status of purified RcsB. To determine if YfiQ acetylated and thus regulated RcsB activity *in vivo*, I tested if the RcsB acetylation profile depended on YfiQ and determined if YfiQ regulated *rprA* transcription.

In vitro acetylation of RcsB with YfiQ and AcCoA

To investigate the effect purified YfiQ on the acetylation status of purified RcsB, Dr. Ekaterina Filippova, a post-doctoral fellow in the laboratory of our collaborator Wayne F. Anderson at Northwestern University, first purified His6-tagged RcsB using gel filtration chromatography, finding that the 23.7 kDa RcsB purified from WT *E. coli* cells resolved into two peaks with estimated molecular mass values of 100 kDa (high molecular weight or peak 1 (RcsB-1)) and 60 kDa (low molecular weight or peak 2 (RcsB-2)) (**Figure 22A**). Dynamic light scattering revealed that monodisperse solutions of RcsB-1 and RcsB-2 have globular species with exclusion radii of 8.9 nm and 7.2 nm, respectively (**Figures 22B and 22C)**.

Taken together, these results are consistent with the formation in solution of both tetramers (RcsB-1) and dimers (RcsB-2).

To determine whether RcsB could be a substrate of YfiQ, Dr. Misty L. Kuhn, another post-doctoral fellow from Dr. Anderson's laboratory, used a biochemical assay that detects AcCoA hydrolysis (188). For both oligomers, AcCoA hydrolysis increased as the concentration of RcsB was increased; incubation of 0.02 mM YfiQ with 15 times the concentration of RcsB (0.30 mM) hydrolyzed more AcCoA than in the presence of equimolar amounts of RcsB (0.02 mM) (**Figure 23B**). This behavior indicates that RcsB can be a substrate of YfiQ.

To identify the RcsB lysines acetylated in the presence of YfiQ, we used mass spectrometric analysis (184,219). Following incubation of either RcsB oligomer with YfiQ and AcCoA, we observed acetylation of Lys-180, consistent with the previous report that YfiQ acetylates Lys-180 *in vitro* (49), but we also observed YfiQ-dependent acetylation of several other RcsB lysines: Lys-125, Lys-127, Lys-149 and Lys-186 (**Table 5, Tables S8C and F** in (218)). Surprisingly, incubation with both AcCoA and YfiQ did not dramatically change the abundance of acetylated lysines relative to incubation with AcCoA alone (**Table 5, Tables S8B and E** in (218)). Anti-acetyl-lysine immunoblot analysis yielded a similar result (**Figure 23A**, compare lanes 9 and 10 to lanes 5 and 6). Instead, the pattern of acetylation changed. For some residues, the level of acetylation increased relative to their status after incubation with AcCoA alone. For other residues, the acetylation decreased (**Table 5**). For example, both RcsB-1 and RcsB-2 exhibited increased SC for acetylated Lys-

125, Lys-180, and Lys-186. In contrast, the SC for acetylated Lys-140 of RcsB-1 decreased by more than five-fold (**Table 5**).

In vitro analysis of YfiQ and the effect of incubation with AcCoA

Anti-acetyllysine immunoblot analysis detected acetylation of purified YfiQ (**Figure 23A**, lane 1). This suggests that YfiQ was acetylated under the conditions used for purification. Indeed, Orbitrap Velos mass spectrometric analysis (184,219) detected 8 acetylated lysines in YfiQ **(Table 6)**.

When YfiQ was incubated with AcCoA, YfiQ acetylation increased (**Figure 23A,** compare lane 2 to lane 1, **Tables S9D and E** in (218)), suggesting that YfiQ might autoacetylate, consistent with reports that some KATs autoacetylate (222-224). Mass spectrometry revealed 11 acetylated lysines, the eight that were acetylated with YfiQ alone plus three more: Lys-13, Lys-149 and Lys-447 (**Table 6, Tables S9C-D** in (218)). In the presence of AcCoA, an average of 39 total SC of acetylated lysines were detected, an increase of nearly two-fold relative to YfiQ without AcCoA (average total 20 SC). Most notably, the acetylated Lys-146 peptide was six-fold more abundant when AcCoA was included in the reaction. We conclude that YfiQ is acetylated on multiple residues and that, like some other protein acetyltransferases (224,225), YfiQ may be regulated by autoacetylation when provided with its acetyl donor AcCoA.

In vitro analysis of RcsB and the effect of incubation with AcCoA

Anti-acetyl-lysine immunoblot analysis also detected acetylation of RcsB-1 and RcsB-2, but this acetylation was only visible after a long exposure (**Figure 23C**),

suggesting that the proportion of RcsB that is acetylated under the conditions used for purification is low. The number of acetylated lysines (10 acetylated lysines in RcsB-1 **(Table 5, Table S8A** in (218)) and 9 acetylated lysines in RcsB-2 **(Table 5, Table S8D** in (218)), the abundance of acetylation, or the average total SC of acetylated peptides (RcsB-1 (22 SC) and RcsB-2 (20 SC)), and the distribution of acetylation were similar between RcsB-1 and RcsB-2, suggesting that the oligomeric structure of RcsB plays a minor role in the regulation of acetylation.

For both RcsB oligomers, incubation with AcCoA dramatically increased acetylation (**Figure 23A,** compare lanes 5 and 6 to lanes 3 and 4) and increased the abundance of acetylated RcsB peptides by about two-fold (**Table 5, Tables S8B and E** in (218)). This observation suggests that RcsB may autoacetylate in the presence of AcCoA, similar to what is reported for the chemotaxis RR CheY, one of the first bacterial proteins to be discovered as regulated by acetylation (46).

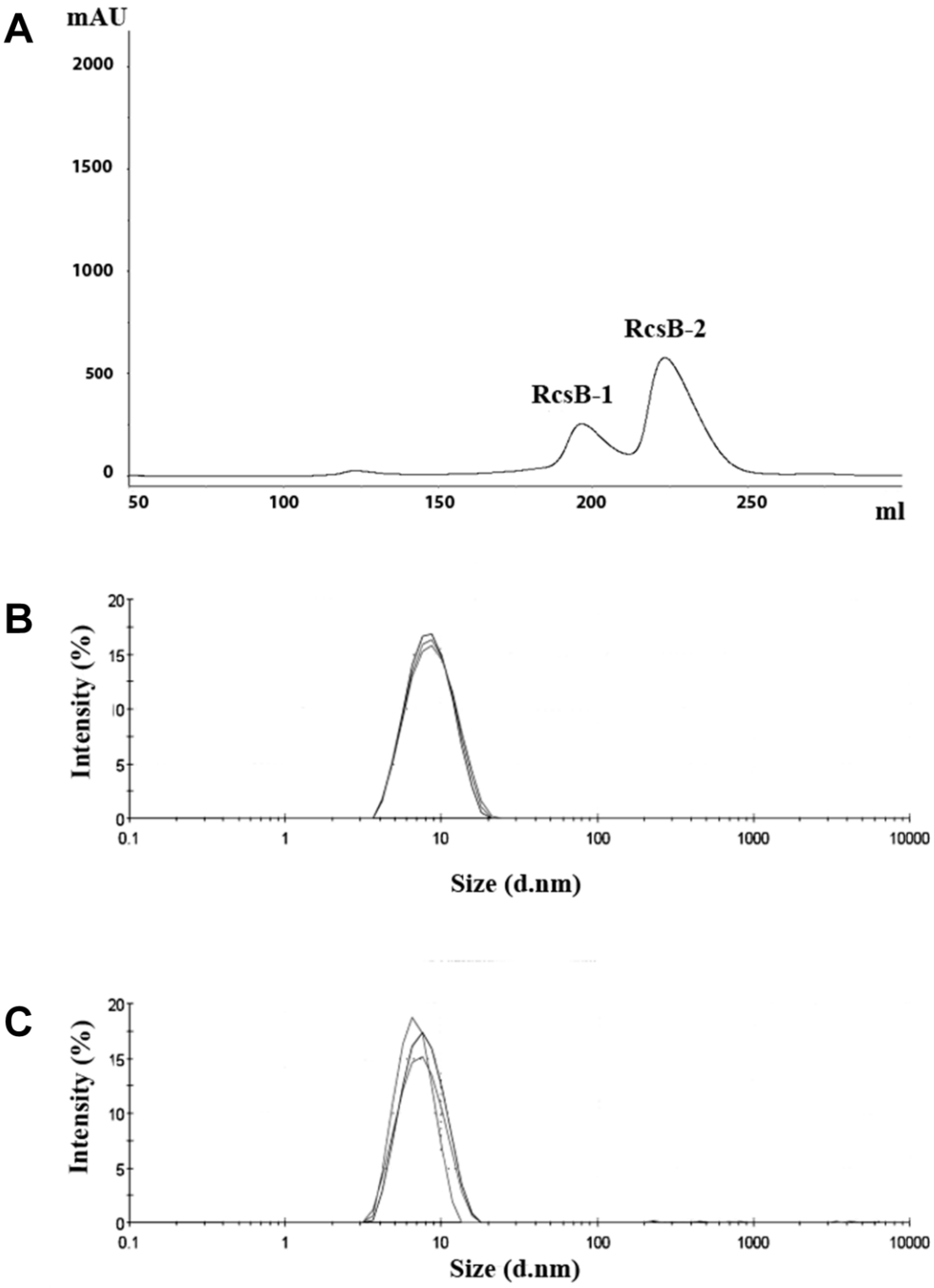
A
mAU
2000
1500
1000
500
0
RcsB-2
RcsB-1
50
100
150
200
250
ml
B
Intensity (%)
20
15
10
5
0
0.1
1
10
100
1000
10000
Size (d.nm)
C
Intensity (%)
20
15
10
5
0
0.1
1
10
100
1000
10000
Size (d.nm)

Figure 22. Gel filtration and dynamic light scattering analysis of RcsB.
Dr. Ekaterina Filippova performed these analyses on purified RcsB1 and RcsB2.
A) Elution profile at 280 nm of the purified RcsB protein in 10 mM Bis–Tris, 500 mM Sodium Chloride, pH 8.3. Flow rate 3.2 ml/min on a gel filtration column (Superdex) attached to FPLC system.
B) Distribution of scattering intensity for RcsB peak 1 (RcsB-1) at ~ 1.0 mg/ml. The estimated molecular weight of RcsB-1 is 110 kDa (tetramer).
C) Distribution of scattering intensity for RcsB peak 2 (RcsB-2) at ~ 1.0 mg/ml. The estimated molecular weight of RcsB-2 is 67 kDa (dimer).

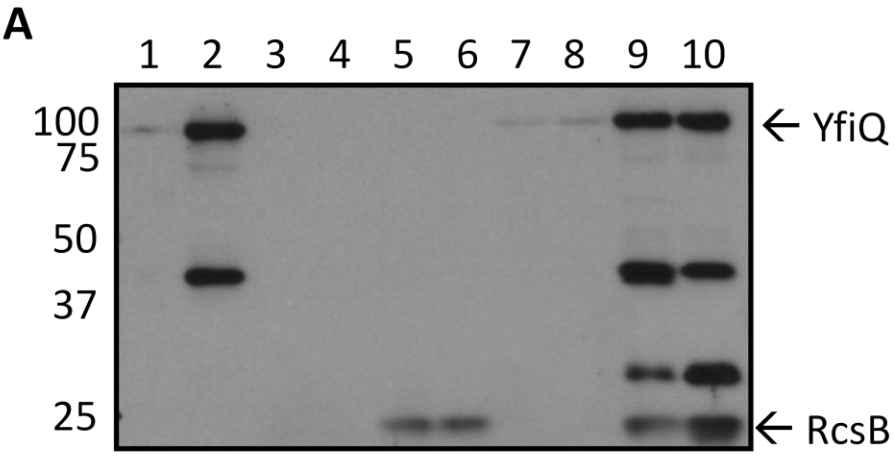
A
1 2 3 4 5 6 7 8 9 10
100
75
50
37
25
← YfiQ
← RcsB

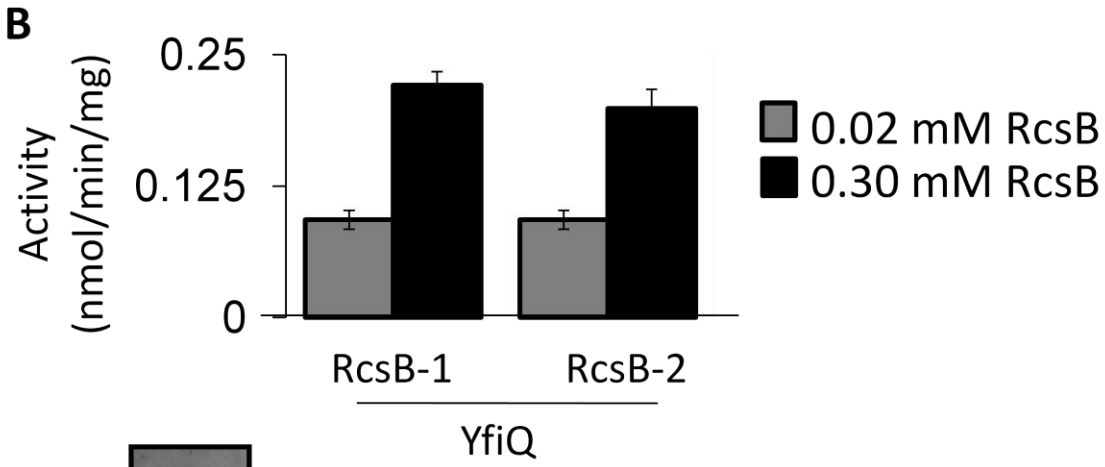
B
Activity (nmol/min/mg)
0.25
0.125
0
RcsB-1
RcsB-2
YfiQ
0.02 mM RcsB
0.30 mM RcsB

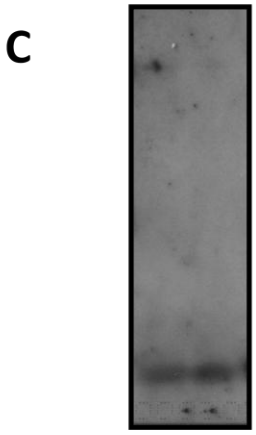
C

Figure 23. *In vitro* acetylation of RcsB

A) *In vitro* acetylation reactions with RcsB, YfiQ, and AcCoA. 50 µl reactions of 21 µM RcsB-1 or -2, 2 µM YfiQ, and 0.4 mM AcCoA were incubated at 37°C for 2 hours. The reactions were quenched with 50 µl 2X SDS-PAGE loading buffer and heated at 95°C for 5 minutes. 15 µl was resolved by 13% SDS-PAGE, proteins were transferred, and acetylated proteins detected by Western immunoblot with anti-acetyl-lysine antibody. Lane 1: YfiQ alone, lane 2: YfiQ + AcCoA, lane 3: RcsB-1 alone, lane 4: RcsB-2 alone, lane 5: RcsB-1 + AcCoA, lane 6: RcsB-2 + AcCoA, lane 7: YfiQ + RcsB-1, lane 8: YfiQ + RcsB-2, lane 9: YfiQ + RcsB-1 + AcCoA, lane 10: YfiQ + RcsB-2 + AcCoA. These results are representative of three independent experiments. The high molecular weight signal in lanes 1, 2, 9 and 10 corresponds to acetylated YfiQ. The acetylated sites were determined using semi-quantitative mass spectrometry (**Tables S9A-E,** (218)). Mass spectrometry also identified the signal visible between the 37-50 kDa markers in lanes 2, 9 and 10 as the 43.3 kDa EF-Tu protein and determined the acetylated sites (**Table S10,** (218)**)**. Mass spectrometry identified the signal between the 25-37 kDa markers in lanes 9 and 10 as the 29.9 kDa RplB protein and determined its acetylated sites (**Table S11,** (218)).

B) Activity of YfiQ using different concentrations of RcsB1 and RcsB2. Reactions were performed using 0.02 mM YfiQ at 25°C for one hour in a 50 µl reaction volume. To initiate the reaction, 0.5 mM AcCoA was used. Activity (nmol/min/mg) is shown as the average of three separate trials. Black bars correspond to 0.02 mM RcsB and red bars to 0.3 mM RcsB. Dr. Misty Kuhn at Northwestern University performed these experiments.

C) Purified RcsB acetylation is detectable by anti-acetyl lysine Western immunoblot analysis. A longer exposure time (5 minutes) of the blot from Figure 23A, showing lanes 3 and 4, which contains purified RcsB peak 1 and peak 2, respectively.

Table 5. Spectral counts of acetylated peptides of RcsB[1,4]

Acetylated lysine	RcsB-1					RcsB-2				
	Average SC[2]			SC Ratio[2]		Average SC			SC Ratio	
	Control	AcCoA	AcCoA+ YfiQ	AcCoA /control	AcCoA+YfiQ /AcCoA	control	AcCoA	AcCoA+ YfiQ	AcCoA /control	AcCoA+YfiQ /AcCoA
63	2.0	1.0	0.0	*0.5*[3]	*0.0*	0.0	0.0	0.0	NA	NA
72	2.0	2.0	1.5	1.0	0.8	0.5	2.5	1.5	**5.0**	*0.6*
118	5.5	7.0	10.0	1.3	1.4	6.0	8.5	10.5	1.4	1.2
125	2.0	4.0	13.5	**2.0**[3]	**3.4**	3.0	4.0	9.0	1.3	**2.3**
127	0.0	1.0	2.0	**>1.0**	**2.0**	0.0	1.0	2.0	**>1.0**	**2.0**
128	3.0	4.0	6.0	1.3	1.5	1.5	4.5	7.0	**3.0**	1.6
140	0.5	19.0	3.0	**38.0**	*0.2*	0.0	3.0	3.5	**>3.0**	1.2
149	1.0	2.0	5.0	**2.0**	**2.5**	2.5	5.0	5.0	**2.0**	1.0
154	3.5	8.0	4.5	**2.3**	*0.6*	3.0	6.5	5.0	**2.2**	0.9
173	2.0	2.0	2.5	1.0	1.3	1.0	2.5	2.0	**2.5**	0.8
180	0.5	1.0	6.0	**2.0**	**6.0**	1.5	2.5	6.5	1.6	**2.3**
186	0.0	1.0	3.0	**>1.0**	**3.0**	1.0	0.5	2.5	*0.5*	**5.0**
Total SC	22	52	57	**2.4**	1.1	20	40.5	54.5	**2.0**	1.3

[1]Average spectral counts (SC) of detected lysine acetylation sites in purified RcsB (control), and purified RcsB incubated with AcCoA (AcCoA) or purified RcsB incubated with AcCoA plus YfiQ (AcCoA+YfiQ).
[2]Using data obtained from Scaffold 3 proteome software, the spectral counts of two replicates for each condition were counted manually, were averaged over the two replicates, and were compared as the ratio of SC detected for RcsB incubated with AcCoA or with AcCoA and YfiQ relative to SC detected with purified RcsB alone.
[3]When the SC of a peptide with an acetylated lysine following AcCoA incubation is substantially more than the SC of the same peptide in the absence of AcCoA or if the SC of a peptide with an acetylated lysine following incubation with both AcCoA and YfiQ is substantially more than the SC of the same peptide in the presence of AcCoA alone, the ratio is underlined. If the ratio is substantially less, then the ratio is italicized. A ratio of >n refers to any acetylated peptide that was not detected in the absence of AcCoA (SC=0), but detected in the presence of AcCoA (SC=n).
[4]The spectral counts of the detected lysine acetylation sites in each replicate and the peptide scores and mass deviations as well as the complete MS/MS spectra and fragment ion series can be found in **Tables S10A-F (218)**, where A-C respectively denote RcsB-1 alone, RcsB-1 incubated with AcCoA, and RcsB-1 incubated with both AcCoA and YfiQ, and D-F respectively denote RcsB-2 alone, RcsB-2 incubated with AcCoA, and RcsB-2 incubated with both AcCoA and YfiQ.

Table 6. Spectral counts of acetylated peptides of purified YfiQ[1,4]

Acetylated lysine	Average SC[2]		SC Ratio[2]
	Control	AcCoA	AcCoA/Control
13	0.0	0.5	>0.5
23	3.5	4.0	1.1
146	0.5	3.0	6.0[3]
149	0.0	2.5	>2.5
228	1.5	3.5	2.3
234	5.5	8.5	1.6
447	0.0	1.0	>1.0
635	5.0	8.0	1.6
637	1.0	3.0	3.0
748	0.5	1.0	2.0
819	2.5	4.0	1.6
Total SC	20.0	39.0	2.0

[1]Average spectral counts (SC) of detected lysine acetylation sites in purified YfiQ (Control), and purified YfiQ incubated with AcCoA (AcCoA).
[2]Using data obtained from Scaffold 3 proteome software, the spectral counts of two replicates for each condition were counted manually, were averaged over the two replicates, and were compared as the ratio of SC detected for YfiQ incubated with AcCoA relative to SC detected with YfiQ alone.
[3]When the SC of a peptide with an acetylated lysine following AcCoA incubation is more than the SC of the same peptide in the absence of AcCoA, the ratio is underlined. A ratio of >n refers to any acetylated peptide that was not detected in the absence of AcCoA (SC=0), but detected in the presence of AcCoA (SC=n).
[4]The spectral counts of the detected lysine acetylation sites in each replicate and the peptide scores and mass deviations as well as the complete MS/MS spectra and fragment ion series can be found in Tables S9B-C and S9D-E (218), where B-C (YfiQ in the absence of AcCoA) and D-E (YfiQ in the presence of AcCoA) denote two replicates.

Additional acetylated proteins

Although RcsB and YfiQ were relatively pure, both proteins included co-purified proteins that were acetylated in the *in vitro* acetylation reactions. Since these acetylated proteins may be physiologically relevant, we used mass spectrometry to identify the protein and to determine the sites of acetylation. Incubation of YfiQ with AcCoA revealed two prominently acetylated bands, with molecular masses about 30 and 40 kDa (**Figure 23A,** lanes 2, 9, and 10). Mass spectrometry identified the smaller protein as the 50S ribosomal subunit protein L2 RplB and the larger protein as the elongation factor EF-Tu (data not shown). RplB co-purified with RcsB and was acetylated on residues Lys-8, Lys-23, and Lys-156 (**Table S10** (218)). EF-Tu co-purified with YfiQ and was acetylated on Lys-177 (**Table S11** (218)), confirming the reports that EF-Tu is acetylated (34,35).

Testing the effect of the lysine acetyltransferase YfiQ on P*rprA* activity

It was reported that YfiQ can acetylate RcsB *in vitro* on one lysine (Lys-180) and inhibit its ability to bind DNA (49) and we were able to independently corroborate these results. However, we found that RcsB is acetylated on multiple lysines *in vivo*. Of these acetylated residues, Lys-180 was not the most acetylated (**Table 2**). These results suggested that the regulation of RcsB by YfiQ *in vivo* may be different than *in vitro* and that YfiQ may not be a physiological regulator of RcsB acetylation. I therefore tested if YfiQ affected P*rprA* activity by deleting *yfiQ*. Contradicting the proposed inhibitory function of YfiQ on RcsB that was demonstrated *in vitro* (49), when *yfiQ* was deleted, P*rprA* activity was reduced (**Figure 24A**). This result suggests that YfiQ activates *rprA* transcription. I also

overexpressed YfiQ and monitored P*rprA* activity. When YfiQ was overexpressed, P*rprA* activity was inhibited, consistent with the reported inhibitory effect of YfiQ on RcsB activity (**Figure 24B**). These results could be explained if the concentration of YfiQ or the level of YfiQ acetyltransferase activity dictates whether *rprA* transcription, which requires RcsB, is inhibited or activated. The other possibility is that overexpression can lead to artifacts that may be misleading.

Analysis of RcsB acetylation in the *yfiQ* null mutant

We propose that YfiQ activates *rprA* transcription. This proposal contradicts the previous report showing that YfiQ inhibits RcsB binding to DNA *in vitro* (49). To determine if YfiQ affects RcsB acetylation *in vivo*, I isolated RcsB from the *yfiQ* mutant and compared the acetylation profile to RcsB isolated from WT cells using mass spectrometry. While not identical, the lysine acetylation sites were quite similar between WT cells and the *yfiQ* mutant (**Table 4, Tables S7A-B** in (218)). Most notably, the overall SC for the *yfiQ* mutant and its parental strain were identical (average total 8.5 SC) and there was no substantial change in the SC for individual acetylated lysines. Thus the acetyltransferase appears to have no effect on the acetylation status of RcsB *in vivo* in this growth condition. We propose that YfiQ enhances *rprA* transcription by acetylating a protein other than RcsB.

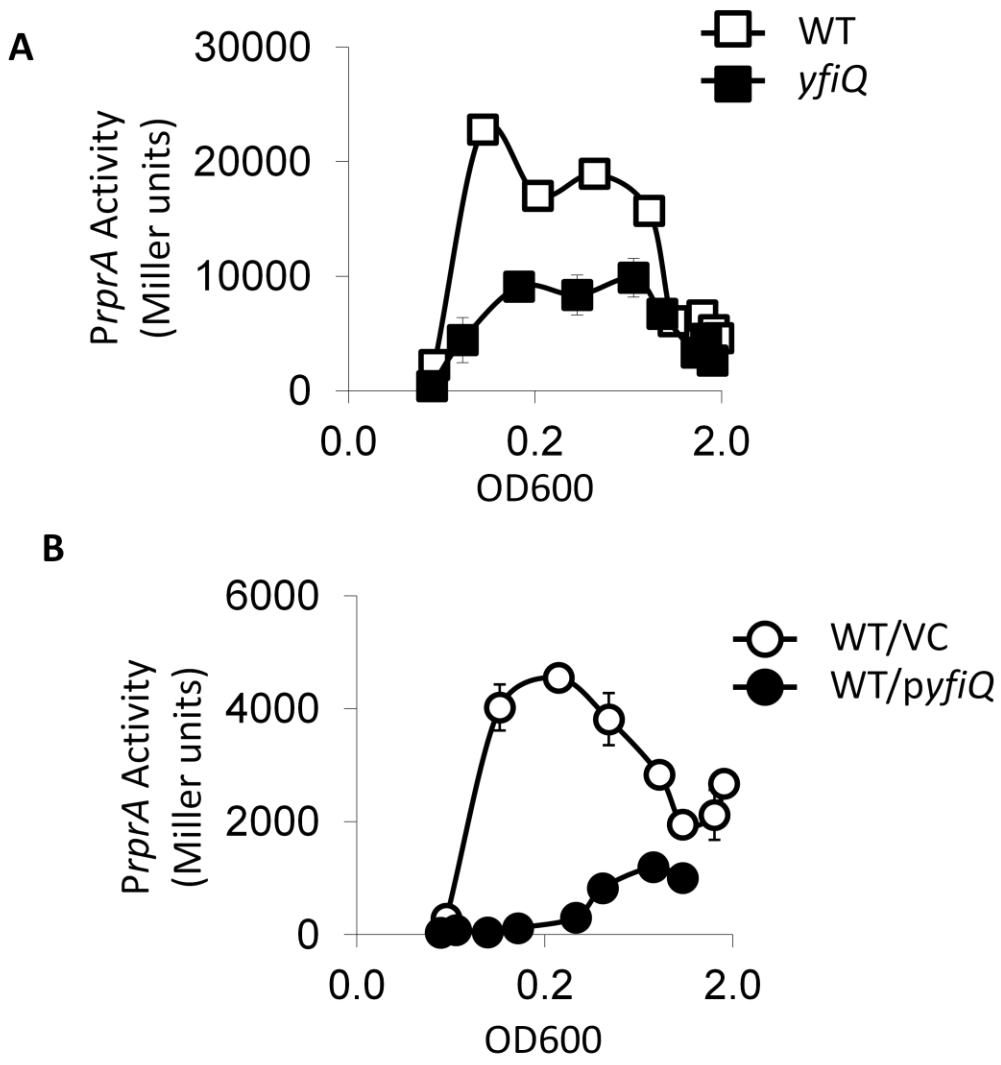

Figure 24. The effect of YfiQ on *rprA* promoter activity

A) P*rprA* activity of WT cells (AJW3759) and the isogenic *yfiQ* null mutant (AJW3797) were grown at 37°C in TB7 with shaking. Samples were harvested for OD600 and β-galactosidase activity measurements. The values represent the average promoter activity of triplicate independent cultures and error bars indicate standard deviations.

B) P*rprA* activity of WT cells (AJW3759) transformed with the YfiQ expression plasmid pCA24n-*yfiQ* (p*yfiQ*) or the pCA24n (VC) were aerated at 37°C in TB7 supplemented with 10 μM IPTG to induce *yfiQ* expression. Samples were harvested for OD600 and β-galactosidase activity measurements. Values represent triplicate independent cultures and standard deviations.

Summary

I confirmed that RcsB is acetylated by YfiQ and AcCoA *in vitro* and that Lys-180 was sensitive to YfiQ. However, I also showed that YfiQ does not appear to regulate RcsB acetylation *in vivo*. The acetylation of RcsB and YfiQ increased in the presence of AcCoA alone, suggesting that autoacetylation may regulate RcsB and YfiQ. Autoacetylation may regulate YfiQ activity, consistent with what has been reported for some eukaryotic acetyltransferases. If autoacetylation regulates RcsB, then RcsB would be the second bacterial protein known to be regulated by autoacetylation, along with the chemotaxis RR CheY (46).

The effect of the spermidine acetyltransferase SpeG on *rprA* regulation

Introduction

GNATs possess conserved sequence motifs and can acetylate many substrates, including proteins but also aminoglycosides (e.g. amikacin), arylalkylamines (e.g. serotonin), and polyamines (e.g. spermidine) (63). In *E. coli*, there are 23 genes that encode GCN5 homologs. 8 are known acetyltransferases and 15 are putative acetyltransferases. 4 of the known acetyltransferases are protein acetyltransferases: RimI, RimJ, and RimL, which are known to acetylate the N-terminus of some ribosomal proteins; YfiQ is the only GNAT that has been reported to exhibit Nε-lysine acetyltransferase activity. YfiQ has been reported to acetylate RcsB *in vitro* (49,218). Despite these biochemical results, there was no physiological evidence for YfiQ acetylating RcsB (**Table 4, Tables S7A-B**, (218)). To determine if some other GNAT impacts *rprA* transcription, I performed a genetic screen of the known and putative GNAT and then determined the mechanism through which one candidate, the spermidine acetyltransferase SpeG, regulated *rprA* transcription.

Determining the effect of overexpressing known and putative acetyltransferases on *rprA* promoter activity

Since a *cobB* mutant increased RcsB acetylation and reduced P*rprA* activity compared to WT cells grown in TB7, I reasoned that if an acetyltransferase did regulate *rprA* transcription, then the acetyltransferase is likely an inhibitor that may

acetylate RcsB. I transformed the WT strain with an inducible plasmid (pCA24N vector) carrying each of the known or putative acetyltransferase genes, 21 of which are available from the ASKA plasmid library collection of *E. coli* open reading frames (185). With the help from a student from Kenyon College, Sarah Cook, these transformants were grown in TB7 and β-galactosidase activity from the P*rprA-lacZ* fusion was measured throughout growth and peak P*rprA* activity during exponential phase was analyzed. Compared to WT cells transformed with the vector control, we observed four general effects of overexpressing the known and putative GNATs on the *rprA* promoter. Overexpression of four known or putative GNATs (*speG*, *rimJ*, *yiiD*, and *yfiQ*) had the greatest impact on P*rprA* activity, reducing activity by almost 80% (**Figure 25**, white bars). The overexpression of seven GNAT genes reduced average promoter activity by approximately 50% or more (**Figure 25,** light gray bars), while five of the GNATs reduced average promoter activity by 20% - 40% (**Figure 25**, dark gray bars). The remaining five genes did not reduce the average promoter activity (**Figure 25**, black bars). Whether the latter subset of genes are actually expressed remains to be determined.

The effect of *speG* mutant on *rprA* promoter activity

The overexpression screen identified SpeG, RimJ, YiiD, and YfiQ as potential inhibitors of *rprA* transcription. Since the *yfiQ* mutation did not appear to affect RcsB acetylation *in vivo* (**Table 4, Tables S7A-B**, (218)), I considered the other three candidates. If one of these GNATs inhibits *rprA* transcription, then a null mutant

lacking that GNAT would be expected to exhibit higher promoter activity than WT cells. From a partial mutant screen, I observed that the *speG* mutant (AJW4589) exhibited increased P*rprA* activity compared to WT cells (AJW3759) (**Figure 26**). Peak exponential P*rprA* activity showed some variability, but the level of activity was always either equal to or greater than WT or the peak activity occurred earlier in the mutant cells than in the WT cells (data not shown). The results suggest that SpeG can be an inhibitor of *rprA* transcription. This SpeG-mediated inhibition may be a conserved function, since overexpression of the *Vibrio cholerae* SpeG homolog (VCA0947) in *E. coli* cells also inhibited P*rprA* activity (**Figure 27**).

Determining the effect of spermidine on *rprA* transcription

SpeG is not known for acetylating proteins. Instead, SpeG is annotated as a spermidine acetyltransferase. Spermidine is a polyamine that is present in all organisms (226). In *E. coli*, spermidine is considered a toxic compound (227) that is neutralized by SpeG-mediated acetylation (spermidine metabolism pathway is shown in **Figure 28,** (228-230)). In the absence of *speG*, the level of spermidine increases (227). I therefore tested whether an increase in exogenous spermidine activates the *rprA* promoter by growing WT cells in the presence of increasing concentrations of spermidine. Instead of activating P*rprA*, exogenous spermidine inhibited (**Figure 29A**). This inhibition can occur through a SpeG-independent mechanism, as a *speG* mutant exhibited spermidine-mediated inhibition of P*rprA* activity (**Figure 29B**). In fact, in the absence of SpeG, P*rprA* may be more sensitive

to spermidine (compare **Figures 29A and B**). However, it should be noted that a direct comparison between WT and *speG* sensitivities to spermidine has not been performed. From these results, I propose that the activation of P*rprA* in a *speG* mutant is not due to an accumulation of spermidine.

Investigating if SpeG can affect *rprA* transcription in the absence of spermidine

The only known function of SpeG is to acetylate spermidine. I therefore tested if the inhibitory effect of SpeG on P*rprA* activity required spermidine. To reduce the intracellular level of spermidine, I deleted the gene that encodes the spermidine synthase SpeE. SpeE synthesizes spermidine from putrescine and decarboxylated-S-adenosylmethionine and SpeG acetylates spermidine using AcCoA as the acetyl donor (**Figure 28**). I compared P*rprA* activity in WT cells and in the isogenic *speG*, *speE*, and *speEG* mutants. The *speE* mutant behaved like WT cells (**Figure 26**), suggesting that spermidine is not required for P*rprA* activity. The *speEG* double mutant exhibited reduced P*rprA* activity compared to WT cells. This result suggests that (1) SpeG inhibition of *rprA* requires spermidine, which is consistent with the finding that exogenous spermidine inhibits *rprA* promoter activity (**Figure 29**), and that (2) in the absence of spermidine, SpeG activates *rprA* transcription (**Figure 26**, dark triangles). I propose that the level of spermidine determines whether SpeG inhibits or activates *rprA* transcription. Since SpeG affects

P*rprA* activity in the absence of its known substrate spermidine, I further propose that SpeG has a novel function.

SpeG does not appear to be a protein acetyltransferase

We originally hypothesized that the novel, spermidine-independent function of SpeG was protein acetylation. We based this hypothesis on the observation that spermidine and lysine have quite similar structures (**Figure 30**) and on the BLAST sequence analysis that suggests that SpeG is similar (e-value of 3e-0.6) to a human thialysine Nε-acetyltransferase called TLAT (or SSAT2), which can exhibit a spermidine-independent effect and can acetylate thialysines and lysines (231). However, I have not been able to provide evidence to support this hypothesis. First, mass spectrometry did not detect a change in RcsB acetylation when RcsB was isolated from the *speG* null mutant compared to WT cells (data not shown). Second, while our collaborator Dr. Misty Kuhn in the Anderson laboratory at Northwestern University demonstrated that purified, His6-tagged SpeG exhibited spermidine and spermine acetyltransferase activity, my immunoblot analysis did not detect an increase in RcsB acetylation when RcsB was incubated with purified SpeG and AcCoA (data not shown). Therefore, we concluded that SpeG is not a protein acetyltransferase and considered the possibility that the effect of SpeG on *rprA* transcription was independent of protein acetylation.

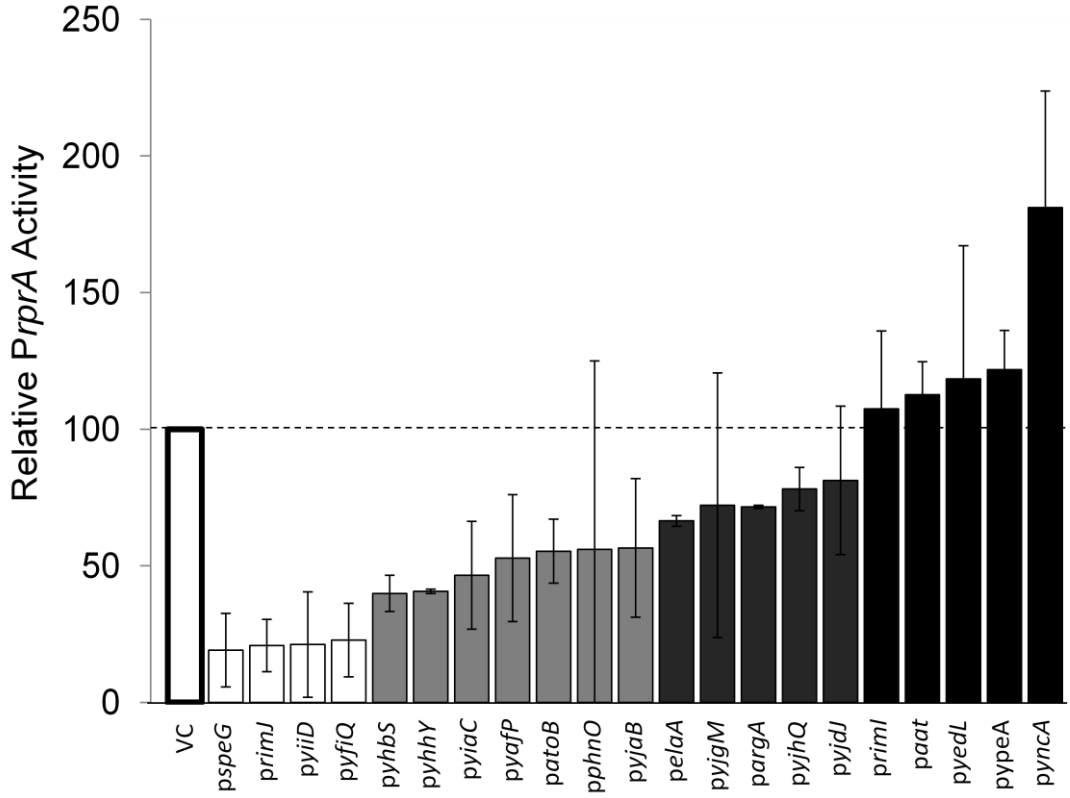

Figure 25. The effect of overexpressing putative or known GNATs on *rprA* promoter activity.

WT λ*rprA* cells (AJW3759) were transformed with either the pCA24n vector control (VC) or an IPTG-inducible plasmid carrying one of the 21 available putative or known acetyltransferase ORFs. Cells were grown in the presence of 5 μM IPTG and growth and promoter activity were assayed. The values represent the means of maximum early to mid-exponential growth +/- standard deviations of five independent experiments done in either duplicate, triplicate, or quadruplicate independent cultures standardized against the VC.

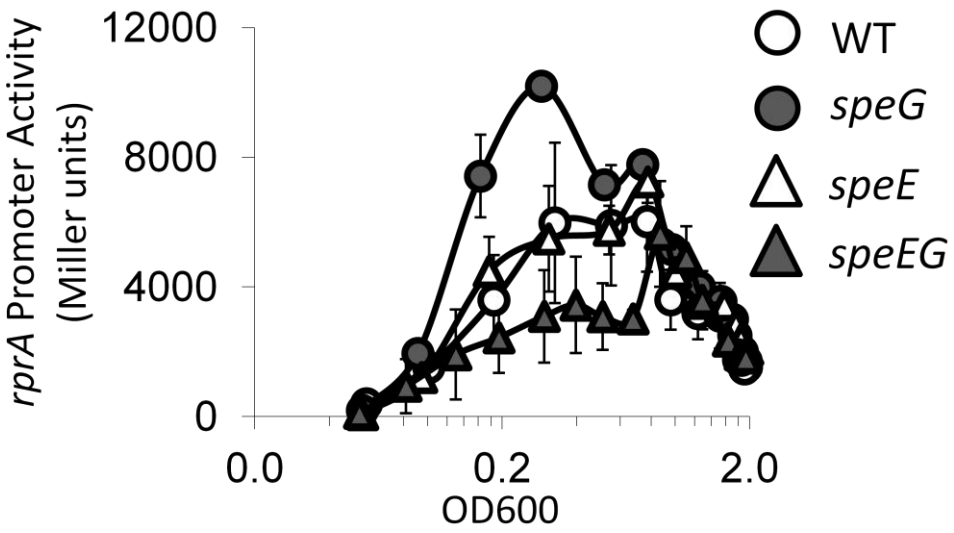

Figure 26. Analyzing the regulation of P*rprA* activity by the spermidine synthetase SpeE and the spermidine acetyltransferase SpeG
WT λ*rprA* cells (AJW3759) and isogenic *speG* (AJW4589), *speE* (AJW4533), or *speE speG* (AJW4592) strains were assayed for cell growth in TB7 and β-galactosidase activity. The values represent average promoter activity with standard deviations of triplicate independent WT, *speE*, and *speE speG* cultures and duplicate independent *speG* mutant culture. In the same experiment, three other, independently constructed *speG* mutants were tested in duplicate. Shown here is one clone that was representative of the four *speG* clones.

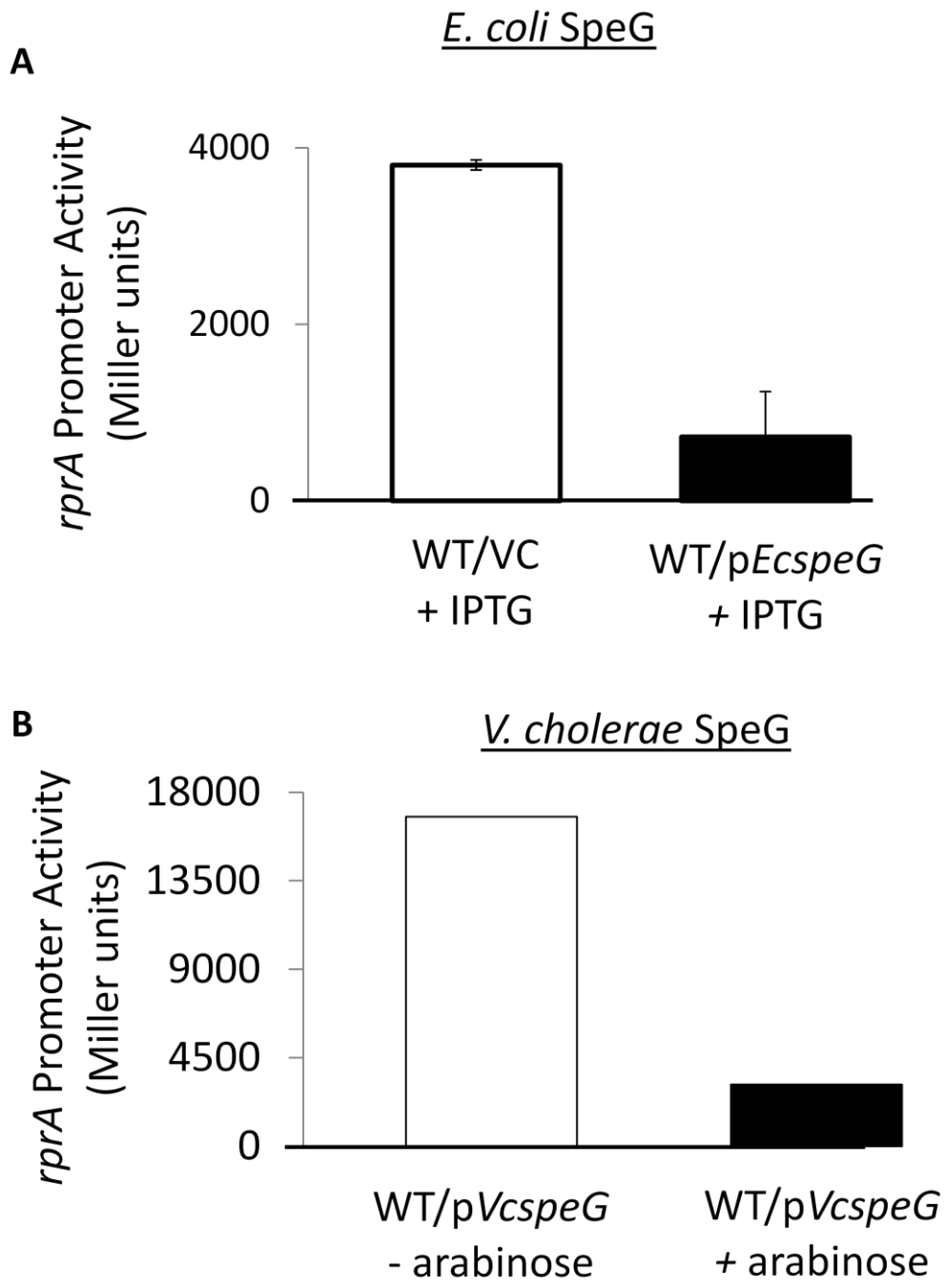

Figure 27. The effect of overexpressing *E. coli* or *V. cholera* SpeG on *rprA* promoter activity

A) P*rprA* activity of WT *E. coli* cells (AJW3759) transformed with the VC (pCA24n) or a plasmid that expresses *E. coli* SpeG under the control of an IPTG-inducible promoter (pCA24n-*speG*). The values represent average promoter activity at OD600 ~0.3 with standard deviation. This experiment was performed in duplicate.
B) P*rprA* activity of WT *E. coli* cells (AJW3759) transformed with a plasmid that expresses *Vibrio cholerae* SpeG under the control of an arabinose-inducible promoter (pBAD24-Vc0947). The values represent promoter activity at OD600 ~0.5 (+ 0.02% arabinose) and OD600 ~0.6 (no arabinose).

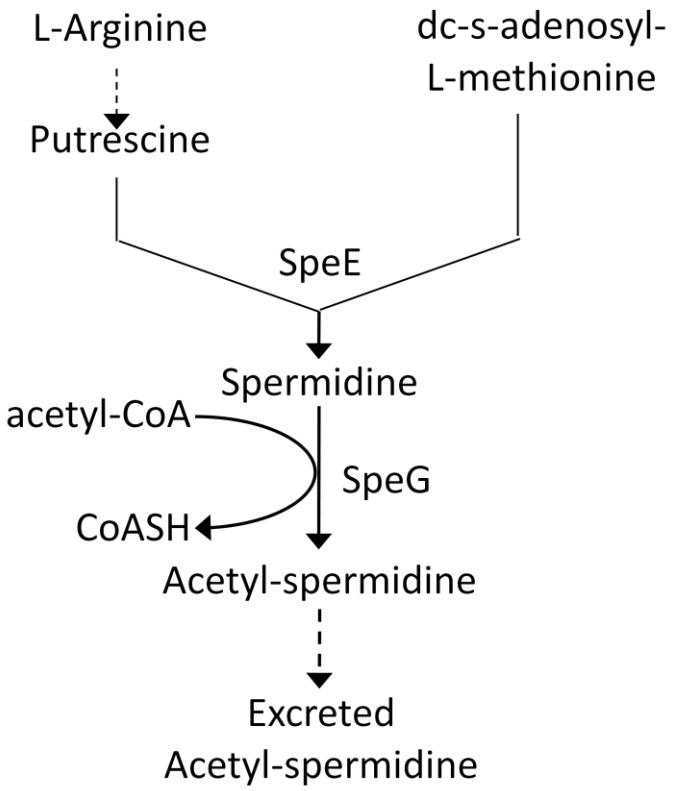

Figure 28. *E. coli s*permidine metabolism.
Arginine metabolism leads to putrescine production. Spermidine synthase SpeE converts putrescine and decarboxylated (dc)-S-adenosylmethionine to spermidine. SpeG acetylates spermidine using acetyl-coenzyme A. Acetylated spermidine is then excreted from the cell.

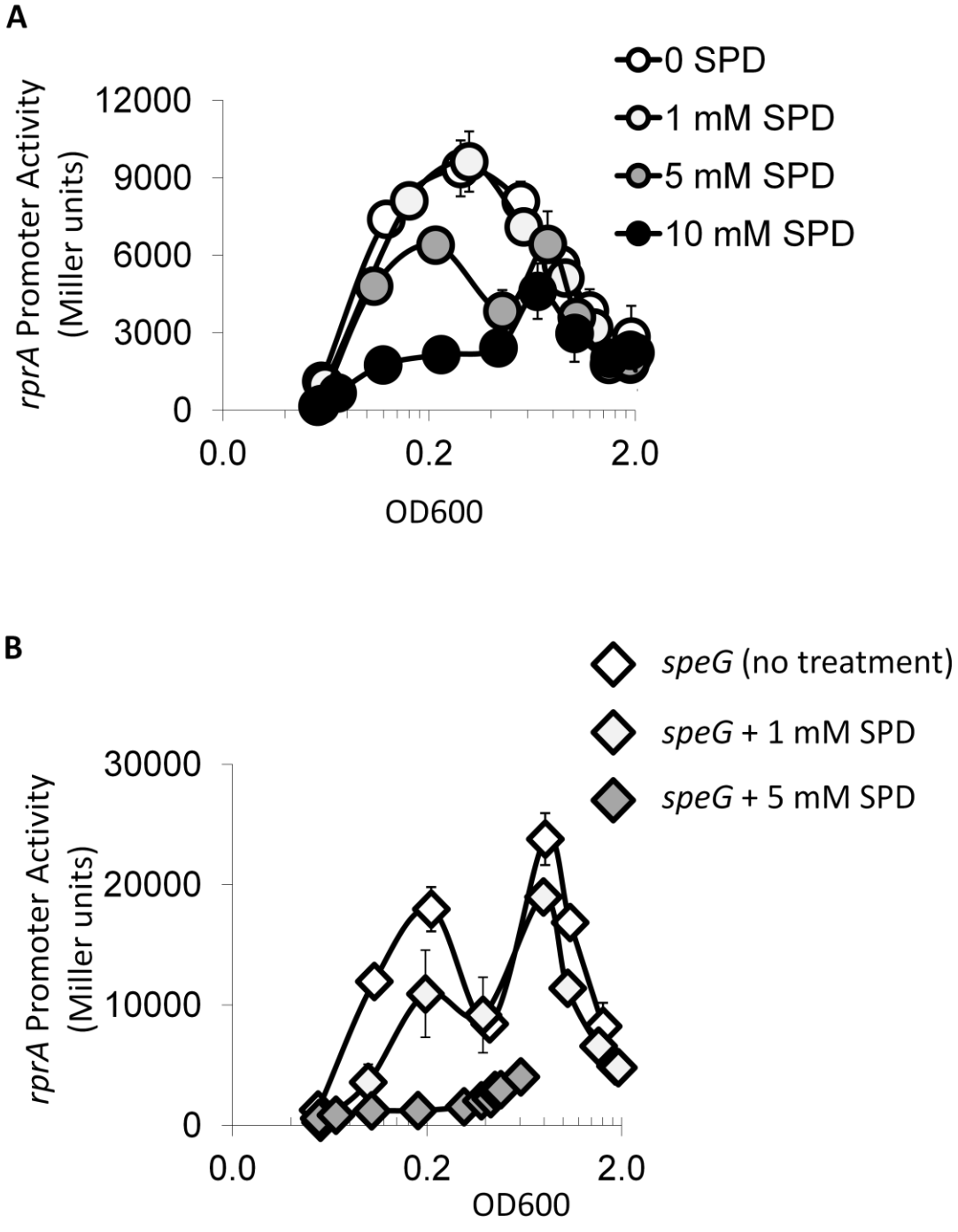
A
0 SPD
1 mM SPD
5 mM SPD
10 mM SPD
rprA Promoter Activity
(Miller units)
12000
9000
6000
3000
0
0.0
0.2
2.0
OD600
B
speG (no treatment)
speG + 1 mM SPD
speG + 5 mM SPD
rprA Promoter Activity
(Miller units)
30000
20000
10000
0
0.0
0.2
2.0
OD600

Figure 29. The effect of exogenous spermidine on *rprA* promoter activity
A) WT λ*rprA* cells (AJW3759) were aerated in TB7 supplemented with increasing concentrations of spermidine (SPD). The values represent average promoter activity with standard deviations of triplicate independent cultures.
B) The *speG* λ*rprA* mutant (AJW4589) was grown in TB7 in the presence of 0, 1 mM, or 5 mM SPD. Samples were harvested at regular intervals and were assayed for OD600 and β-galactosidase activity.

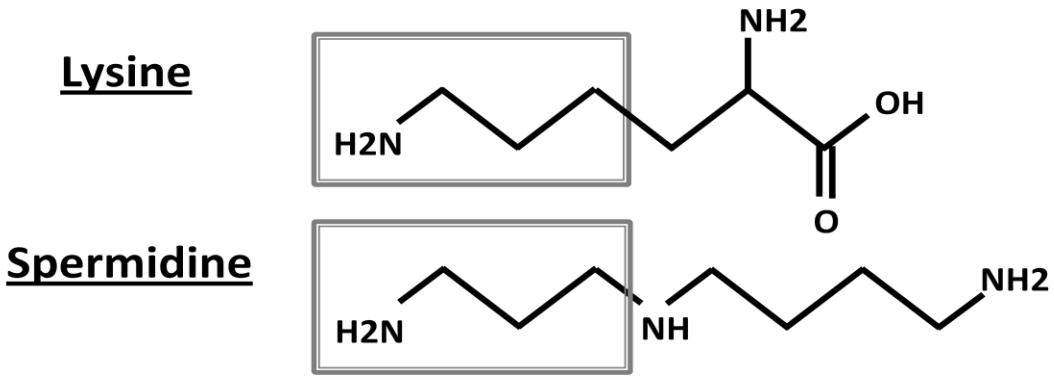

Figure 30. The structures of lysine and spermidine.
The boxed regions highlight the structural similarities between lysine and spermidine.

Functional analysis of RcsB on SpeG acetyltransferase activity

The possibility that SpeG affected *rprA* transcription led to a collaboration with Drs. Misty Kuhn and Ekaterina Filippova in the Anderson laboratory. The Anderson laboratory is part of the Center for Structural Genomics of Infectious Diseases and its primary goal is to determine the structures of proteins that can be representative of major protein families and then use structural analysis to understand biological function. They were able to crystallize SpeG from *Vibrio cholerae*, as a representative of the N-acyltransferase superfamily, and discovered that SpeG forms a dodecamer (Filippova *et al.* unpublished data). Kuhn measured SpeG spermine and spermidine acetyltransferase activity with Ellman's reagent (5,5'-dithiobis(2-nitro-benzoic acid)), which reacts with the free sulfhydryl group of CoA (188). If SpeG can acetylate its substrates using AcCoA, free CoA is release and

detected spectrophotometrically. They found that SpeG could acetylate spermine and spermidine and that when RcsB was present, SpeG acetyltransferase activity was inhibited through a direct interaction with RcsB (Kuhn and Hu *et al*., unpublished). Together, we propose that RcsB and SpeG can inhibit each other and that this interaction may have consequences on spermidine metabolism and regulation of the Rcs regulon.

Summary

I hypothesize that acetylation of RcsB inhibits *rprA* transcription. To identify acetyltransferases that could possibly regulate RcsB activity, I used a combination of overexpression and deletion analyses to screen more than 20 genes that had some sequence similarity to yeast KAT GCN5. While several GNAT family members inhibited P*rprA* activity, SpeG was the only candidate that, when deleted, activated the P*rprA.* From an epistasis analysis of SpeG and the spermidine synthase SpeE, I propose that SpeG inhibits *rprA* transcription when the level of spermidine is high and that SpeG can activate *rprA* transcription when spermidine is absent or low. However, SpeG inhibition of RcsB does not appear to involve protein acetylation; instead, SpeG and RcsB inhibit the other's function through some other mechanism. This study revealed novel functions for SpeG and RcsB as regulators of transcription and metabolism, respectively.

Analysis of AcP as an Acetyl Donor for Protein Acetylation in *E. coli*

Introduction

Protein acetylation is proposed to occur when AcCoA donates an acetyl group to the amino terminus of a lysyl side chain. However, it was reported in 1975 that AcP could non-enzymatically donate an acetyl to histone proteins (201). More recently, I reported that several RcsB lysines exhibit increased acetylation when the intracellular concentration of AcP is high (218) and Dr. Bruno Lima reported that an AcP phenotype involved the acetylation of certain lysine residues on RNA polymerase (48). We therefore hypothesize that AcP is an acetyl donor for protein acetylation in *E. coli.* Bozena Zemaitaitis tested this hypothesis and found that acetylation is dramatically increased especially during exponential growth when the concentration of AcP accumulates and that this increase in acetylation depended on AcP. These results are consistent with a recent report that demonstrated that AcP regulates *E. coli* acetylation (202). To determine if protein acetylation can occur by AcP, I performed *in vitro* acetylation of purified proteins. To determine if the primary amino acid sequence may regulate acetylation by AcP, I studied the AcP-sensitive sites identified by global quantitative mass spectrometry.

In vitro analysis of protein acetylation by AcP

Since global protein acetylation increases in the absence of *ackA*, a condition that accumulates intracellular AcP, and since this increase in acetylation depends on AcP, we hypothesize that AcP is an acetyl donor for protein acetylation in *E. coli.* I

tested this hypothesis by determining if AcP can donate acetyl groups to proteins *in vitro.* I used LpdA, a metabolic enzyme, to study AcP as a regulator of protein acetylation because the members of the Anderson laboratory at Northwestern University have purified LpdA in abundance and LpdA has proven to provide highly reproducible results. LpdA was analyzed by Drs. Brad Gibson and Birgit Schilling, research associate Dylan Sorensen, and bioinformaticist Alexandria D'Souza at The Buck Institute for Research on Aging using semi-quantitative mass spectrometry, spectral counting. They determined that LpdA was between 80-85% pure (mass spectrometric data not shown, **Figure 31A**). I incubated various concentrations of purified LpdA, with increasing concentrations of AcP for 1 hour at 37°C in 150 mM Tris HCl (pH 7.3 at room temperature), 10% glycerol, 10 mM $MgCl_2$, and 150 mM NaCl. To stop the reaction, an equal volume of 2X SDS loading buffer was added and the reactions were heated at 95°C for 10 minutes. I detected acetylation by anti-acetyl lysine immunoblot analyses. In the absence of AcP, some acetylation was detectable, indicating that LpdA is acetylated *in vivo* (**Figure 31**). *In vitro* acetylation increased with AcP concentration. An increase in acetylation was detected with as low as 5 mM AcP, a concentration of AcP that is comparable to the level of AcP that has been measured in WT *E. coli* cells (123). I have repeated this analysis, and I have not been able to saturate LpdA acetylation, even at the highest concentration tested, 80 mM AcP. Acetylation is also LpdA concentration-dependent, as an increasing amount of LpdA correlated with an increase in acetylation when AcP was held

constant at 80 mM (**Figure 31B**). This increase in acetylation is not due an artifact of basic pH, a condition that activates the lysine for acetylation through deprotonation, because pH decreases as AcP is hydrolyzed (**Figure 32**). Therefore, I conclude that AcP can donate acetyl groups to LpdA.

We also have found that other proteins are acetylated when incubated with AcP. I have preliminary evidence to suggest that purified RcsB is acetylated when incubated with AcP and Robert Davis (a graduate student in the Wolfe laboratory) has similar evidence for the transcription factor CRP. Similarly, Dr. Bruno Lima detected that certain subunits of purified RNA polymerase are acetylated in the presence of AcP. Finally, Dr. Misty Kuhn was able to demonstrate acetylation of the central metabolic enzymes GapA and TpiA by X-ray crystallography. Therefore, we propose that AcP can acetylate many proteins.

Kinetic analysis of LpdA acetylation in the presence of AcP

To study the reactivity of AcP with LpdA and its lysines, I characterized the kinetics of acetylation by AcP using LpdA. Physiologically relevant concentrations of AcP range between 3 mM in WT cells and 15 mM in the *ackA* mutant (123). Therefore, to study the kinetics of LpdA acetylation by AcP, I incubated 1.25 μM LpdA with increasing concentrations of AcP (0, 5, 10, 15, and 20 mM AcP) for various lengths of time at 37°C at pH 7. To accommodate the large number of samples and to avoid reduced reaction volumes due to condensation during long

incubation times, these *in vitro* protein acetylation reactions were performed using the PCR machine, which can hold many samples and has a hot lid. Acetylation was determined by both anti-acetyl lysine immunoblot analyses and quantitative mass spectrometry. The mass spectrometric analyses were performed in two technical replicates, on two independent experiments, by our collaborators at The Buck Institute for Research on Aging. LpdA acetylation was, again, AcP concentration-dependent, with the highest level of acetylation in the presence of 20 mM. When LpdA was incubated with 5 mM AcP for less than 1 hour, LpdA acetylation was not detectable by immunoblot analysis (**Figure 33A**) or by mass spectrometry (data not shown). Instead, acetylation using 5 mM AcP appears to require at least 1 to 2 hours to be detectable. Acetylation with 10, 15, and 20 mM AcP was detectable within 30 minutes to an hour (**Figure 33**). Using mass spectrometry, we monitored acetylated LpdA lysines over time with 10 and 20 mM AcP (**Figure 34**) and the fold increase in acetylation was measured relative to the no AcP control. Six LpdA lysine residues were detected to be acetylated in the presence of 10 mM AcP (**Figure 34A**). The kinetics of acetylation appear to be similar for each lysine, with acetylation occurring quickly within the first hour of incubation; from hours one to seven, the rates were similar and constant. The number of acetylated lysines and the rate of acetylation increased when LpdA was incubated with 20 mM AcP. In addition to five of the lysines that were detected to be acetylation with 10 mM AcP, six additional residues were acetylated with 20 mM AcP (**Figure 34B**). In contrast to the kinetics

of acetylation with 10 mM AcP, the rate of early acetylation (within the first hour) in the presence of 20 mM AcP, varied widely for each acetylated lysine: both Lys-229 and Lys-339 exhibited the slowest early rates of acetylation, the kinetics of which were comparable to acetylation performed with 10 mM AcP, while Lys-85, Lys-220, Lys-256, and Lys-284 were amongst those lysines that reacted quickly with AcP. Generally, the rates of acetylation remained constant after the first hour since the abundance of acetylation after 1 hour correlated with the early rates of acetylation for each lysine.

The amount of acetylation does not appear to be limited by AcP hydrolysis. Using a method (182) that I adapted from a published protocol (232,233), I measured the amount of AcP present in LpdA *in vitro* acetylation reactions. AcP acetylates hydroxylamine efficiently; the resultant acetyl hydroxamate reacts with ferric ions, which is detected spectrophotometrically at 540 nm. While AcP does deteriorate over time when incubated at 37°C, by 7 hours, the amount of remaining AcP is in excess relative to the number of available LpdA lysines in the reactions (**Figure 35**). For instance, after 7 hours, almost 4 mM AcP is present from a reaction that started with 10 mM AcP and 1.25 μM LpdA.

These data suggest that the concentration of AcP regulates the number of acetylated lysines, the rate of acetylation, and the abundance of acetylation. Additionally, these reactions were performed in the absence of an acetyltransferase,

suggesting that acetyl transfer from AcP occurs directly to lysines on proteins through a non-enzymatic reaction.

Analysis of the AcP-sensitive primary amino acid sequences

The mechanism that regulates the specificity of the non-enzymatic acetylation of lysines by AcP was unknown. We considered that the microenvironment surrounding the lysine can affect the reactivity of the lysine side chain. Under physiological pH, lysine predominately exists in its non-reactive, protonated state. The capacity for lysine to act as a nucleophile and attack the carbonyl carbon on AcP is dependent on the deprotonation of the lysine side chain. Activating the lysine side chain can occur by the presence of neighboring amino acids acting as a general base at neutral pH. We thus determined whether specificity of acetylation is regulated by the primary amino acid sequence.

I determined if an acetylation motif existed *in vivo*. I analyzed the acetylated sites identified by our collaborators at the Buck Institute using quantitative mass spectrometry, comparing 543 sites that were identified in at least 3 out of 4 bioreplicates and exhibited at least a 2-fold increase in acetylation in the *ackA* mutant compared to its WT parent, with a P value <0.05. A sequence logo using the primary amino acid sequence, from -10 to +10 relative to the acetylated lysine, was generated using WebLogo, a web-based application developed at University of California-Berkley to identify consensus motifs (234). There was a high prevalence

of negatively charged residues (glutamate and aspartate) in the -1 position, adjacent to the acetylated lysine residue (**Figure 36**).

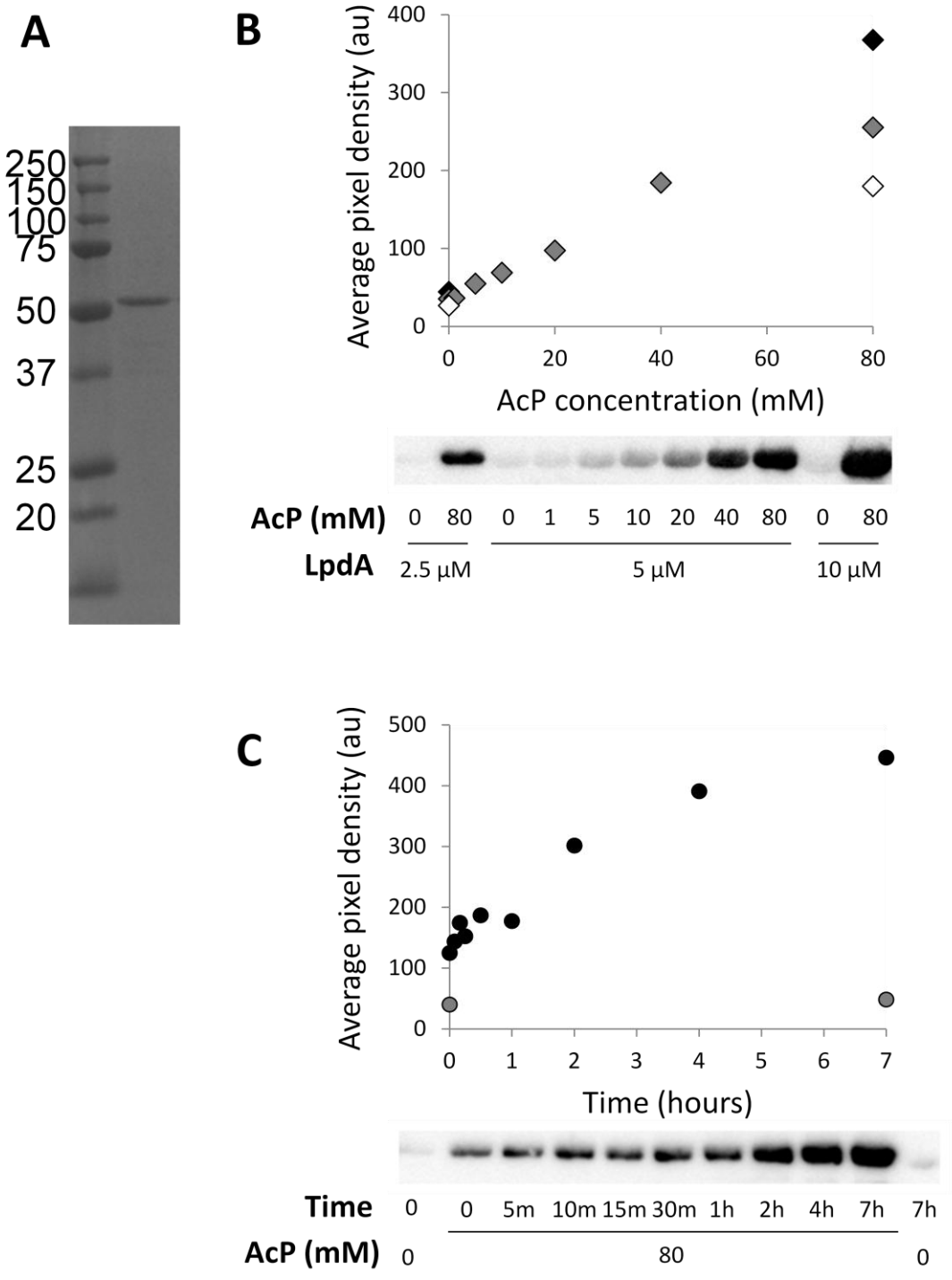
A
250
150
100
75
50
37
25
20
B
Average pixel density (au)
400
300
200
100
0
0
20
40
60
80
AcP concentration (mM)
AcP (mM)
0 80 0 1 5 10 20 40 80 0 80
LpdA
2.5 µM
5 µM
10 µM
C
Average pixel density (au)
500
400
300
200
100
0
0 1 2 3 4 5 6 7
Time (hours)
Time
0 0 5m 10m 15m 30m 1h 2h 4h 7h 7h
AcP (mM)
0 80 0

Figure 31. *In vitro* acetylation of LpdA with AcP
A) Coomassie-stained SDS-polyacrylamide gel containing purified LpdA
B) AcP and LpdA were incubated together for 1 hour at 37°C. Acetylation was detected by anti-acetyllysine immunoblot analysis and quantification was performed using AlphaView.
C) 1.25 μM LpdA was incubated with 0 or 80 mM AcP and incubated at 37°C for the indicated length of time. Acetylation was detected by anti-acetyllysine immunoblot analysis and quantification was performed using AlphaView.

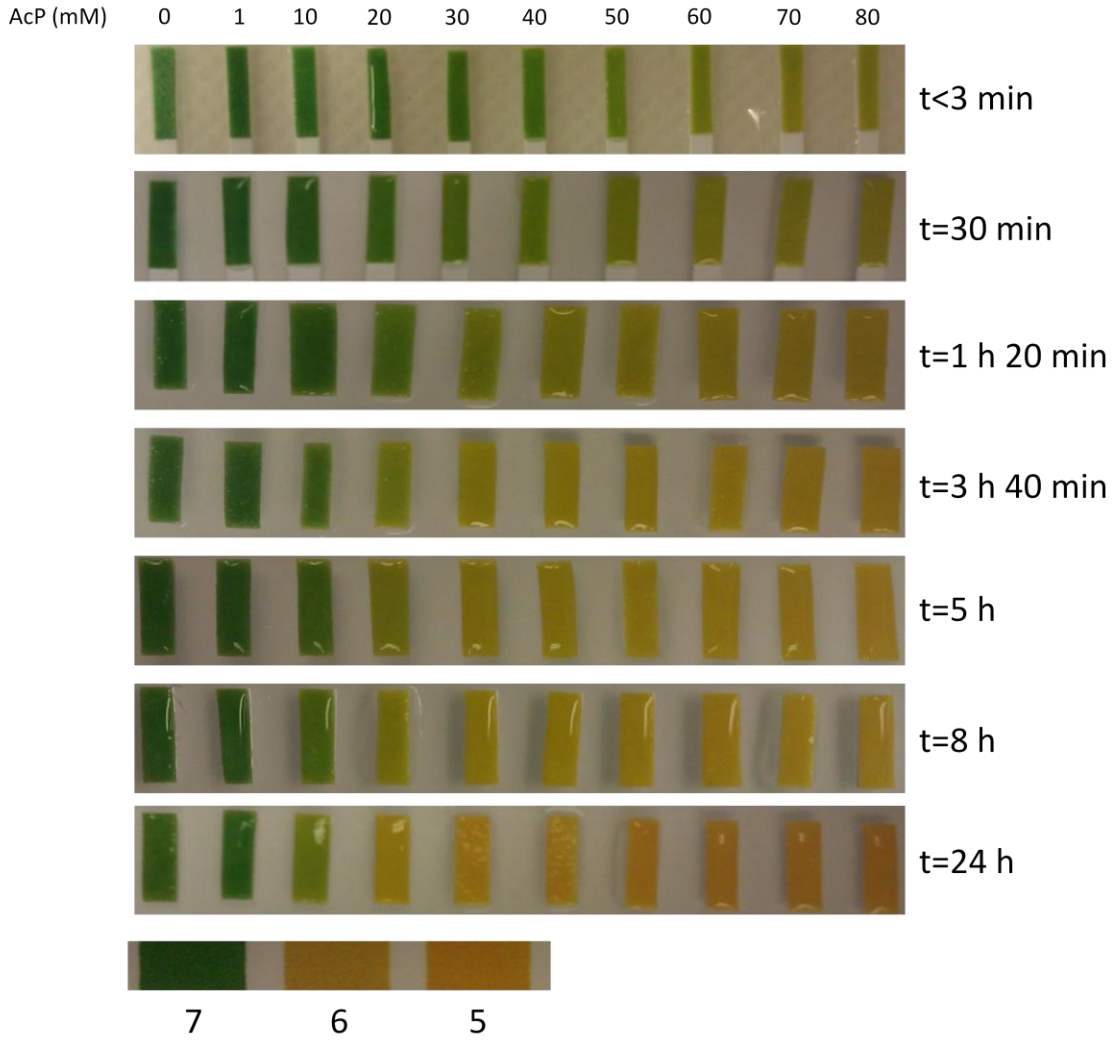

Figure 32. The effect of AcP hydrolysis on pH.
The indicated concentrations of AcP was incubated at 37°C in 150 mM Tris-HCl pH 7, 10mM $MgCl_2$, 150 mM NaCl, and 10% glycerol. Approximately 5 µl was spotted onto a pH test strip at multiple points in time.

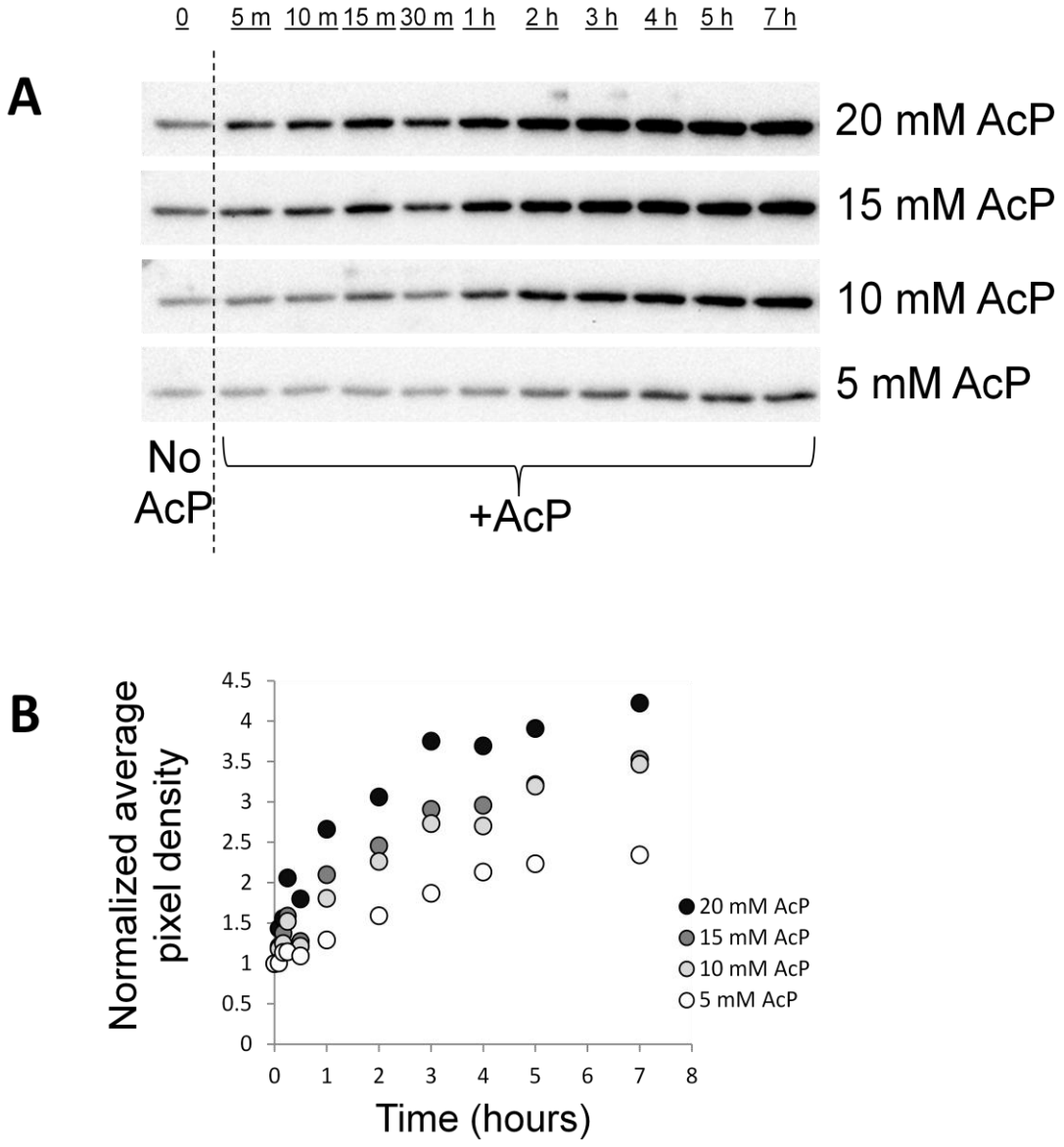

Figure 33. *In vitro* acetylation of LpdA using AcP as an acetyl group donor is sensitive to time of incubation and concentration of AcP.

AcP (0, 5, 10, 15, 20 mM) was incubated with 1.25 μM LpdA for various lengths of time (5 minutes, 10 minutes, 15 minutes, 30 minutes, 1 hr, 2 hr, 3 hr, 4 hr, 5 hr, and 7 hr) at 37°C. An anti-acetyllysine immunoblot analysis (A) and a quantification of acetylation was performed with AlphaView. The pixel densities were normalized to the signal in the absence of AcP (B).

A

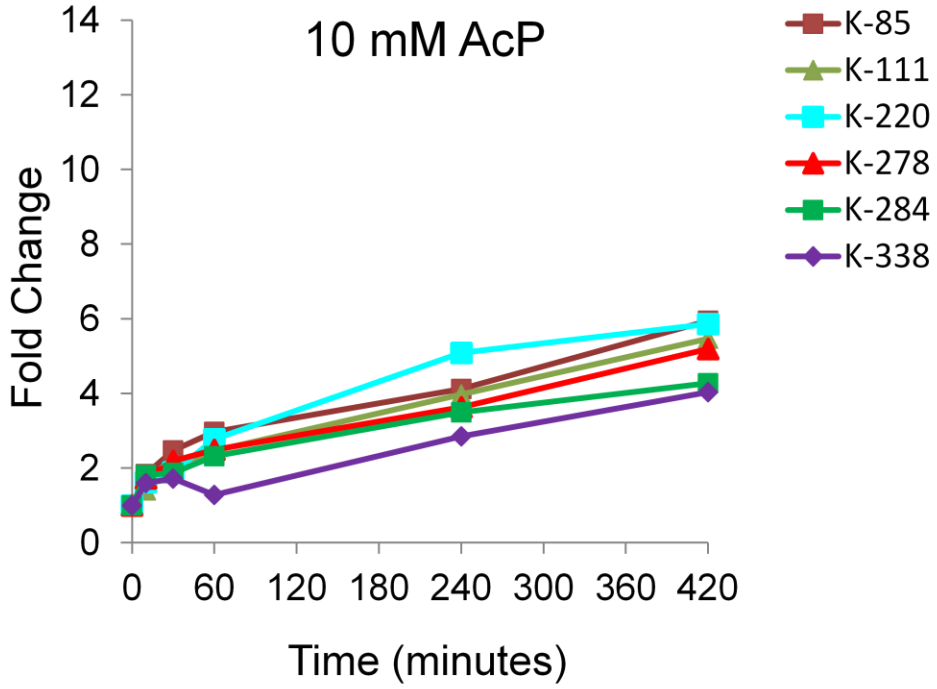
10 mM AcP
Fold Change
Time (minutes)
0
2
4
6
8
10
12
14
0
60
120
180
240
300
360
420
K-85
K-111
K-220
K-278
K-284
K-338

B

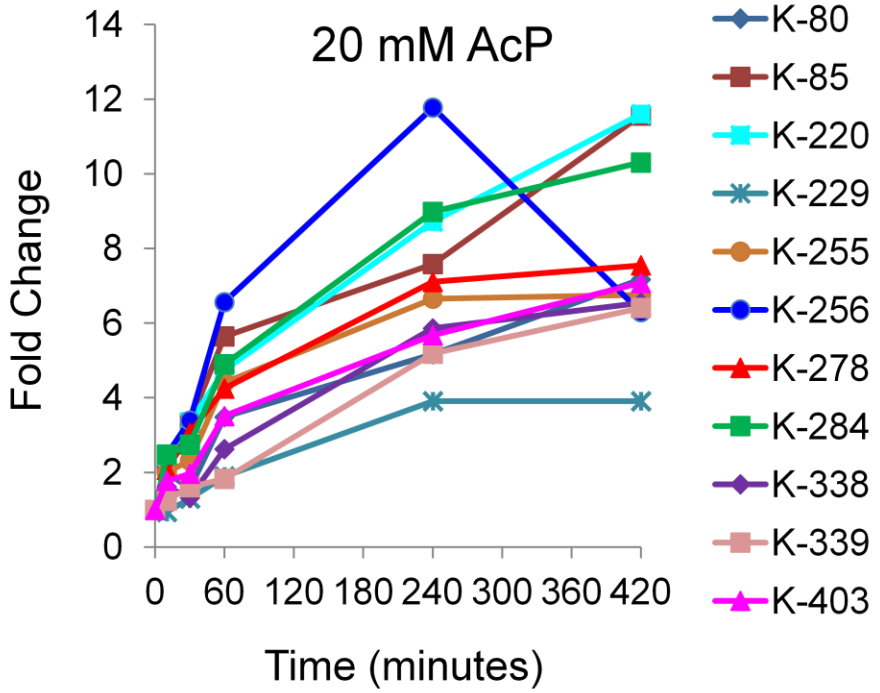
20 mM AcP
Fold Change
Time (minutes)
0
2
4
6
8
10
12
14
0
60
120
180
240
300
360
420
K-80
K-85
K-220
K-229
K-255
K-256
K-278
K-284
K-338
K-339
K-403

Figure 34. Quantitative mass spectrometric analysis of AcP on LpdA acetylation.

The experiment described in Figure 32 was performed in duplicate on separate days. These experimental duplicates were analyzed by Dr. Birgit Schilling, who analyzed the samples in technical duplicates by quantitative mass spectrometry. Fold-change in acetylation was plotted for each lysine as a ratio of acetylation in the presence of 10 mM AcP (A) or 20 mM AcP (B) compared to no AcP.

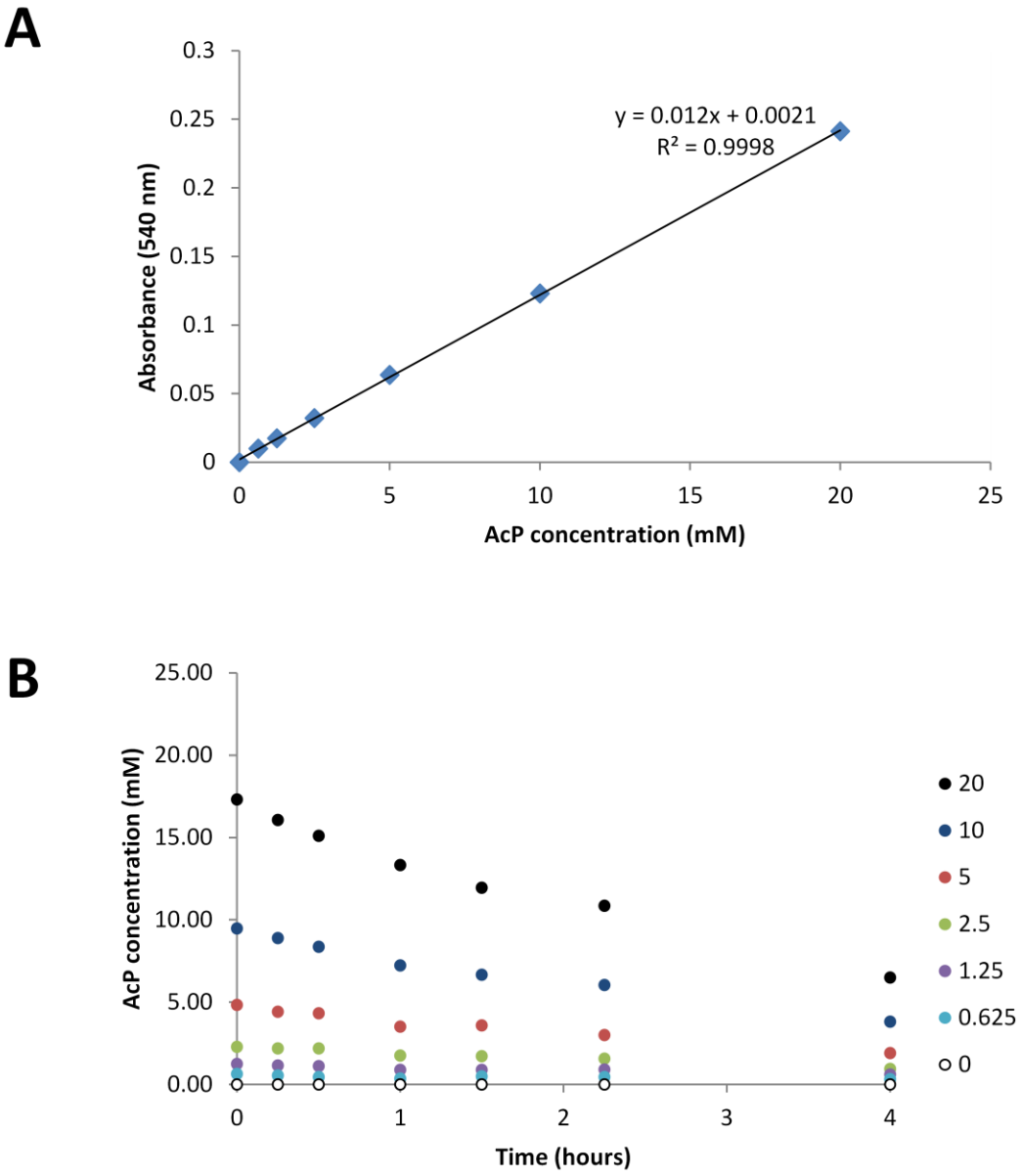

Figure 35. AcP measurements in *in vitro* acetylation reactions using hydroxylamine.

A) AcP phosphate standard curve. 0, 0.625, 1.25, 2.5, 5, 10, and 20 mM AcP was suspended in *in vitro* transcription buffer in the absence of LpdA to a final volume of 300 µl. 50 µl of neutralized hydroxylamine HCl was added and incubated at 60°C for 5 minutes. 100 µl of development solution was added and the absorbance was read

spectrophotometrically at 540 nm. The hydroxylamine assay was adapted from Fowler *et al.*, 2011 Journal of Visualized Experiments.
B) The level of AcP was measured when the indicated concentration of AcP was incubated with 1.25 μM LpdA at 37°C for various lengths of time using the hydroxylamine assay. The concentration of AcP was determined by comparing the measured absorbance to the standard curve.

A

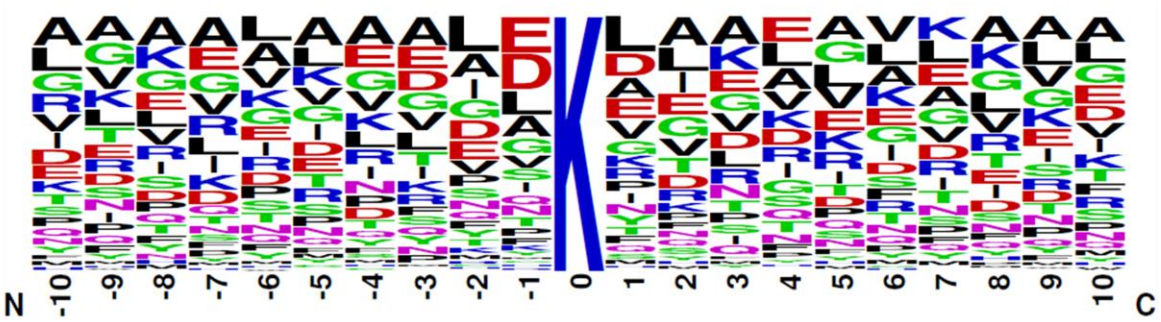

B

		Position relative to acetyl-K										
		-5	-4	-3	-2	-1	0	1	2	3	4	5
Amino acid composition	A	11.79%	11.42%	11.79%	9.76%	8.66%		8.47%	11.79%	11.42%	8.84%	9.58%
	C	1.84%	1.10%	0.37%	1.10%	1.29%		0.92%	0.18%	0.00%	0.37%	0.92%
	D	6.08%	4.97%	8.47%	7.92%	14.36%		9.39%	5.89%	7.00%	6.81%	4.42%
	E	6.08%	9.02%	9.02%	7.73%	14.55%		8.47%	8.66%	8.66%	10.31%	8.29%
	F	2.76%	2.58%	4.24%	3.68%	3.31%		3.50%	3.31%	1.66%	3.13%	2.58%
	G	7.18%	8.84%	7.92%	8.10%	6.63%		6.08%	8.47%	7.73%	6.08%	9.02%
	H	0.74%	1.47%	0.74%	1.10%	1.29%		1.47%	1.66%	0.92%	1.29%	1.66%
	I	7.00%	5.52%	5.34%	8.47%	4.60%		4.42%	8.84%	4.24%	6.26%	5.52%
	K	7.73%	7.55%	4.97%	2.76%	2.58%		4.79%	4.05%	9.76%	7.18%	7.73%
	L	7.92%	6.81%	7.55%	14.18%	9.94%		14.18%	9.76%	6.81%	9.76%	9.02%
	M	2.03%	1.84%	1.47%	2.39%	1.47%		2.03%	1.66%	1.66%	0.92%	1.66%
	N	3.87%	5.52%	3.50%	4.24%	4.42%		4.42%	3.31%	5.71%	4.05%	3.50%
	P	4.42%	5.16%	3.50%	4.79%	3.50%		4.60%	3.50%	4.42%	2.76%	4.42%
	Q	3.50%	3.31%	3.87%	4.05%	4.60%		3.31%	3.31%	4.24%	4.97%	4.24%
	R	5.71%	6.63%	4.60%	1.84%	1.29%		4.79%	4.97%	6.63%	6.45%	7.37%
	S	5.34%	2.21%	4.05%	4.60%	4.97%		2.58%	3.31%	4.42%	5.34%	3.68%
	T	5.89%	3.87%	6.08%	2.95%	4.24%		3.68%	6.63%	4.97%	4.97%	4.79%
	V	7.37%	8.10%	7.92%	5.89%	5.52%		7.92%	7.55%	7.73%	7.92%	9.02%
	W	0.74%	0.74%	0.74%	0.92%	0.74%		0.55%	0.92%	0.37%	0.74%	0.18%
	Y	2.03%	3.31%	3.87%	3.50%	2.03%		4.42%	2.21%	1.66%	1.84%	2.39%

Figure 36. An analysis of the amino acid composition and position relative to acetylated lysines.
Sequence logo (A) and frequency table (B) showing the amino acid composition and position relative to the acetylated lysine. 543 sites that exhibited significantly upregulated sites relative to WT with a P value < 0.05 were analyzed using WebLogo. Acetylated lysines that were within 10 amino acids of the start (28 sites) or stop codon (24 sites) were not part of this analysis.

These results are in contrast to the AcP chemical acetylation profile obtained from a peptide-based array analysis called SAMDI (surface-assembled monolayers for matrix assisted laser desorption/ionization time-of-flight mass spectrometry) (235). A peptide library is immobilized onto a chip. The 5 or 6 amino acid peptides are lysine-containing sequences that randomize the -1 and +1 positions. Dr. Misty Kuhn and Dr. Michael Scholle (in Milan Mrksich's lab at Northwestern University) incubated the peptide array with AcP at 30°C for 1 hour and detected acetylation by mass spectrometry. Using this assay, they found that positively charged residues enhanced the acetylation of the adjacent lysine, while negatively charged residues inhibited (data not shown).

From these results, I propose that non-enzymatic acetylation of lysines by AcP is a balance between negatively and positively charged local residues, which activate the lysine for acetylation and increase the local concentration of AcP. Previous reports have demonstrated that two families of acetyltransferases (GNAT and MYST) utilize negatively charged glutamate or aspartate in their catalytic site to deprotonate and thus activate the lysine side chain for acetylation (64,236).

Therefore, negatively charged residues may promote lysine deprotonation at neutral pH for AcP dependent acetylation. The positively charge residues may increase the electrostatic interaction between the negative phosphate group of AcP and the positively charged lysine side chain, bringing AcP close to a potentially active lysine substrate.

Summary

Since high AcP correlated with an increase in RcsB (218) and RNA polymerase acetylation (48), we hypothesized that AcP regulated global protein acetylation in *E. coli.* This hypothesis is consistent with a recent publication, which primarily studied the effect of AcP on starved and growth arrested *E. coli* cells (202). We have demonstrated that there is a substantial increase in global acetylation that is dependent on high intracellular level of AcP and that AcP can undergo direct acetyl transfer to lysine-containing proteins and peptides. We propose that acetylation with AcP is non-enzymatic and that the neighboring amino acids can influence lysine acetylation. This research contributes to the understanding of a potentially novel, global regulator of acetylation in *E. coli* and potentially other bacteria that exhibit AcP-dependent acetylation of proteins.

CHAPTER FOUR

DISCUSSION

What is the effect of non-enzymatic acetylation?

Acetylation, like all PTMs, can increase the functionality of the proteome by generating potentially different isoforms of a protein. Nε-lysine acetylation, like many other PTMs, is a reversible modification. This reversibility allows the protein to return to its original state and to turn off a response. The discovery that AcP and AcCoA can non-enzymatically donate acetyl groups to proteins implies that a separate enzyme may not be necessary for some acetylation to occur *in vivo*. Without the requirement for a KAT, the cell may by-pass the metabolic cost and time needed to activate transcription and translation of the enzyme. Non-enzymatic acetylation, therefore, could be a fast, initial cellular response by which the cell can adapt to particular stresses by altering the intracellular concentrations of these acetyl donors.

If non-enzymatic modifications are not limited to lysines that are accessible to KATs, then some acetylated sites may be inaccessible to KDACs. If so, then some non-enzymatically acetylated lysines may not be reversible. Intuitively, acetylation that occurs non-enzymatically and irreversibly is a high risk situation. If proteins are prone to undergo modification then acetylation of certain sites may be deleterious to the cell. Thus, a mechanism to regulate non-enzymatic acetylation is necessary. Our results suggest that some of this control is at the level of the targeted

proteins. Other mechanisms of regulation could be through protein degradation, compensatory PTMs, or adaptive mutations that could suppress or limit the effect of the irreversible modification.

What is the effect of multiple acetyl donors on bacterial physiology?

Multiple acetyl donors could allow for more levels of regulation, such as at the level of synthesis and degradation of the acetyl donor or mechanisms of acetyl transfer and removal specific for each acetyl donor. Since AcCoA and AcP are metabolic intermediates of the same pathway, it is possible that certain stimuli can affect both molecules and the cell can activate a more robust and rapid response than with either AcCoA or AcP alone. However, if there are stimuli that can differentially regulate the AcCoA and AcP pools, then distinct AcCoA- or AcP-sensitive cellular responses are possible.

The mechanisms that regulate acetylation by either AcCoA or AcP may impact the differences between these AcCoA- or AcP-sensitive responses. KATs are known to acetylate proteins by binding to the CoA moiety of AcCoA through their CoA binding motif. Since CoA and phosphate are structurally different, AcP is unlikely to depend on the known KATs for acetylation. This difference in mechanisms of acetylation by AcCoA and AcP may impact specificity of acetylation.

The chemical structures of AcCoA and AcP are likely to affect specifity. The standard state free energies of hydrolysis for the thioester and phosphoester bonds

for AcCoA (-31.5 kJ/mol) and AcP (-43.3 kJ/mol), respectively, are different. Thus, expelling the phosphate group from AcP is thermodynamically more favorable than CoASH from AcCoA. This difference could impact the sites that are targeted for acetylation. However, given that KATs can bind AcCoA and catalyze the reaction, it is possible that certain KAT-dependent acetylations with AcCoA could be kinetically more favorable *in vivo.*

Due to these similarities and differences between AcCoA and AcP, the cell could coordinate appropriate responses to a variety of extra- and intracellular stimuli.

What is the effect of acetylation on RcsB?

I hypothesize that acetylation inhibits RcsB activity, at least in part, through acetylation of Lys-154. In the absence of AckA or the deacetylase CobB, P*rprA* activity was reduced (**Figure 19A**) and RcsB acetylation increased (**Table 4**). In particular, acetylation of Lys-154 increased. A genetic mimic of acetylated Lys-154 (RcsB-K154Q) had no activity at the *rprA* promoter and the genetic mimic of non-acetylated Lys-154 (RcsB-K154R) had WT levels of activity (**Figure 20A**), which suggests that acetylation of Lys-154 inhibits RcsB activity. Site-specific acetylation of Lys-154 (220) followed by *in vitro* transcription assays could directly test the effect of Lys-154 acetylation on *rprA*.

According to a reported structural analysis of *E. amylovora* RcsB carboxy terminal domain, Lys-154 is positioned in the amino terminus of the seventh alpha helix (172). Pristovsek and colleagues suggest that this is a supporting helix based on homology to similar structurally characterized RRs. They also found that, among several other residues in the effector domain, Lys-154 was involved in binding to an RcsA-RcsB heterodimer DNA sequence. Additionally, some RRs employ basic residues in the amino terminus of the supporting helix to interact with DNA (176). If acetylation of Lys-154 was responsible for the inhibited *rprA* transcription seen in the *cobB* or *ackA* mutants, then expressing a genetic mimic of non-acetylated Lys-154 should suppress the inhibition. I tested this prediction by transforming the single copy plasmid that expressed WT RcsB or the RcsB(K154R) mutant into the *ackA rcsB* double mutant lysogenized with the P*rprA-lacZ* fusion. The RcsB(K154R) mutant had the same level of activity as WT RcsB in the absence of *cobB* instead of the expected higher activity (data not shown). This preliminary evidence suggests that Lys-154 is not solely responsible for the effects seen in the *cobB* mutant and, possibly, the *ackA* mutant. There are likely other targets within or outside of RcsB that are involved in regulating *rprA* transcription.

Acetylation was also detected on several other residues on RcsB (**Figure 4C**). Mass spectrometry determined that several RcsB residues were acetylated *in vivo* or *in vitro*. Although the sites that were modified were not identical, acetylation did occur frequently in the region between Lys-72 and Lys-186. This region includes

several parts of the protein that are putatively important in RcsB function. 5 out of the 11 acetylated lysines centered on the linker region. The linker is critical for OmpR and PhoB effector function. The linker was reported to be important in regulating physical interactions between the REC and effector domains and transducing the activation signal from the REC domain to the effector domain (169). Acetylation of the linker could perturb some aspect of the REC-effector domain relationship. Although increased acetylation of the HTH (α8 - α9) occurred in the *in vitro* acetylation reactions only, it is possible that under certain conditions, an elevation in the intracellular concentration of AcCoA or AcP may lead to acetylation of these sites in the HTH. Acetylation of Lys-180 effectively eliminated RcsB binding to the *flhD* DNA (49). This mechanism of acetylating the HTH may be part of a stress response in which activation of the RcsB regulon is not preferable for the cell and RcsB activity is quickly turned off.

The ability of the RcsB-K154 mutants to inhibit migration on semi-solid agar plates as well as WT RcsB is intriguing (**Figure 20B**). RcsB is a repressor of the master regulator of flagellar biosynthesis *flhDC* transcription. A DNase I protection assay found that a mimic of phosphorylated RcsB(D56E) protected a 20 nucleotide region centered at +12 and RcsB repression of *flhDC* promoter activity required this region (163). Therefore, RcsB repression of *flhDC* transcription requires DNA binding. Lys-154 is a DNA-binding residue but Lys-154 mutants were capable of binding and inhibiting migration (**Figure 20B**). It is known that several other

transcription factors bind and regulate *flhDC* expression. RcsB-K154 mutants may be able to bind DNA in the presence of these transcription factors. This possibility is supported by reports showing that RcsB binding to DNA either requires or is enhanced by the addition of proteins such as RNAP (164) or RcsA (163,172). These results may implicate a role for an RcsB co-repressor. This co-repressor is probably not RcsA because it was reported that RcsA is not required for flagellar biosynthesis and affected migration only when overexpressed (125). Alternatively, RcsB-K154 mutants may have no defect in binding to DNA but, instead, affect a later event in the initiation of *rprA* transcription, such as the recruitment of RNAP.

From the inhibition of migration assays, I found that a mutant that lacked the phosphoryl acceptor site Asp-56 of RcsB was still capable of inhibiting migration (**Figure 20B**). These results suggest that phosphorylation is not required for RcsB repression of *flhDC.* Similar to the previous discussion, interaction with co-regulators may suppress the need for phosphorylation in DNA binding. This hypothesis can be tested by mutating the known DNA binding sites for *flhDC* transcription factors and determine if RcsB(D56A) can repress *flhDC* promoter activity and migration. Another exciting possibility is that phosphorylation of RcsB is not required for binding to DNA, but is important in the activation of transcription, perhaps recruitment of RNAP to form the closed complex or isomerization to the open complex. This model is consistent with a previous report demonstrating that the phosphorylated genetic mimic RcsB(D56E) activates *osmCp1*

by recruiting RNAP to the DNA (164). Although this report did not show that Asp-56 was required for DNA binding, the RcsB(D56E) mutant was incapable of binding to DNA alone, suggesting that phosphorylation is not sufficient to for RcsB DNA binding. Because I showed that the phosphorylation-deficient mutant RcsB(D56A) can inhibit migration (**Figure 20B**) but cannot activate *rprA* transcription (**Figure 16B**), I hypothesize that for RcsB, phosphorylation is critical for activation of transcription independently of inducing DNA binding.

Does autoacetylation regulate RcsB?

Although YfiQ can acetylate RcsB *in vitro* (**Figure 23, (49)**), YfiQ does not appear to be the physiological regulator of RcsB acetylation because the acetylation status of purified RcsB from the *yfiQ* mutant was similar to that from WT cells (**Table 4**). However, it does seem that YfiQ can activate RcsB-regulated phenotypes because a deletion of *yfiQ* reduced P*rprA* activity (**Figure 24A**) and enhanced migration in semi-solid agar (J. Escalante-Semerena, personal communication). Members of the Wolfe laboratory have evidence to support the hypothesis that the function of YfiQ is predominately to regulate Acs activity and that this regulation could affect metabolism on gluconeogenic carbon sources. Therefore, the mechanism by which RcsB acetylation occurs *in vivo* remains unknown.

Two scenarios are possible. RcsB acetylation could involve another protein acetyltransferease or RcsB acetylation occurs independently of an acetyltransferase. An unknown acetyltransferase is possible. Evidence from the Wolfe laboratory

suggests that YfiQ is not a significant regulator of global acetylation and there are over 20 GNAT homologs in *E. coli.* One could screen the requirement for any one of these GNATs in AcP-independent acetylation by constructing *ackA pta gnat* triple mutants and screening for changes in acetylation by anti-acetyllysine immunoblot analyses.

Another possible mechanism of acetylation may be autoacetylation because purified RcsB is acetylated when incubated with AcCoA alone (**Figure 23** and **Table 5, (49)**) or AcP alone (data not shown). It is unlikely that purified RcsB was contaminated by an acetyltransferase, as in-solution mass spectrometric analysis did not detect a contaminating YfiQ or another acetyltransferase (data not shown). Autoacetylation of several other proteins have been reported (46,223,237,238), including proteins in the mitochondrion, where little is known about potential mitochondrial lysine acetyltransferase(s) and the conditions are favorable for AcCoA-dependent lysine acetylation, i.e., alkaline pH (~8.0) and high AcCoA concentration (~5 mM) (73,239,240). Also, RR CheY (46) and Acs (45) can autoacetylate with AcCoA. Seven lysines were acetylated when CheY was incubated with AcCoA alone (46).

To determine if RcsB is regulated by autoacetylation *in vivo* is extremely difficult, if not impossible. One would have to know all the enzymes that regulate RcsB acetylation, which is unknown, and determine if acetylation occurs in the absence of these enzymes. Currently, we know that YfiQ is likely not involved in

acetylating RcsB. Acs can acetylate CheY with AcCoA or acetate (and ATP) as acetyl donors (45). One could test if Acs regulates RcsB acetylation by purifying RcsB in an *acs* mutant followed by *in vitro* acetylation reactions between RcsB, Acs, and acetate and ATP. Finding the answer to the general question of whether autoacetylation of proteins occurs *in vivo* may not be feasible.

What mechanisms regulate RcsB deacetylation?

When RcsB was acetylated only on Lys-180, CobB was reported to deacetylate RcsB *in vitro* (49). I found that the *cobB* mutant or nicotinamide-exposed WT cells showed reduced P*rprA* activity (**Figure 19**). These results are consistent with CobB activating P*rprA* activity and suggest that CobB activates by deacetylating some inhibitory acetylated protein. The inhibitory acetylated protein may be RcsB because RcsB is hyperacetylated in the *cobB* mutant (**Tables 2** and **4**). I propose that CobB regulates the deacetylation of certain RcsB lysines *in vivo.* To determine if CobB can deacetylate RcsB, RcsB that is acetylated at CobB-sensitive lysines (e.g. Lys-118 and Lys-154) can be generated and incubated with CobB and NAD^+. This method of site-specific acetylation can also contribute to understanding the functions of specific lysines when acetylated (220). Unfortunately, this approach has not yet been successful in our hands and may require optimization before application.

Other lysines (e.g., Lys-72 and Lys-125) appeared to be insensitive to CobB, suggesting that CobB does not regulate these sites. Although one explanation would

be that some acetylated lysines are not deacetylated, it is unlikely to be the case. Lysine acetylation is known to be dynamic and, to the best of my knowledge, irreversible acetylation of internal lysines has not been reported. Another possibility is that CobB activity is relatively low under these experimental conditions (BW25113 strain in TB7 growth medium and aerated at 37°C) and a deletion of CobB reveals the preferred but not all of the substrates. It is possible to identify the suboptimal CobB substrates by activating CobB activity in WT cells, using a sirtuin-specific activator such as resveratrol (241), and then compare RcsB acetylation to the resveratrol-treated *cobB* mutant. This small-scale experiment could be adjusted to identify more targets of CobB *in vivo* on a global scale. The identification of novel CobB targets by mass spectrometry and structural biology has begun in collaboration with the Mrksich and Anderson laboratories at Northwestern University. known.

Our lab has evidence to suggest that there may be other mechanisms of deacetylation in *E. coli.* However, this study into a novel deacetylase would need further analysis. We found that CobB is likely the only sirtuin deacetylase since the acetylation profile of the nicotinamide-exposed *cobB* mutant was identical to the non-treated *cobB* mutant. This is consistent with the sirtuin phylogenetic analyses identifying only CobB in *E. coli* (78,79). Kenyon College summer student Sarah Cook and I performed a screen for a HDAC-like *E. coli* enzyme using HDAC-specific inhibitors (i.e. butyrate and propionate). These inhibitors were able to induce an

increase in acetylation and the acetylation profile was different compared to the *cobB* mutant (data not shown). However, inconsistent with the presence of another KDAC in *E. coli*, no lysine deacetylation activity was detected when a *cobB* crude extract was incubated with acetylated peptides by SAMDI (unpublished data). We currently do not know how the HDAC inhibitors can induce acetylation. If the effect of these inhibitors is through a HDAC-like enzyme, one could screen for a HDAC-like enzyme by deleting genes that encode putative amidohydrolases and determine which mutant enhances acetylation.

Could RcsB be co-regulated by phosphorylation and acetylation?

I propose that the *rprA* promoter is regulated by phosphorylation and Nε-lysine acetylation. It was reported that *rprA* transcription increases when RcsC kinase activity is stimulated by overexpressing the lipoprotein RcsF (157). The activation of *rprA* transcription required RcsB (157). My results are consistent with phosphorylation regulating and activating RcsB: P*rprA* activity requires the phosphoryl acceptor site Asp-56 of RcsB (**Figure 16B**), RcsF overexpression increased P*rprA* activity (**Figure 17B**), and RcsC when RcsC is not overexpressed (**Figure 17A**). It was also reported that AcP might activate RcsB when RcsC functions as a net phosphatase (125). I demonstrated that AcP is an activator of the P*rprA* (**Figure 17A**) and that AcP can donate phosphoryl groups to RcsB (**Figure 18**). To confirm that AcP is a physiological phosphoryl donor for RcsB, *in vivo* detection of AcP dependent phosphorylation of RcsB would need to be performed. If

AcP can indeed act as a phosphoryl donor to RcsB then these results suggest that RRs like RcsB can be activated by both the SK and AcP, not just when the SK is acting as a net phosphatase. The implication of two phosphoryl donors co-regulating RcsB is unknown but presumably involves generating a robust RcsB response when the condition is appropriate. This genetic analysis of RcsB regulation by its SK and AcP are similar to a study of the *Xenorhabdus* OmpR, which is an inhibitor of antibiotic production upon phosphorylation. Either the deletion of the SK EnvZ or the absence of AcP led to increased antibiotic production (215,242). It would be important to test whether the absence of both EnvZ and AcP has an additive effect on antibiotic production.

If AcP activates RcsB by donating phosphoryl groups to RcsB *in vivo*, then why is *rprA* transcription reduced in the *ackA* mutant? The answer appears to involve acetylation of RcsB. Because RcsB is regulated by phosphorylation at Asp-56 and acetylation on multiple lysines, in what manner is RcsB co-regulated by both modifications? For example, p53 activity is inhibited if Lys-317 is acetylated (24) and Acs is inhibited if Lys-609 is acetylated (131,132). RcsB activity could be regulated by single 'off-on' modifications like p53 and Acs. Alternatively, PTM could occur sequentially. p53 is modified by multiple PTMs on many sites and p53 activity is differentially regulated depending on its modification(s). Phosphorylated Ser-15 on p53 appears to initiate a sequential PTM relay (23,25-27). A kinetic characterization of RcsB autoacetylation using AcCoA or AcP would provide insight

into the chemistry of RcsB autoacetylation. By analyzing the relationship between the velocity of acetylation and the concentration of AcCoA or AcP, the shape of the curve would indicate whether acetylation of RcsB is cooperative, in which acetylation of one site might facilitate acetylation of other sites. Finally, acetylation and phosphorylation could occur simultaneously and these different combinations could result in various outcomes on RcsB activity. RcsB may be regulated by a combination of these three possibilities as well. Similar to p53 for eukaryotes, RcsB may become a prototype for the PTM code in bacteria.

The possibility that RcsB is controlled by multiple PTMs suggests that there is an advantage to RcsB evolving such a complex regulatory program. RcsB regulates over 100 genes, involved in many aspects of bacterial physiology. I predict that RcsB acetylation affects other genes besides *rprA*. Intuitively, a simple phosphorylation-dependent 'on-off' switch is not sophisticated enough to provide specific control over the RcsB regulon. The possibility of phosphorylation, multiple acetylated lysines, and different oligomeric states (dimers and possibly tetramers) regulating RcsB amplifies the number of functionally distinct forms of RcsB. This increased diversity could regulate RcsB affinity to promoters and to interacting proteins.

What regulates glucose-induced osmC *transcription?*

While several research groups have performed thorough investigations into the regulation of *osmC* transcription, we may have discovered a novel mechanism that activates *osmC* transcription. *osmC* is reported to be regulated by two

overlapping promoters: *osmCp1* and *osmCp2*. *osmCp2* is closer to the translational start site and is dependent on the sigma factor that regulates stationary phase stress responses (σ^S), is activated by the leucine-responsive transcription factor LRP, and is indirectly inhibited by the nucleoid-associated protein H-NS. *osmCp1* is activated by both RcsB and NhaR (165) and is repressed by both LRP and H-NS (243).

I have found that a high AcCoA:CoA ratio activates *osmC* transcription. This mechanism appears to not require the αCTD of RNAP, which is distinct from the glucose-induced, high AcCoA:CoA ratio-regulated response from the stress-responsive *cpxP* promoter. The *cpxP* response to glucose in WT cells and the *ackA* mutant depended on specific lysine residues on the αCTD (47,48).

Glucose activated a transcriptional promoter-*lacZ* fusion that included both *osmCp1* and *osmCp2.* The targeted promoter is currently unknown and, from what is known about *osmCp1* and *osmCp2* regulation, glucose-induced *osmC* transcription appears to be similar in some aspects but there are differences. Glucose-exposed cells activated *osmC* transcription between late exponential and early stationary phase. Suggesting that a high AcCoA:CoA ratio is involved in glucose-induced transcription, reducing the AcCoA:CoA ratio using PHB or CoaA overexpression decreased this response. Glucose activated *osmC* independently of RR and its cognate SK RcsC. This Rcs-independent regulation is reminiscent of the RcsB-independent osmotic response at *osmCp1,* in which the *osmCp1* response to 0.5 M NaCl did not require RcsC, RcsB, or the co-activator RcsA (164). The *osmCp1*

response to osmotic shock in LB growth medium does, however, require the transcriptional regulator NhaR (166). One could test whether NhaR is required for the glucose-induced *osmC* response. However, there is a possibility that glucose does not activate through *osmCp1* because the osmotically-induced response occurs during exponential phase (164), whereas the glucose-induced response occurs during the transition into stationary phase (**Figure 5**). RcsB-independent, stationary phase activation of *osmC* transcription is similar to the reported mechanism of *osmCp2* activation. This promoter is activated in stationary phase by σ^S (244) which, together with the RNAP holoenzyme, can control genes under starvation conditions or upon transitioning into stationary phase. Since σ^S is largely responsible for *osmCp2* induction in stationary phase and the gene *rpoS* that encodes σ^S is not essential, one could delete *rpoS* and determine if the glucose-activated *osmC* transcription requires σ^S. However, *osmCp2* is transiently activated in lag phase when cells are grown in LB medium, which is not apparent when cells are grown in TB7 (**Figure 5**). Therefore, the high AcCoA:CoA activation of *osmC* transcription in stationary phase does not completely resemble the known regulation of either *osmCp1* or *osmCp2*. In addition to screening mutants of known regulators, one could test the effect of glucose on the *osmC* promoter region that carries nucleotide substitutions that disrupt either *osmCp1* or *osmCp2*, similar to studies of osmotically-induced *osmC* transcription (166).

Glucose-induced *osmC* transcription requires the acetyl-coenzyme A synthetase Acs (**Figure 14A**). It is reported that Acs activity is inhibited by the *S. enterica* KAT Pat (132), a homolog of *E. coli* YfiQ. Although YfiQ is not required for glucose-induced *osmC* transcription, *osmC* transcription is dampened in both the glucose-exposed *yfiQ* mutant and the non-treated-*yfiQ* mutant relative to the WT cells (**Figure 13A**). In the absence of YfiQ, Acs is not acetylated on Lys-609 (132). If the effect of YfiQ requires Acs, then I hypothesize that acetylated Acs activates and/or non-acetylated Acs inhibits the *osmC* transcription. This hypothesis that Acs directly regulates *osmC* transcription and that the acetylation state affects Acs transcriptional activity can be tested using *in vitro* transcription assays with RNAP, Acs, and a DNA template containing the *osmC* promoter. Acetylated Acs at Lys-609 can be either purified from the *cobB* mutant or generated by site-specific acetylation (220). However, to the best of my knowledge, there are no reports that show Acs can function as a transcription factor. Another possibility is that Acs is indirectly affecting *osmC* transcription. Acs may either directly or indirectly modify proteins posttranslationally, in a manner that could control *osmC* transcription. Acs may alter the metabolism of either AcCoA or AcP, both of which can modify proteins. Alternatively, Acs may directly mediate the modification of proteins that directly or indirectly affect *osmC* transcription. For instance, Acs was reported to acetylate the chemotaxis RR CheY (45). To determine if Acs can affect protein acetylation, one could delete *acs* and compare the acetylation profile to WT cells by anti-acetyllysine

immunoblot analysis. If there is a difference, then mass spectrometry would determine the proteins that are acetylated through an Acs-regulated mechanism.

By understanding the effect of Acs at the *osmC* promoter, we can also have a better indication of its function in other Acs regulated functions. Robert Davis from the Wolfe laboratory has evidence to suggest that YfiQ has an important function in regulating cellular metabolism on gluconeogenic carbon sources. In the absence of *yfiQ*, cells grow poorly on certain gluconeogenic carbon sources and grow similar to WT cells on glycolytic carbon sources. This growth defect on gluconeogenic carbon requires Acs. It is possible that Acs is important when cells are grown on gluconeogenic carbon sources because Acs regulates the acetylation status of enzymes in gluconeogesis. We can test this hypothesis by performing immunoblot analysis and mass spectrometry on an *acs* mutant grown in the presence of gluconeogenic carbon sources compared to glycolytic conditions.

What is the function of SpeG on RcsB activity?

The spermidine acetyltransferase SpeG appears to inhibit RcsB activity through a spermidine-dependent manner. The overexpression of SpeG inhibited RcsB-dependent P*rprA* activity (**Figures 25 and 27**), while the *speG* mutant enhanced P*rprA* activity (**Figure 26**). These results suggest that SpeG inhibits RcsB activity. SpeG inhibition of P*rprA* activity may be dependent on spermidine because P*rprA* in the *speE speG* double mutant that lacks SpeG and does not produce spermidine is lower than the *speG* mutant. Another interpretation could be that in

the absence of SpeG, spermidine activates *rprA* transcription; however, spermidine-exposed *speG* mutant showed a concentration-dependent reduction in P*rprA* activity (**Figure 29B**).

Spermidine-mediated inhibition of RcsB activity may involve a direct interaction between the RcsB and SpeG. Our collaborators at the Anderson laboratory at Northwestern University have evidence to suggest that SpeG can acetylate spermidine *in vitro*. However, when RcsB is present, spermidine acetyltransferase activity is inhibited. Although a detailed mechanism still needs to be elucidated, RcsB inhibition of SpeG activity appears to be direct, by forming a spermidine acetyltransferase inactive complex.

Furthermore, there are aspects of the epistasis experiment between SpeG and SpeE that add more intrigue to the relationship between spermidine, SpeG, and RcsB. In the absence of spermidine production (*speE* mutant), SpeG appears to be an activator of *rprA* transcription. P*rprA* in the absence of both spermidine and SpeG (*speE speG* double mutant) was reduced compared to the *speE* mutant (**Figure 26**).

How does SpeG activate RcsB? The answer is unknown but there is evidence to suggest that RcsB binds poorly to its DNA targets unless a co-activator is present. For example, RcsB did not bind to the RcsB homodimer consensus DNA sequence in *osmCp1* in the absence of RNAP in an electrophoretic mobility shift assay (164). Additionally, RcsB binding to three RcsB-regulated promoters, P*amsG*, P*wza*, and P*cpsA*, was weak and unstable with K_D values between 2×10^{-6} and 6×10^{-6} and half-

lives less than a second. In the presence of the co-activator RcsA, stability increased and K_D values were at least one order magnitude smaller (172). Therefore, the mechanism through which SpeG can activate *rprA* transcription may involve enhancing RcsB DNA affinity.

Why does growth phase regulate glucose-induced rprA *transciption?*

The timing of glucose exposure affected the *rprA* response to glucose in stationary phase, suggesting that the phase of growth regulates glucose-induced *rprA* transcription. Only when cells were exposed to glucose early in growth (i.e. lag phase and early exponential phase) was there an *rprA* promoter response in stationary phase (**Figure 7**). These results have been independently reproduced by David Christensen, a graduate student in the Wolfe laboratory. The importance of exposure early in growth could suggest that lag phase and early exponential phase present some common factor(s) that is critical for the *rprA* response to glucose. It is understood that the transcriptomic and metabolic profiles change throughout different phases of growth. Therefore, an unknown early transcription factor(s), enzyme(s), or metabolite(s) might be important for a stationary phase *rprA* response. Similarly, one may wonder why the *rprA* response glucose occurs in stationary phase and not at any other point in growth. The dependence on early glucose exposure regulating a stationary phase response is not specific to *rprA* transcription; this effect is also seen in glucose-induced protein acetylation. The Wolfe laboratory has evidence for glucose stimulated acetylation in stationary

phase. David Christensen has tested whether the timing of glucose exposure affected the induction of stationary phase acetylation by anti-acetyllysine immunoblot analysis. He found that glucose-induced acetylation in stationary phase occurred only when cells were exposed to glucose early in growth. Currently, the mechanism of growth phase-dependent, glucose-induced *rprA* transcription and global protein acetylation is yet unclear.

How does AcP non-enzymatically acetylate proteins?

In 1975, Ramponi and colleages reported that AcP can nonenzymatically donate acetyl groups to histone tails *in vitro* (201). However, there has been no evidence that this effect was relevant *in vivo.* The discovery that AcCoA is not the only physiologically relevant acetyl donor and that AcP contributes to acetylation in bacteria constitutes a significant shift in lysine acetylation dogma. While working on my thesis, which contributed to the hypothesis that that AcP is a novel physiologically relevant acetyl donor, a paper was published showing very similar results (202). Weinert and coworkers used a quantitative mass spectrometric approach and determined that the global level of *E. coli* lysine acetylation in stationary phase is significantly greater than in exponential phase, indicating that acetylation increases in cells that experience little to no growth, but only if provided with a carbon source (glucose or acetate) that can be metabolized to AcP. Indeed, exponential phase cells that were arrested for growth exhibited an increase in acetylation. Increased acetylation depended on the presence of the metabolite and

signaling molecule acetyl phosphate (AcP), was partially inhibited by the KDAC CobB, and was mostly independent of the KAT YfiQ. In the absence of a KAT, AcP could donate acetyl groups to purified adenylate kinase and bovine serum albumin, which suggests that AcP can modify proteins through a non-enzymatic mechanism.

The *ackA* mutant accumulates AcP and acetylated proteins during exponential growth (Kuhn *et al. in preparation*). Since AcP is a highly reactive electrophile that can also donate phosphoryl groups to RRs, I tested whether this effect of AcP on acetylation is a direct chemical reaction by performing *in vitro* acetylation experiments with AcP and LpdA. AcP is an acetyl donor to LpdA (**Figures 31**, **33,** and **34**) and several other proteins. I found that acetylation of LpdA is concentration dependent. The number of acetylated lysines increased and the kinetics of lysine acetylation were more variable in the presence of higher concentrations of AcP.

An analysis of the modified sites *in vivo* and *in vitro* may have provided some insight into the regulation of AcP-dependent, non-enzymatic acetylation of proteins. We tested if the primary amino acid sequence influences the specificity of non-enzymatic acetylation. Our collaborators Drs. Kuhn and Scholle incubated a peptide array with randomized residues flanking the lysine with AcP and acetylation was detected by mass spectrometry (235). This approach identifies sequence characteristics that provide the most favorable conditions for acetylation by AcP. They discovered that AcP donated acetyl groups preferentially to lysines that were

flanked by positively charged residues. In contrast, adjacent negatively charged residues were strictly inhibitory (Kuhn *et al.*, *in preparation*).

We collaborated with Drs. Gibson and Schilling at The Buck Institute for Research on Aging, who performed label-free quantitative mass spectrometry (239) on WT cells and the *ackA* mutant. From their mass spectrometric data, I analyzed over 500 unique sites that were at least 2-fold more acetylated in the *ackA* mutant compared to WT cells. This analysis showed that the -1 and +1 positions tend to be negatively charged aspartate and glutamate, with a low frequency of positively charged lysine, arginine, and histidine (**Figure 36**). Specifically, 30% of the amino acids in the -1 position were aspartate or glutamate, and these residues represented 20% of the amino acids in the +1 position. This is in contrast to 5% and 11% of amino acids in the -1 and +1 positions, respectively, being lysine, arginine, and histidine.

Taken together, the sequence preferences identified *in vitro* and *in vivo* may provide some understanding of the mechanism of acetylation using AcP. However, it is important to note that peptide array identified sequence preferences do not necessarily indicate physiologically relevant sequences. For example, peptide arrays have been used to determine KDAC-specific sequences. Acetylated peptide arrays were incubated with one of four KDACs and deacetylation was detected by mass spectrometry (235). The most frequently deacetylated peptides can, but do not always, represent the sequences of acetylated targets *in vivo* (29,235). Instead, these

peptide arrays indicate optimal substrates. To account for modified lysines that are adjacent to non-permissive residues, it has been hypothesized that physiological targets have suboptimal sequence characteristics to allow for regulation by enzymes (235).

Since acetylation by AcP can occur non-enzymatically, our collaborators and I propose that chemical acetylation is regulated by residues that are either adjacent on the linear polypeptide sequence or close to the lysine in the tertiary structure. The outcome of acetylation is a balance of optimal, suboptimal, and inhibitory residues. I propose that these residues have different capacities to promote acetylation, depending on their ability to either activate the lysine for acetylation or increase the local concentration of AcP. It has been reported that KATs have mechanisms to activate lysines by deprotonation and residues that position AcCoA near the lysine. Deprotonation of lysines can occur through 'proton wires' that shuttle the positive charge away from the lysine side chain or through conserved catalytic residues that act as general bases. It is possible for adjacent negatively charged aspartate and glutamine to act as general bases on lysine. As for the positively charged residues, they may increase the concentration or the probability of AcP being near a potentially activated lysine through electrostatic interactions with the electronegative phosphoryl group. This hypothesis can be tested. Gcn5 Glu-173 is a conserved residue that is essential for catalytic activity by functioning as a general base at physiological pH (68). The E173Q variant of Gcn5 was unable to

acetylate histone protein at neutral pH but was capable of acetylation at high pH, a condition that artificially deprotonates lysines. These results are consistent with Glu-173 acting as a general base. Similar experiments could be performed with acetylation substrates of AcP to test putative general base residues.

Differences in pH could also explain the widely different results seen in the peptide array compared to the *in vivo* analysis of AcP-sensitive acetylated sites. The peptide array was performed at pH 8 and I have observed that acetylation with AcP and LpdA is pH-sensitive (data not shown). A basic condition is optimized for non-enzymatic acetylation of lysines because the proportion of deprotonated and active lysines is greater than at neutral pH. The preference for positively charged residues adjacent to the acetylated lysine might indicate that at higher pH, the rate of acetylation is determined by the presence of AcP near the activated lysine. One could test whether the preferences for certain peptide sequences change at different pH.

Concluding Remarks

Our collaborators and I have discovered that *E. coli* applies many different mechanisms to regulate cellular processes. Specifically, RcsB activity appears to be regulated by both phosphorylation and acetylation. Activation by phosphorylation can come from either Rcs signaling or from AcP. RcsB can exist in multiple oligomeric states and potentially affect cellular physiology independently of its transcriptional activity. Lastly, AcP is a novel, highly reactive, bifunctional molecule

that can modify proteins by functioning either as a phosphoryl donor or as an acetyl group donor. Although acetylation by AcP can occur non-enzymatically, the reaction appears to be regulated in part by the charges of neighboring residues. This study highlights the importance of non-enzymatic reactions in cellular physiology and advances our understanding of how the effects of reactive small molecules like AcP are regulated.

REFERENCES

1. Karve, T. M., and Cheema, A. K. (2011). Small changes huge impact: the role of protein posttranslational modifications in cellular homeostasis and disease. *J Amino Acids*, *2011*, 207691.

2. Prabakaran, S., Lippens, G., Steen, H., and Gunawardena, J. (2012). Post-translational modification: nature's escape from genetic imprisonment and the basis for dynamic information encoding. *Wiley Interdiscip Rev Syst Biol Med*, *4*, 565-583.

3. Boyer, R. (2006). Posttranslational Modification of Proteins: Expanding Nature's Inventory. *Biochemistry and Molecular Biology Education*, *34*, 461-462.

4. Hu, L. I., Lima, B. P., and Wolfe, A. J. (2010). Bacterial protein acetylation: the dawning of a new age. *Mol Microbiol*, *77*, 15-21.

5. Phillips, D. M. (1963). The presence of acetyl groups of histones. *Biochem J*, *87*, 258-263.

6. Arnesen, T., Van Damme, P., Polevoda, B., Helsens, K., Evjenth, R., Colaert, N., Varhaug, J. E., Vandekerckhove, J., Lillehaug, J. R., Sherman, F., and Gevaert, K. (2009). Proteomics analyses reveal the evolutionary conservation and divergence of N-terminal acetyltransferases from yeast and humans. *Proc Natl Acad Sci U S A*, *106*, 8157-8162.

7. Walker, J.-P. (1963). The NH2-terminal residues of the proteins from cell-free extracts of E. coli. *J Mol Biol*, *7*, 483-496.

8. Gautschi, M., Just, S., Mun, A., Ross, S., Rucknagel, P., Dubaquie, Y., Ehrenhofer-Murray, A., and Rospert, S. (2003). The yeast N(alpha)-acetyltransferase NatA is quantitatively anchored to the ribosome and interacts with nascent polypeptides. *Mol Cell Biol*, *23*, 7403-7414.

9. Pestana, A., and Pitot, H. C. (1975). Acetylation of nascent polypeptide chains on rat liver polyribosomes in vivo and in vitro. *Biochemistry*, *14*, 1404-1412.

10. Pestana, A., and Pitot, H. C. (1975). Acetylation of ribosome-associated proteins in vitro by an acetyltransferanse bound to rat liver ribosomes. *Biochemistry*, *14*, 1397-1403.

11. Polevoda, B., Brown, S., Cardillo, T. S., Rigby, S., and Sherman, F. (2008). Yeast N(alpha)-terminal acetyltransferases are associated with ribosomes. *J Cell Biochem*, *103*, 492-508.

12. Polevoda, B., Arnesen, T., and Sherman, F. (2009). A synopsis of eukaryotic Nalpha-terminal acetyltransferases: nomenclature, subunits and substrates. *BMC Proc*, *3 Suppl 6*, S2.

13. Polevoda, B., and Sherman, F. (2003). N-terminal acetyltransferases and sequence requirements for N-terminal acetylation of eukaryotic proteins. *J Mol Biol*, *325*, 595-622.

14. Perrot, M., Massoni, A., and Boucherie, H. (2008). Sequence requirements for Nalpha-terminal acetylation of yeast proteins by NatA. *Yeast*, *25*, 513-527.

15. Hershko, A., Heller, H., Eytan, E., Kaklij, G., and Rose, I. A. (1984). Role of the alpha-amino group of protein in ubiquitin-mediated protein breakdown. *Proc Natl Acad Sci U S A*, *81*, 7021-7025.

16. Hwang, C. S., Shemorry, A., and Varshavsky, A. (2010). N-terminal acetylation of cellular proteins creates specific degradation signals. *Science*, *327*, 973-977.

17. Barak, R., Welch, M., Yanovsky, A., Oosawa, K., and Eisenbach, M. (1992). Acetyladenylate or its derivative acetylates the chemotaxis protein CheY in vitro and increases its activity at the flagellar switch. *Biochemistry*, *31*, 10099-10107.

18. Gershey, E. L., Vidali, G., and Allfrey, V. G. (1968). Chemical studies of histone acetylation. The occurrence of epsilon-N-acetyllysine in the f2a1 histone. *J Biol Chem*, *243*, 5018-5022.

19. Allfrey, V. G., Faulkner, R., and Mirsky, A. E. (1964). Acetylation and Methylation of Histones and Their Possible Role in the Regulation of Rna Synthesis. *Proc Natl Acad Sci U S A, 51*, 786-794.

20. Strahl, B. D., and Allis, C. D. (2000). The language of covalent histone modifications. *Nature, 403*, 41-45.

21. Jenuwein, T., and Allis, C. D. (2001). Translating the histone code. *Science, 293*, 1074-1080.

22. Green, D. R., and Kroemer, G. (2009). Cytoplasmic functions of the tumour suppressor p53. *Nature, 458*, 1127-1130.

23. Meek, D. W., and Anderson, C. W. (2009). Posttranslational modification of p53: cooperative integrators of function. *Cold Spring Harb Perspect Biol, 1*, a000950.

24. Chao, C., Wu, Z., Mazur, S. J., Borges, H., Rossi, M., Lin, T., Wang, J. Y., Anderson, C. W., Appella, E., and Xu, Y. (2006). Acetylation of mouse p53 at lysine 317 negatively regulates p53 apoptotic activities after DNA damage. *Mol Cell Biol, 26*, 6859-6869.

25. Gu, W., Shi, X. L., and Roeder, R. G. (1997). Synergistic activation of transcription by CBP and p53. *Nature, 387*, 819-823.

26. Tang, Y., Zhao, W., Chen, Y., Zhao, Y., and Gu, W. (2008). Acetylation is indispensable for p53 activation. *Cell, 133*, 612-626.

27. Lill, N. L., Grossman, S. R., Ginsberg, D., DeCaprio, J., and Livingston, D. M. (1997). Binding and modulation of p53 by p300/CBP coactivators. *Nature, 387*, 823-827.

28. Gu, B., and Zhu, W. G. (2012). Surf the post-translational modification network of p53 regulation. *Int J Biol Sci, 8*, 672-684.

29. Choudhary, C., Kumar, C., Gnad, F., Nielsen, M. L., Rehman, M., Walther, T. C., Olsen, J. V., and Mann, M. (2009). Lysine acetylation targets protein complexes and co-regulates major cellular functions. *Science*, *325*, 834-840.

30. Kim, S. C., Sprung, R., Chen, Y., Xu, Y., Ball, H., Pei, J., Cheng, T., Kho, Y., Xiao, H., Xiao, L., Grishin, N. V., White, M., Yang, X. J., and Zhao, Y. (2006). Substrate and functional diversity of lysine acetylation revealed by a proteomics survey. *Mol Cell*, *23*, 607-618.

31. Zhao, S., Xu, W., Jiang, W., Yu, W., Lin, Y., Zhang, T., Yao, J., Zhou, L., Zeng, Y., Li, H., Li, Y., Shi, J., An, W., Hancock, S. M., He, F., Qin, L., Chin, J., Yang, P., Chen, X., Lei, Q., Xiong, Y., and Guan, K. L. (2010). Regulation of cellular metabolism by protein lysine acetylation. *Science*, *327*, 1000-1004.

32. Gray, M. W., Burger, G., and Lang, B. F. (1999). Mitochondrial evolution. *Science*, *283*, 1476-1481.

33. Pallen, M. J. (2011). Time to recognise that mitochondria are bacteria? *Trends Microbiol*, *19*, 58-64.

34. Yu, B. J., Kim, J. A., Moon, J. H., Ryu, S. E., and Pan, J. G. (2008). The diversity of lysine-acetylated proteins in Escherichia coli. *J Microbiol Biotechnol*, *18*, 1529-1536.

35. Zhang, J., Sprung, R., Pei, J., Tan, X., Kim, S., Zhu, H., Liu, C. F., Grishin, N. V., and Zhao, Y. (2009). Lysine acetylation is a highly abundant and evolutionarily conserved modification in *Escherichia coli*. *Mol Cell Proteomics*, *8*, 215-225.

36. Wang, Q., Zhang, Y., Yang, C., Xiong, H., Lin, Y., Yao, J., Li, H., Xie, L., Zhao, W., Yao, Y., Ning, Z. B., Zeng, R., Xiong, Y., Guan, K. L., Zhao, S., and Zhao, G. P. (2010). Acetylation of metabolic enzymes coordinates carbon source utilization and metabolic flux. *Science*, *327*, 1004-1007.

37. Kim, D., Yu, B. J., Kim, J. A., Lee, Y. J., Choi, S. G., Kang, S., and Pan, J. G. (2013). The acetylproteome of Gram-positive model bacterium *Bacillus subtilis*. *Proteomics*, *13*, 1726-1736.

38. Soufi, B., Soares, N. C., Ravikumar, V., and Macek, B. (2012). Proteomics reveals evidence of cross-talk between protein modifications in bacteria: focus on acetylation and phosphorylation. *Curr Opin Microbiol*, *15*, 357-363.

39. van Noort, V., Seebacher, J., Bader, S., Mohammed, S., Vonkova, I., Betts, M. J., Kuhner, S., Kumar, R., Maier, T., O'Flaherty, M., Rybin, V., Schmeisky, A., Yus, E., Stulke, J., Serrano, L., Russell, R. B., Heck, A. J., Bork, P., and Gavin, A. C. (2012). Cross-talk between phosphorylation and lysine acetylation in a genome-reduced bacterium. *Mol Syst Biol*, *8*, 571.

40. Okanishi, H., Kim, K., Masui, R., and Kuramitsu, S. (2013). Acetylome with structural mapping reveals the significance of lysine acetylation in *Thermus thermophilus*. *J Proteome Res*,

41. Li, R., Gu, J., Chen, Y. Y., Xiao, C. L., Wang, L. W., Zhang, Z. P., Bi, L. J., Wei, H. P., Wang, X. D., Deng, J. Y., and Zhang, X. E. (2010). CobB regulates *Escherichia coli* chemotaxis by deacetylating the response regulator CheY. *Mol Microbiol*, *76*, 1162-1174.

42. Yan, J., Barak, R., Liarzi, O., Shainskaya, A., and Eisenbach, M. (2008). In vivo acetylation of CheY, a response regulator in chemotaxis of *Escherichia coli*. *J Mol Biol*, *376*, 1260-1271.

43. Eisenbach, M. (2007). A hitchhiker's guide through advances and conceptual changes in chemotaxis. *J Cell Physiol*, *213*, 574-580.

44. Liarzi, O., Barak, R., Bronner, V., Dines, M., Sagi, Y., Shainskaya, A., and Eisenbach, M. (2010). Acetylation represses the binding of CheY to its target proteins. *Mol Microbiol*, *76*, 932-943.

45. Barak, R., Prasad, K., Shainskaya, A., Wolfe, A. J., and Eisenbach, M. (2004). Acetylation of the chemotaxis response regulator CheY by acetyl-CoA synthetase purified from Escherichia coli. *J Mol Biol*, *342*, 383-401.

46. Barak, R., Yan, J., Shainskaya, A., and Eisenbach, M. (2006). The chemotaxis response regulator CheY can catalyze its own acetylation. *J Mol Biol*, *359*, 251-265.

47. Lima, B. P., Antelmann, H., Gronau, K., Chi, B. K., Becher, D., Brinsmade, S. R., and Wolfe, A. J. (2011). Involvement of protein acetylation in glucose-induced transcription of a stress-responsive promoter. *Mol Microbiol*, *81*, 1190-1204.

48. Lima, B. P., Huyen, T. T., Bäsell, K., Becher, D., Antelmann, H., and Wolfe, A. J. (2012). Inhibition of Acetyl phosphate-dependent transcription by an acetylatable lysine on RNA polymerase. *J Biol Chem*, *287*, 32147-32160.

49. Thao, S., Chen, C. S., Zhu, H., and Escalante-Semerena, J. C. (2010). Nepsilon-lysine acetylation of a bacterial transcription factor inhibits Its DNA-binding activity. *PLoS One*, *5*, e15123.

50. Liang, W., Malhotra, A., and Deutscher, M. P. (2011). Acetylation regulates the stability of a bacterial protein: growth stage-dependent modification of RNase R. *Mol Cell*, *44*, 160-166.

51. Liang, W., and Deutscher, M. P. (2012). Post-translational modification of RNase R is regulated by stress-dependent reduction in the acetylating enzyme Pka (YfiQ). *RNA*, *18*, 37-41.

52. Liang, W., and Deutscher, M. P. (2010). A novel mechanism for ribonuclease regulation: transfer-messenger RNA (tmRNA) and its associated protein SmpB regulate the stability of RNase R. *J Biol Chem*, *285*, 29054-29058.

53. Liang, W., and Deutscher, M. P. (2012). Transfer-messenger RNA-SmpB protein regulates ribonuclease R turnover by promoting binding of HslUV and Lon proteases. *J Biol Chem*, *287*, 33472-33479.

54. Shaw, K. J., Rather, P. N., Hare, R. S., and Miller, G. H. (1993). Molecular genetics of aminoglycoside resistance genes and familial relationships of the aminoglycoside-modifying enzymes. *Microbiol Rev*, *57*, 138-163.

55. Vetting, M. W., LP, S. d. C., Yu, M., Hegde, S. S., Magnet, S., Roderick, S. L., and Blanchard, J. S. (2005). Structure and functions of the GNAT superfamily of acetyltransferases. *Arch Biochem Biophys*, *433*, 212-226.

56. Marmorstein, R., and Roth, S. Y. (2001). Histone acetyltransferases: function, structure, and catalysis. *Curr Opin Genet Dev*, *11*, 155-161.

57. Bannister, A. J., and Kouzarides, T. (1996). The CBP co-activator is a histone acetyltransferase. *Nature*, *384*, 641-643.

58. Spencer, T. E., Jenster, G., Burcin, M. M., Allis, C. D., Zhou, J., Mizzen, C. A., McKenna, N. J., Onate, S. A., Tsai, S. Y., Tsai, M. J., and O'Malley, B. W. (1997). Steroid receptor coactivator-1 is a histone acetyltransferase. *Nature*, *389*, 194-198.

59. Mizzen, C. A., Yang, X. J., Kokubo, T., Brownell, J. E., Bannister, A. J., Owen-Hughes, T., Workman, J., Wang, L., Berger, S. L., Kouzarides, T., Nakatani, Y., and Allis, C. D. (1996). The TAF(II)250 subunit of TFIID has histone acetyltransferase activity. *Cell*, *87*, 1261-1270.

60. Neuwald, A. F., and Landsman, D. (1997). GCN5-related histone N-acetyltransferases belong to a diverse superfamily that includes the yeast SPT10 protein. *Trends Biochem Sci*, *22*, 154-155.

61. Lu, L., Berkey, K. A., and Casero, R. A., Jr. (1996). RGFGIGS is an amino acid sequence required for acetyl coenzyme A binding and activity of human spermidine/spermine N1acetyltransferase. *J Biol Chem*, *271*, 18920-18924.

62. Wolf, E., Vassilev, A., Makino, Y., Sali, A., Nakatani, Y., and Burley, S. K. (1998). Crystal structure of a GCN5-related N-acetyltransferase: *Serratia marcescens* aminoglycoside 3-N-acetyltransferase. *Cell*, *94*, 439-449.

63. Dyda, F., Klein, D. C., and Hickman, A. B. (2000). GCN5-related N-acetyltransferases: a structural overview. *Annu Rev Biophys Biomol Struct*, *29*, 81-103.

64. Berndsen, C. E., Albaugh, B. N., Tan, S., and Denu, J. M. (2007). Catalytic mechanism of a MYST family histone acetyltransferase. *Biochemistry*, *46*, 623-629.

65. Yan, Y., Harper, S., Speicher, D. W., and Marmorstein, R. (2002). The catalytic mechanism of the ESA1 histone acetyltransferase involves a self-acetylated intermediate. *Nat Struct Biol*, *9*, 862-869.

66. Jiang, J., Lu, J., Lu, D., Liang, Z., Li, L., Ouyang, S., Kong, X., Jiang, H., Shen, B., and Luo, C. (2012). Investigation of the acetylation mechanism by GCN5 histone acetyltransferase. *PLoS One*, *7*, e36660.

67. Trievel, R. C., Rojas, J. R., Sterner, D. E., Venkataramani, R. N., Wang, L., Zhou, J., Allis, C. D., Berger, S. L., and Marmorstein, R. (1999). Crystal structure and mechanism of histone acetylation of the yeast GCN5 transcriptional coactivator. *Proc Natl Acad Sci U S A*, *96*, 8931-8936.

68. Tanner, K. G., Trievel, R. C., Kuo, M. H., Howard, R. M., Berger, S. L., Allis, C. D., Marmorstein, R., and Denu, J. M. (1999). Catalytic mechanism and function of invariant glutamic acid 173 from the histone acetyltransferase GCN5 transcriptional coactivator. *J Biol Chem*, *274*, 18157-18160.

69. Liszczak, G., Arnesen, T., and Marmorstein, R. (2011). Structure of a ternary Naa50p (NAT5/SAN) N-terminal acetyltransferase complex reveals the molecular basis for substrate-specific acetylation. *J Biol Chem*, *286*, 37002-37010.

70. Nambi, S., Basu, N., and Visweswariah, S. S. (2010). cAMP-regulated protein lysine acetylases in mycobacteria. *J Biol Chem*, *285*, 24313-24323.

71. Zhao, G., Jin, Z., Allewell, N. M., Tuchman, M., and Shi, D. (2013). Crystal structure of the N-acetyltransferase domain of human N-acetyl-L-glutamate synthase in complex with N-acetyl-L-glutamate provides insights into its catalytic and regulatory mechanisms. *PLoS One*, *8*, e70369.

72. Brent, M. M., Iwata, A., Carten, J., Zhao, K., and Marmorstein, R. (2009). Structure and biochemical characterization of protein acetyltransferase from *Sulfolobus solfataricus*. *J Biol Chem*, *284*, 19412-19419.

73. Scott, I., Webster, B. R., Li, J. H., and Sack, M. N. (2012). Identification of a molecular component of the mitochondrial acetyltransferase programme: a novel role for GCN5L1. *Biochem J*, *443*, 655-661.

74. Yoshida, M., Horinouchi, S., and Beppu, T. (1995). Trichostatin A and trapoxin: novel chemical probes for the role of histone acetylation in chromatin structure and function. *Bioessays*, *17*, 423-430.

75. Taunton, J., Hassig, C. A., and Schreiber, S. L. (1996). A mammalian histone deacetylase related to the yeast transcriptional regulator Rpd3p. *Science*, *272*, 408-411.

76. de Ruijter, A. J., van Gennip, A. H., Caron, H. N., Kemp, S., and van Kuilenburg, A. B. (2003). Histone deacetylases (HDACs): characterization of the classical HDAC family. *Biochem J*, *370*, 737-749.

77. Gregoretti, I. V., Lee, Y. M., and Goodson, H. V. (2004). Molecular evolution of the histone deacetylase family: functional implications of phylogenetic analysis. *J Mol Biol*, *338*, 17-31.

78. Greiss, S., and Gartner, A. (2009). Sirtuin/Sir2 phylogeny, evolutionary considerations and structural conservation. *Mol Cells*, *28*, 407-415.

79. Frye, R. A. (2000). Phylogenetic classification of prokaryotic and eukaryotic Sir2-like proteins. *Biochem Biophys Res Commun*, *273*, 793-798.

80. Hildmann, C., Riester, D., and Schwienhorst, A. (2007). Histone deacetylases--an important class of cellular regulators with a variety of functions. *Appl Microbiol Biotechnol*, *75*, 487-497.

81. Hubbert, C., Guardiola, A., Shao, R., Kawaguchi, Y., Ito, A., Nixon, A., Yoshida, M., Wang, X. F., and Yao, T. P. (2002). HDAC6 is a microtubule-associated deacetylase. *Nature*, *417*, 455-458.

82. Ito, A., Kawaguchi, Y., Lai, C. H., Kovacs, J. J., Higashimoto, Y., Appella, E., and Yao, T. P. (2002). MDM2-HDAC1-mediated deacetylation of p53 is required for its degradation. *EMBO J*, *21*, 6236-6245.

83. Hirschey, M. D. (2011). Old enzymes, new tricks: sirtuins are NAD(+)-dependent de-acylases. *Cell Metab*, *14*, 718-719.

84. Finnin, M. S., Donigian, J. R., Cohen, A., Richon, V. M., Rifkind, R. A., Marks, P. A., Breslow, R., and Pavletich, N. P. (1999). Structures of a histone deacetylase homologue bound to the TSA and SAHA inhibitors. *Nature*, *401*, 188-193.

85. Gallinari, P., Di Marco, S., Jones, P., Pallaoro, M., and Steinkuhler, C. (2007). HDACs, histone deacetylation and gene transcription: from molecular biology to cancer therapeutics. *Cell Res*, *17*, 195-211.

86. Marmorstein, R. (2001). Structure of histone deacetylases: insights into substrate recognition and catalysis. *Structure*, *9*, 1127-1133.

87. Somoza, J. R., Skene, R. J., Katz, B. A., Mol, C., Ho, J. D., Jennings, A. J., Luong, C., Arvai, A., Buggy, J. J., Chi, E., Tang, J., Sang, B. C., Verner, E., Wynands, R., Leahy, E. M., Dougan, D. R., Snell, G., Navre, M., Knuth, M. W., Swanson, R. V., McRee, D. E., and Tari, L. W. (2004). Structural snapshots of human HDAC8 provide insights into the class I histone deacetylases. *Structure*, *12*, 1325-1334.

88. Vannini, A., Volpari, C., Filocamo, G., Casavola, E. C., Brunetti, M., Renzoni, D., Chakravarty, P., Paolini, C., De Francesco, R., Gallinari, P., Steinkuhler, C., and Di Marco, S. (2004). Crystal structure of a eukaryotic zinc-dependent histone deacetylase, human HDAC8, complexed with a hydroxamic acid inhibitor. *Proc Natl Acad Sci U S A*, *101*, 15064-15069.

89. Miller, E. S., Heidelberg, J. F., Eisen, J. A., Nelson, W. C., Durkin, A. S., Ciecko, A., Feldblyum, T. V., White, O., Paulsen, I. T., Nierman, W. C., Lee, J., Szczypinski, B., and Fraser, C. M. (2003). Complete genome sequence of the broad-host-range vibriophage KVP40: comparative genomics of a T4-related bacteriophage. *J Bacteriol*, *185*, 5220-5233.

90. Du, J., Zhou, Y., Su, X., Yu, J. J., Khan, S., Jiang, H., Kim, J., Woo, J., Kim, J. H., Choi, B. H., He, B., Chen, W., Zhang, S., Cerione, R. A., Auwerx, J., Hao, Q., and Lin, H. (2011). Sirt5 is a NAD-dependent protein lysine demalonylase and desuccinylase. *Science*, *334*, 806-809.

91. Klar, A. J., Fogel, S., and Macleod, K. (1979). MAR1-a Regulator of the HMa and HMalpha Loci in *Saccharomyces cerevisiae*. *Genetics*, *93*, 37-50.

92. Feldman, J. L., Dittenhafer-Reed, K. E., and Denu, J. M. (2012). Sirtuin catalysis and regulation. *J Biol Chem*, *287*, 42419-42427.

93. Yuan, H., and Marmorstein, R. (2012). Structural basis for sirtuin activity and inhibition. *J Biol Chem*, *287*, 42428-42435.

94. Sauve, A. A. (2010). Sirtuin chemical mechanisms. *Biochim Biophys Acta*, *1804*, 1591-1603.

95. Avalos, J. L., Boeke, J. D., and Wolberger, C. (2004). Structural basis for the mechanism and regulation of Sir2 enzymes. *Mol Cell*, *13*, 639-648.

96. Zhao, K., Harshaw, R., Chai, X., and Marmorstein, R. (2004). Structural basis for nicotinamide cleavage and ADP-ribose transfer by NAD(+)-dependent Sir2 histone/protein deacetylases. *Proc Natl Acad Sci U S A*, *101*, 8563-8568.

97. Smith, B. C., and Denu, J. M. (2006). Sir2 protein deacetylases: evidence for chemical intermediates and functions of a conserved histidine. *Biochemistry*, *45*, 272-282.

98. Tong, L., and Denu, J. M. (2010). Function and metabolism of sirtuin metabolite O-acetyl-ADP-ribose. *Biochim Biophys Acta*, *1804*, 1617-1625.

99. Trzebiatowski, J. R., O'Toole, G. A., and Escalante-Semerena, J. C. (1994). The *cobT* gene of *Salmonella typhimurium* encodes the NaMN: 5,6-dimethylbenzimidazole phosphoribosyltransferase responsible for the synthesis of N1-(5-phospho-alpha-D-ribosyl)-5,6-dimethylbenzimidazole, an intermediate in the synthesis of the nucleotide loop of cobalamin. *J Bacteriol*, *176*, 3568-3575.

100. Tsang, A. W., and Escalante-Semerena, J. C. (1998). CobB, a new member of the SIR2 family of eucaryotic regulatory proteins, is required to compensate for the lack of nicotinate mononucleotide:5,6-dimethylbenzimidazole phosphoribosyltransferase activity in *cobT* mutants during cobalamin biosynthesis in *Salmonella typhimurium* LT2. *J Biol Chem*, *273*, 31788-31794.

101. Frye, R. A. (1999). Characterization of five human cDNAs with homology to the yeast SIR2 gene: Sir2-like proteins (sirtuins) metabolize NAD and may have protein ADP-ribosyltransferase activity. *Biochem Biophys Res Commun*, *260*, 273-279.

102. Smith, J. S., Brachmann, C. B., Celic, I., Kenna, M. A., Muhammad, S., Starai, V. J., Avalos, J. L., Escalante-Semerena, J. C., Grubmeyer, C., Wolberger, C., and Boeke, J. D. (2000). A phylogenetically conserved NAD+-dependent protein deacetylase activity in the Sir2 protein family. *Proc Natl Acad Sci U S A*, *97*, 6658-6663.

103. Houtkooper, R. H., Pirinen, E., and Auwerx, J. (2012). Sirtuins as regulators of metabolism and healthspan. *Nat Rev Mol Cell Biol*, *13*, 225-238.

104. Sauve, A. A., Wolberger, C., Schramm, V. L., and Boeke, J. D. (2006). The biochemistry of sirtuins. *Annu Rev Biochem*, *75*, 435-465.

105. Avalos, J. L., Bever, K. M., and Wolberger, C. (2005). Mechanism of sirtuin inhibition by nicotinamide: altering the NAD(+) cosubstrate specificity of a Sir2 enzyme. *Mol Cell*, *17*, 855-868.

106. Deutscher, J. (2008). The mechanisms of carbon catabolite repression in bacteria. *Curr Opin Microbiol*, *11*, 87-93.

107. Deutscher, J., Francke, C., and Postma, P. W. (2006). How phosphotransferase system-related protein phosphorylation regulates carbohydrate metabolism in bacteria. *Microbiol Mol Biol Rev*, *70*, 939-1031.

108. Wolfe, A. J. (2005). The acetate switch. *Microbiol Mol Biol Rev*, *69*, 12-50.

109. Zheng, D., Constantinidou, C., Hobman, J. L., and Minchin, S. D. (2004). Identification of the CRP regulon using in vitro and in vivo transcriptional profiling. *Nucleic Acids Res*, *32*, 5874-5893.

110. Chohnan, S., Izawa, H., Nishihara, H., and Takamura, Y. (1998). Changes in size of intracellular pools of coenzyme A and its thioesters in *Escherichia coli* K-12 cells to various carbon sources and stresses. *Biosci Biotechnol Biochem*, *62*, 1122-1128.

111. Chohnan, S., and Takamura, Y. (1991). A simple micromethod for measurement of CoASH and its use in measuring intracellular levels of CoASH and short chain acyl-CoAs in *Escherichia coli* K12 cells. *Agric Biol Chem*, *55*, 87-94.

112. Vallari, D. S., and Jackowski, S. (1988). Biosynthesis and degradation both contribute to the regulation of coenzyme A content in Escherichia coli. *J Bacteriol*, *170*, 3961-3966.

113. Vallari, D. S., Jackowski, S., and Rock, C. O. (1987). Regulation of pantothenate kinase by coenzyme A and its thioesters. *J Biol Chem*, *262*, 2468-2471.

114. Vallari, D. S., and Rock, C. O. (1987). Isolation and characterization of temperature-sensitive pantothenate kinase (coaA) mutants of Escherichia coli. *J Bacteriol*, *169*, 5795-5800.

115. Chohnan, S., Furukawa, H., Fujio, T., Nishihara, H., and Takamura, Y. (1997). Changes in the size and composition of intracellular pools of nonesterified coenzyme A and coenzyme A thioesters in aerobic and facultatively anaerobic bacteria. *Appl Environ Microbiol*, *63*, 553-560.

116. Jackowski, S., and Rock, C. O. (1986). Consequences of reduced intracellular coenzyme A content in *Escherichia coli*. *J Bacteriol*, *166*, 866-871.

117. Cummings, J. H. (1981). Short chain fatty acids in the human colon. *Gut*, *22*, 763-779.

118. Cummings, J. H., Pomare, E. W., Branch, W. J., Naylor, C. P., and Macfarlane, G. T. (1987). Short chain fatty acids in human large intestine, portal, hepatic and venous blood. *Gut*, *28*, 1221-1227.

119. Starai, V. J., and Escalante-Semerena, J. C. (2004). Acetyl-coenzyme A synthetase (AMP forming). *Cell Mol Life Sci*, *61*, 2020-2030.

120. Ingram-Smith, C., Martin, S. R., and Smith, K. S. (2006). Acetate kinase: not just a bacterial enzyme. *Trends Microbiol*, *14*, 249-253.

121. Kumari, S., Tishel, R., Eisenbach, M., and Wolfe, A. J. (1995). Cloning, characterization, and functional expression of *acs*, the gene which encodes acetyl coenzyme A synthetase in *Escherichia coli*. *J Bacteriol*, *177*, 2878-2886.

122. **Howland, J.** (1990) *Biochemistry: By D Voet and J G Voet* John Wiley and Sons, New York

123. Klein, A. H., Shulla, A., Reimann, S. A., Keating, D. H., and Wolfe, A. J. (2007). The intracellular concentration of acetyl phosphate in Escherichia coli is sufficient for direct phosphorylation of two-component response regulators. *J Bacteriol*, *189*, 5574-5581.

124. Wolfe, A. J., Chang, D. E., Walker, J. D., Seitz-Partridge, J. E., Vidaurri, M. D., Lange, C. F., Pruss, B. M., Henk, M. C., Larkin, J. C., and Conway, T. (2003). Evidence that acetyl phosphate functions as a global signal during biofilm development. *Mol Microbiol*, *48*, 977-988.

125. Fredericks, C. E., Shibata, S., Aizawa, S., Reimann, S. A., and Wolfe, A. J. (2006). Acetyl phosphate-sensitive regulation of flagellar biogenesis and capsular biosynthesis depends on the Rcs phosphorelay. *Mol Microbiol*, *61*, 734-747.

126. Liu, X., Pena Sandoval, G. R., Wanner, B. L., Jung, W. S., Georgellis, D., and Kwon, O. (2009). Evidence against the physiological role of acetyl phosphate in the phosphorylation of the ArcA response regulator in *Escherichia coli*. *J Microbiol*, *47*, 657-662.

127. Mizrahi, I., Biran, D., and Ron, E. Z. (2009). Involvement of the Pta-AckA pathway in protein folding and aggregation. *Res Microbiol*, *160*, 80-84.

128. McCleary, W. R., and Stock, J. B. (1994). Acetyl phosphate and the activation of two-component response regulators. *J Biol Chem*, *269*, 31567-31572.

129. Brown, T. D., Jones-Mortimer, M. C., and Kornberg, H. L. (1977). The enzymic interconversion of acetate and acetyl-coenzyme A in *Escherichia coli*. *J Gen Microbiol*, *102*, 327-336.

130. Starai, V. J., Takahashi, H., Boeke, J. D., and Escalante-Semerena, J. C. (2003). Short-chain fatty acid activation by acyl-coenzyme A synthetases requires SIR2 protein function in *Salmonella enterica* and *Saccharomyces cerevisiae*. *Genetics*, *163*, 545-555.

131. Starai, V. J., Celic, I., Cole, R. N., Boeke, J. D., and Escalante-Semerena, J. C. (2002). Sir2-dependent activation of acetyl-CoA synthetase by deacetylation of active lysine. *Science*, *298*, 2390-2392.

132. Starai, V. J., and Escalante-Semerena, J. C. (2004). Identification of the protein acetyltransferase (Pat) enzyme that acetylates acetyl-CoA synthetase in Salmonella enterica. *J Mol Biol*, *340*, 1005-1012.

133. Hoch, J. A. (2000). Two-component and phosphorelay signal transduction. *Curr Opin Microbiol*, *3*, 165-170.

134. Stock, A. M., Robinson, V. L., and Goudreau, P. N. (2000). Two-component signal transduction. *Annu Rev Biochem*, *69*, 183-215.

135. Mitrophanov, A. Y., and Groisman, E. A. (2008). Signal integration in bacterial two-component regulatory systems. *Genes Dev*, *22*, 2601-2611.

136. Bekker, M., Teixeira de Mattos, M. J., and Hellingwerf, K. J. (2006). The role of two-component regulation systems in the physiology of the bacterial cell. *Sci Prog*, *89*, 213-242.

137. West, A. H., and Stock, A. M. (2001). Histidine kinases and response regulator proteins in two-component signaling systems. *Trends Biochem Sci*, *26*, 369-376.

138. Mizuno, T. (1997). Compilation of all genes encoding two-component phosphotransfer signal transducers in the genome of Escherichia coli. *DNA Res*, *4*, 161-168.

139. Ulrich, L. E., and Zhulin, I. B. (2007). MiST: a microbial signal transduction database. *Nucleic Acids Res*, *35*, D386-390.

140. Ulrich, L. E., and Zhulin, I. B. (2010). The MiST2 database: a comprehensive genomics resource on microbial signal transduction. *Nucleic Acids Res*, *38*, D401-407.

141. Forst, S., Comeau, D., Norioka, S., and Inouye, M. (1987). Localization and membrane topology of EnvZ, a protein involved in osmoregulation of OmpF and OmpC in Escherichia coli. *J Biol Chem*, *262*, 16433-16438.

142. Skerker, J. M., Prasol, M. S., Perchuk, B. S., Biondi, E. G., and Laub, M. T. (2005). Two-component signal transduction pathways regulating growth and cell cycle progression in a bacterium: a system-level analysis. *PLoS Biol*, *3*, e334.

143. Gao, R., Mack, T. R., and Stock, A. M. (2007). Bacterial response regulators: versatile regulatory strategies from common domains. *Trends Biochem Sci*, *32*, 225-234.

144. Bourret, R. B. (2010). Receiver domain structure and function in response regulator proteins. *Curr Opin Microbiol*, *13*, 142-149.

145. Chamnongpol, S., and Groisman, E. A. (2000). Acetyl phosphate-dependent activation of a mutant PhoP response regulator that functions independently of its cognate sensor kinase. *J Mol Biol*, *300*, 291-305.

146. Gueriri, I., Bay, S., Dubrac, S., Cyncynatus, C., and Msadek, T. (2008). The Pta-AckA pathway controlling acetyl phosphate levels and the phosphorylation state of the DegU orphan response regulator both play a role in regulating Listeria monocytogenes motility and chemotaxis. *Mol Microbiol*, *70*, 1342-1357.

147. Hiratsu, K., Nakata, A., Shinagawa, H., and Makino, K. (1995). Autophosphorylation and activation of transcriptional activator PhoB of Escherichia coli by acetyl phosphate in vitro. *Gene*, *161*, 7-10.

148. Kim, S. B., Shin, B. S., Choi, S. K., Kim, C. K., and Park, S. H. (2001). Involvement of acetyl phosphate in the in vivo activation of the response regulator ComA in Bacillus subtilis. *FEMS Microbiol Lett*, *195*, 179-183.

149. McCleary, W. R., Stock, J. B., and Ninfa, A. J. (1993). Is acetyl phosphate a global signal in *Escherichia coli*? *J Bacteriol*, *175*, 2793-2798.

150. Pruss, B. M. (1998). Acetyl phosphate and the phosphorylation of OmpR are involved in the regulation of the cell division rate in Escherichia coli. *Arch Microbiol*, *170*, 141-146.

151. Wanner, B. L., and Wilmes-Riesenberg, M. R. (1992). Involvement of phosphotransacetylase, acetate kinase, and acetyl phosphate synthesis in control of the phosphate regulon in *Escherichia coli*. *J Bacteriol*, *174*, 2124-2130.

152. Da Re, S. S., Deville-Bonne, D., Tolstykh, T., M, V. r., and Stock, J. B. (1999). Kinetics of CheY phosphorylation by small molecule phosphodonors. *FEBS Lett*, *457*, 323-326.

153. Mayover, T. L., Halkides, C. J., and Stewart, R. C. (1999). Kinetic characterization of CheY phosphorylation reactions: comparison of P-CheA and small-molecule phosphodonors. *Biochemistry*, *38*, 2259-2271.

154. Volkman, B. F., Lipson, D., Wemmer, D. E., and Kern, D. (2001). Two-state allosteric behavior in a single-domain signaling protein. *Science*, *291*, 2429-2433.

155. Laubacher, M. E., and Ades, S. E. (2008). The Rcs phosphorelay is a cell envelope stress response activated by peptidoglycan stress and contributes to intrinsic antibiotic resistance. *J Bacteriol*, *190*, 2065-2074.

156. Majdalani, N., and Gottesman, S. (2005). The Rcs phosphorelay: a complex signal transduction system. *Annu Rev Microbiol*, *59*, 379-405.

157. Majdalani, N., Heck, M., Stout, V., and Gottesman, S. (2005). Role of RcsF in signaling to the Rcs phosphorelay pathway in *Escherichia coli*. *J Bacteriol*, *187*, 6770-6778.

158. Majdalani, N., Hernandez, D., and Gottesman, S. (2002). Regulation and mode of action of the second small RNA activator of RpoS translation, RprA. *Mol Microbiol, 46*, 813-826.

159. Castanie-Cornet, M. P., Cam, K., and Jacq, A. (2006). RcsF is an outer membrane lipoprotein involved in the RcsCDB phosphorelay signaling pathway in Escherichia coli. *J Bacteriol, 188*, 4264-4270.

160. Gervais, F. G., and Drapeau, G. R. (1992). Identification, cloning, and characterization of rcsF, a new regulator gene for exopolysaccharide synthesis that suppresses the division mutation ftsZ84 in Escherichia coli K-12. *J Bacteriol, 174*, 8016-8022.

161. Torres-Cabassa, A. S., and Gottesman, S. (1987). Capsule synthesis in Escherichia coli K-12 is regulated by proteolysis. *J Bacteriol, 169*, 981-989.

162. Gottesman, S., Trisler, P., and Torres-Cabassa, A. (1985). Regulation of capsular polysaccharide synthesis in Escherichia coli K-12: characterization of three regulatory genes. *J Bacteriol, 162*, 1111-1119.

163. Francez-Charlot, A., Laugel, B., Van Gemert, A., Dubarry, N., Wiorowski, F., Castanie-Cornet, M. P., Gutierrez, C., and Cam, K. (2003). RcsCDB His-Asp phosphorelay system negatively regulates the *flhDC* operon in *Escherichia coli*. *Mol Microbiol, 49*, 823-832.

164. Davalos-Garcia, M., Conter, A., Toesca, I., Gutierrez, C., and Cam, K. (2001). Regulation of *osmC* gene expression by the two-component system RcsB-RcsC in *Escherichia coli*. *J Bacteriol, 183*, 5870-5876.

165. Sturny, R., Cam, K., Gutierrez, C., and Conter, A. (2003). NhaR and RcsB independently regulate the *osmCp1* promoter of *Escherichia coli* at overlapping regulatory sites. *J Bacteriol, 185*, 4298-4304.

166. Toesca, I., Perard, C., Bouvier, J., Gutierrez, C., and Conter, A. (2001). The transcriptional activator NhaR is responsible for the osmotic induction of *osmC(p1)*, a promoter of the stress-inducible gene *osmC* in *Escherichia coli*. *Microbiology, 147*, 2795-2803.

167. Majdalani, N., Chen, S., Murrow, J., St John, K., and Gottesman, S. (2001). Regulation of RpoS by a novel small RNA: the characterization of RprA. *Mol Microbiol*, *39*, 1382-1394.

168. McCullen, C. A., Benhammou, J. N., Majdalani, N., and Gottesman, S. (2010). Mechanism of positive regulation by DsrA and RprA small noncoding RNAs: pairing increases translation and protects *rpoS* mRNA from degradation. *J Bacteriol*, *192*, 5559-5571.

169. Walthers, D., Tran, V. K., and Kenney, L. J. (2003). Interdomain linkers of homologous response regulators determine their mechanism of action. *J Bacteriol*, *185*, 317-324.

170. Dyson, H. J., and Wright, P. E. (2005). Intrinsically unstructured proteins and their functions. *Nat Rev Mol Cell Biol*, *6*, 197-208.

171. Collins, M. O., Yu, L., Campuzano, I., Grant, S. G., and Choudhary, J. S. (2008). Phosphoproteomic analysis of the mouse brain cytosol reveals a predominance of protein phosphorylation in regions of intrinsic sequence disorder. *Mol Cell Proteomics*, *7*, 1331-1348.

172. Pristovsek, P., Sengupta, K., Lohr, F., Schafer, B., von Trebra, M. W., Ruterjans, H., and Bernhard, F. (2003). Structural analysis of the DNA-binding domain of the *Erwinia amylovora* RcsB protein and its interaction with the RcsAB box. *J Biol Chem*, *278*, 17752-17759.

173. Baikalov, I., Schroder, I., Kaczor-Grzeskowiak, M., Grzeskowiak, K., Gunsalus, R. P., and Dickerson, R. E. (1996). Structure of the *Escherichia coli* response regulator NarL. *Biochemistry*, *35*, 11053-11061.

174. Ducros, V. M., Lewis, R. J., Verma, C. S., Dodson, E. J., Leonard, G., Turkenburg, J. P., Murshudov, G. N., Wilkinson, A. J., and Brannigan, J. A. (2001). Crystal structure of GerE, the ultimate transcriptional regulator of spore formation in *Bacillus subtilis*. *J Mol Biol*, *306*, 759-771.

175. Vannini, A., Volpari, C., Gargioli, C., Muraglia, E., Cortese, R., De Francesco, R., Neddermann, P., and Marco, S. D. (2002). The crystal structure of the quorum sensing protein TraR bound to its autoinducer and target DNA. *EMBO J*, *21*, 4393-4401.

176. Avarind, L., Anantharaman, V., Balaji, S., Babu, M. M., and Iyer, L. M. (2005). The many faces of the helix-turn-helix domain: Transcription regulation and beyond. *FEMS Microbiol Rev*, *29*, 231-262.

177. Powell, B. S., Rivas, M. P., Court, D. L., Nakamura, Y., and Turnbough, C. L., Jr. (1994). Rapid confirmation of single copy lambda prophage integration by PCR. *Nucleic Acids Res*, *22*, 5765-5766.

178. Simons, R. W., Houman, F., and Kleckner, N. (1987). Improved single and multicopy lac-based cloning vectors for protein and operon fusions. *Gene*, *53*, 85-96.

179. Keating, D. H., Shulla, A., Klein, A. H., and Wolfe, A. J. (2008). Optimized two-dimensional thin layer chromatography to monitor the intracellular concentration of acetyl phosphate and other small phosphorylated molecules. *Biol Proced Online*, *10*, 36-46.

180. Marsh, P. (1986). Ptac-85, an E. coli vector for expression of non-fusion proteins. *Nucleic Acids Res*, *14*, 3603.

181. Lintner, R. E., Mishra, P. K., Srivastava, P., Martinez-Vaz, B. M., Khodursky, A. B., and Blumenthal, R. M. (2008). Limited functional conservation of a global regulator among related bacterial genera: Lrp in *Escherichia*, *Proteus* and *Vibrio*. *BMC Microbiol*, *8*, 60.

182. Fowler, M. L., Ingram-Smith, C. J., and Smith, K. S. (2011). Direct detection of the acetate-forming activity of the enzyme acetate kinase. *J Vis Exp*,

183. DiGiuseppe, P. A., and Silhavy, T. J. (2003). Signal detection and target gene induction by the CpxRA two-component system. *J Bacteriol*, *185*, 2432-2440.

184. Chi, B. K., Gronau, K., Mader, U., Hessling, B., Becher, D., and Antelmann, H. (2011). S-bacillithiolation protects against hypochlorite stress in *Bacillus subtilis* as revealed by transcriptomics and redox proteomics. *Mol Cell Proteomics*, *10*, M111 009506.

185. Kitagawa, M., Ara, T., Arifuzzaman, M., Ioka-Nakamichi, T., Inamoto, E., Toyonaga, H., and Mori, H. (2005). Complete set of ORF clones of *Escherichia coli* ASKA library (a complete set of *E. coli* K-12 ORF archive): unique resources for biological research. *DNA Res*, *12*, 291-299.

186. Dieckman, L., Gu, M., Stols, L., Donnelly, M. I., and Collart, F. R. (2002). High throughput methods for gene cloning and expression. *Protein Expr Purif*, *25*, 1-7.

187. Millard, C. S., Stols, L., Quartey, P., Kim, Y., Dementieva, I., and Donnelly, M. I. (2003). A less laborious approach to the high-throughput production of recombinant proteins in *Escherichia coli* using 2-liter plastic bottles. *Protein Expr Purif*, *29*, 311-320.

188. Kuhn, M. L., Majorek, K. A., Minor, W., and Anderson, W. F. (2013). Broad-substrate screen as a tool to identify substrates for bacterial Gcn5-related N-acetyltransferases with unknown substrate specificity. *Protein Sci*, *22*, 222-230.

189. Datsenko, K. A., and Wanner, B. L. (2000). One-step inactivation of chromosomal genes in Escherichia coli K-12 using PCR products. *Proc Natl Acad Sci U S A*, *97*, 6640-6645.

190. Kumari, S., Beatty, C. M., Browning, D. F., Busby, S. J., Simel, E. J., Hovel-Miner, G., and Wolfe, A. J. (2000). Regulation of acetyl coenzyme A synthetase in Escherichia coli. *J Bacteriol*, *182*, 4173-4179.

191. Baba, T., Ara, T., Hasegawa, M., Takai, Y., Okumura, Y., Baba, M., Datsenko, K. A., Tomita, M., Wanner, B. L., and Mori, H. (2006). Construction of Escherichia coli K-12 in-frame, single-gene knockout mutants: the Keio collection. *Mol Syst Biol*, *2*, 2006 0008.

192. Zuber, M., Hoover, T. A., and Court, D. L. (1995). Analysis of a Coxiella burnetti gene product that activates capsule synthesis in Escherichia coli: requirement for the heat shock chaperone DnaK and the two-component regulator RcsC. *J Bacteriol*, *177*, 4238-4244.

193. Gutierrez, C., and Devedjian, J. C. (1991). Osmotic induction of gene osmC expression in Escherichia coli K12. *J Mol Biol*, *220*, 959-973.

194. Boulanger, A., Francez-Charlot, A., Conter, A., Castanie-Cornet, M. P., Cam, K., and Gutierrez, C. (2005). Multistress regulation in Escherichia coli: expression of osmB involves two independent promoters responding either to sigmaS or to the RcsCDB His-Asp phosphorelay. *J Bacteriol*, *187*, 3282-3286.

195. Amann, E., Ochs, B., and Abel, K. J. (1988). Tightly regulated tac promoter vectors useful for the expression of unfused and fused proteins in Escherichia coli. *Gene*, *69*, 301-315.

196. Ferrieres, L., and Clarke, D. J. (2003). The RcsC sensor kinase is required for normal biofilm formation in Escherichia coli K-12 and controls the expression of a regulon in response to growth on a solid surface. *Mol Microbiol*, *50*, 1665-1682.

197. Clarke, D. J., Joyce, S. A., Toutain, C. M., Jacq, A., and Holland, I. B. (2002). Genetic analysis of the RcsC sensor kinase from Escherichia coli K-12. *J Bacteriol*, *184*, 1204-1208.

198. Gaal, T., Ross, W., Blatter, E. E., Tang, H., Jia, X., Krishnan, V. V., Assa-Munt, N., Ebright, R. H., and Gourse, R. L. (1996). DNA-binding determinants of the alpha subunit of RNA polymerase: novel DNA-binding domain architecture. *Genes Dev*, *10*, 16-26.

199. Carballes, F., Bertrand, C., Bouche, J. P., and Cam, K. (1999). Regulation of Escherichia coli cell division genes ftsA and ftsZ by the two-component system rcsC-rcsB. *Mol Microbiol*, *34*, 442-450.

200. Clarke, D. J. (2010). The Rcs phosphorelay: more than just a two-component pathway. *Future Microbiol*, *5*, 1173-1184.

201. Ramponi, G., Manao, G., and Camici, G. (1975). Nonenzymatic acetylation of histones with acetyl phosphate and acetyl adenylate. *Biochemistry*, *14*, 2681-2685.

202. Weinert, B. T., Iesmantavicius, V., Wagner, S. A., Scholz, C., Gummesson, B., Beli, P., Nystrom, T., and Choudhary, C. (2013). Acetyl-Phosphate Is a Critical Determinant of Lysine Acetylation in E. coli. *Mol Cell*,

203. Pokholok, D. K., Harbison, C. T., Levine, S., Cole, M., Hannett, N. M., Lee, T. I., Bell, G. W., Walker, K., Rolfe, P. A., Herbolsheimer, E., Zeitlinger, J., Lewitter, F., Gifford, D. K., and Young, R. A. (2005). Genome-wide map of nucleosome acetylation and methylation in yeast. *Cell*, *122*, 517-527.

204. Wang, X., and Hayes, J. J. (2008). Acetylation mimics within individual core histone tail domains indicate distinct roles in regulating the stability of higher-order chromatin structure. *Mol Cell Biol*, *28*, 227-236.

205. Barak, R., and Eisenbach, M. (2004). Co-regulation of acetylation and phosphorylation of CheY, a response regulator in chemotaxis of Escherichia coli. *J Mol Biol*, *342*, 375-381.

206. Pruss, B. M., Besemann, C., Denton, A., and Wolfe, A. J. (2006). A complex transcription network controls the early stages of biofilm development by Escherichia coli. *J Bacteriol*, *188*, 3731-3739.

207. Wang, Q., Zhao, Y., McClelland, M., and Harshey, R. M. (2007). The RcsCDB signaling system and swarming motility in Salmonella enterica serovar typhimurium: dual regulation of flagellar and SPI-2 virulence genes. *J Bacteriol*, *189*, 8447-8457.

208. Hankermeyer, C. R., and Tjeerdema, R. S. (1999). Polyhydroxybutyrate: plastic made and degraded by microorganisms. *Rev Environ Contam Toxicol*, *159*, 1-24.

209. Spiekermann, P., Rehm, B. H., Kalscheuer, R., Baumeister, D., and Steinbuchel, A. (1999). A sensitive, viable-colony staining method using Nile red for direct screening of bacteria that accumulate polyhydroxyalkanoic acids and other lipid storage compounds. *Arch Microbiol*, *171*, 73-80.

210. Ostle, A. G., and Holt, J. G. (1982). Nile blue A as a fluorescent stain for poly-beta-hydroxybutyrate. *Appl Environ Microbiol*, *44*, 238-241.

211. Song, W. J., and Jackowski, S. (1992). Cloning, sequencing, and expression of the pantothenate kinase (coaA) gene of Escherichia coli. *J Bacteriol*, *174*, 6411-6417.

212. Russo, F. D., and Silhavy, T. J. (1992). Alpha: the Cinderella subunit of RNA polymerase. *J Biol Chem*, *267*, 14515-14518.

213. Ishihama, A., Shimamoto, N., Aiba, H., Kawakami, K., Nashimoto, H., Tsugawa, A., and Uchida, H. (1980). Temperature-sensitive mutations in the alpha subunit gene of Escherichia coli RNA polymerase. *J Mol Biol*, *137*, 137-150.

214. Hayward, R. S., Igarashi, K., and Ishihama, A. (1991). Functional specialization within the alpha-subunit of Escherichia coli RNA polymerase. *J Mol Biol*, *221*, 23-29.

215. Wolfe, A. J. (2010). Physiologically relevant small phosphodonors link metabolism to signal transduction. *Curr Opin Microbiol*, *13*, 204-209.

216. Denu, J. M. (2005). Vitamin B3 and sirtuin function. *Trends Biochem Sci*, *30*, 479-483.

217. Lundgren, D. H., Hwang, S. I., Wu, L., and Han, D. K. (2010). Role of spectral counting in quantitative proteomics. *Expert Rev Proteomics*, *7*, 39-53.

218. Hu, L. I., Chi, B. K., Kuhn, M. L., Filippova, E. V., Walker-Peddakotla, A. J., Basell, K., Becher, D., Anderson, W. F., Antelmann, H., and Wolfe, A. J. (2013). Acetylation of the Response Regulator RcsB Controls Transcription from a Small RNA Promoter. *J Bacteriol*, *195*, 4174-4186.

219. Chi, B. K., Gronau, K., Mäder, U., Hessling, B., Becher, D., and Antelmann, H. (2011). S-bacillithiolation protects against hypochlorite stress in Bacillus subtilis as revealed by transcriptomics and redox proteomics. *Mol Cell Proteomics*, *10*, M111 009506.

220. Neumann, H., Hancock, S. M., Buning, R., Routh, A., Chapman, L., Somers, J., Owen-Hughes, T., van Noort, J., Rhodes, D., and Chin, J. W. (2009). A method for genetically installing site-specific acetylation in recombinant histones defines the effects of H3 K56 acetylation. *Mol Cell*, *36*, 153-163.

221. Dang, W., Steffen, K. K., Perry, R., Dorsey, J. A., Johnson, F. B., Shilatifard, A., Kaeberlein, M., Kennedy, B. K., and Berger, S. L. (2009). Histone H4 lysine 16 acetylation regulates cellular lifespan. *Nature*, *459*, 802-807.

222. Albaugh, B. N., Arnold, K. M., Lee, S., and Denu, J. M. (2011). Autoacetylation of the histone acetyltransferase Rtt109. *J Biol Chem*, *286*, 24694-24701.

223. Santos-Rosa, H., Valls, E., Kouzarides, T., and Martinez-Balbas, M. (2003). Mechanisms of P/CAF auto-acetylation. *Nucleic Acids Res*, *31*, 4285-4292.

224. Wang, J., and Chen, J. (2010). SIRT1 regulates autoacetylation and histone acetyltransferase activity of TIP60. *J Biol Chem*, *285*, 11458-11464.

225. Thompson, P. R., Wang, D., Wang, L., Fulco, M., Pediconi, N., Zhang, D., An, W., Ge, Q., Roeder, R. G., Wong, J., Levrero, M., Sartorelli, V., Cotter, R. J., and Cole, P. A. (2004). Regulation of the p300 HAT domain via a novel activation loop. *Nat Struct Mol Biol*, *11*, 308-315.

226. Igarashi, K., and Kashiwagi, K. (2010). Modulation of cellular function by polyamines. *Int J Biochem Cell Biol*, *42*, 39-51.

227. Fukuchi, J., Kashiwagi, K., Yamagishi, M., Ishihama, A., and Igarashi, K. (1995). Decrease in cell viability due to the accumulation of spermidine in spermidine acetyltransferase-deficient mutant of Escherichia coli. *J Biol Chem*, *270*, 18831-18835.

228. Carper, S. W., Willis, D. G., Manning, K. A., and Gerner, E. W. (1991). Spermidine acetylation in response to a variety of stresses in Escherichia coli. *J Biol Chem*, *266*, 12439-12441.

229. Matsui, I., Kamei, M., Otani, S., Morisawa, S., and Pegg, A. E. (1982). Occurrence and induction of spermidine-N1-acetyltransferase in Escherichia coli. *Biochem Biophys Res Commun*, *106*, 1155-1160.

230. Fukuchi, J., Kashiwagi, K., Takio, K., and Igarashi, K. (1994). Properties and structure of spermidine acetyltransferase in Escherichia coli. *J Biol Chem*, *269*, 22581-22585.

231. Coleman, C. S., Stanley, B. A., Jones, A. D., and Pegg, A. E. (2004). Spermidine/spermine-N1-acetyltransferase-2 (SSAT2) acetylates thialysine and is not involved in polyamine metabolism. *Biochem J*, *384*, 139-148.

232. Lipmann, F., and Tuttle, L. C. (1945). *J Biol Chem*, *159*, 21-28.

233. Rose, I. A. (1955). *Methods in Enz.*, *1*, 591-595.

234. Crooks, G. E., Hon, G., Chandonia, J. M., and Brenner, S. E. (2004). WebLogo: a sequence logo generator. *Genome Res*, *14*, 1188-1190.

235. Gurard-Levin, Z. A., Kilian, K. A., Kim, J., Bahr, K., and Mrksich, M. (2010). Peptide arrays identify isoform-selective substrates for profiling endogenous lysine deacetylase activity. *ACS Chem Biol*, *5*, 863-873.

236. Albaugh, B. N., Arnold, K. M., and Denu, J. M. (2011). KAT(ching) metabolism by the tail: insight into the links between lysine acetyltransferases and metabolism. *Chembiochem*, *12*, 290-298.

237. Karanam, B., Jiang, L., Wang, L., Kelleher, N. L., and Cole, P. A. (2006). Kinetic and mass spectrometric analysis of p300 histone acetyltransferase domain autoacetylation. *J Biol Chem*, *281*, 40292-40301.

238. Yang, C., Wu, J., and Zheng, Y. G. (2012). Function of the active site lysine autoacetylation in Tip60 catalysis. *PLoS One*, *7*, e32886.

239. Rardin, M. J., Newman, J. C., Held, J. M., Cusack, M. P., Sorensen, D. J., Li, B., Schilling, B., Mooney, S. D., Kahn, C. R., Verdin, E., and Gibson, B. W. (2013). Label-free quantitative proteomics of the lysine acetylome in mitochondria identifies substrates of SIRT3 in metabolic pathways. *Proc Natl Acad Sci U S A*, *110*, 6601-6606.

240. Wagner, G. R., and Payne, R. M. (2011). Mitochondrial acetylation and diseases of aging. *J Aging Res*, *2011*, 234875.

241. Hubbard, B. P., Gomes, A. P., Dai, H., Li, J., Case, A. W., Considine, T., Riera, T. V., Lee, J. E., E, S. Y., Lamming, D. W., Pentelute, B. L., Schuman, E. R., Stevens, L. A., Ling, A. J., Armour, S. M., Michan, S., Zhao, H., Jiang, Y., Sweitzer, S. M., Blum, C. A., Disch, J. S., Ng, P. Y., Howitz, K. T., Rolo, A. P., Hamuro, Y., Moss, J., Perni, R. B., Ellis, J. L., Vlasuk, G. P., and Sinclair, D. A. (2013). Evidence for a common mechanism of SIRT1 regulation by allosteric activators. *Science*, *339*, 1216-1219.

242. Park, D., Ciezki, K., van der Hoeven, R., Singh, S., Reimer, D., Bode, H. B., and Forst, S. (2009). Genetic analysis of xenocoumacin antibiotic production in the mutualistic bacterium Xenorhabdus nematophila. *Mol Microbiol*, *73*, 938-949.

243. Bouvier, J., Gordia, S., Kampmann, G., Lange, R., Hengge-Aronis, R., and Gutierrez, C. (1998). Interplay between global regulators of Escherichia coli: effect of RpoS, Lrp and H-NS on transcription of the gene osmC. *Mol Microbiol*, *28*, 971-980.

244. Gordia, S., and Gutierrez, C. (1996). Growth-phase-dependent expression of the osmotically inducible gene osmC of Escherichia coli K-12. *Mol Microbiol*, *19*, 729-736.

VITA

Linda I-Lin Hu was born in Philadelphia, PA and was raised in Havertown by parents George and Betty Hu. She has an older sister Mimi Hu. Linda currently resides in Lombard, IL with her husband Nestor Alvarado.

She received her Bachelor of Science in Biological Sciences at University of Notre Dame in Notre Dame, IN in 2004. She worked for Caterpillar as an oil analyst in Bensalem, PA for a year. She then worked for Argonne National Laboratories in Lemont, IL as a chemical analyst for two years.

In August of 2007, Linda joined the Department of Microbiology and Immunology at Loyola University Medical Center in Maywood, IL. She studied in the laboratory of Dr. David Keating for about a half a year before joining the laboratory of Dr. Alan Wolfe, where she studied the regulation of an *E. coli* stress response. Linda received many opportunities to mentor high school students, undergraduates, medical students, and graduate students. She also presented her research at several microbiology conferences. At one of these meetings, she was recognized as a Bacterial Locomotion and Signal Transduction Board of Directors' Award for an Outstanding Talk Finalist in 2011.

After completing her Ph.D., Linda will be pursuing her post-doctoral training in the laboratory of Dr. Douglas Weibel in the Department of Biochemistry at University of Wisconsin – Madison.

DISSERTATION APPROVAL SHEET

The dissertation submitted by Linda I-Lin Hu has been read and approved by the following committee:

Alan J. Wolfe, Ph.D., Director
Professor of Microbiology and Immunology
Loyola University Chicago Stritch School of Medicine

Karen L. Visick, Ph.D.
Professor of Microbiology and Immunology
Loyola University Chicago Stritch School of Medicine

Adam Driks, Ph.D.
Professor of Microbiology and Immunology
Loyola University Chicago Stritch School of Medicine

Thomas M. Gallagher, Ph.D.
Professor of Microbiology and Immunology
Loyola University Chicago Stritch School of Medicine

Christopher M. Wiethoff, Ph.D.
Assistant Professor of Microbiology and Immunology
Loyola University Chicago Stritch School of Medicine

Sean Crosson, Ph.D.
Associate Professor of Biochemistry and Molecular Biophysics
The University of Chicago Stritch School of Medicine

The final copies have been examined by the director of the dissertation and the signature which appears below verifies the fact that any necessary changes have been incorporated and that the dissertation is now given final approval by the committee with reference to content and form. The dissertation is therefore accepted in partial fulfillment of the requirements for the degree of Doctor of Philosophy

_____ _____

Date Director's Signature